

Medical University of South Carolina

**MEDICA**

---

MUSC Theses and Dissertations

---

2014

## Dual-specificity Phosphatase-1 Regulates the Inflammatory Milieu in Head and Neck Squamous Cell Carcinoma

Xiaoyi Zhang

*Medical University of South Carolina*

Follow this and additional works at: <https://medica-musc.researchcommons.org/theses>

---

### Recommended Citation

Zhang, Xiaoyi, "Dual-specificity Phosphatase-1 Regulates the Inflammatory Milieu in Head and Neck Squamous Cell Carcinoma" (2014). *MUSC Theses and Dissertations*. 514.

<https://medica-musc.researchcommons.org/theses/514>

This Dissertation is brought to you for free and open access by MEDICA. It has been accepted for inclusion in MUSC Theses and Dissertations by an authorized administrator of MEDICA. For more information, please contact [medica@musc.edu](mailto:medica@musc.edu).

**Dual-specificity Phosphatase-1 Regulates the Inflammatory Milieu in Head and  
Neck Squamous Cell Carcinoma**

by

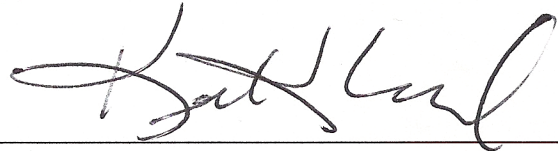
Xiaoyi Zhang

A dissertation submitted to the faculty of the Medical University of South Carolina in  
partial fulfillment of the requirement for the degree of doctorate of philosophy in the  
College of Graduate Studies.

Department of Oral Health Sciences

2014

Approved by:



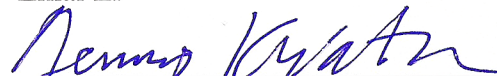
Chairman, Keith Kirkwood



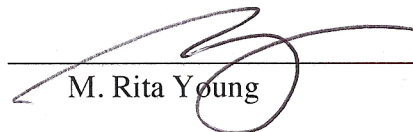
Terry Day



Zihai Li



Dennis Watson



M. Rita Young

**Abstract Title**

Dual-specificity Phosphatase-1 Regulates the Inflammatory Milieu in Head and Neck  
Squamous Cell Carcinoma

by

Xiaoyi Zhang

An abstract of a dissertation conducted under the guidance of Keith Kirkwood

## **Abstract**

Head and neck cancer accounts for approximately 6% of diagnosed malignancies in the United States, with an estimated 35,000 incidences and over 7,000 deaths every year. Head and neck squamous cell carcinoma (HNSCC) comprises the majority of head and neck cancers, with a worldwide incidence of more than 500,000 cases. Head and neck cancer patients often present in advanced stages of disease, and despite ongoing research, survival rates remain lower than other more common malignancies. Cytokines and pro-inflammatory factors have been shown to have a critical role in the various steps of malignant transformation, including tumor growth, survival, invasion, angiogenesis, and metastasis. Mitogen-activated protein kinases (MAPK), such as p38, JNK, and ERK, relay information from extracellular signals to the effectors that control these diverse cellular processes. Negative regulation of MAPK activity is provided by MAPK phosphatases that dephosphorylate MAPK proteins. The founding member of this class of phosphatases is dual-specificity phosphatase-1 (DUSP1) and has been shown to be crucial for negatively regulating innate immune responses. Initial studies revealed significant over-expression of DUSP1 in a range of human epithelial tumors including prostate, colon, and bladder, with loss of DUSP1 expression in tumors of higher histological grade and in metastases. Based on the above, this study hypothesized that DUSP1 is a negative regulator of tumor-promoting inflammation in head and neck cancer. To test this hypothesis, we first assessed the effect of *Dusp1* deficiency in animal models of tumor progression. *Dusp1* deficiency enhanced tumor progression in a carcinogen-induced model of oral cancer with higher levels of inflammatory infiltrate and gene expression. Deficiency in hematopoietic-derived cells by bone marrow transplant



did not recapitulate the advanced disease phenotype seen in *Dusp1* deficient animals. However, *Dusp1* deficiency also enhanced the progression of subcutaneous syngeneic breast and prostate allograft tumors. Examination of *Dusp1* deficient bone marrow macrophages revealed enhanced expression of inflammatory cytokine IL-1 $\beta$  after stimulation with lipopolysaccharide. Elevated levels of IL-1 $\beta$  were shown to be due to increased *de novo* transcription in addition to enhanced mRNA stability. Inflammasome activation was not affected by *Dusp1* deficiency. Lastly, in human HNSCC tissues, both mRNA and protein DUSP1 was decreased in tumor compared to adjacent non-tumor samples, and IL-1 $\beta$  protein was increased. These studies demonstrate DUSP1 expression is deregulated in HNSCC and suggests an important role for DUSP1 as a negative regulator of tumor-promoting inflammation through suppression of inflammatory cytokines, such as IL-1 $\beta$ . Understanding the role of these inflammatory mediators and the upstream signaling pathways in the tumor microenvironment in head and neck cancer may yield novel therapeutic targets for prevention and treatment.

## **Dedication**

This dissertation is dedicated to my parents, who instilled in me an early curiosity and appreciation for learning, and have always served as examples of diligence and hard work. Thank you for your constant love and support.

## Table of Contents

ABSTRACT.....	iv
LIST OF FIGURES AND LEGENDS.....	x
KEY TO SYMBOLS AND ABBREVIATIONS.....	xii
ACKNOWLEDGEMENTS.....	xvi
<b>CHAPTER 1. Background &amp; Significance.....</b>	<b>1</b>
1.1    Head and neck squamous cell carcinoma.....	1
Importance of the problem.....	1
Etiological factors in HNSCC.....	1
Signaling pathways deregulated in HNSCC.....	2
1.2    Mitogen-activated protein kinases and regulation.....	6
Overview of MAPK signaling.....	6
Overview of dual-specificity phosphatases.....	6
MAPK phosphatase structure and function.....	7
1.3    Dual-specificity phosphatase-1.....	8
Regulation of <i>DUSP1</i> expression.....	8
Regulation of <i>DUSP1</i> activity.....	11
Phenotype of <i>Dusp1</i> deficient mice.....	13
Regulation of inflammation by <i>DUSP1</i> .....	15
Expression of <i>DUSP1</i> in cancer.....	19
1.4    Cancer-associated inflammation.....	26
Inflammatory signaling pathways activated in cancer.....	26
The HNSCC tumor microenvironment.....	29
Inflammatory cell recruitment and activation.....	30
Roles of macrophages in cancer.....	32
Cytokines, chemokines, and inflammatory mediators.....	33
Roles of interleukin 1- $\beta$ in cancer biology.....	34
1.5    Hypothesis & Specific Aims.....	38
<b>CHAPTER 2. Materials and Methods.....</b>	<b>40</b>
2.1    Generation of animals.....	40
2.2    Carcinogen-induced oral cancer model.....	41
2.3    Bone marrow transplantation.....	42
2.4    Subcutaneous syngeneic tumor model.....	43
2.5    Human tissue samples.....	44
2.6    Histology.....	44
2.7    Immunohistochemistry.....	45

2.8 Primary bone marrow-derived macrophage isolation.....	46
2.9 Macrophage polarization.....	47
2.10 Inflammasome activation.....	47
2.11 Protein isolation.....	48
2.12 Western blotting.....	49
2.13 Enzyme-linked immunosorbent assay.....	50
2.14 RNA isolation and quantitative PCR.....	50
2.15 Quantitative PCR array.....	52
2.16 Nanostring.....	52
2.17 mRNA decay.....	53
2.18 Flow cytometry.....	53
2.19 Statistical analyses.....	55
<b>CHAPTER 3. <i>Dusp1</i> deficiency enhances tumor growth and progression.....</b>	<b>56</b>
3.1 Rationale & Hypothesis.....	56
3.2 Results.....	57
<i>Dusp1</i> deficient mice are more susceptible to carcinogen-induced oral cancer.....	57
<i>Dusp1</i> deficient tumors contain higher levels of inflammation.....	65
Effects of <i>Dusp1</i> deficiency on MAPK activation in oral tumor epithelium.....	78
Effect of hematopoietic <i>Dusp1</i> deficiency in carcinogen-induced oral cancer...	82
<i>Dusp1</i> deficient mice support enhanced syngeneic tumor growth.....	84
3.3 Summary & Discussion.....	90
<b>CHAPTER 4. <i>Dusp1</i> regulates inflammatory mediators <i>ex vivo</i>.....</b>	<b>99</b>
4.1 Rationale & Hypothesis.....	99
4.2 Results.....	100
Macrophage polarization is not skewed in <i>Dusp1</i> deficient primary cells.....	100
<i>Dusp1</i> deficient tumor tissues express significantly higher levels of inflammatory chemokines and cytokines.....	103
<i>Dusp1</i> deficient macrophages express more <i>Il1b</i> mRNA after stimulation.....	104
<i>Il1b</i> mRNA stability is enhanced in <i>Dusp1</i> deficient macrophages.....	108
<i>Dusp1</i> deficiency does not affect inflammasome activation.....	109
4.3 Summary & Discussion.....	112
<b>CHAPTER 5. Assessment of <i>DUSP1</i> expression in human HNSCC.....</b>	<b>117</b>
5.1 Rationale & Hypothesis.....	117
5.2 Results.....	117
Decreased <i>DUSP1</i> expression in human HNSCC.....	117
<i>DUSP1</i> expression in other HNSCC datasets.....	119

Correlation between <i>DUSP1</i> expression and cytokine levels in HNSCC.....	120
5.3 Summary & Discussion.....	121
<b>CHAPTER 6. General Discussion &amp; Future Directions.....</b>	<b>124</b>
<b>APPENDICES.....</b>	<b>128</b>
Appendix A. Comparison of inflammatory cytokine, chemokine and receptor expression in wild-type and <i>Dusp1</i> deficient tumor tissue by targeted qPCR array.....	128
Appendix B. Comparison of the expression levels of MAPK signaling pathway members in wild-type and <i>Dusp1</i> deficient tumor tissue by targeted qPCR array.....	129
Appendix C. Nanostring gene counts from wild-type and <i>Dusp1</i> deficient tumor tissues.....	130
<b>REFERENCES.....</b>	<b>149</b>
<b>BIOGRAPHY.....</b>	<b>184</b>

## List of Figures

Figure 1-1. Schematic of <i>DUSP1</i> gene.....	9
Figure 1-2. DUSP1/MKP-1 negatively regulates inflammatory cytokine production.....	17
Figure 3-1. Induction of squamous cell carcinoma by 4-nitroquinoline 1-oxide treatment.....	58
Figure 3-2. Tumor-free survival is decreased in <i>Dusp1</i> deficient animals.....	59
Figure 3-3. Gender does not affect 4NQO progression in wild-type or <i>Dusp1</i> deficient animals.....	59
Figure 3-4. Weight gain is decreased in <i>Dusp1</i> deficient mice treated with 4NQO.....	60
Figure 3-5. <i>Dusp1</i> deficiency does not affect weight gain in vehicle treatment groups...	61
Figure 3-6. Representative panel of tongue tissues at the time of collection.....	62
Figure 3-7. Enhanced esophageal tumor burden in <i>Dusp1</i> deficient animals.....	63
Figure 3-8. Tumor burden is increased in <i>Dusp1</i> deficient animals.....	64
Figure 3-9. <i>Dusp1</i> deficiency enhances histological disease progression.....	64
Figure 3-10. <i>Dusp1</i> deficient lesions have enhanced inflammatory infiltrate.....	66
Figure 3-11. Quantification of immunohistochemistry for macrophages in wild-type and <i>Dusp1</i> deficient tissues.....	67
Figure 3-12. Quantification of immunohistochemistry for monocyte-myeloid lineage infiltrate in tumor tissues.....	68
Figure 3-13. Gene expression from tumor tissues by Nanostring analysis.....	69
Figure 3-14. Flow cytometry analysis of T cells in tumor-bearing mice.....	71
Figure 3-15. Flow cytometry analysis of T regulatory cells in tumor-bearing mice.....	72
Figure 3-16. Flow cytometry analysis of B cells in tumor-bearing mice.....	73
Figure 3-17. Flow cytometry analysis of dendritic cells in tumor-bearing mice.....	75
Figure 3-18. Flow cytometry analysis of natural killer cells in tumor-bearing mice.....	76
Figure 3-19. Flow cytometry analysis of myeloid lineage cells in tumor-bearing mice...	77
Figure 3-20. MAPK expression and activity in wild-type and <i>Dusp1</i> deficient tissues...	79
Figure 3-21. Densitometry analysis of Western blots for phosphorylated and total forms of p38 $\alpha$ , JNK1/2, and ERK1/2 MAPK in tissues.....	80
Figure 3-22. Immunohistochemistry of phosphorylated MAPK in oral tumor tissues...	81
Figure 3-23. Quantification of MAPK and Ki67 immunohistochemistry staining.....	82
Figure 3-24. Weight gain in chimeric wild-type and <i>Dusp1</i> deficient mice treated with 4NQO.....	84
Figure 3-25. Expression of <i>DUSP1</i> by microarray analysis in prostate cancer.....	85
Figure 3-26. Effect of <i>DUSP1</i> expression on progression-free survival in breast cancer.	86
Figure 3-27. Subcutaneous syngeneic tumor growth in wild-type and <i>Dusp1</i> deficient animals. ....	88
Figure 3-28. Inflammation scores of syngeneic subcutaneous tumors in wild-type and <i>Dusp1</i> deficient animals.....	89
Figure 3-29. Inhibition of p38 $\alpha$ MAPK in wild-type and <i>Dusp1</i> deficient mice with subcutaneous syngeneic EO771 tumors.....	89
Figure 4-1. Effect of <i>Dusp1</i> deficiency on macrophage polarization.....	102
Figure 4-2. Increased <i>Il1b</i> gene expression in <i>Dusp1</i> deficient tumor tissues.....	104
Figure 4-3. <i>Il1b</i> mRNA is increased in <i>Dusp1</i> deficient macrophages after stimulation with LPS. ....	105

Figure 4-4. <i>Il1b</i> expression is increased after stimulation with 4NQO-derived conditioned media.....	106
Figure 4-5. <i>Il1b</i> primary transcripts are increased in <i>Dusp1</i> deficient macrophages after LPS stimulation.....	107
Figure 4-6. The 3'-untranslated region of <i>IL1B</i> contains AU-rich elements.....	108
Figure 4-7. <i>Dusp1</i> deficiency differentially affects <i>Il1b</i> mRNA stability.....	109
Figure 4-8. IL-1 $\beta$ and caspase-1 expression in 4NQO tissues.....	110
Figure 4-9. IL-1 $\beta$ secretion by wild-type and <i>Dusp1</i> deficient macrophages after inflammasome activation.....	111
Figure 4-10. IL-1 $\beta$ expression is increased in <i>Dusp1</i> deficient macrophages.....	112
Figure 5-1. <i>DUSP1</i> mRNA is decreased in human HNSCC.....	119
Figure 5-2. <i>DUSP1</i> and <i>IL1B</i> expression in human HNSCC.....	119
Figure 5-3. <i>DUSP1</i> and <i>IL1B</i> mRNA in HNSCC from available microarray datasets...	120

## **Key to Symbols and Abbreviations Used**

<b>4NQO</b>	4-nitroquinoline 1-oxide
<b><math>\alpha</math>-MEM</b>	$\alpha$ -minimum essential medium
<b>ACK</b>	ammonium chloride potassium
<b>ActD</b>	actinomycin D
<b>AP</b>	activator protein
<b>ARE</b>	AU-rich element
<b>ATP</b>	adenosine triphosphate
<b>AUF1</b>	AU-rich element RNA binding protein 1
<b>BSA</b>	bovine serum albumin
<b>CCL</b>	chemokine (C-C motif) ligand
<b>CCR</b>	chemokine (C-C motif) receptor
<b>CSF-1</b>	colony stimulating factor-1
<b>CTF/NF-1</b>	CCAAT box-binding transcription factor/nuclear factor-1
<b>CXCL</b>	chemokine (C-X-C motif) ligand
<b>CXCR</b>	chemokine (C-X-C motif) receptor
<b>DMEM</b>	Dulbecco's modified Eagle's medium
<b>DUSP1</b>	dual-specificity phosphatase 1
<b>EDTA</b>	ethylenediaminetetraacetic acid
<b>ELISA</b>	enzyme-linked immunosorbent assay
<b>EGFR</b>	epidermal growth factor receptor
<b>ERK</b>	extracellular regulated kinase
<b>FBS</b>	fetal bovine serum



<b>GM-CSF</b>	granulocyte macrophage colony-stimulating factor
<b>H&amp;E</b>	hematoxylin and eosin
<b>HNSCC</b>	head and neck squamous cell carcinoma
<b>HPV</b>	human papilloma virus
<b>HSP</b>	heat shock protein
<b>HuR</b>	human antigen R
<b>IFN-<math>\gamma</math></b>	interferon- $\gamma$
<b>I<math>\kappa</math>B</b>	inhibitor of $\kappa$ B
<b>IL</b>	interleukin
<b>IL-1R</b>	interleukin-1 receptor
<b>IL-1RA</b>	interleukin-1 receptor antagonist
<b>IMDM</b>	Iscove's modified Dulbecco's medium
<b>JAK/STAT</b>	Janus kinase/signal transducer and activator of transcription
<b>JNK</b>	Jun N-terminal kinase
<b>KIM</b>	kinase interaction motif
<b>KO</b>	knockout
<b>LPS</b>	lipopolysaccharide
<b>MAPK</b>	mitogen-activated protein kinase
<b>MAPKKK</b>	mitogen-activated protein kinase kinase kinase
<b>M-CSF</b>	macrophage colony-stimulating factor
<b>MDSC</b>	myeloid-derived suppressor cell
<b>MEF</b>	mouse embryonic fibroblast
<b>MKK</b>	mitogen-activated protein kinase kinase

<b>MMP</b>	matrix metalloproteinase
<b>miRNA</b>	(miR) microRNA
<b>MAPKAPK2 (MK2)</b>	MAPK-activated protein kinase 2
<b>MKP-1</b>	mitogen-activated protein kinase phosphatase-1
<b>MyD88</b>	myeloid differentiation primary response 88
<b>NF-<math>\kappa</math>B</b>	nuclear factor $\kappa$ B
<b>NLR</b>	Nod-like receptor
<b>OSCC</b>	oral squamous cell carcinoma
<b>PAC-1</b>	phosphatase in activated T-cells
<b>PAMPs</b>	pathogen-associated molecular patterns
<b>PBS</b>	phosphate buffered saline
<b>PCR</b>	polymerase chain reaction
<b>PD-1</b>	programmed cell death-1
<b>PGE<sub>2</sub></b>	prostaglandin E <sub>2</sub>
<b>PI3K-AKT</b>	phosphatidylinositol-4,5-bisphosphate 3-kinase/protein kinase B
<b>PMSF</b>	phenylmethanesulfonyl fluoride
<b>PTEN</b>	phosphatase and tensin homolog
<b>Raf</b>	rapidly accelerated fibrosarcoma
<b>Ras</b>	rat sarcoma
<b>RIPA</b>	radioimmunoprecipitation assay
<b>RNA</b>	ribonucleic acid
<b>RNAi</b>	RNA interference
<b>RPMI</b>	Roswell Park Memorial Institute medium

<b>shRNA</b>	short hairpin RNA
<b>siRNA</b>	small interfering RNA
<b>SP-1</b>	specificity protein 1
<b>TAM</b>	tumor-associated macrophage
<b>TBS</b>	Tris-buffered saline
<b>TBS-T</b>	Tris-buffered saline with 0.1% Tween-20
<b>TGF-<math>\beta</math></b>	transforming growth factor- $\beta$
<b>TLR</b>	Toll-like receptor
<b>TNF-<math>\alpha</math></b>	tumor necrosis factor- $\alpha$
<b>TTP</b>	tristetraprolin
<b>UTR</b>	untranslated region
<b>VEGF</b>	vascular endothelial growth factor
<b>WT</b>	wild-type
<b>ZEB</b>	zinc finger E-box-binding homeobox

## **Acknowledgments**

This work would not have been possible without the contributions of several people. I would like to thank Dr. Hong Yu for her help with the carcinogen-induced model from the very beginning and spending countless hours of pathology scoring, Kimberlee Lisicki for monitoring the animals in the 4NQO model and processing all the tissues for histology, Kylie Martin for her guidance with any and all histological questions, and Johannes Aartun for his assistance with immunohistochemistry staining and quantification. My time in the laboratory was spent with wonderful people who have become close friends. I am thankful to Erica Nelson and Tara Byrum for managing an endless stream of mice and Bethany Herbert, Mike Valerio, and Heidi Steinkamp for their encouragement, commiseration, and always being available for an impromptu pow-wow. Nisha D'Silva provided her oral pathology expertise in initial characterization of the animal model and in preparation of this work for publication. My committee members Drs. Terry Day, Zihai Li, Dennis Watson, and Rita Young have contributed significant insight to this project as it has developed over the years, and I am extremely grateful for their time in guiding this work as well as my own career development. Lastly, I would like to thank my mentor Dr. Keith Kirkwood who welcomed me into his laboratory. I am grateful for his faith in me as we ventured into new territory and thankful for his patience, his enthusiasm, and his sincerity and candor. He continues to strive for excellence as a clinician-scientist and spurs me to do the same. Thank you for your mentorship.

## **CHAPTER 1. Background & Significance**

### **1.1 Head and neck squamous cell carcinoma**

#### ***Importance of the problem***

Head and neck cancers encompass a set of malignancies that affect the oral cavity, nasal cavity and sinuses, nasopharynx, oropharynx, laryngopharynx, and salivary glands. Head and neck squamous cell carcinoma (HNSCC) comprises over 90% of these cancers and is the sixth most commonly diagnosed cancer in the world (1). Of HNSCCs, cancers of the oral cavity are the most common, with 263,900 new cases of oral squamous cell carcinomas (OSCC) diagnosed worldwide and an estimated 42,000 new cases in the United States in 2014 (2, 3).

Current treatments available to patients diagnosed with HNSCC include surgical resection, radiation, and chemotherapies, performed alone or in combination, depending upon disease stage. Since the 1960s, great improvements have been in reconstructive methods to improve functional outcomes and reduce associated morbidities, yet overall survival rates have not significantly changed (4).

#### ***Etiological factors in HNSCC***

Tobacco remains an important risk factor for HNSCC, as upwards of 80% of cases are attributed, in part, to tobacco exposure (5). Smokers have ten times the risk of

HNSCC compared to patients who have never smoked (6). In the United States, public health campaigns and significant health education efforts have begun reduce prevalence of tobacco use, leading to an overall trend toward decreased HNSCC incidence (5, 6). However, tobacco exposure remains an important causative agent in HNSCC for many countries outside the developed world.

Although the national incidence of HNSCC has been decreasing due to changes in tobacco use, a rapid increase in oropharyngeal squamous cell carcinoma has been reported in a younger population of adults, associated with the presence of the human papilloma virus (HPV) (7, 8). Of the 100 characterized HPV subtypes, the predominant subtype associated with oncogenesis is HPV-16, which accounts for over 90% of HPV-associated HNSCC (9, 10). The majority of HPV-associated HNSCCs are found within the oropharynx, while the rate is much lower for tumors found within the oral cavity (11).

### ***Signaling pathways deregulated in HNSCC***

HPV-mediated carcinogenesis is driven by the E6 and E7 viral oncoproteins expressed by the DNA virus. The ubiquitin ligase E6 inhibits p53 tumor suppressor function by targeting it for proteosomal degradation (12), and E7 inhibits the retinoblastoma protein (pRB) releasing its inhibition of cyclin-dependent kinase inhibitors, including p21, p27, and p16 (13). Overexpression of p16, by immunohistochemistry, has become commonly used as a detection tool for identifying tissues with HPV infection (14). As HPV-associated HNSCC incidence continues to rise, the clinical, pathological, and etiological distinctions with significantly improved prognosis and therapeutic outcomes from HPV-negative HNSCC are gaining recognition

(15, 16). However, the biological mechanisms underlying these characteristics remain unclear.

HPV-negative HNSCCs typically contain TP53 mutations, the most common in HNSCC (17), in addition to mutations in other tumor suppressors which enhance genomic instability and resistance to typical cytotoxic regimens (18). In contrast, TP53 mutations are significantly decreased in HPV-positive HNSCCs concomitant with fewer overall mutation rates (19). Unlike HPV-positive HNSCCs, where p16 is overexpressed, in HPV-negative HNSCC tissues, exome sequencing studies have found mutation rates and copy number losses in the CDKN2A gene that encodes both p16INK4A and p14INK4B at 7% and 20-30% respectively (20, 21). As data continue to emerge, there is a growing appreciation for the distinction between HPV-positive and negative disease in HNSCC to support the stratification of patients by HPV status for prognostic and predictive assessments.

HNSCC proliferation is driven predominantly by activation of the epidermal growth factor receptor (EGFR), phosphatidylinositol-3-kinase-AKT (PI3K-AKT), and Janus kinase-signal transducer and activator of transcription (JAK-STAT) pathways (22). EGFR is a cell surface receptor that binds ligands such as epidermal growth factor, amphiregulin, and  $\beta$ -cellulin, which initiates receptor dimerization, tyrosine kinase activation and autophosphorylation, driving downstream signaling cascades. By driving cellular proliferation and survival, EGFR is an oncogene with reports of mutations and gene amplification in HNSCC (23, 24). As EGFR expression varies among HNSCC tissue sites, with higher levels in the oral cavity and pharynx compared to the larynx (25), the signaling pathways within different tumor sites likely vary.

Cetuximab is a chimeric monoclonal antibody that targets EGFR and was the first approved biologic agent for HNSCC. In patients with locally advanced or recurrent and metastatic disease, the addition of cetuximab to radiation or platinum chemotherapies improves overall survival (26, 27). However, resistance to cetuximab often develops, due to expression of a constitutively active EGFRvIII deletion mutant in the cancer cells (28, 29). Although antibody and vaccine therapies are being developed to target this mutant variant, results have not yet been extended to HNSCC (30, 31).

A number of cytokine receptors activate intracellular signaling cascades through JAKs, non-receptor tyrosine kinases constitutively bound to cytokine receptors that transphosphorylate receptors after ligand binding. Activated cytokine receptors phosphorylate STAT proteins, which translocate into the nucleus to initiate target gene transcription as dimerized transcription factors (32). In HNSCC carcinogenesis, the JAK-STAT pathway has been shown to promote tumor cell survival and growth as well as angiogenesis and suppression of anti-tumor immunity within the microenvironment (33). Increased STAT3 expression has been shown in cancer cell lines, human tumor tissues, and is an early molecular event in patients with tobacco-associated HNSCC (34, 35). STAT5 has also been shown to promote tumor growth as well as epithelial-mesenchymal transition in HNSCC and may contribute to chemoresistance (36, 37). In addition to efforts to shut down STAT3 signaling downstream of EGFR using kinase inhibitors, such as erlotinib (38, 39), a recent in-human trial describes effective downregulation of STAT3 target genes in HNSCC tissues using an anti-STAT3 oligonucleotide (40).

MicroRNAs (miRNAs) are small non-coding RNAs of 18-22 nucleotides in length that regulate a host of cellular processes through altering gene expression. After



transcription by RNA polymerase II as primary-miRNAs, they are processed within the nucleus into pre-miRNAs that are transported into the cytoplasm for further processing by the ribonuclease Dicer to form a mature miRNA. Upon association with the RNA-induced silencing complex (RISC), the miRNA can associate with its target mRNAs through interactions most often within the 3'-untranslated region (UTR) to effect gene silencing. Partial complementarity with its target mRNA sequence instead results in suppression of protein synthesis by translational repression (41).

Like coding genes, miRNAs have been identified that are oncogenic and overexpressed in cancer or tumor suppressive and down-regulated in cancers. In HNSCC, the tumor suppressive miRNAs let-7, miR-125a/b, miR-200a, and miR-133a/b have been reported to regulate important signaling targets such as oncogenic KRAS, EGFR, the EMT-associated transcription factors ZEB1 and ZEB2, and the metabolic regulator pyruvate kinase 2, respectively (42-47). Oncogenic miRNAs that are overexpressed in HNSCC include miR-106b-25, miR-17-92, miR-106a which downregulate the p21 cyclin dependent kinase inhibitor and RB1 (48) as well as miRNA-205 which may target the tumor suppressor phosphatase and tensin homolog (PTEN) (49). Although an open-source database of deregulated miRNAs in HNSCC has been established (50), the functional impact of these miRNAs and whether they are suitable targets for therapy have yet to be determined.

## **1.2 Mitogen-activated protein kinases and regulation**

### ***Overview of MAPK signaling***

Mitogen-activated protein kinases (MAPKs) comprise a number of signal transduction pathways that coordinate cellular responses to a variety of intra- and extra-cellular stimuli (51, 52). MAPKs phosphorylate serine and threonine residues to regulate cellular functions including proliferation, differentiation, survival, and death, through its actions on gene transcription, protein translation, stability, localization, and enzymatic activity (53, 54). Thus, MAPKs are key players in physiological processes, including development, immune and metabolic homeostasis, as well as pathological responses in human diseases including obesity, autoimmune disorders, and cancer (55-58).

MAPK pathways typically include an activation cascade of three members: the MAPK kinase kinase (MKKK), a MAPK kinase (MKK), and the MAPK, each of which serves as a substrate for the previous kinase for activation (59). Dual phosphorylation of both a threonine and a tyrosine residue within the activation loop domain are required. The major mammalian MAPK pathways include the extracellular signal-regulated kinases (ERKs) 1 and 2, the p38 MAPK family including p38 $\alpha$ , p38 $\beta$ , p38 $\gamma$ , and p38 $\delta$ , the c-jun N-terminal kinases (JNKs) 1, 2, and 3, and the ERK5 pathway (60). Other less well-characterized MAPKs include ERK3, ERK4, ERK7, and ERK8 (61).

### ***Overview of dual-specificity phosphatases***

The functional outcome of MAPK signaling is controlled, largely in part, by the duration of pathway activation (62). Thus, MAPK pathway activation is carefully balanced by both the activation of upstream pathway kinases as well as a number of

negative regulatory mechanisms. Direct inactivation of MAPK signaling can occur through dephosphorylation by specific protein phosphatases at either the threonine or tyrosine residue, as phosphorylation of both is required for activation. Dephosphorylation can be performed by type 1 and type 2 serine/threonine phosphatases, protein tyrosine phosphatases, or dual-specificity tyrosine and threonine phosphatases (DUSPs) (63). Although all of these family members may play a role, the largest of these groups are the dual-specificity phosphatases and MAPK phosphatases (MKPs).

### ***MAPK phosphatase structure and function***

Within the dual-specificity phosphatases, the MAPK phosphatases are a specific sub-family of phosphatases dedicated to MAPK regulation, all of which share a N-terminal noncatalytic domain and a C-terminal catalytic domain, containing the protein phosphatase consensus active site (64). The N-terminal domain serves a number of functions, including a docking site for MAPK substrates, and localization sequences (65). A kinase interacting domain (KIM) was identified within the N-terminus and shown to be responsible for MAPK binding through a cognate MAPK motif (66, 67). MKP-mediated dephosphorylation occurs through two separate binding, dephosphorylation, and release cycles, first of the tyrosine and then the threonine residue (68, 69). Substrate specificity overlap may have risen from gene duplication with divergence across evolution; however, tissue and cellular localization, in addition to phosphatase-independent mechanisms of regulation must also be considered (70).

The ten catalytically active MAPK phosphatases in mammalian cells can be subdivided into three families based on cellular localization, substrate specificity, and

sequence homology. The stress-inducible, nuclear MKPs include DUSP1/MKP-1, DUSP2, DUSP4/MKP-2, and DUSP5. ERK-selective, cytoplasmic MKPs include DUSP6/MKP-3, DUSP7/MKP-X, and DUSP9/MKP-4. Lastly, the JNK and p38-selective MKPs, which are found both in the nucleus and cytoplasm, include DUSP8, DUSP10/MKP-5, and DUSP16/MKP-7 (71, 72).

### **1.3 Dual-specificity phosphatase-1**

The archetype of the MAPK phosphatases is DUSP1/MKP-1, an inducible nuclear phosphatase that has been shown to bind and dephosphorylate p38, JNK, and ERK MAPKs both *in vitro* and *in vivo* (66, 73). However, the KIM of DUSP1 has been shown to be necessary only for interaction with p38 and ERK MAPKs. The KIM mutant in which the arginine residues have been substituted with alanine can still bind and dephosphorylate JNK both *in vitro* and *in vivo* with the same efficiency (66). Interaction of MKPs with their MAPK substrates has been shown, for DUSP6/MKP-3 as well as DUSP1, and DUSP2, to induce conformational changes that enhance enzymatic activity (66, 74-77). In the absence of a three-dimensional structural conformation, understanding DUSP1 function and activity has come from mutagenesis studies and characterization in different cells and tissues.

#### ***Regulation of DUSP1 expression***

*DUSP1* was initially identified as one of a set of genes expressed during the G0/G1 transition in cultured murine cells (78) and is widely expressed in a number of tissues (72). The human *DUSP1* gene is located in chromosome 5 and contains four

exons and three introns, encoding a transcript of approximately 2.4kb shown in Figure 1-1 (79). Transcription is induced following a variety of stimuli, including growth factors, cytokines, lipopolysaccharide (LPS), and other cellular stressors, such as hypoxia, and heat shock (65, 80, 81). Transcriptional regulation occurs through regions within the *DUSP1* promoter and upstream regulatory regions containing cAMP responsive elements, glucocorticoid responsive elements, the vitamin D responsive element, as well as binding sites for activator protein 1 (AP-1), nuclear factor (NF)- $\kappa$ B, specificity protein 1 (SP-1), and controlled amino acid treatment (CAAT)-binding transcription factor/nuclear factor 1 (CTF/NF-1) (79, 82-86). Epigenetic regulation includes histone H3 phosphorylation and acetylation that also modulate stress-induced *DUSP1* gene transcription (87). More recently, promoter methylation has been described as a mechanism of *DUSP1* downregulation in both the prostate cancer cell line PC-3 and HNSCC tissues (88, 89).

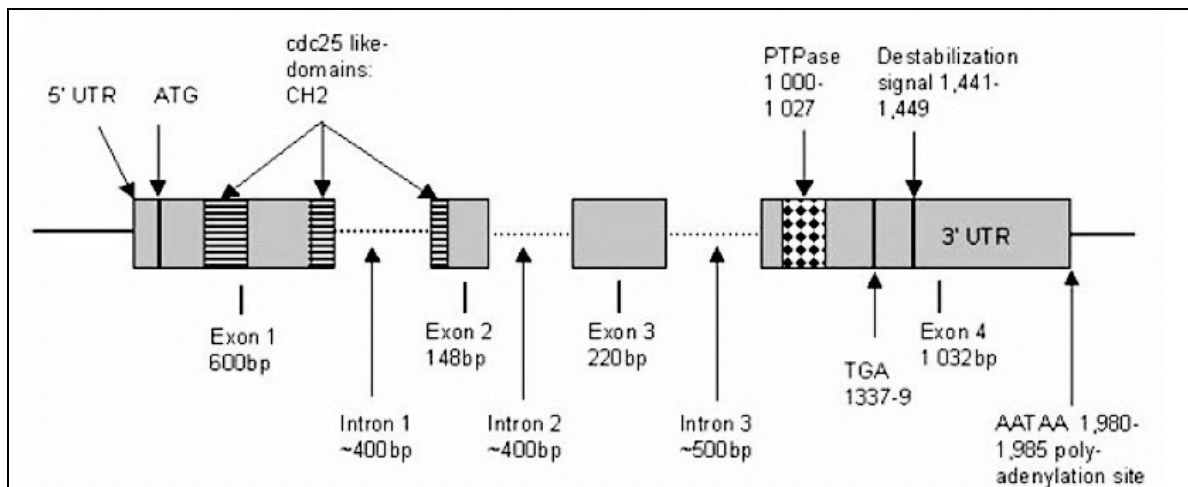


Figure 1-1. Schematic of *DUSP1* gene. The *DUSP1* gene is located on chromosome 5 and includes 4 exons and 3 introns. The mature transcript is 2.4kb long. The N-terminus contains 2 cdc25-like domains and a noncanonical nuclear localization motif. The C-terminus contains the phosphatase domain. Adapted from Boutros et al. 2008 (70).

As an immediate-early response gene, a number of factors induce transcription of *DUSP1*, including serum in fibroblasts (90), dexamethasone (91, 92) and glucagon in hepatocytes (93), insulin in a hepatoma cell line (94), and atrial natriuretic peptide in human umbilical vein endothelial cells (95). Stressors such as heat shock in dermal fibroblasts (96) and murine macrophages (97), osmotic shock in rat hepatoma (94, 98), hypoxia (99, 100), cobalt chloride, a hypoxic mimic (101), and tissue ischemia (102, 103) also increase transcription. Similar effects are also seen following exposure to DNA damaging agents such as reactive oxygen species from hydrogen peroxide treatment (96), ultraviolet radiation (104, 105), and gamma-radiation (106). Although a multitude of conditions regulate *DUSP1* mRNA, it is unclear whether reported increases are a result of *de novo* synthesis or increased mRNA stability.

The *DUSP1* mRNA has a half-life of 1 to 2h, depending upon the induction method (78). Post-transcriptional regulation of *DUSP1* includes negative regulation by miR-101, following LPS stimulation, to enhance the strength and duration of the inflammatory response (107) and control by the RNA binding proteins Hu antigen R (HuR) and nuclear factor 90 (NF90), which enhance *DUSP1* transcript stability through interactions with the 3'UTR (108). In addition to phosphorylation, DUSP1 can be modified following oxidative stress through S-glutathionylation, targeting it for proteasomal degradation (109).

Protein expression of DUSP1 can be increased with exposure to many of the same stimuli as those which induce expression, including insulin (110, 111), glucagon (93), dexamethasone (91, 92), EGF (112), hypoxia (99, 113-115), and peroxide (116). However, it is still unclear whether these increases in protein are due to elevated levels of

*de novo* translation or enhanced protein stabilization. As with transcriptional stimulation, these inducing factors are not specific to DUSP1 and increase a large number of targets to generate their cellular responses. DUSP1 protein half-life has been reported to be between 40min (117) and 2h (85). Modulation of protein half-life is differentially regulated by a number of mechanisms. Heat shock has been shown to reversibly aggregate DUSP1 protein through HSP72, to preserve its function (118). A p38 inhibitor, SB203580, partially blocked cisplatin-induced, ERK-mediated accumulation of DUSP1 protein, independent of transcriptional effects (119).

### ***Regulation of DUSP1 activity***

The large number of family members and overlapping substrate specificity suggest redundancy in the negative regulation of MAPKs by MKPs. However, the combination of differing subcellular localization, MAPK specificity, and temporal control of activity suggest these phosphatases can modulate MAPK signaling with greater finesse than simply turning them on or off. A noncanonical nuclear localization signal was identified, through a series of deletion and mutation experiments, in the N-terminus of DUSP1 (120), and is conserved among the nuclear MKPs. This LXXLL motif targets DUSP1 to the nucleus (120), where it exerts its phosphatase action (72, 120). Spatially, MKP binding can serve as an anchor to MAPKs, restricting them to a particular cellular compartment for nonenzymatic purposes (121, 122). Reports of cytoplasmic localization have been made in different human tumor tissue samples (123). In addition, treatment of a human lymphoblastic cell line with nerve growth factor increased *DUSP1* mRNA and protein levels with translocation of the protein to the mitochondria (124). The

significance of these reports and understanding what impact DUSP1 has outside the nucleus has yet to be addressed. The C-terminus of DUSP1 contains a region which autoinhibits phosphatase activity, as a truncated mutant had higher phosphatase activity without change in substrate specificity (125). Determining whether this domain plays a part in interaction with other proteins may reveal additional levels of regulation.

DUSP1 has greater affinity for p38MAPK and JNK than ERK1/2 (126) but also minor activity for ERK5 (127). A model of DUSP1 regulation of ERK activity independent of dephosphorylation suggests its binding prevents ERK1/2 interaction with its downstream targets (112) or translocation into the nucleus. DUSP1 is unable to recognize or inactivate p38 $\gamma$  or p38 $\delta$  (66), despite significant sequence homology to p38 $\alpha$ . Although initial RNAi experiments suggested DUSP1 could interact with and inactivate STAT1 protein to regulate interferon-responses (128), subsequent *in vitro* analyses failed to demonstrate protein-protein interactions or phosphatase activity or downregulation of interferon-induced transcription (66). RNAi knockdown of *DUSP1* highlighted phosphorylated-histone H3 at serine 10 as a potential dephosphorylation target, in response to thrombin and vascular endothelial growth factor (129). Although kinetics demonstrated histone H3 dephosphorylation coincided with DUSP1 expression, similar results from *Dusp1* deficient mouse embryonic fibroblasts do not support a DUSP1-dependent mechanism of action (130).

Typically, MKPs are expressed at low levels basally and up-regulated following exposure to stimuli as an immediate early or delayed early response gene (131, 132). Subsequent modulation by MAPKs, such as ERK, forms an autoregulatory feedback loop for MAPK signaling (133). ERK phosphorylation of DUSP1 at serine 359 and 364 has



been shown to increase protein stability, as a mechanism of negative feedback control (134, 135). Alternatively, ERK phosphorylation at residues serine 296 and 323 recruit ubiquitin ligases to enhance DUSP1 degradation (136-138). DUSP1 has also been shown to be acetylated by p300 acetyltransferase on lysine 57, following Toll-like receptor 4 (TLR4) stimulation (138). Due to its close proximity to the KIM, substrate specificity for p38 is enhanced, increasing its negative feedback effect (139).

In summary, MAPK regulation by MKPs depends on a number of factors including spatial localization and cellular shuttling of MAPKs, substrate MAPK concentration, temporal delays in transcriptional feedback, and other post-translational modifications. The unique properties of MKPs place them as central coordinators of MAPK signaling and crosstalk with other pathways. Understanding these regulatory mechanisms will enable more sophisticated targeting of deregulated pathways in disease.

### ***Phenotype of *Dusp1* deficient mice***

When first developed, *Dusp1* deficient mice were reported to have no overt phenotype, with no differences in cellular proliferation between primary embryonic fibroblasts from wild-type or *Dusp1* deficient animals (140). Between wild-type and knockout littermates, no differences were readily detected during development or in adulthood within the neurological, cardiac, endocrinological, and hematological organ systems (141). Subsequent studies have identified an important role for *Dusp1* in regulation of key cellular processes in these organ systems in pathologic states, detailed below.

Numerous groups have identified a crucial role for DUSP1 as a negative regulator of innate immunity, in models of infection, sepsis, periodontal disease, and arthritis (142-147). Challenges with endotoxin have demonstrated *Dusp1* deficient mice are significantly more susceptible to immune activation, with increased leukocyte infiltration, severe hypotension, and increased mortality (141-144, 148, 149). In a periodontal model, *Dusp1* deficient mice developed more severe bone loss with increased inflammatory infiltrate and osteoclast formation (150), reversed with adenoviral transfer of *Dusp1* into the tissues (151). In these models, macrophages from knockout mice express elevated levels of cytokines, chemokines, and inflammatory enzymes. In a model of collagen-induced arthritis, *Dusp1* deficient mice displayed increased disease incidence, earlier disease onset, and accelerated disease progression, associated with increased serum TNF- $\alpha$  and IL-6 levels as well as increased inflammatory cell infiltrate and osteoclast formation (141, 152).

In models of *Escherichia coli* sepsis, *Dusp1* deficient mice had more severe inflammatory responses with increased mortality but also had impaired bacterial clearance (153). Other models of infection include polymicrobial peritonitis (154) and pulmonary infection with *Chlamydomphila pneumoniae* (155), which yielded similar results. Impaired clearance may be due to excess production of the anti-inflammatory cytokine interleukin-10, inhibition of which relieved splenic bacterial load by neutralizing antibody or on *Dusp1/Il10* double knockout mice in the case of *Escherichia coli* sepsis (153). *Dusp1* deficient mice challenged with two strains of the gram-positive bacterium *Staphylococcus aureus* showed no difference in mortality or bacterial burden

(156). However, heat-killed bacteria yielded enhanced inflammatory response and mortality.

Additional studies have shown that *Dusp1* deficient mice are resistant to diet-induced obesity, with increased MAPK activity in both skeletal muscle and white adipose tissue (157). Recently, JNK activity in macrophages was shown to be necessary for insulin resistance induced by high-fat diet, with macrophage-specific JNK deletion protecting mice from obesity-induced insulin-resistance, macrophage infiltrate, and pro-inflammatory polarization (158).

Few studies have examined the effects of increased *Dusp1* expression in animals. Constitutive cardiac transgenic mice expressing 4-fold higher levels of *Dusp1* die within the first two weeks of life in the absence of developmental hypertrophy, whereas mice with 2-fold higher levels survive with only moderate cardiac morphology, as determined by histology and echocardiography (159).

Given the phenotype of *Dusp1* deficient mice with normal development and fertility, it suggests phosphatases are capable of compensating for *Dusp1* during development. The question remains what compensatory mechanisms are in play and why they fail to do so during stress.

### ***Regulation of inflammation by DUSP1***

The initiation of an inflammatory response can occur when components of the bacterial cell wall, such as LPS, engage with host immune cells via Toll-like receptors. Resulting activation drives the transcription of pro-inflammatory cytokines through activation of NF- $\kappa$ B and the MAPK signaling pathways, detailed above. In addition to

transcriptional initiation, p38 $\alpha$ MAPK increases mRNA stability of targets (160), via MAPKAPK2 (MK2) which phosphorylates RNA binding proteins such as tristetraprolin (TTP) (160), heterogeneous nuclear ribonucleoprotein A0 (161), and poly(A)-binding protein (162). These RNA binding proteins interact with AU-rich elements within the 3'UTR of targets such as *DUSP1* (163), *VEGF* (164), and *MMP* (165, 166), targeting them for decay in the absence of an activating stimulus. Activation of toll-like receptors also drives *DUSP1* expression through the adaptor molecules myeloid differentiation factor 88 (MyD88) and toll-interleukin 1 receptor (TIR) domain-containing adaptor inducing IFN- $\beta$  (TRIF) in macrophages (144). As an early response gene, *DUSP1* is crucial to quell the production of inflammatory cytokines in a timely manner, summarized in Figure 1-2.

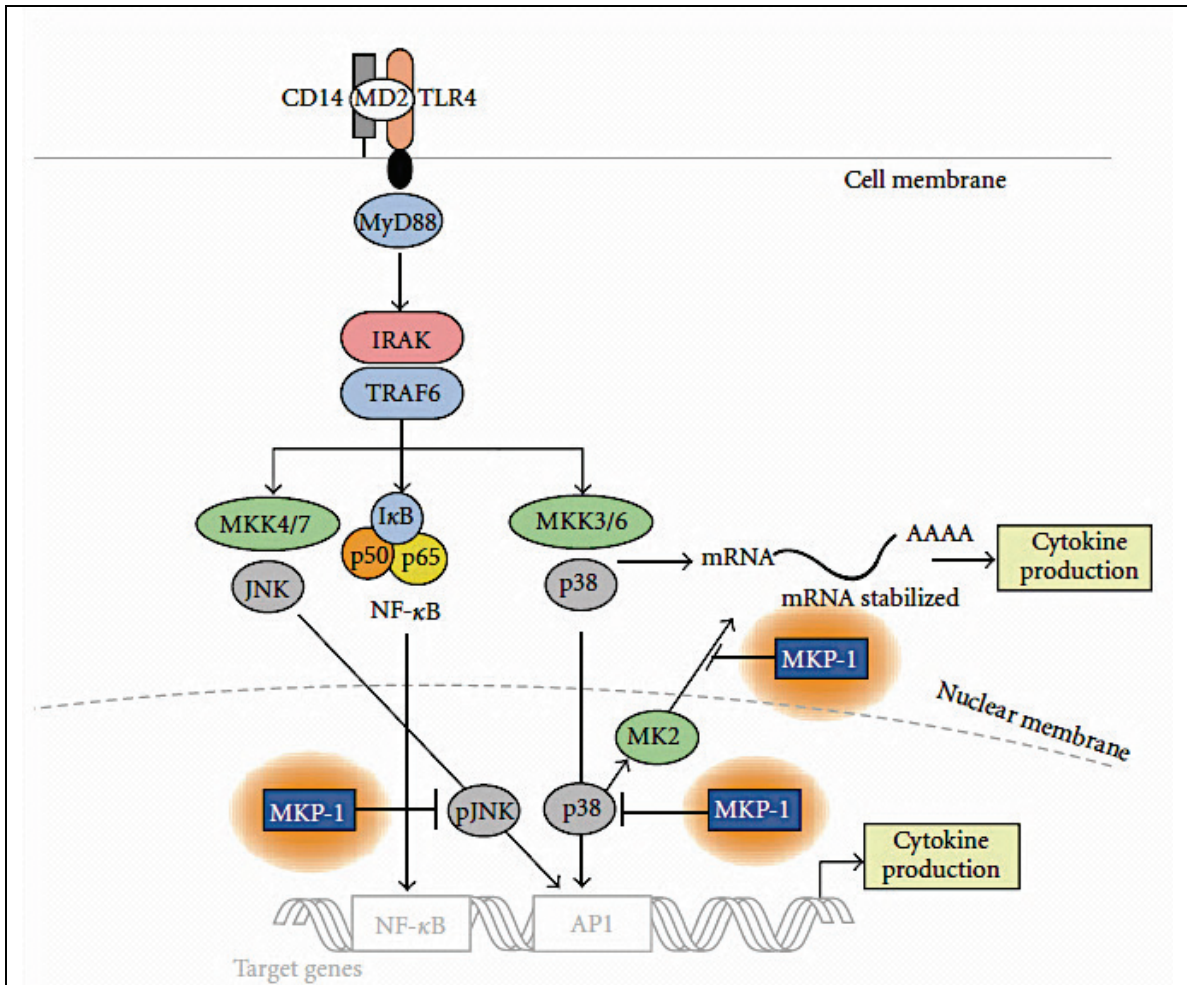


Figure 1-2. DUSP1/MKP-1 negatively regulates inflammatory cytokine production. In response to TLR4 activation, signaling cascades induce the phosphorylation of p38 and JNK MAPK to stimulate production of inflammatory cytokines and other mediators. The induction of DUSP1/MKP-1 dephosphorylates MAPKs to inhibit this process by two mechanisms: decreasing transcriptional activation and inhibiting MK2-dependent increases in mRNA stability. Adapted from Li et al. 2012 (167).

Glucocorticoids exert an anti-inflammatory effect in macrophages, in part, through DUSP1 inactivation of p38 MAPK (168, 169). The upstream region of the *DUSP1* gene contains functional glucocorticoid response elements at -1.3kb and -4.6kb, which function alongside p300 to initiate transcription after glucocorticoid stimulus (82, 170). In vitro treatment with dexamethasone induces *DUSP1* expression, initially

identified by microarray analysis (91). Dexamethasone failed to inhibit p38 and JNK dephosphorylation in *Dusp1* deficient macrophages and had little effect in a dorsal air pouch model of inflammation (171). In asthma patients, single nucleotide polymorphisms in the *DUSP1* gene have been associated with response to inhaled glucocorticoid therapy (172). However, dexamethasone also exerts anti-inflammatory effects through alternative pathways, as some dose-dependent anti-inflammatory responses are still seen in *Dusp1* deficient animals (173).

Despite their enhanced susceptibility to innate immune challenges, *Dusp1* deficient mice display normal thymocyte development and have no difference in total number or ratio of CD4<sup>+</sup> and CD8<sup>+</sup> T cells, compared to wild-type mice (147). However, T cells from *Dusp1* deficient mice display impaired IL-2 release and proliferation, with decreased Th1 and Th17 responses following T cell receptor stimulation or exposure to antigen, in an influenza vaccination model (147). In a Th17-driven disease model, experimental autoimmune encephalomyelitis, *Dusp1* deficient mice were relatively protected with decreased levels of IFN- $\gamma$  and IL-17 in infiltrating CD4<sup>+</sup> T cells (147). In an elegant chimera model, Huang et al. demonstrated *Dusp1* deficiency in dendritic cells impaired IL-12 production and subsequent Th1 response, while enhancing IL-6 production and promoting a Th17 response (146). Furthermore, the production of induced regulatory T cells was negatively regulated by *Dusp1* through inhibition of TGF- $\beta$ 2 production in deficient dendritic cells (146).

These studies demonstrate *Dusp1* deficiency, through both enhanced and prolonged activation of its MAPK substrates, impacts the duration of inflammation in response to innate stimuli. In addition to prolonged inflammation, *Dusp1* can also

regulate adaptive immunity through the alteration of secreted cytokines, which mediate interaction with innate cells and guide the developing immune response.

### ***Expression of DUSP1 in cancer***

As a negative regulator of MAPK signaling, DUSP1 may have a tumor suppressive role (123). *DUSP1* gene expression has been examined in a number of malignant tissues and cell lines. In bladder, breast, prostate, and colon cancers, expression of *DUSP1* gene was shown to decrease in late stage, more aggressive disease, with loss of *DUSP1* in nearly 80% of metastatic tissues examined (174). It is unclear whether *DUSP1* expression is serving a direct role as a metastasis suppressor or the loss of *DUSP1* is a bystander effect. *In vitro* studies suggest that *DUSP1* expression may serve key roles in curtailing filopodia formation and cell motility, in studies of ovarian cancer cell lines in which *DUSP1* was re-expressed, although the mechanism for this phenotype is unclear (175). However, studies of *DUSP1* expression in tumor tissues are mostly limited to characterization of mRNA levels by *in situ* hybridization and protein levels by immunohistochemistry. The functional role of *DUSP1* in cancer remains undefined.

In prostate cancer, *DUSP1* mRNA expression decreases with increasing tumor grade (174, 176). Similarly, in lymph node metastases of prostate cancer, *DUSP1* mRNA was absent (176). Both *DUSP1* mRNA and protein have been detected in the basal cells of prostatic acini (174, 176). In assessing matched patient tissues, an inverse relationship was observed between *DUSP1* expression and JNK1 activity but not ERK1 (176). Across all tumor grades, *DUSP1* expression, both mRNA and protein, decreased following

hormone ablation. A later study showed similar findings of lower *DUSP1* expression in hormone-refractory prostate compared to untreated carcinomas and benign hyperplasia controls (177).

In human lobular and ductal breast carcinomas, lesions had higher levels of *DUSP1* mRNA than the constitutive expression seen in surrounding tissue with loss of expression in late stage and metastatic disease (174). However, tissues with positive *DUSP1* expression strongly correlated *DUSP1* with HER2 and EGFR expression as well as ERK1/2 (174), which may be due in part to positive feedback regulation of *DUSP1* expression through stimulation of the Raf-MEK-ERK pathway.

In normal bladder urothelium, *DUSP1* mRNA is expressed at only very low levels. However, in increasing histological tumor grade, *DUSP1* expression is inversely related, with more expression in in situ lesions than high-grade carcinomas (174). Another group found low *DUSP1* expression, in conjunction with high JNK1 expression, correlated with higher tumor grade, invasion, and vascularity in human urothelial carcinomas (178). *In vitro* chorioallantoic membrane assays with cell lines corroborated a relationship between low *DUSP1* expression supporting JNK-mediated angiogenesis (178).

Human colon adenocarcinomas show a similar pattern of *DUSP1* expression inversely correlating with tumor histologic grade (174). In the human EB-1 colon cancer cell line, p53-dependent expression of *DUSP1* could induce apoptosis in response to stress (179). In turn, *DUSP1* protein inactivation of JNK could allow for the targeting of p53 by nonphosphorylated JNK for ubiquitination and degradation (180). In human gastric adenocarcinomas, *DUSP1* expression is increased compared to control tissues



from healthy donors, alongside increased ERK1/2 activity (181). However, p38 and JNK1/2 activity were not assessed in this study.

Compared to normal controls or benign lesions, DUSP1 protein expression is reduced in low-grade ovarian carcinomas. However, in high-grade lesions, DUSP1 protein expression greatly varies, with a significant correlation with shorter progression-free survival, but not overall survival (182). In both cancer cell lines and primary ovarian cancer tissues, *DUSP1* gene expression was decreased compared to immortalized cell lines or normal ovarian control tissues, decreasing with increasing disease stage (175). In a xenograft model, nude mice bearing cell lines conditionally expressing *DUSP1* had decreased tumor burden compared to control cell lines (175).

In the work by Loda et al., minimal *DUSP1* expression was detected in hepatocellular carcinomas by *in situ* hybridization (174). Another group found in *DUSP1* negative tumors, an inverse relationship with increased size and serum levels of the tumor burden marker  $\alpha$ -fetoprotein compared to *DUSP1* positive tumors (183). They also suggest *DUSP1* may serve as a predictive biomarker for survival post-hepatectomy (183). In NSCLC cell lines, *DUSP1* expression was increased compared to small cell lung cancer cell lines (184). However, there was no relationship between *DUSP1* expression with other variables such as clinical or pathological stage or MAPK phosphorylation status. Overall, increased DUSP1 protein expression correlated with improved survival, based on percentage of tumor nuclei staining positive for DUSP1 by immunohistochemistry (184).

Gain of *DUSP1* expression has been associated with cancer progression, chemoresistance, and poor prognosis (123). This rise in *DUSP1* expression may be

secondary to increased MAPK activity, as one subset of MAPK-responsive transcripts that are elevated in tumorigenesis. When elevated, DUSP1 protein expression can inhibit the apoptotic pathways initiated by chemotherapies, through targeting JNK and p38 MAPKs (119, 185-187). In a number of tissue contexts, it appears DUSP1 activation is necessary for cell survival by inhibiting pro-apoptotic p38 and JNK signaling. Despite a substrate preference for JNK (66), induction of *DUSP1* gene expression can also occur through ERK or p38-dependent pathways (87, 105, 188, 189). In response to ultraviolet radiation, p38 activity induces *DUSP1* expression to inhibit JNK-mediated apoptosis (105, 190). In cortical development, *DUSP1* induction also represses JNK signaling, but in an ERK-dependent manner, to guide axonal branching (190). In untreated mesangial cells, ectopic expression of *DUSP1* induced apoptosis. However, in the context of hydrogen peroxide treatment, *DUSP1* had an anti-apoptotic effect, suggesting *DUSP1* may inhibit basal MAPK activity in the absence of a stress-activated MAPK target (191).

As a member of several cellular stress-response pathways, *DUSP1* expression has been suggested to enhance chemoresistance in some cancers (92, 192). Cisplatin is a mainstay in chemotherapeutic treatment of HNSCC, as a DNA cross-linking agent that blocks transcription and DNA synthesis (193, 194). Cisplatin treatment was shown to up-regulate *DUSP1* expression in human lung and ovarian cancer cell lines (119). Mouse embryonic fibroblasts from *Dusp1* deficient mice were more sensitive to cisplatin-induced apoptosis, reversed by treatment with the JNK inhibitor SP600125 (119). DNA fragmentation was reduced in cells transduced with *DUSP1* adenovirus after treatment with chemotherapies including paclitaxel, doxorubicin, and mechlorethamine and combination regimens as well as in MEFS from wild-type mice compared to *Dusp1*

deficient mice, via JNK inhibition (186). In the breast cancer cell line MDA-MB-231 paclitaxel-induced caspase-3/7 activation was reduced in the presence of *DUSP1* expression (195). In addition to mediating apoptosis, caspases 3 and 7 can activate p38, ERK1/2 and JNK MAPKs through cleavage products of Mst1 (196). Other non-apoptotic roles for caspase-3/7 include cellular maturation, differentiation, and cytokine activation (197).

Treatment of the prostate cancer cell line PC-3 with histone deacetylase inhibitor trichostatin A (198) and DNA methyltransferase inhibitor decitabine up-regulated *DUSP1* gene expression (177), suggesting epigenetic regulation is responsible for downregulation in these cells and can be reversed with pharmacotherapy. Although hormone-refractory prostate carcinomas showed decreased expression of *DUSP1* mRNA and protein, no differences were detected in untreated prostate carcinomas compared to benign prostate hyperplasia control tissues (177).

Dexamethasone is a glucocorticoid with pleiotropic effects, currently used as an antiemetic or to reduce adverse effects or toxicity as a part of a chemotherapeutic regimen. Studies have shown dexamethasone treatment prior to chemotherapy with paclitaxel or doxorubicin protects breast cancer cells from apoptosis (91), with similar effects seen in cell cultures with ectopic *DUSP1* expression. This effect was abrogated in the presence of siRNA targeting *DUSP1*. Surprisingly, targeting *DUSP1* by RNAi increased JNK and ERK1/2 phosphorylation with no effect on p38 activity (92). Although these studies suggest *DUSP1* plays a part in dexamethasone-induced chemoresistance in breast cancer cell lines, the mechanism is still unclear.

As many as half of cancer patients receive concurrent radiotherapy with chemotherapy (199). In HNSCC, radiation therapy can be given at curative doses for early stage disease as well as an adjuvant therapy for more aggressive disease. Gamma-radiation can also induce *DUSP1* expression, *in vitro* and in irradiated nude mice, resulting in ERK1/2 dephosphorylation (106, 200). Ultraviolet radiation-induced apoptosis can be inhibited by ectopic *DUSP1* expression in the U937 human monocytic cell line (104), through the inhibition of JNK1 activity. However, low dose short wavelength UVC radiation can decrease *DUSP1* gene expression in human fibroblasts deficient in transcription-coupled repair (201).

Originally identified in a set of genes expressed in the G0/G1 cell cycle transition (78), *DUSP1* has been better characterized as a negative regulator of the G0/G1 transition, with constitutive expression blocking G1 cycle gene expression, including cyclin D1 (175, 202, 203). Thus, it is not surprising that in several *in vitro* systems, *DUSP1* overexpression leads to cell cycle inhibition. Transfection of a phosphatase-dead *DUSP1* dominant-negative mutant enhanced platinum-induced cell death independent of c-Jun-activation (185). This protective effect may be, in part, due to sequestration of JNK from other inactivating phosphatases to promote AP-1-mediated cell cycle progression (204).

Conditional expression of *DUSP1* in U28 and M18 ovarian carcinoma cell lines decreased intraperitoneal tumor growth in nude mice, compared to tumors expressing vector controls (175). Surprisingly, this effect was not seen in subcutaneous xenografts. Similarly, *DUSP1* inhibition by RNAi in xenografts of pancreatic cell lines PANC-1 and T3M4 also resulted in delayed tumorigenicity in nude mice (205). *DUSP1* knockdown also impaired anchorage-independent growth of these cell lines in soft agar assays (205).

Similar results were seen in transfected cell lines A2780 and UCI101 (175). *DUSP1* has also been implicated in expression of the melanocyte-specific transcription factor Microphthalmia. When overexpressed, *DUSP1* rescues Microphthalmia from ERK-mediated degradation to enhance melanocyte differentiation (206), suggesting induction of *DUSP1* expression may enhance tumor control, in part, through promoting differentiation. The functional impact of loss or gain of *DUSP1* expression on differentiation and cell cycle progression likely varies across tumor tissues.

As previously discussed, *DUSP1* mRNA and protein are increased in the presence of hypoxia or ischemia in a number of systems. Response to VEGF and thrombin treatment is reduced in *Dusp1* deficient aorta sections, suggesting a supportive role of *Dusp1* in endothelial sprouting (207). However, in tumor cells, low levels of *DUSP1* expression may promote angiogenesis through p38- and JNK-mediated chemotaxis and VEGF response (208, 209). When induced, *DUSP1* can inhibit HIF-1 activity through inactivation of ERK (114) by reducing phosphorylation of the cofactor p300 (115), an acetyltransferase (210). Studies of stress-induced transcriptional activation of *DUSP1* suggest a role of chromatin remodeling through histone H3 phosphorylation and acetylation (87), but a clear mechanism has yet to be defined.

In summary, these studies suggest *DUSP1* expression is deregulated in human malignancies. In several but not all tumor tissues, *DUSP1* expression is lost with disease progression and is associated with advanced stage and decreased survival. A number of cellular processes, including differentiation, cell cycle progression, and anti-apoptotic signal can be altered by modulating *DUSP1* levels. However, the functional impact of these changes is unclear and warrants further investigation.

#### **1.4 Cancer-associated inflammation**

The ability of inflammatory conditions to promote tumor progression has been observed in a number of malignancies. These associations include hepatitis infection in hepatocellular carcinoma, asbestos and silica exposure with lung carcinoma, *Helicobacter pylori* infection with gastric carcinoma, and Schistosomiasis with bladder carcinoma (211-215). In these situations, inflammation occurs initially as a protective measure against pathogen exposure or a foreign irritant. As immune cells are recruited, an inflammatory response develops with release of cytokines, chemokines, and reactive oxidants. Many of these mediators, highly expressed in cases of dysregulated inflammation, have been shown to promote tumor growth and invasion, enhance mutagenesis, and increase angiogenesis and lymphangiogenesis (216). As such, these inflammatory mediators not only support tumorigenesis but may also promote tumor progression.

#### ***Inflammatory signaling pathways activated in cancer***

The Toll-like receptor family contains highly conserved transmembrane proteins, which recognize both microbial products and endogenous molecules released during cell death (217). As a first line of defense, these receptors on immune cells activate signaling pathways crucial for activation of innate immunity and following induction of adaptive immunity (218, 219). TLRs are also expressed on cancer cells, where they may promote cell growth, enhance survival and resistance to cytotoxic stressors (217, 220). Previous

reports have identified an association between TLR4 expression and HNSCC progression, through induction of IL-6, IL-8, VEGF, and GM-CSF (221, 222). Treatment of HNSCC cell lines with lipopolysaccharide (LPS) enhanced cell proliferation, migration, invasion, and cytokine production (223). Aside from LPS, other endogenous ligands for TLR4 include S100A and HMGB1 (217, 224).

Downstream of the TLR pathway, through adaptor molecule MyD88, NF- $\kappa$ B can be activated in both immune and tumor cells to drive expression of inflammatory cytokines, prostaglandin synthase enzymes, pro-angiogenic factors, and adhesion molecules, as well as pro-survival anti-apoptotic genes. NF- $\kappa$ B is a key regulator of innate immunity and inflammation, with dysregulation of NF- $\kappa$ B pathways often observed in many cancers (225). The family is composed of NF- $\kappa$ B1 (p105/p50), NF- $\kappa$ B2 (p100/p52), RelA (p65), and RelB, inactivated in a complex with inhibitor- $\kappa$ B (I $\kappa$ B) proteins within the cytoplasm. Upon stimulation, kinase cascades phosphorylate I $\kappa$ B, leading to its ubiquitination and proteasomal degradation. The released dimers translocate to the nucleus to enact target gene transactivation (226).

A number of studies have demonstrated that NF- $\kappa$ B activity promotes tumor initiation and progression within the lower gastrointestinal tract and liver (225, 227, 228). For example, specific inhibition of NF- $\kappa$ B activity within leukocytes, through myeloid-specific I $\kappa$ K $\beta$  deletion, protected animals from colitis-associated cancer (227). MAPK cross-talk can occur through MEKK1 activation of I $\kappa$ B $\alpha$  kinase, leading to the phosphorylation and degradation of I $\kappa$ B $\alpha$ . The kinase can also be phosphorylated by JNK, also targeting it for polyubiquitination and degradation, leading to the activation of the NF- $\kappa$ B signaling pathway (229). Blocking NF- $\kappa$ B function in HNSCC results in

decreased IL-6 mRNA expression and secretion as well as reduced tumor growth (230, 231). Inhibition of p65, activating kinase IKK1 or IKK2, and expression of dominant negative mutants of I $\kappa$ B $\alpha$  have also demonstrated the pro-survival pro-tumorigenic function of this pathway (230, 232).

Prostaglandin E<sub>2</sub> (PGE<sub>2</sub>) has been shown to be increased in HNSCC tissues. This secreted factor promotes tumor growth, inhibits apoptosis, and enhances tumor cell invasion, metastasis, and supports angiogenesis (233). Synthesis of PGE<sub>2</sub> is regulated by the rate-limiting cyclooxygenase (COX) enzymes. Of the two isoforms, COX-2 is up-regulated in inflammation as well as premalignant and malignant tissues, as a target gene of both NF- $\kappa$ B and MAPK pathways. COX-2 has been shown to be overexpressed in both oral premalignant lesions as well as HNSCC, with its expression correlated with increased invasiveness and angiogenesis (234). *In vitro* treatment of cell lines of oral squamous cell carcinoma, the most common subtype of HNSCC, reduced cellular proliferation and expression of matrix metalloproteases (235). However, clinical trials to inhibit cyclooxygenase activity to reduce oral leukoplakia have not been effective (236, 237). A trial with the COX-2 inhibitor celecoxib also failed to demonstrate reduction in oral premalignant lesions, with decreased interest as concerns for cardiotoxicity arise (236). Early studies of 25-hydroxyvitamin D<sub>3</sub> suggested treatment of HNSCC patients could impair the recruitment and development of immunosuppressive CD34<sup>+</sup> cells within the tumor, yet no effect on plasma IL-1 $\beta$ , IL-6, or TGF- $\beta$  was observed (238).

Growing evidence supports the pro-tumorigenic role of inflammation in many malignancies, including HNSCC. TLR signaling pathways drive production inflammatory mediators, which contribute to disease development and progression, in



part through MAPK activation. Thus, there is a need to understand the potential roles of MAPK signaling and phosphatase regulation in controlling chronic inflammation-mediated tumorigenesis as well as anti-tumor immunity.

### ***The HNSCC tumor microenvironment***

Malignancies develop in a multi-factorial process, resulting from the interaction of genomic alterations and altered gene expression within the context of a tumor-supportive microenvironment. The tumor microenvironment is composed of resident stromal cell populations, such as fibroblasts and endothelial cells, but also infiltrating immune cells, such as macrophages, lymphocytes, natural killer (NK) cells, dendritic cells (DCs), eosinophils, and neutrophils (239-241). The relationships between inflammatory cells and cancer are complex, with great variability among tumor types, tissue sites, and other factors within the microenvironment. Understanding these relationships and how they support anti-tumor immunity, enhance disease progression, or generate a heterogeneous commixture of the two remains an avenue for exploration.

In HNSCC patients with lymph node metastases, there were significantly decreased numbers of tumor-infiltrating CD8<sup>+</sup> T cells (242). One mechanism of evading the adaptive immune system is the secretion of gangliosides by tumor cells which serve to down-regulate expression of major histocompatibility complex I by T cells (243). The secretion of Fas ligand to induce apoptosis in T cells has also been proposed to be another mechanism of avoiding cytotoxic killing (244). Intratumoral CD8<sup>+</sup> T cells within HNSCC also have increased expression of programmed death-1 (PD-1) (245), a signal for immune checkpoints to inhibit T cell activation, through interaction with PD-1L, found on

HNSCC cells (246). Within HNSCC tissues, immune cell infiltration occurs mostly within the underlying stroma, with increasing levels of Foxp3<sup>+</sup> T regulatory cells in later stages of disease (247).

In addition to T cells, innate immune cells are powerful players within the tumor microenvironment. Dendritic cells are highly specialized antigen-presenting cells, able to stimulate adaptive immune T cell responses. In the context of cytokines such as TGF- $\beta$  and IL-10, they can also promote the development of an immunosuppressive environment by driving regulatory T cell differentiation (248, 249). In many solid tumors, the majority of infiltrating immune cells is comprised of tumor-associated macrophages (TAMs) (240, 250, 251). Although macrophages have the potential to inhibit tumor progression and enhance anti-tumor immunity, TAMs often express factors that both support tumor progression directly and also suppress the anti-tumor response. In breast, bladder, and ovarian carcinomas, TAMs display a skewed pro-tumor phenotype (252-254). M1-polarized macrophages produce the pro-inflammatory cytokines IL-12, IL-23, and IFN- $\gamma$  (255). M2-polarized macrophages produce cytokines including IL-10 and TGF- $\beta$  to promote wound healing and angiogenesis. In HNSCC, infiltrating TAMs seem to closely resemble the M2 phenotype and in high levels, correlate with increased tumor stage and lymph node involvement and extracapsular spread (256-258).

### ***Inflammatory cell recruitment and activation***

Macrophages infiltrating the tumor are derived from monocytes in circulation that home to the tumor site and differentiate (254, 259). Chemokines activate the migratory response of hematopoietic cells in normal trafficking to sites of inflammation and also for

homeostatic migration to lymphoid organs (260, 261). Chemokine receptors, in turn, may facilitate a number of processes necessary for metastasis including endothelial attachment, cell migration and extravasation, angiogenesis, and pro-proliferative and survival signaling (262).

CSF-1 is crucial for hematopoiesis and myeloid cell development (263). In addition to enhancing monocyte recruitment, it may act secondarily by supporting subsequent differentiation into macrophages at the tumor site (264). Although CSF-1 has the ability to activate macrophages, promoting phagocytosis and release of cytotoxic products, its ability to promote tumor progression suggests a dual role, possibly for its secreted rather than membrane-bound form (265). Members of the TGF family have also been suggested to participate in monocyte recruitment to tumors. These proteins may play a number of roles, regulating the functions of epithelial cells, endothelium, as well as immune cells. TGF- $\beta$ 1 in HNSCC was shown to enhance peripheral blood monocyte migration and their production of proangiogenic factors, such as IL-8 and vascular endothelial growth factor (VEGF) (266, 267). Genetic deletion of TGF- $\beta$  signaling in a mouse model of chemical carcinogenesis in the skin resulted in reduced TAM infiltration (268).

The chemokine C-X-C motif ligand (CXCL) 12 (CXCL12) and chemokine C-X-C motif receptor (CXCR) 4 (CXCR4) have been identified in HNSCC tissues with some associations with poor survival (269-271) and lymph node metastases (271, 272). Interest in CXCR4 antagonists as inhibitors of tumor angiogenesis and metastases continues with promising results from animal studies (271, 273). A key to unlocking potential therapeutic targets in these chemokine networks will be an understanding of the

regulatory pathways driving their expression and their function within the tumor microenvironment.

### ***Roles of macrophages in cancer***

Differentiated cells of the myeloid monocyte-macrophage lineage display a broad diversity with extensive plasticity among phenotypes, which guide the functional outcome of interactions with immune cells (274). TAMs constitute the predominant leukocyte population within the tumor microenvironment that drives the inflammatory response. Based on phenotypic marker expression and functional properties, TAMs closely resemble M2-polarized macrophages with some distinctions (253, 275). Focusing on M2-polarized cells reveals sub-categories of macrophages, which can drive a predominantly T helper 2 response, T regulatory cell response, or B cell response via immune complex and LPS stimulation (274).

Within the tumor microenvironment, a number of factors, including IL-10 and TGF- $\beta$ , promote the differentiation of recruited monocytes toward M2-polarized macrophages (252, 276). TAMs enhance malignancies through secretion of cytokines, growth factors, matrix proteases (277-279), and pro-angiogenic growth factors and chemokines (278, 280). In addition, accumulation of TAMs within regions of hypoxia promotes a pro-angiogenic switch in those cells (280). Metabolic changes, such as tumor-secreted lactic acid, can also promote induction of the IL-23/IL-17 inflammatory pathway in TAMs, limiting induction of anti-tumor IL-12/Th1 responses (281). TAMs and myeloid-derived suppressor cells (MDSCs) themselves express a large repertoire of immunosuppressive mediators which inhibit antitumor immunity by targeting cytotoxic T

cell activation, as well as further promoting the development of regulatory T cells and enhancing M2 polarization (282-285).

### ***Cytokines, chemokines, and inflammatory mediators***

Immune cells impact tumor progression through the release of soluble factors to support angiogenesis, tumor cell proliferation, and tissue remodeling (250, 252, 286, 287). In addition, immunosuppressive effects of these inflammatory mediators inhibit potential anti-tumor responses from cytotoxic T lymphocytes, NK cells, macrophages, and neutrophils, skewing the immune phenotype to a pro-tumor response (286, 288). Chemokines such as IL-8 and CXCL1 recruit neutrophils, monocytes, and endothelial cells to promote the inflammatory response as well as local angiogenesis, enhancing local invasion and metastasis (289). Chemokines also attract MDSCs, immature myeloid-lineage cells that have been shown to be important effectors of angiogenesis (282, 290). Signaling from these secreted growth factors and other mediators initiate signal transduction pathways which can further promote malignant transformation, such as the MAPK, NF- $\kappa$ B, and PI3K/Akt pathways (289).

By these mechanisms, altered cytokine, chemokine, and growth factor expression influences the development of a number of cancers, including HNSCC (291, 292). Factors such as IL-1 $\alpha$ , IL-6, IL-8, CXCL1, GM-CSF, and VEGF have been identified both in secretions from HNSCC cell lines, from within tumor samples, and also in patient sera (230, 231, 293). For a number of these secreted factors, increasing levels have been associated with disease progression and recurrence, with decreases associated with therapeutic response (231). IL-6 has been shown to correlate with poor prognosis in

HNSCC (294), in part through induction of VEGF and an invasive phenotype in tumor cells (295). Whether targeting these secreted mediators will have a beneficial effect on disease progression requires further investigation.

### ***Roles of interleukin-1 $\beta$ in cancer biology***

The interleukin-1 family contains IL-1 $\alpha$  and IL-1 $\beta$  members that exert potent pro-inflammatory effects in a pleiotropic manner, produced by macrophages in response to inflammatory stimuli. Located on chromosome 2, this gene family produces the pro-inflammatory cytokines IL-1 $\alpha$  and IL-1 $\beta$ , in addition to the antagonist, interleukin 1-receptor antagonist (IL-1RA). The agonist members, IL-1 $\alpha$  and IL-1 $\beta$ , activate an inflammatory response through the IL-1 receptor (IL-1R), but also induce the expression of a panel of inflammatory molecules across a diverse panel of stromal and immune cells. Low levels of IL-1 $\alpha$  expression within healthy cells, released during necrosis may activate immune responses (296), through binding IL-1RI on immune surveillance cells, bearing MHC class I, B7.1, B7.2, L-selectin, and NKG2D ligands (297, 298). However, IL-1 $\beta$  expression is tightly controlled at multiple regulatory points and is only secreted in the presence of inflammatory stimuli.

Genetic knockout mice lacking IL-1 $\beta$  are protected from B16 local and lung metastases (299). In models of carcinogen-induced tumorigenesis, both tumor and immune cell-derived IL-1 $\beta$  contribute to enhanced tumor cell adhesion and invasion, increased angiogenesis within the microenvironment, and local immune suppression (300). In prostate cancer, IL-1 $\beta$  was identified as a macrophage-secreted factor with the ability to alter androgen receptor signaling modulators to enhance hormonal therapy

resistance (301). In human studies, IL-1 $\beta$  polymorphisms were associated with increased risk of gastric carcinoma (302). In transgenic mice, expression of human IL-1 $\beta$  within stomach tissue generated spontaneous gastric inflammation and cancer, associated with the recruitment of MDSCs (303).

IL-1 $\beta$  has been well characterized as a pro-metastatic factor (304, 305) and is one of a number of secreted factors increased in progressing or resistant oral tumors (306, 307). In HNSCC cell lines, IL-1 $\beta$  exposure promoted epithelial-mesenchymal transitions through the up-regulation of Snail, proposed to occur through COX-2 activation (308). In oral keratinocytes, the induction of Snail expression was shown to increase pro-inflammatory cytokine expression (309), generating a cycle of tumor-promoting inflammation. Although previous reports have identified IL-1 $\alpha$  as a constitutively expressed cytokine in a panel of HNSCC cell lines, IL-1 $\beta$  secretion was not detected (310), supporting the role of stromal cells as a cellular source of this cytokine in HNSCC.

Expression of IL-1 $\beta$  is tightly regulated at both the mRNA and protein level. Like other early response cytokine genes, IL-1 $\beta$  mRNA can be regulated post-transcriptionally through AU-rich elements (AREs) within its 3' untranslated region (UTR) (311). The precise interactions of specific RNA binding proteins and the IL-1 $\beta$  3'UTR and whether other RNA binding factors such as miRNAs are involved in this process have not yet been addressed. In addition to post-transcriptional regulation, IL-1 $\beta$  is also regulated post-translationally by inflammasome activation. All members of the NLR (nucleotide binding, lots of leucine-rich repeats containing) gene family contain a nucleotide-binding domain, a leucine-rich repeats (LRR) domain in the C-terminus, and an effector domain in the N-terminus, such as CARD or PYRIN (312). In activation complexes, these

proteins are key to host responses to pathogen and damage-associated molecular patterns (313, 314), including viral DNA (315) and RNA (316), extracellular ATP (317), and reactive oxygen species (318). Following activation, the NLR proteins assemble a multimeric protein complex, the inflammasome, to cleave pro-caspase-1 into its mature form, which in turn cleaves the 36 proform of IL-1 $\beta$  and IL-18 into their mature secreted forms (313).

Within the NLRP family, genetic variants and experimental deletions have identified a regulatory role for these proteins in colorectal carcinogenesis (319-322). However, discordant roles for NLRP family members have been identified by different research groups. In murine models, deficiencies in *Nlrp3* and *Casp1* were shown to reduce severity of colitis-associated cancer (323, 324), whereas mice lacking *Nlrp3*, *Nlrp6*, *Nlpr12*, *Pycard*, and *Casp1* were shown to be more susceptible to the model compared to wild-type animals (319, 321, 325-328). Interpretation of results from bone marrow-reconstitution experiments should be taken in consideration that previous characterizations of engraftment have shown particularly poor reconstitution of intestinal lamina propria and intraepithelial lymphocytes despite high splenic reconstitution (329). Thus, these discrepancies may be due, in part, to differing roles of inflammasome signaling in immune cells versus intestinal epithelium (325), as well as the potential impact of varying microflora among animals from different institutions.

Like, other cytokines, IL-1 $\beta$  expression is deregulated in human cancers. As a early pro-inflammatory mediator, IL-1 $\beta$  initiates a downstream cascade of inflammatory molecules to potentiate its effect, activating stromal cells, other immune cells, and also tumor cells. With increasing interest in the blockade of IL-1 $\beta$  signaling in cancer therapy,



the need remains to characterize cellular sources of IL-1 $\beta$  within the tumor and surrounding microenvironment and delineate the regulatory mechanisms involved for the development of efficient therapeutic targets.

## 1.5 Hypothesis & Specific Aims

DUSP1 has been shown to be an important regulator of innate immune activity, with exuberant over-production of inflammatory cytokines in *Dusp1* deficient animals following immune challenge. Although levels of *DUSP1* expression have been shown to be lost in a number of human cancers with advanced tumor stage, whether this change in *DUSP1* expression is directly related to disease progression or simply a bystander effect of altered cancer signaling pathways is unknown. We hypothesized that DUSP1 is a negative regulator of tumor-promoting inflammation in head and neck squamous cell carcinoma. This hypothesis was tested with the following specific aims.

Specific Aim 1 addressed how *Dusp1* deficiency affects tumor progression in an animal model. Wild-type and *Dusp1* deficient mice were challenged with 4-nitroquinoline 1-oxide (4NQO) to initiate the development of oral squamous cell carcinoma. The effects of *Dusp1* deficiency were examined by assessing disease onset, tumor burden, and histological tumor grade. To understand how *Dusp1* alters the tumor microenvironment, Nanostring analysis and qPCR arrays were performed to quantitate the mRNA expression levels of inflammatory mediators in wild-type and knockout tumor tissues. Flow cytometry analysis further assessed the numbers of innate and adaptive immune cells present within the spleen and draining lymph nodes from tumor-bearing wild-type and knockout mice. To determine whether *Dusp1* deficiency in the hematopoietic compartment was sufficient to recapitulate the enhanced disease phenotype observed, bone marrow chimeras were generated from wild-type and *Dusp1* deficient mice, challenged with 4-nitroquinoline 1-oxide, and monitored for disease progression. Lastly, tumor progression was assessed using a syngeneic subcutaneous

tumor cell injection in wild-type and *Dusp1* deficient mice using three different cancer cell lines, with enhanced tumor growth in *Dusp1* deficient mice inhibited by intraperitoneal injections of the p38 inhibitor SB203580.

Specific Aim 2 addressed the mechanism by which *Dusp1* regulates inflammation in macrophages. The effect of *Dusp1* deficiency on macrophage polarization to M1 or M2 phenotypes was examined *in vitro*. Wild-type and *Dusp1* deficient wild-type bone marrow-derived macrophages were challenged with inflammatory stimuli including lipopolysaccharide and tumor cell-conditioned media to assess expression of *Il1b* mRNA. Total levels of *Il1b* mRNA and primary mRNA were assessed at steady-state levels by qPCR. Rates of mRNA decay were quantified by qPCR following actinomycin D treatment. Lastly, the effects of *Dusp1* deficiency on inflammasome activation and IL-1 $\beta$  secretion were assessed by western blotting and ELISA from primary macrophages.

Specific Aim 3 addressed how *DUSP1* expression is altered in human head and neck squamous cell carcinoma. The levels of *DUSP1* mRNA and protein were examined in matched tissues from human head and neck squamous cell carcinoma tissues and adjacent non-tumor tissues. In addition, the mRNA and protein expression levels of IL-1 $\beta$  were quantified in these samples. Publicly available datasets from human head and neck squamous cell carcinoma tissues were also examined for significant alterations in *DUSP1* expression and IL-1 $\beta$ , identified in the animal model in Specific Aim 1.

## CHAPTER 2. Materials and Methods

### 2.1 Generation of animals

All animal studies were carried out in accordance with NIH guidelines, in compliance with the Guide for the Care and Use of Laboratory Animals, and protocols were approved by the Medical University of South Carolina (MUSC) Institutional Animal Care and Use Committee. *Dusp1<sup>-/-</sup>* (KO) and *Dusp1<sup>+/+</sup>* (WT) mice, on a C57/129 mixed genetic background were obtained through a Material Transfer Agreement from Bristol-Myers Squibb (NY) and bred at MUSC. Every five generations, homozygous wild-type and knockout breeder pairs were replaced with littermates from *Dusp1<sup>-/+</sup>* heterozygous breeder pairs to prevent genetic drift. Litters from these C57/129 background mice were used for all experiments with the exception of allograft and chimeric experiments, which necessitated a C57BL/6 genetic background. For allograft and bone marrow transplants, *Dusp1<sup>-/-</sup>* mice were backcrossed to a C57BL/6NCrl background (Charles River Laboratories) for ten generations, alternating male and female C57BL/6 mates. Homozygous *Dusp1<sup>-/-</sup>* and *Dusp1<sup>+/+</sup>* breeder pairs for colony maintenance were established from heterozygous *Dusp1<sup>-/+</sup>* breeder pairs. Every five generations, *Dusp1<sup>-/-</sup>* mice were backcrossed with C57BL/6J mice (The Jackson Laboratory) to prevent genetic drift.

## 2.2 Carcinogen-induced oral cancer model

Male and female mice aged 6-8 weeks old and weighing 16-22g were housed in appropriate sterile filter-capped cages and fed and given water *ad libitum*. A stock solution of 4-nitroquinoline 1-oxide (4NQO) (Sigma-Aldrich) dissolved in propylene glycol (4mg/mL) was diluted in the drinking water to a final concentration of 25µg/mL for mice on a mixed genetic background or 50µg/mL for mice on a C57BL/6 genetic background. 4NQO concentration was decreased for mice on the mixed C57/129 genetic background, compared to C57BL/6, due to enhanced toxicity in an initial pilot study. These results are in accordance with previous reports that mice on a C57BL/6 genetic background are more resistant to other models of carcinogenesis. Drinking water was protected from light exposure and prepared weekly. Animals were given either water with propylene glycol vehicle controls or 4NQO in the drinking water for 16 weeks, after which all cages were reverted to regular water and monitored until week 28-32. Animals were euthanized at week 28 (C57BL/6 background) or 32 (C57/129 background) or when greater than 20% weight loss was documented. Full autopsies were performed, and tissues were immediately collected in 10% buffered formalin for histology or snap frozen for homogenization. All animals were monitored daily for general behavioral abnormalities and any sign of toxicity or illness.

Weekly examinations were performed under anesthesia [3-5% isoflurane mixed with oxygen] to document pathologic changes within the oral cavity. Images were recorded using an Olympus SZ40 Stereo Zoom Microscope at 6.7x magnification and

Hitachi KP-D20B CCD color camera, and disease onset was determined by a blinded observer. Survival rates were estimated from the first date of visible oral tumor formation, using the Kaplan-Meier method, and differences between the curves were compared using the log-rank test.

### **2.3 Bone marrow transplantation**

Male and female mice aged 8-10 weeks old and weighing 18-24g were used to generate bone marrow chimeras through lethal irradiation and hematopoietic reconstitution by bone marrow transplant. The day before irradiation of recipient mice, access to food but not water was restricted to limit radiation-induced gastrointestinal toxicity. Mice received 2 doses of 550 cGy, spaced 4 hours apart, from a JL Shepherd Model 143 137 Cesium irradiator. The following day, irradiated mice received 200 $\mu$ L injections of  $2 \times 10^6$  red blood cell-depleted whole bone marrow in phosphate-buffered saline (PBS) through the lateral tail vein. Animals were monitored for signs of radiation-induced illness and given access to soft gel-based diets for a week following treatment. At 6-8 weeks post-transplant, engraftment was assessed by flow cytometry analysis of peripheral blood for the markers CD45.2 from *Dusp1*<sup>-/-</sup> and *Dusp1*<sup>+/+</sup> mice and the congenic marker CD45.1 from C57/Ly5.1 mice (NCI, Frederick). Successful engraftment was determined as greater than 80% expression of the donor marker. After validation, animals began 4NQO treatment at 50 $\mu$ g/mL for 16 weeks, as described above, followed by 12 weeks of regular water. Weights were monitored as a surrogate for disease burden throughout the model.

## **2.4 Subcutaneous syngeneic tumor model**

Male and female *Dusp1*<sup>-/-</sup> and *Dusp1*<sup>+/+</sup> mice on a C57BL/6 genetic background aged 8-10 weeks old and weighing 18-24g were implanted with syngeneic cancer cell lines. Animals were anesthetized by isoflurane inhalation (3-5% mixed with oxygen), and fur on the dorsal flank was removed with an electric razor. EO771, TRAMP-C2, or B16F10 tumor cells were subcutaneously injected in 100 – 200 $\mu$ L volumes of PBS over the right flank using 27 gauge x 1/2” tuberculin needles. After injections, animals were monitored daily for signs of illness. Tumor progression was monitored by assessing tumor volume, calculated as (length x width<sup>2</sup>)/2 with digital calipers every other day. Animals were sacrificed if tumor volume exceeded 1500mm<sup>3</sup> or tumors developed extensive non-healing ulcerations. During tissue collection, tumor tissues were split and either fixed in 10% buffered formalin for 48 hours or snap frozen in liquid nitrogen. Animals were also examined for any signs of metastatic lesions or other illness.

## **2.5 Human tissue samples**

Previously collected snap-frozen tissues from patients diagnosed with head and neck squamous cell carcinoma were acquired from the MUSC Hollings Cancer Center Tissue Biorepository in compliance with protocols approved by the MUSC Institutional Review Board. Tissue samples were collected fresh from the surgical pathology grossing room. A representative sample of the tissue sample was placed in Optimum Cutting Temperature (OCT) compound with the remaining tissue frozen in liquid nitrogen. Tissue pathology and tumor percentage within the representative frozen section was verified by

hematoxylin and eosin (H&E) staining by the Tissue Biorepository research pathologist. Non-tumor adjacent tissue was obtained from the same patient during the same surgical procedure and underwent the same collection procedure. The non-tumor adjacent tissue was also verified by H&E staining to contain no abnormal pathology.

## **2.6 Histology**

Formalin-fixed paraffin-embedded tissues were used for histological scores and immunohistochemistry. Tissues were sectioned at 7 $\mu$ m thickness by rotary microtome and placed onto glass slides before drying overnight. Slides were deparaffinized in three five minute washes of xylene and rehydrated through three five minute washes of 100%, 95%, and 90% ethanol before staining. Tissue sections were stained with hematoxylin and eosin before examination by two pathologists, blinded to experimental group. Histological scores were graded as normal, hyperplasia, dysplasia, in situ squamous cell carcinoma, or invasive squamous cell carcinoma. For tissue samples with multiple lesions, the most severe histological score was used for analysis. Inflammation was scored on a 0–4 scale (0, normal mucosa; 1, minimal inflammation (occasional scattered granulocytes and leukocytes); 2, mild inflammation (scattered granulocytes with occasional infiltrates); 3, moderate inflammation (scattered granulocytes with patchy infiltrates); and 4, severe inflammation (multiple extensive areas with abundant granulocytes and marked infiltrates), as previously described (330). For animals with multiple lesions of varying inflammation, the highest inflammation score was used for analysis.



## 2.7 Immunohistochemistry

Tissue slides were deparaffinized and rehydrated, as described above, before performing antigen retrieval in ethylenediaminetetraacetic acid (EDTA) buffer (1mM EDTA, 0.05% Tween-20, pH 8.0) or in citrate buffer (10mM sodium citrate, 0.05% Tween-20, pH 6.0) at 100°C for 30min. Sections were blocked in 10% goat serum in PBS and incubated with the following primary antibodies in blocking buffer at 4°C overnight: F4/80 at 1:500, phospho-p38 MAPK, phospho-ERK1/2, phospho-SAPK/JNK (Cell Signaling) at 1:1000, Ki67 (Abcam) at 1:100, and isotype controls (Santa Cruz) at corresponding  $\mu\text{g/mL}$  dilutions to the primary antibody. After washing in PBS, slides were sequentially incubated with biotinylated secondary antibody at 1:200 and avidin-biotin complex (Santa Cruz) at 1:1:50 before developing in 3,3-diaminobenzidine (Vector Labs), according the manufacturers' protocols. Slides were washed, counterstained with Gill's hematoxylin No. 2 (Sigma-Aldrich), dehydrated overnight, and transferred to xylene before mounting with CytoSeal mounting media (ThermoScientific).

Staining was scored by a research pathologist, blinded to animal identification and experimental group. Immunohistochemistry scores were calculated by the Quick-Score method of multiplying the intensity coefficient and the frequency of positivity coefficient (331). The intensity coefficient was scored as 0 (negative), 1 (low), 2 (moderate) or 3 (strong), and the positivity coefficient was scored based on the percentage of positively staining cells (0 = no positive staining, 1 = 1-19% positive, 2 = 20-39% positive, 3 = 40-59% positive, 4 = 60-79% positive, and 5 = 80-100% positive). The resulting product was categorized from 0 to 5 yielding the IHC staining score as follows: 0 = negative score, 1 = 1-3, 2 = 4-6, 3 = 7-9, 4 = 10-12, and 5 = 13-15. For F4/80<sup>+</sup> cell counts, tumor-positive

fields of view were acquired at 10X magnification and quantified using Viziopharm acquisition and analysis software v. 4.48.201 (Hoersholm, Denmark), in a blinded manner, and expressed as the number of positive cells in each histologically defined area.

## **2.8 Primary bone marrow-derived macrophage isolation**

Bone marrow cells were obtained from age and sex-matched 8-12 week-old *Dusp1<sup>-/-</sup>* and *Dusp1<sup>+/+</sup>* mice. Animals were euthanized by CO<sub>2</sub> inhalation, followed by cervical dislocation. After spraying with 70% ethanol, six bones from each mouse, humerus, femur, tibia, were removed and cleaned with a Kimwipe to remove muscle and connective tissue. Bones were sprayed with 70% ethanol and moved to a sterile cell culture dish. In the cell culture hood, one epiphysis was removed from each bone, and the bones were placed, three to a tube, cut side down, into sterile 0.5 mL tubes within a 1.5 mL tube. The 0.5 mL tubes each contained a small hole bored using a heated 20 gauge needle. Bone marrow cells were flushed by centrifuging the tubes for a 5 second pulse in a tabletop centrifuge. Following isolation, red blood cells were lysed with ammonium chloride potassium (ACK) lysis buffer for 2 minutes before plating remaining cells.

Isolated bone marrow cells were differentiated for 6-7 days in Iscove's Modified Dulbecco's Medium (IMDM, Life Technologies) or  $\alpha$ -minimum essential media ( $\alpha$ -MEM, Life Technologies) supplemented with 2mM glutamine, 10% HyClone characterized endotoxin-free fetal bovine serum (FBS) (ThermoScientific), penicillin (100U/mL, Sigma-Aldrich), streptomycin (100 $\mu$ g/mL, Sigma-Aldrich), and 10ng/mL macrophage colony-stimulating factor (M-CSF, R&D Systems). During differentiation,

bone marrow cells were plated in untreated plastic tissue culture dishes with media replenishment every two days. Bone marrow-derived macrophages were released from culture dishes with Cellstripper solution (Cellgro) and plated the day prior to treatment. All inflammasome treatments were performed in serum-free IMDM supplemented with 10ng/mL M-CSF. All other treatments were performed in complete  $\alpha$ -MEM diluted 5-fold in serum-free  $\alpha$ -MEM.

## **2.9 Macrophage polarization**

Primary bone marrow-derived macrophages were cultured, as described in section 2.8, and plated the day prior to treatment in  $\alpha$ -MEM with 10% FBS, antibiotics, and 10ng/mL M-CSF. Macrophages were plated at a density of  $1.5 \times 10^6$  cells in 2mL media in a 6-well dish. Treatments were performed for 24 hours in low serum  $\alpha$ -MEM, prepared from complete media diluted 5-fold in serum-free  $\alpha$ -MEM, containing either LPS (100ng/mL) and recombinant mouse interferon- $\gamma$  (IFN- $\gamma$ , 20ng/mL, R&D Systems) or recombinant mouse IL-4 (10ng/mL, R&D Systems), to polarize cells to a M1 or M2 phenotype, respectively. Supernatants were collected and centrifuged at  $1,000 \times g$  for 10 minutes at  $4^\circ\text{C}$  to remove cellular debris before analysis of cytokine expression by ELISA. Cell lysates were collected in protein lysis buffer, as described in section 2.11. RNA was collected for qPCR analysis, as described in section 2.14.

## **2.10 Inflammasome activation**

Primary bone marrow-derived macrophages were cultured, as described in section 2.8, and plated the day prior to treatment in IMDM with 10% FBS and antibiotics with

10ng/mL M-CSF. Macrophages were plated at a density of  $1 \times 10^6$  cells per 1mL media in 12-well dishes or  $2.5 \times 10^6$  cells per 2mL media in 6-well dishes. Macrophages were primed with LPS (100ng/mL) from *Aggregatibacter actinomycetemcomitans* (strain Y4, serotype B), extracted by the hot phenol-water method (332), and diluted in PBS. After priming for 4 hours, cells were washed twice with serum-free IMDM before treatment with adenosine tri-phosphate (5mM ATP, Sigma-Aldrich) or nigericin (10 $\mu$ M, Sigma-Aldrich) for 30 or 60 minutes, respectively, to induce inflammasome activation. Supernatants were collected and centrifuged at 1,000 x g for 10 minutes at 4°C to remove cellular debris before IL-1 $\beta$  detection by ELISA. Cell lysates were collected in protein lysis buffer, described in section 2.11.

## **2.11 Protein isolation**

Prior to protein collection, cell culture media was removed, and adherent cells were washed with PBS. Cell lysates were scraped in a 50 $\mu$ L volume of radioimmunoprecipitation assay (RIPA) buffer supplemented with phenylmethylsulfonyl fluoride (PMSF, 1mM), and the protease and phosphatase inhibitors cOmplete protease inhibitor cocktail and phosSTOP (Roche), according to manufacturer's guidelines. Murine and human tissues, previously snap frozen, were thawed on ice and homogenized with a rotor stator homogenizer in the same lysis buffer in a 500 $\mu$ L volume in a 5mL round bottom tube. Following homogenization, tissue lysates were sonicated at 50% amplitude for five 1 second pulses. Cellular and tissue debris was removed by centrifugation at 14,000 x g for 15 minutes at 4°C and transferring the supernatant. Tissue samples and supernatants were filter-concentrated in a table-top centrifuge,

removing excess buffer and proteins smaller than 3kDa, following manufacturer's protocol using a 30 minute centrifugation time (Millipore).

## **2.12 Western blotting**

Protein samples were quantified by bicinchoninic acid assay immediately prior to electrophoresis. Samples from inflammasome experiments were analyzed on 15% acrylamide gels. All other samples were analyzed on 10% acrylamide gels. All acrylamide gels contained 4% acrylamide stacking phases and were prepared within 24 hours prior to electrophoresis, using 30% acrylamide/bis solution (37.5:1), tetramethylethylenediamine, and ammonium persulfate (Bio-Rad). Protein samples of 30 - 50 $\mu$ g were loaded into each well and electrophoresed before transfer in Towbin buffer onto polyvinylidene fluoride membranes with 0.2 $\mu$ m pore size (Bio-Rad). Membranes were blocked from non-specific binding with 5% non-fat dry milk in Tris buffered saline, containing 0.1% Tween-20 (TBS-T), for 30 minutes. Membranes were then incubated in primary antibody, prepared in 5% bovine serum albumin in TBS-T, overnight at 4°C with gentle rocking.

The following antibodies were used: DUSP1/MKP-1 (Millipore), caspase 1 p20 (Millipore) and p10 (Santa Cruz), IL-1 $\beta$  (Abcam) at 1:500,  $\beta$ -actin, phospho- and total p-38 MAPK GAPDH, phospho- and total-ERK1/2 MAPK, phospho- and total-SAPK/JNK1/2 MAPK, GAPDH, and  $\alpha$ -tubulin (Cell Signaling). All primary antibodies were used at 1:1000 dilutions unless stated otherwise and incubated overnight at 4°C with gentle agitation. Membranes were washed three times in TBS-T for 5 minutes before incubating in secondary antibodies, diluted 1:1000 in 5% non-fat dry milk in TBS-T.

Secondary antibodies were horseradish peroxidase-conjugated anti-rabbit and anti-biotin antibodies (Cell Signaling). After secondary antibody incubation for 1 hour at room temperature, membranes were washed five times for 5 minutes in TBS-T and incubated in prepared SuperSignal WestPico chemiluminescent substrate (Pierce) before exposing on X-ray film (ThermoScientific). Images of X-ray films were captured on a Gel Doc imaging systems and saved as TIFF files.

### **2.13 Enzyme-linked immunosorbent assay**

Supernatants, previously collected with cellular debris removed by centrifugation, were thawed from -80°C for ELISA analysis. Single aliquots of supernatant were used to avoid freeze-thaw. Cytokine secretion in supernatants was detected using the Mouse IL-1 beta/IL-1F2, IL-1RA, IL-12p40, and IL-10 DuoSet ELISAs (R&D Systems). Levels of IL-1 $\beta$  in tissue lysates and sera were detected using the Mouse IL-1 $\beta$  ELISA for Lysates (Ray Biotech). All samples were prepared in triplicate and analyzed alongside a standard curve, prepared in triplicate. Concentration was calculated from the standard curve using a 4-parameter logistic nonlinear regression model, per manufacturer's recommendations.

### **2.14 RNA isolation and quantitative PCR**

RNA isolation was performed using QIAprep RNeasy spin columns (Qiagen) for quantitative PCR array analysis of tumor tissue lysates. Column eluents were assessed for RNA integrity on the Agilent Bioanalyzer using the RNA 6000 Pico chip, and only samples with RNA integrity  $\geq 7$  were used for qPCR array analysis. TRIzol (Invitrogen) was used for preparation of all other samples. After addition of chloroform to TRIzol, the

aqueous phase was transferred, and isolated RNA was precipitated in isopropanol. All RNA for qPCR arrays were prepared with on-column DNase treatment, per manufacturer's protocol (Qiagen). Isolated RNA was washed with 75% ethanol and resuspended in RNase and DNase-free water. Concentration was determined by Beer-Lambert law, using absorbance at 260 and 280nm measured by NanoDrop spectrophotometer (ThermoScientific).

Complementary DNA was prepared from 500ng of total RNA using random hexamers, according to manufacturer's protocol (Applied Biosystems). Gene expression was determined using the following probe-primer TaqMan sets for delta-delta Ct calculations: *Ptprc* (Mm01293577\_m1), *I11b* (Mm00434228\_m1), *Cxcl1* (Mm04207460\_m1), *I112b* (Mm00434174\_m1), *Nos2* (Mm00440502\_m1), *I110* (Mm00439614\_m1), *Arg1* (Mm00475988\_m1), *Gapdh* (Mm99999915\_g1), 16s rRNA (Mm04260181\_s1), *DUSP1* (Hs00610256\_g1), and *ACTB* (Hs01060665\_g1). Quantitation of primary *I11b* mRNA was performed using the following SYBR Green primer pairs for delta-delta Ct calculations: *I11b* exon 3 forward 5'-TGA CCT GTT CTT TGA AGT TGA CG-3', *I11b* intron 3 forward 5'-CCT TGG TGT TCT CTG GGG TTG-3', *I11b* intron 3 reverse 5'-TAT CCC TTC CCG TTT GGG TT-3', *I11b* exon 4 reverse 5'-CGA GAT TTG AAG CTG GAT GCT C-3', *Actb* exon 2 forward 5'-CCA ACC GTG AAA AGA TGA CC-3', *Actb* intron 2 reverse 5'-ATG GGA GAA CGG CAG AAG A-3'. Samples were prepared in duplicate and amplified on the StepOnePlus PCR System (Applied Biosystems).

### **2.15 Quantitative PCR array**

RNA samples were prepared, as described in section 2.14, using the QIAGEN RNeasy mini kit with on-column DNase digestion. After validation of RNA integrity on the Agilent Bioanalyzer RNA 6000 Pico chip, samples were prepared for qPCR array analysis using the RT<sup>2</sup> Prolifer PCR array system (SA Biosciences). For each sample, 1µg RNA was transcribed to cDNA using the RT First Strand synthesis kit and prepared for amplification using a SYBR Green qPCR master mix with ROX reference dye (SA Biosciences). Samples were amplified on the StepOnePlus PCR system (Applied Biosystems) using the following two arrays, Mouse MAP Kinase Signaling Pathway and Mouse Inflammatory Cytokine and Receptors (SA Biosciences).

### **2.16 Nanostring**

Samples for Nanostring analysis were prepared by TRIzol extraction, as described in section 2.14. The nCounter analysis system (NanoString Technologies, Seattle, WA) was used to screen for gene expression using two specific probes (capture and reporter) for each gene of interest, in a custom panel. Total RNA, 250ng of each sample, was hybridized with customized Reporter and Capture ProbeSets according to the manufacturer's instructions to directly label mRNAs with molecular barcodes without reverse transcription or amplification. Manufacturer probe sets were designed and validated for mRNA specificity to preclude the need for DNase treatment or RNA integrity > RIN 7 as in qPCR arrays. Hybridized samples were recovered in the NanoString Prep Station, and mRNA molecules were enumerated with the nCounter. For analysis of expression, each sample profile was normalized to the geometric mean of 4



reference genes, *Eif4a2*, *Oaz1*, *Ncln*, and *Gfra2*, chosen for their lowest variance among all experimental samples.

### **2.17 mRNA decay**

Primary bone marrow-derived macrophages from *Dusp1*<sup>-/-</sup> and *Dusp1*<sup>+/+</sup> were cultured, as described in section 2.8, and plated the day prior to treatment in  $\alpha$ -MEM with 10% FBS, antibiotics, and 10ng/mL M-CSF. Macrophages were plated at a density of  $1.5 \times 10^6$  cells in 2mL media in a 6-well dish. Cells were treated in low serum media, consisting of complete  $\alpha$ -MEM diluted 5-fold in serum-free  $\alpha$ -MEM. Macrophages were stimulated with LPS (100ng/mL) for 4 hours, before the addition of ActD (5 $\mu$ g/mL, Sigma-Aldrich). Media was removed, and adherent cells were washed with PBS before collecting RNA by TRIzol extraction, as described in section 2.14. RNA was collected from cells treated with LPS for 4 hours alone, in addition to cells treated with actinomycin D for 15, 30, 45, 60, and 90 minutes. Relative quantification of mRNA expression by the  $2^{(-\Delta\Delta Ct)}$  method was used to generate a semi-logarithmic curve of mRNA expression over time to calculate the mRNA half-life from the linear regression, under the assumption of first-order kinetics.

### **2.18 Flow cytometry**

Spleens and cervical lymph nodes were isolated from tumor-bearing *Dusp1*<sup>-/-</sup> and *Dusp1*<sup>+/+</sup> mice on a C57BL/6 genetic background 28 weeks after beginning 4NQO treatment. Organs were crushed through a 40 $\mu$ m nylon filter to generate a single cell suspension. Red blood cells from splenocyte preparations were lysed in ACK lysis buffer

for 2 minutes, and the concentration of remaining viable cells were counted on a hemacytometer prior to staining. Peripheral blood was collected from the lateral tail vein in 3mg/mL EDTA in PBS. The majority of red blood cells were separated in 1% dextran T500, and remaining red blood cells were lysed in ACK lysis buffer for 2 minutes. Viable cells were enumerated by hemacytometer prior to staining.

Cells were prepared in  $1 \times 10^5$  –  $1 \times 10^6$  cells per staining sample in PBS buffer containing 0.5% BSA and 2mM EDTA. Non-specific staining through Fc receptor binding was blocked by incubation with FcR blocking reagent (Miltenyi Biotec) for 10 minutes on ice. Fluorescently-labeled antibodies diluted in staining buffer were added for an additional 30 minutes on ice. Samples were washed with staining buffer before resuspension in running buffer for analysis. Propidium iodide was added to each sample for dead cell exclusion. Samples stained for intracellular Foxp3 expression were stained with Fixable Viability Dye for dead cell exclusion (eBioscience). Prior to each flow cytometry experiment, calibration was performed, and instrument settings were adjusted for compensation of all necessary fluorophores using single antibody staining controls on the MACSQuant Analyzer (Miltenyi Biotec).

These murine-specific antibodies were used for staining at the following concentrations: CD45.1-APC (1:50), CD45.2-FITC (1:50), CD4-FITC (1:1500), CD62L-PE (1:1000), CD69-eFluor450 (1:500), IgM-PE (1:200), IgD-eFluor450 (1:500), CD40-APC (1:800), NK1.1-PE (1:500), CD3-FITC (1:2000), F4/80-PE (1:1000), MHCII-PE (1:500), PDCA-1-FITC (1:1000), CD4-FITC (1:1500), CD25-PE (1:1000), Foxp3-APC (1:500), rat IgG<sub>2a</sub>-APC (1:500) (eBioscience), Ly6C-FITC (1:500, Novus Biologicals), Ly6G-Pacific Blue (1:500, BioLegend), CD8-APC (1:10), B220-FITC (1:10), CD11b-

APC (1:11), CD11c-APC (1:10) (Miltenyi Biotec). Intracellular staining with antibodies against Foxp3 or its isotype control was performed following staining with Fixable Viability dye and cell surface markers and incubation in permeabilization and fixation, according to manufacturer's protocols (eBioscience). Flow cytometry data were collected from a live cell gate using either propidium iodide or Fixable Viability Dye to exclude dead cells. A total of 10,000 events were collected for each sample. Analysis was performed on MACSQuantify software (Miltenyi Biotec).

## **2.19 Statistical analyses**

When comparing effect of genotype, a two-sample Student's *t*-test was performed using the Satterthwaite method for unequal variances, Mann-Whitney U-test in absence of normal distribution, or pooled method for all other comparisons. For distributions of categorical scores, a Fischer's Exact test was used. A repeated measures mixed model, with random intercept and time effect, was used to test effect of genotype on weight gain and inhibitor treatment by genotype interaction. Survival analyses (event = tumor volume  $\geq 1500\text{mm}^3$ ) with Kaplan-Meier estimates were performed using a log-rank test. Adjusted *p*-values using Tukey-Kramer multiple comparisons method are provided when comparing least square mean estimates. Analysis of human samples with matched tumor and adjacent tissues were assessed by paired Student's *t*-test. Data analysis was performed using GraphPad Prism version 4.00 (GraphPad Software) with repeated measures mixed models using SAS 9.4; *p* values of  $< 0.05$  were considered statistically significant. Error bars represent standard error of the mean.

## **CHAPTER 3. *Dusp1* deficiency enhances tumor growth and progression.**

### **3.1 Rationale & Hypothesis**

Although the expression of *DUSP1* has been shown to be deregulated in a number of human cancers, with expression lost or increased depending on tumor type, the functional impact of this phosphatase on tumor development and progression has not been examined. As a negative regulator of MAPK signaling, DUSP1 has the potential to influence a broad array of cellular functions driven by MAPK activation. Despite extensive characterization by *in situ* hybridization and immunohistochemistry, there lacks an understanding of how *DUSP1* gene and protein expression levels alter cancer phenotype.

Previous studies have demonstrated DUSP1 is a crucial component to control inflammation in response to acute immune challenges, such as endotoxin. More recently, DUSP1 has also been shown to play a role in shaping the adaptive immune response to bacterial and fungal pathogens. The contribution of chronic inflammation to tumor progression has gained recognition, especially in oral cancer, where the tissue site is subjected to a highly dense array of microbial products. The following studies were designed to test the hypothesis that *Dusp1* deficiency enhances tumor growth and progression, using two *in vivo* cancer models.

### 3.2 Results

#### *Dusp1* deficient mice are more susceptible to carcinogen-induced oral cancer.

To understand how DUSP1 regulates tumor development and progression in oral cancer, *Dusp1* wild-type and deficient mice were treated with 4-nitroquinoline 1-oxide (4NQO) in the drinking water. As a DNA adduct-forming agent, which generates successive DNA damage, 4NQO mimics chronic tobacco exposure, a risk factor for HNSCC, resulting in progressive epithelial neoplasia that culminates in the formation of oral squamous cell carcinomas (Figure 3-1). The development of oral lesions was monitored by weekly examinations performed under anesthesia, and the first onset of visible oral tumors was documented. Oral tumor-free survival curves show a significant enhancement of disease progression, by approximately 2-3 weeks, in *Dusp1* deficient mice (Figure 3-2). Additional tumor sites were discovered on necropsy, primarily within the esophagus, as previously reported (333), with a minority of *Dusp1* deficient animals demonstrating tumor invasion in the cervical lymph nodes. Studies from our laboratory have identified a gender bias in *Dusp1* deficient mice in other models of inflammation, as well as skeletal homeostasis (334) (unpublished studies). However, no difference in disease onset was noted between *Dusp1* deficient male and female mice (n = 19 per group, p = 0.4163) or wild-type male and female mice (n = 18 per group, p = 0.6824) (Figure 3-3).

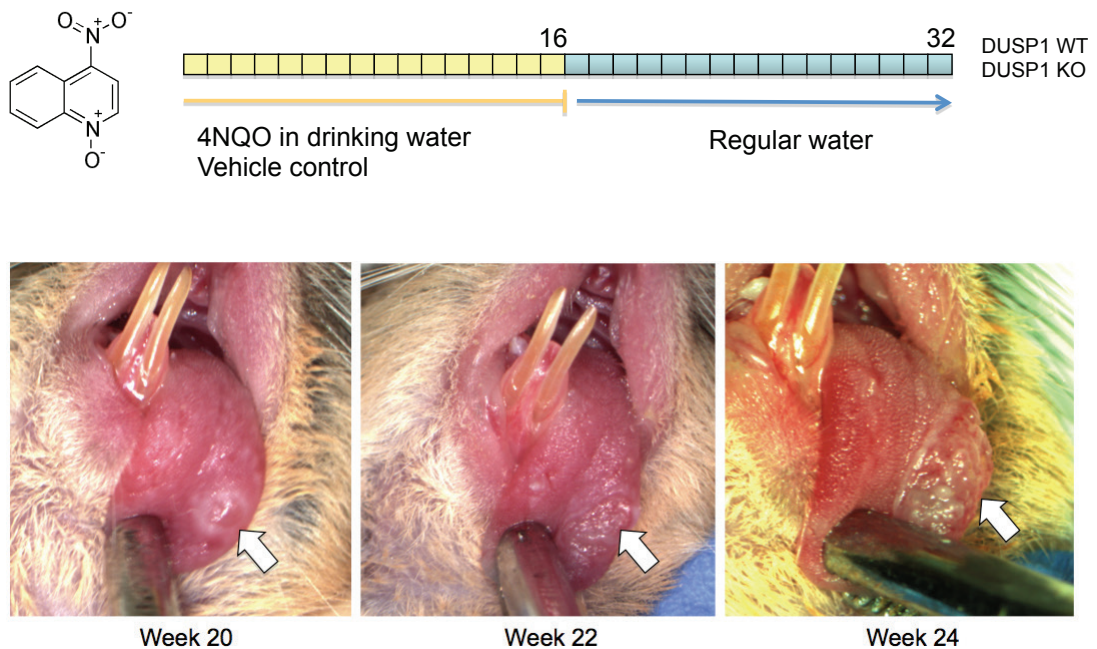


Figure 3-1. Induction of squamous cell carcinoma by 4-nitroquinoline 1-oxide treatment. Animals were treated with 4-nitroquinoline 1-oxide (4NQO), a DNA-adduct-forming agent, chemical structure shown, in the drinking water for 16 weeks. After 4NQO treatment, animals were switched to regular drinking water and monitored for the development of oral lesions during biweekly examinations. A representative series of images depict the typical progression of disease.

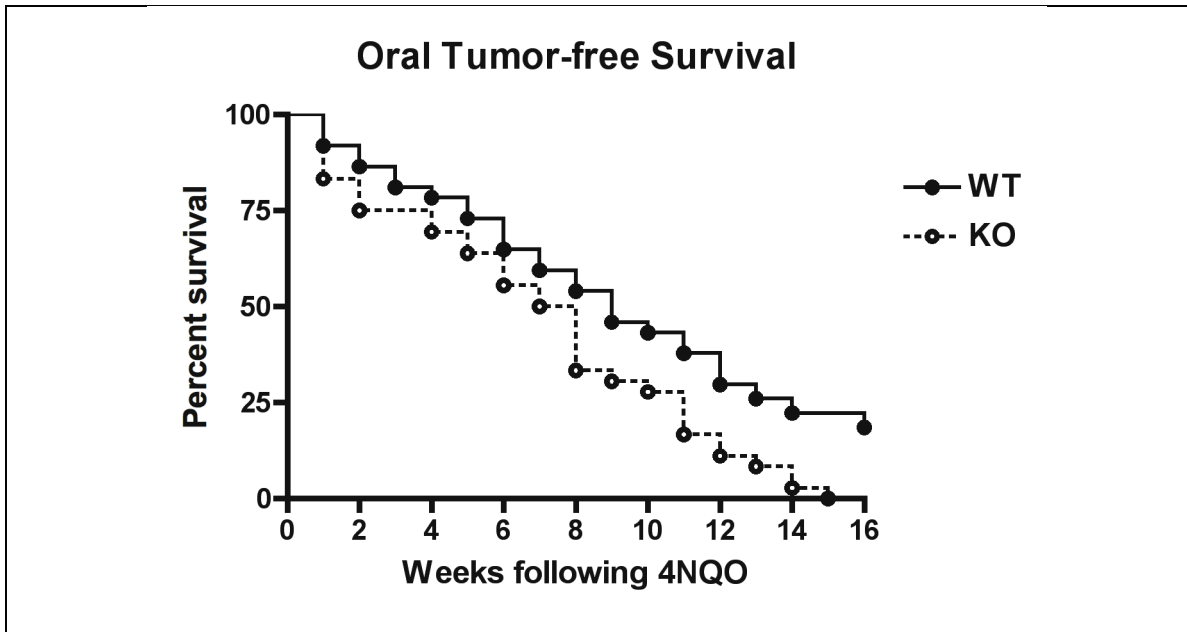


Figure 3-2. Tumor-free survival is decreased in *Dusp1* deficient animals. Following 4NQO treatment, the development of oral tumors was monitored through biweekly oral examinations under anesthesia. Tumor-free survival was assessed as the time until the first visible oral lesion. n = 36. Log-rank test, p = 0.0137.

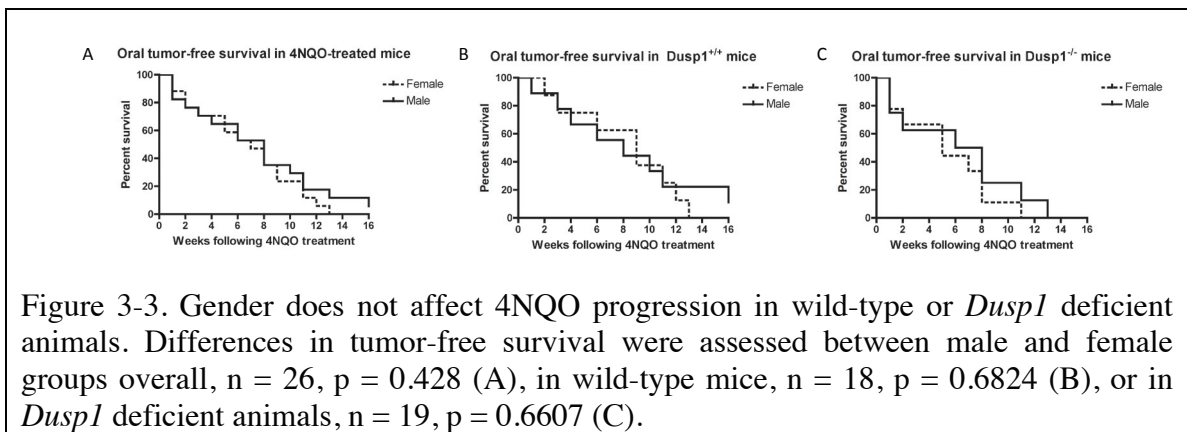


Figure 3-3. Gender does not affect 4NQO progression in wild-type or *Dusp1* deficient animals. Differences in tumor-free survival were assessed between male and female groups overall, n = 26, p = 0.428 (A), in wild-type mice, n = 18, p = 0.6824 (B), or in *Dusp1* deficient animals, n = 19, p = 0.6607 (C).

Weight gain was also monitored weekly as a surrogate for disease burden. *Dusp1* deficient mice ceased gaining weight at approximately 12-14 weeks, while wild-type mice continued weight gain until 15-16 weeks (Figure 3-4). *Dusp1* deficient mice have been shown to be resistance to diet-induced obesity, and previous studies have identified a role for DUSP1 in regulating metabolism within adipocyte and skeletal muscle tissue

(335, 336). However, *Dusp1* deficient and wild-type mice in vehicle treatment groups showed no difference in weight gain throughout the course of the model (Figure 3-5).

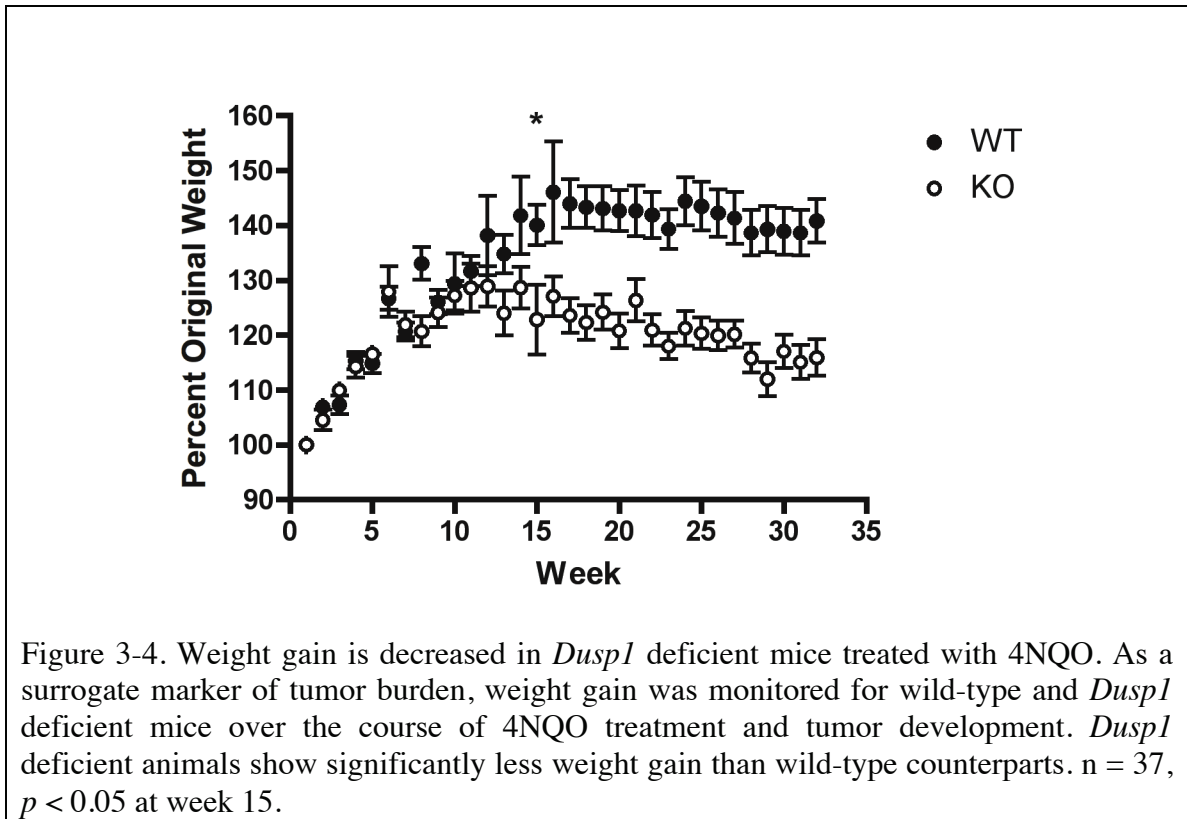


Figure 3-4. Weight gain is decreased in *Dusp1* deficient mice treated with 4NQO. As a surrogate marker of tumor burden, weight gain was monitored for wild-type and *Dusp1* deficient mice over the course of 4NQO treatment and tumor development. *Dusp1* deficient animals show significantly less weight gain than wild-type counterparts.  $n = 37$ ,  $p < 0.05$  at week 15.



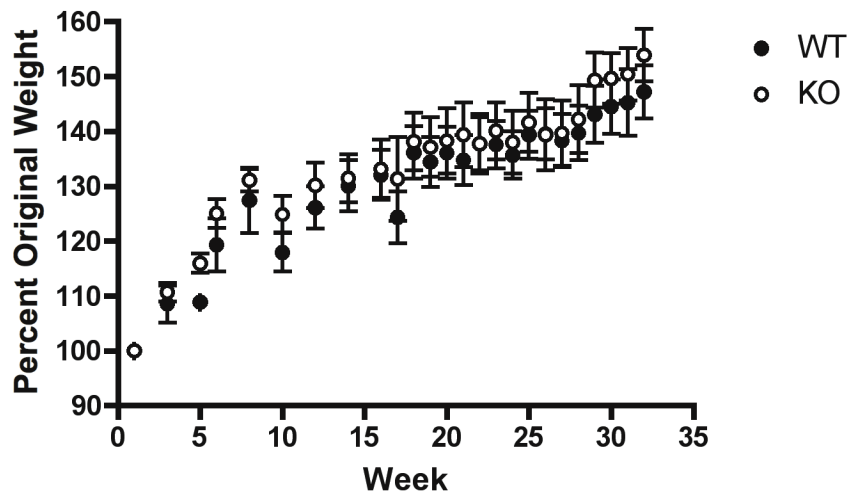


Figure 3-5. *Dusp1* deficiency does not affect weight gain in vehicle treatment groups. No differences were detected in weight gain between wild-type and *Dusp1* deficient mice throughout the course of the model. n = 15-17.

After 16 weeks of 4NQO treatment, animals were monitored for an additional 16 weeks and then euthanized for tissue collection. Any animal that lost greater than 20% of its original weight before 32 weeks was also sacrificed, under the assumption of severe tumor burden. At the time of tissue collection, full necropsies were performed, and major organs, including spleen, liver, lung, heart, esophagus, and cervical lymph nodes were collected for histological analysis. Total tumor burden on the tongue and esophagus were measured at that time with digital calipers. At the time of collection, nearly all animals had visible oral lesions. However, *Dusp1* deficient animals had larger oral tumors, and only *Dusp1* deficient animals had cases of cervical lymph node involvement or distant lung metastases (Figure 3-6). Furthermore, 4NQO treatment resulted in significantly enhanced esophageal tumor burden in *Dusp1* deficient animals (Figure 3-7).

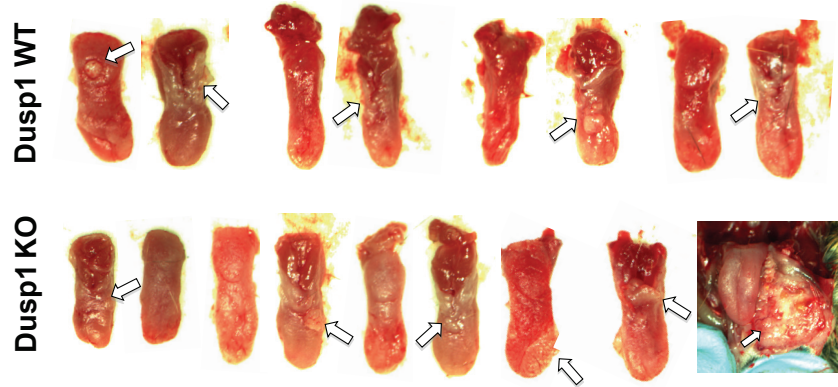


Figure 3-6. Representative panel of tongue tissues at the time of collection. After 32 weeks, animals were euthanized for tissue collection. By gross inspection, the majority of all animals had developed oral tumors. Views of the dorsal and ventral tongue from a representative panel of 4 wild-type and *Dusp1* deficient animals are shown. Instances of cervical lymph node metastasis were only observed within the *Dusp1* deficient group.

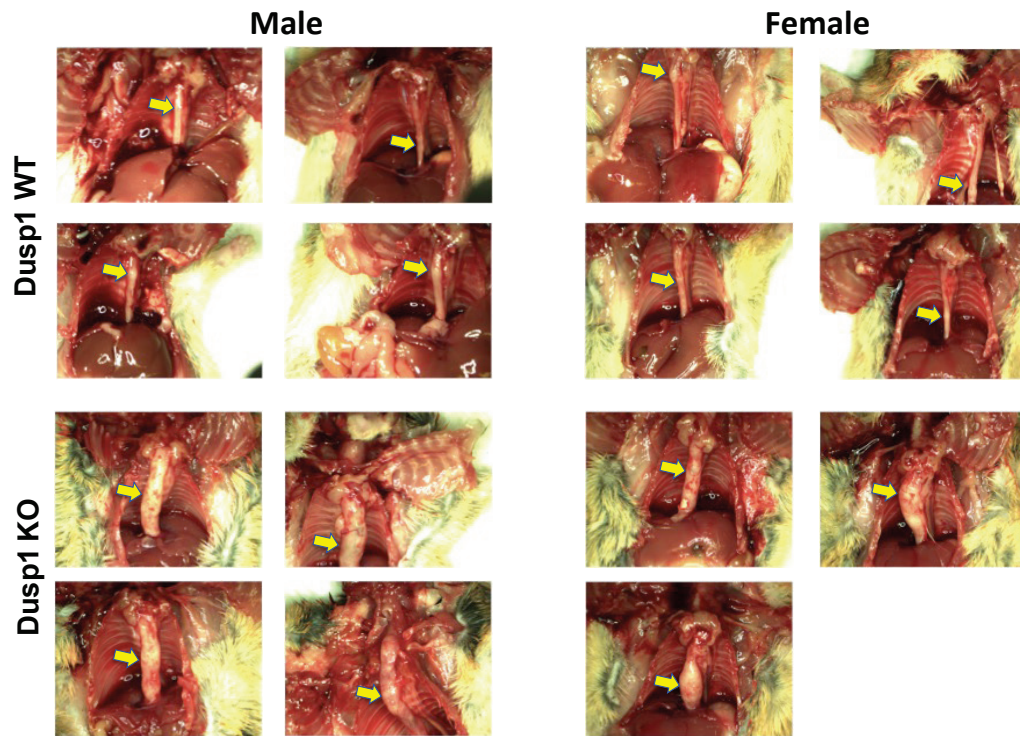


Figure 3-7. Enhanced esophageal tumor burden in *Dusp1* deficient animals. Esophageal tumors were detected within both wild-type and *Dusp1* deficient groups upon tissue collection. Images were taken at the 32 week timepoint. The heart and lungs were removed from the chest cavity to obtain a view of the esophagus. Male animals are shown on the left. Female animals are shown on the right. Wild-type animals are shown above. *Dusp1* deficient animals are shown below. Yellow arrows indicate grossly visible esophageal tumors.

Analysis of tumor burden at the model endpoint revealed significantly enhanced tumor burden, defined as cumulative tumor volume per individual animal, in *Dusp1* deficient mice (Figure 3-8). Histological tumor score, on a scale of normal, hyperplasia, dysplasia, *in situ* squamous cell carcinoma, and invasive squamous cell carcinoma, revealed advanced disease progression in the *Dusp1* deficient mice, with nearly all tissues

in the invasive SCC category, compared to wild-type mice which were more evenly distributed across dysplasia, *in situ*, and invasive lesions (Figure 3-9).

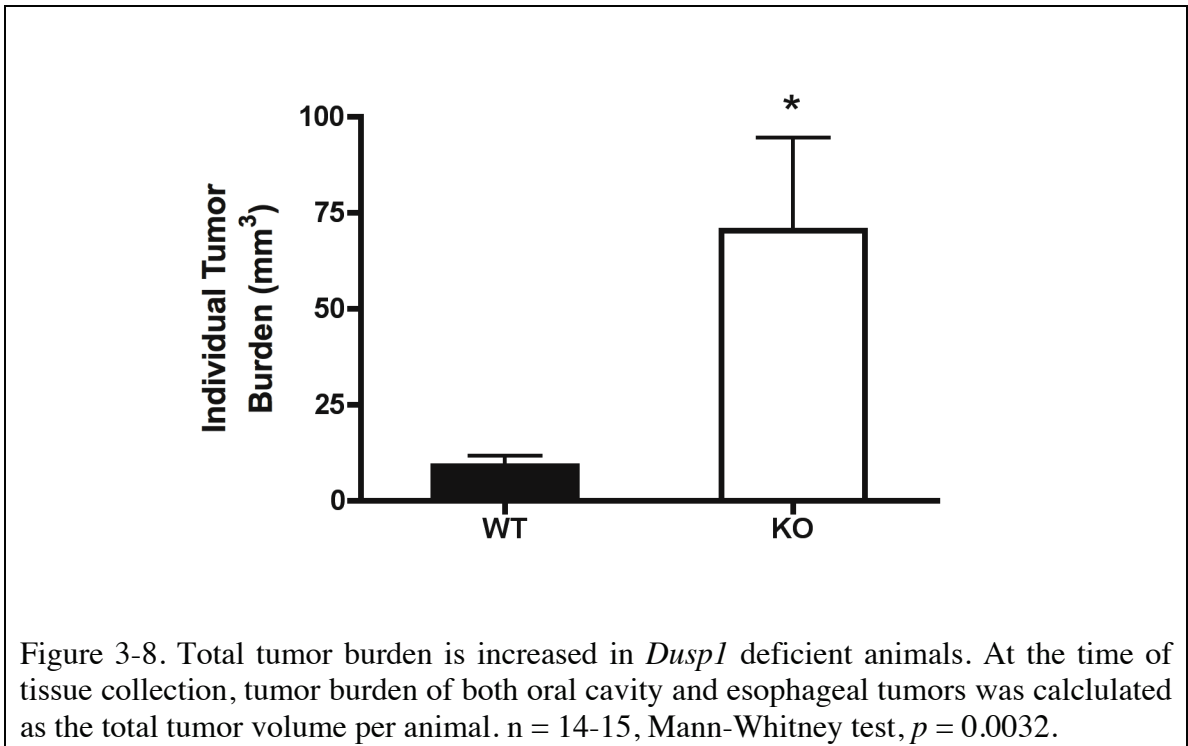


Figure 3-8. Total tumor burden is increased in *Dusp1* deficient animals. At the time of tissue collection, tumor burden of both oral cavity and esophageal tumors was calculated as the total tumor volume per animal. n = 14-15, Mann-Whitney test,  $p = 0.0032$ .

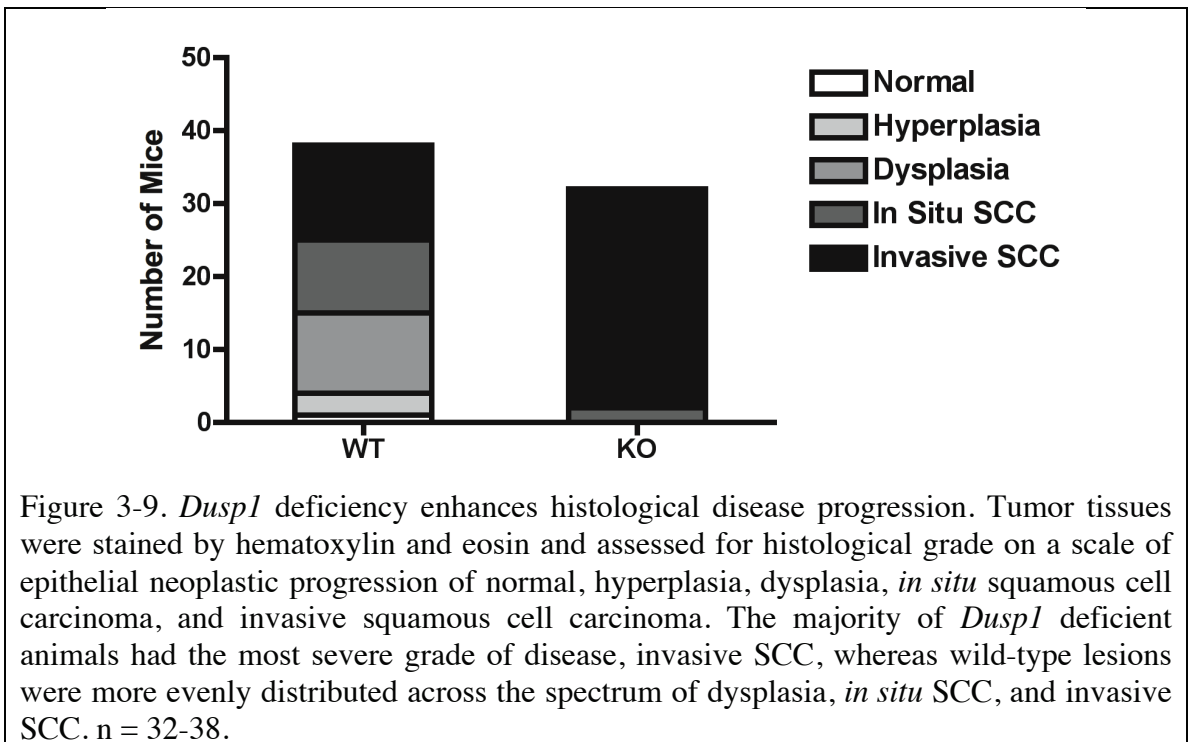


Figure 3-9. *Dusp1* deficiency enhances histological disease progression. Tumor tissues were stained by hematoxylin and eosin and assessed for histological grade on a scale of epithelial neoplastic progression of normal, hyperplasia, dysplasia, *in situ* squamous cell carcinoma, and invasive squamous cell carcinoma. The majority of *Dusp1* deficient animals had the most severe grade of disease, invasive SCC, whereas wild-type lesions were more evenly distributed across the spectrum of dysplasia, *in situ* SCC, and invasive SCC. n = 32-38.

***Dusp1* deficient tumors contain higher levels of inflammation.**

Histological examination of hematoxylin and eosin-stained tumor sections revealed marked inflammatory infiltrate in *Dusp1* deficient samples (Figure 3-10A). Tissue sections were scored for inflammation on a scale of 0–4 (0, normal mucosa; 1, minimal inflammation (occasional scattered granulocytes and leukocytes); 2, mild inflammation (scattered granulocytes with occasional infiltrates); 3, moderate inflammation (scattered granulocytes with patchy infiltrates); and 4, severe inflammation (multiple extensive areas with abundant granulocytes and marked infiltrates), as previously described (330). Histologically scored inflammation was significantly enhanced in *Dusp1* deficient tumor samples (Figure 3-10B). Levels of *Ptprc*, encoding the pan-leukocyte marker CD45, were quantified by qPCR in tumor tissues and also suggest an enhanced immune cell presence within *Dusp1* deficient tumors (Figure 3-10C).

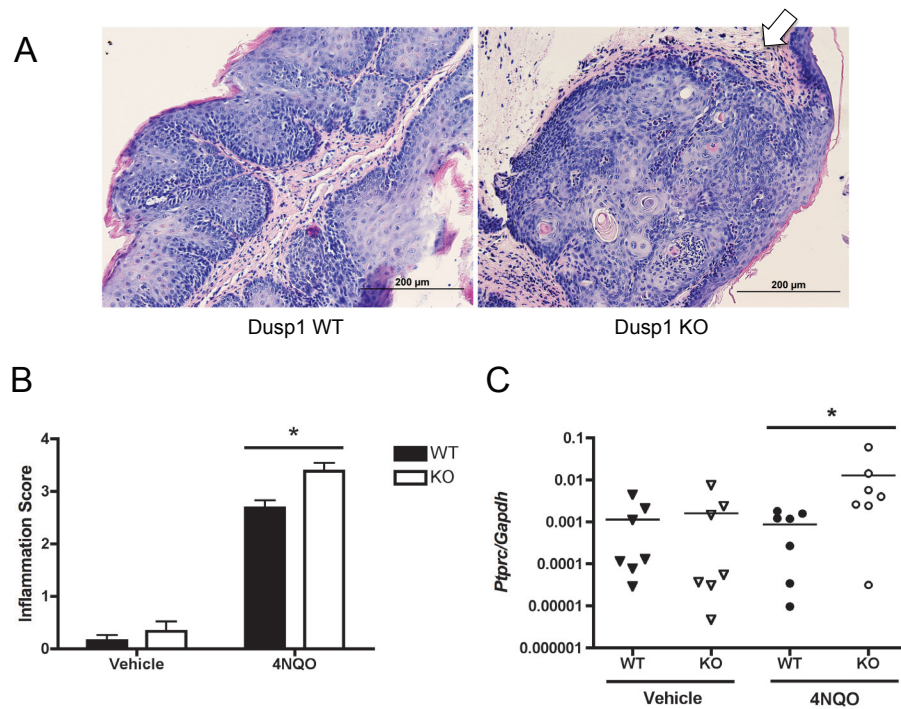


Figure 3-10. *Dusp1* deficient lesions have enhanced inflammatory infiltrate. (A) Hematoxylin and eosin-stained tissue sections show enhanced inflammatory infiltrate, indicated by the white arrow, surrounding the epithelial lesions in *Dusp1* deficient mice. (B) A histological inflammation score was generated based on numbers of infiltrating leukocyte and granulocytes, demonstrating significantly enhanced inflammation in the *Dusp1* deficient tumor tissues, compared to wild-type. n = 12-13 (vehicle), 31 (4NQO), Mann-Whitney test,  $p = 0.0005$ . (C) Expression of the pan-leukocyte marker *Ptpcr* (CD45) by qPCR was performed as a measure of leukocyte infiltrate in tissues from wild-type and *Dusp1* deficient animals. In tumor-bearing mice, *Ptpcr* was significantly elevated in *Dusp1* deficient tissues. n = 7, Mann-Whitney test,  $p = 0.0175$ .

Immunohistochemistry for the murine tissue macrophage marker F4/80 identified a notable macrophage presence within 4NQO-induced lesions. IHC analysis of a broader panel of tissue sections revealed enhanced macrophage infiltrate in tumor tissues, compared to vehicle control-treated animals, but no significant difference between wild-type and *Dusp1* deficient mice (Figure 3-11). Immunohistochemistry was also performed

for the monocyte-macrophage lineage marker CD11b and the myeloid-derived suppressor cell marker Ly6G, which demonstrated no significant difference in CD11b-positive cells but increased numbers of Ly6G-positive cells in *Dusp1* deficient tumors compared to wild-type tumor tissues (Figure 3-12).

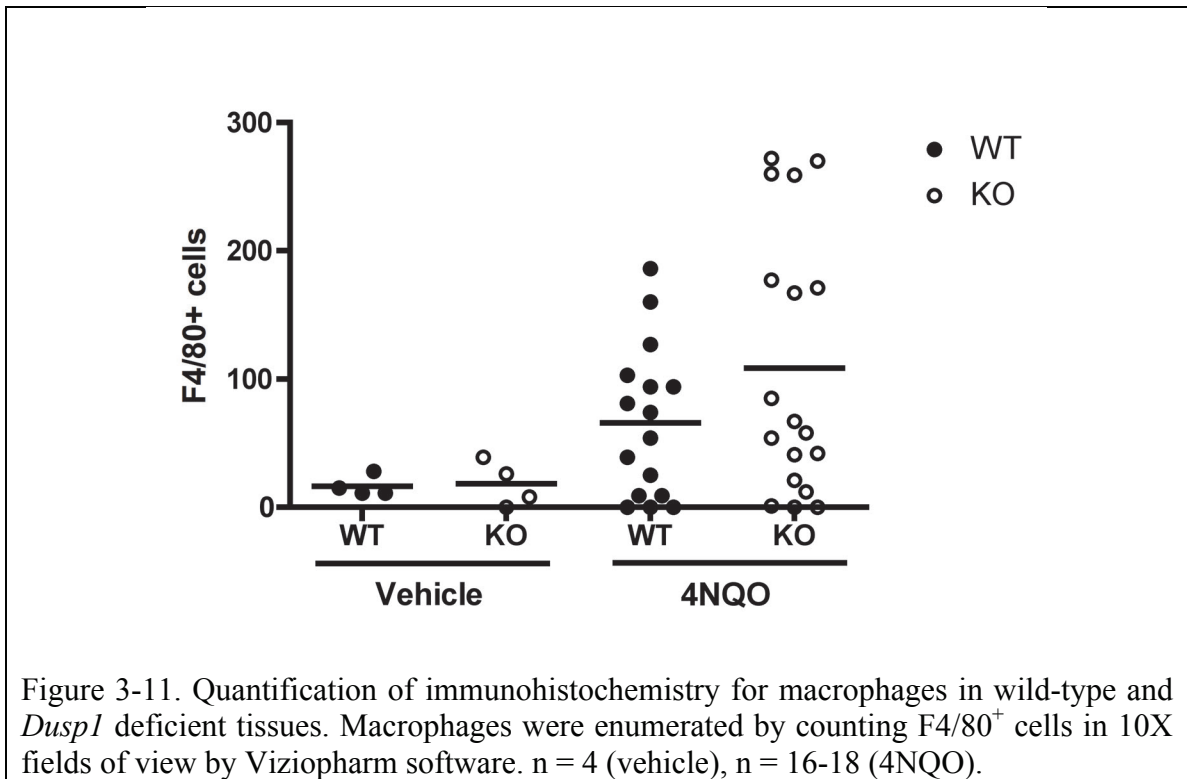


Figure 3-11. Quantification of immunohistochemistry for macrophages in wild-type and *Dusp1* deficient tissues. Macrophages were enumerated by counting F4/80<sup>+</sup> cells in 10X fields of view by Viziopharm software. n = 4 (vehicle), n = 16-18 (4NQO).

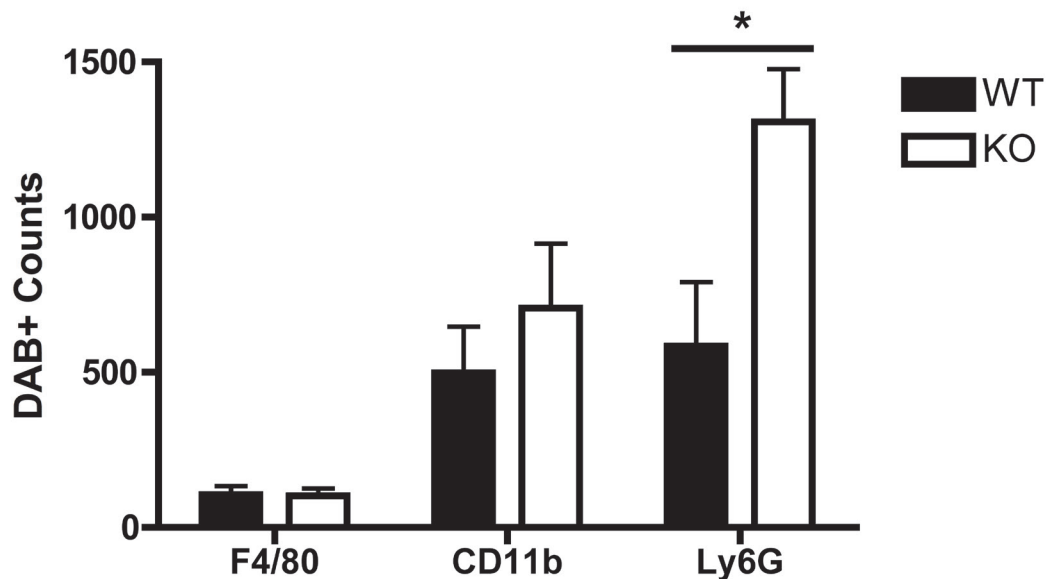
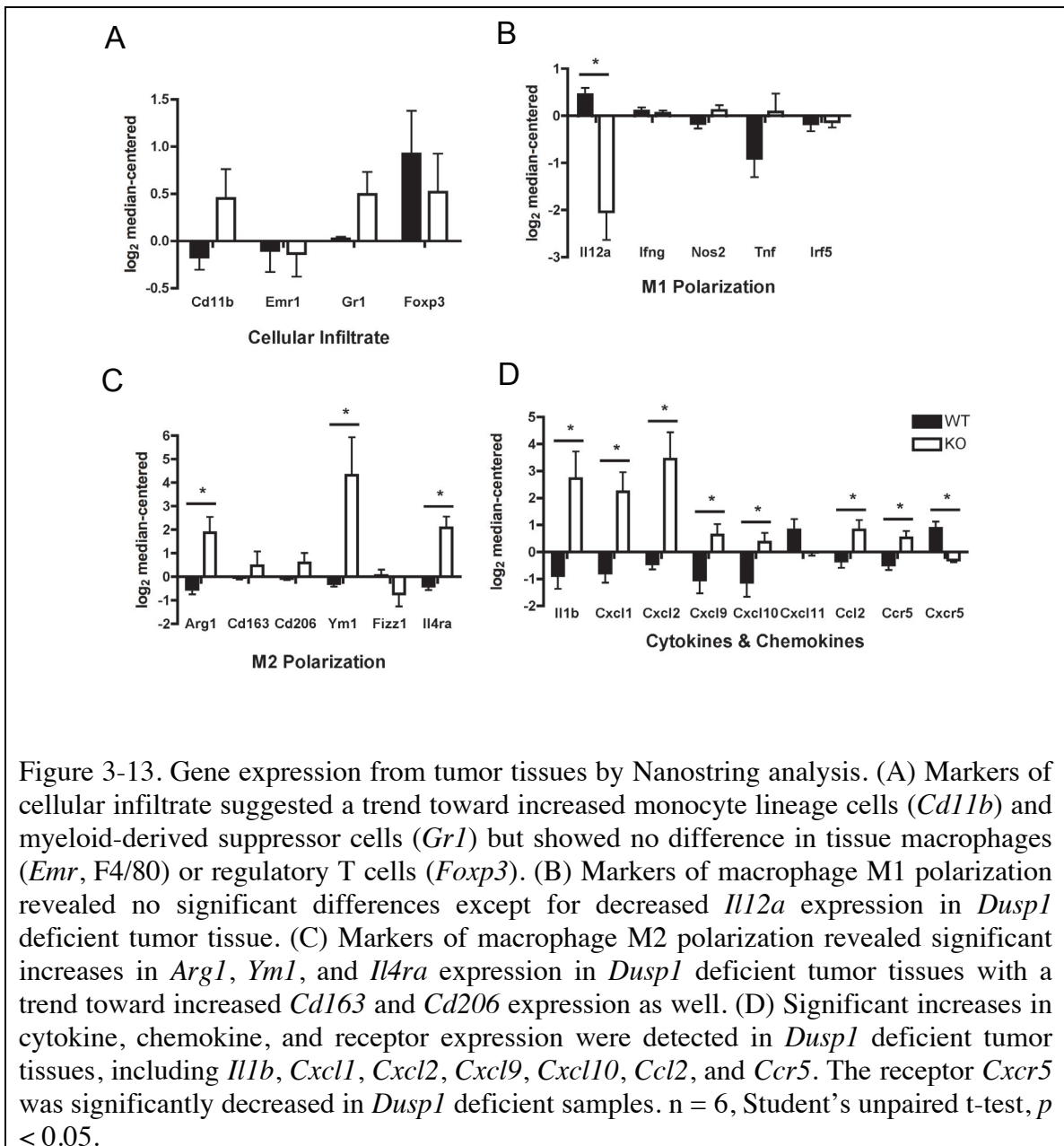


Figure 3-12. Quantification of immunohistochemistry for monocyte-myeloid lineage infiltrate in tumor tissues. Macrophages, monocyte-derived cells, and granulocytic cells were enumerated by counting F4/80<sup>+</sup>, CD11b<sup>+</sup>, or Ly6G<sup>+</sup> cells, respectively, by Viziopharm software in 10X field of view. No significant differences were detected in F4/80 or CD11b expression between wild-type and *Dusp1* deficient tumor tissues, but significantly increased numbers of Ly6G<sup>+</sup> cells were present in *Dusp1* deficient tumor tissues, compared to wild-type. n = 17-18 (F4/80), 8 (CD11b), 8-9 (Ly6G). p = 0.0176 (Ly6G).

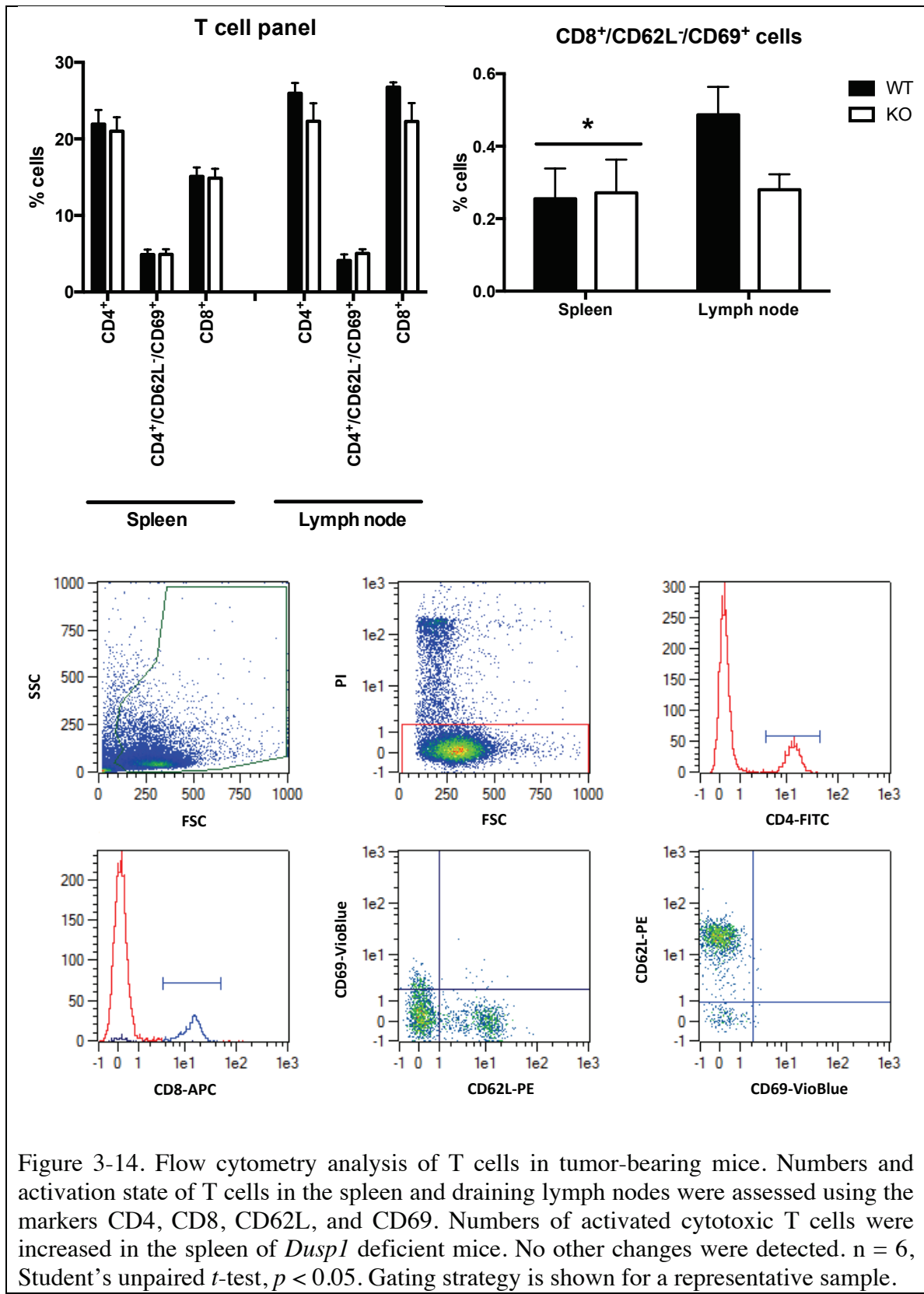
To understand how *Dusp1* deficiency alters the tumor environment, Nanostring analysis was performed on a set of tumor tissues from wild-type and *Dusp1* deficient mice. This quantitative analysis of mRNAs revealed alterations in a number of gene sets. Markers of cellular infiltrate did not show any significant differences in *Foxp3*, indicative of T regulatory cells, but suggested a trend toward increased *Cd11b* and *Gr1* expression. Similar to immunohistochemistry studies, no significant difference was detected in *Emr1*, encoding the murine macrophage marker F4/80 (Figure 3-13A). Markers of macrophage polarization, including *Nos2*, *Ifng*, *Tnf*, and *Irf5*, revealed no significant alterations in expression of M1-polarized macrophages, with the exception of decreased *Il12a* (Figure

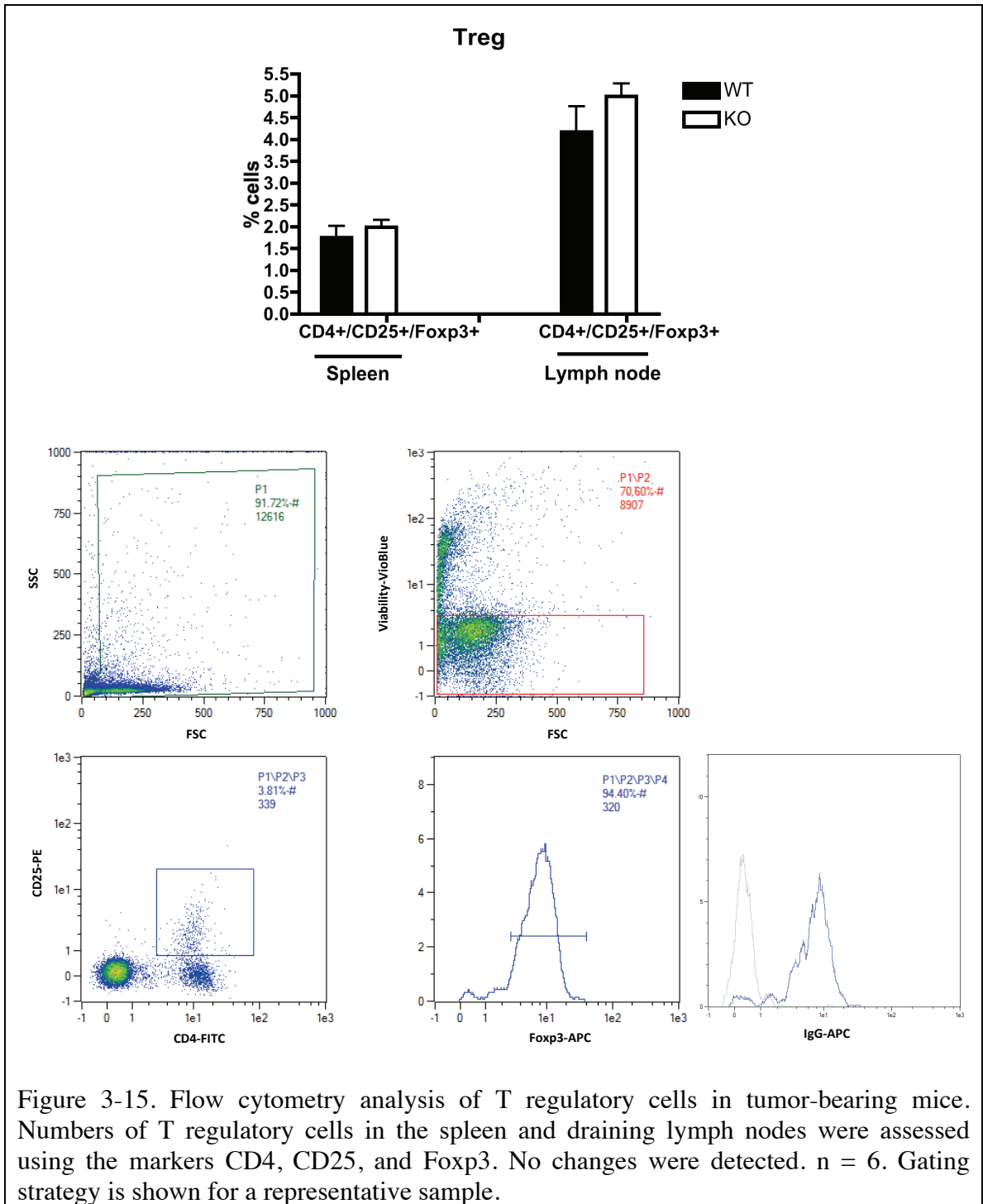


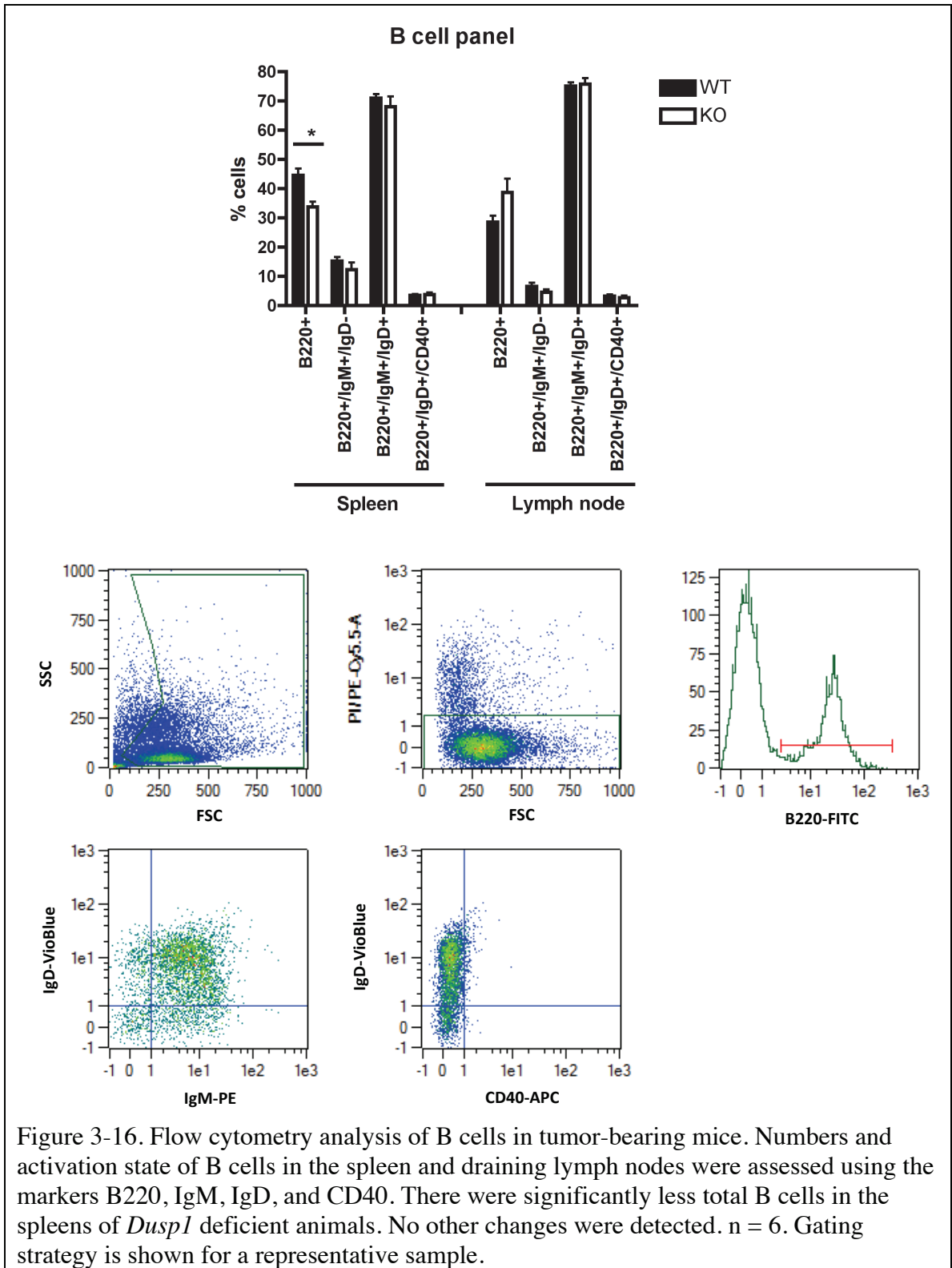
3-13B). However, several markers of M2-polarization were significantly increased in *Dusp1* deficient tumor tissues, including *Arg1* and *Il4ra*, with a trend toward increased *Cd163*, *Cd206*, *Ym1* and *Fizz1* (Figure 3-13C). Most significant were increased levels of inflammatory cytokines, chemokines, and several receptors. In this panel, *Il1b*, *Cxcl1*, *Cxcl2*, *Cxcl9*, *Cxcl10*, *Ccl2*, and *Ccr5* were all significantly elevated (Figure 3-13D). The receptor *Cxcr5* was also significantly down-regulated.



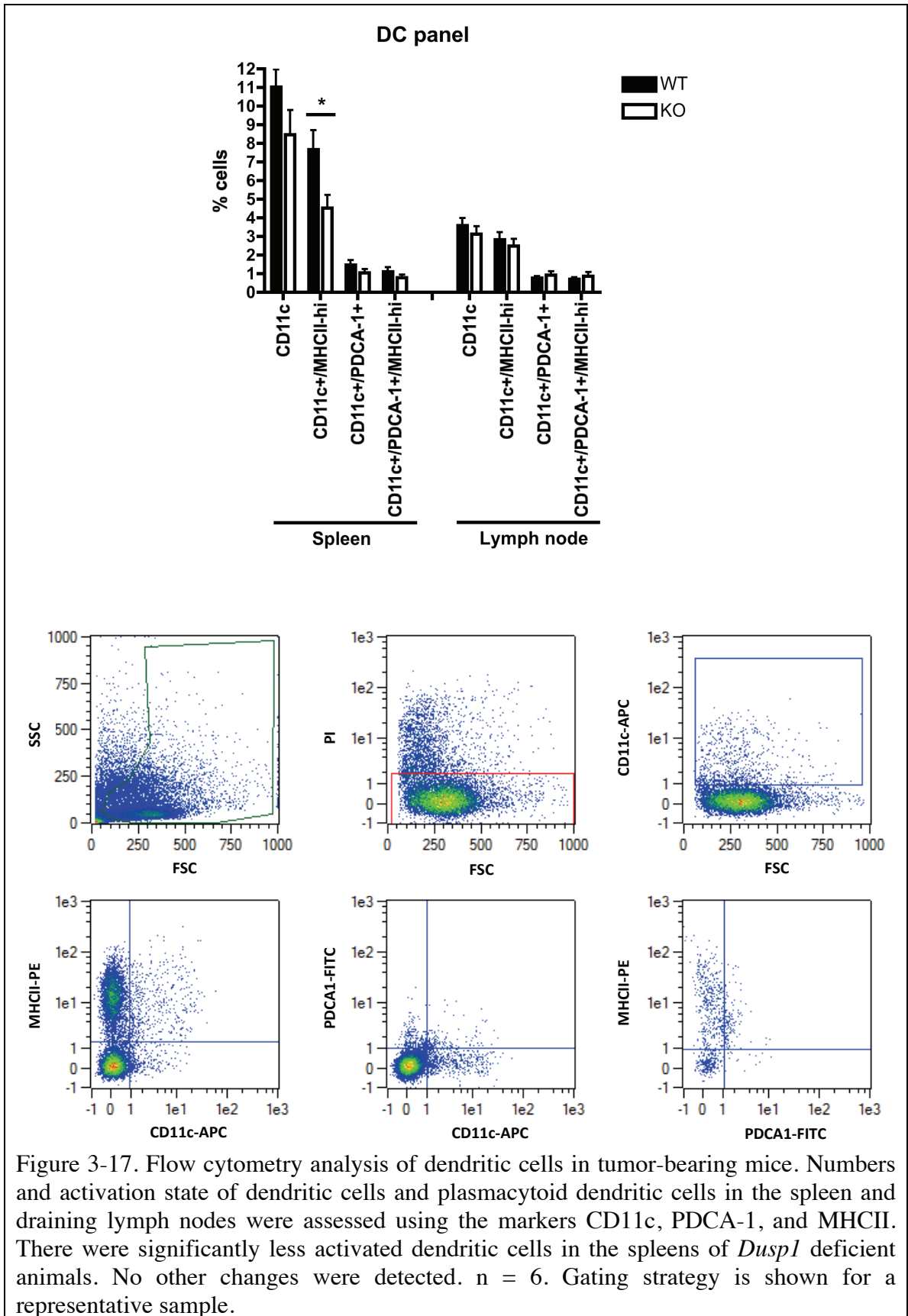
Flow cytometry analysis of immune cell populations within the spleen and draining cervical lymph nodes was performed to discern how *Dusp1* deficiency alters the cellular constituents within the immune system in tumor-bearing mice. The number of CD4<sup>+</sup> T helper and CD8<sup>+</sup> cytotoxic T cells was assessed, in addition to activation status, as determined by CD69<sup>+</sup> and CD62L<sup>-</sup> staining. No significant alteration in T cell numbers or activation was noted except for a moderate but significant increase in activated cytotoxic T cells within the spleen of *Dusp1* deficient mice (Figure 3-14). No significant differences were detected in levels of T regulatory cells, defined as CD4<sup>+</sup>/CD25<sup>+</sup>/Foxp3<sup>+</sup>, in either spleen or draining lymph nodes from wild-type and *Dusp1* deficient mice (Figure 3-15). Total number of B220<sup>+</sup> B cells was significantly decreased in the spleen of *Dusp1* deficient mice, but no differences in markers of B cell maturation or activation were detected in populations of B220<sup>+</sup>/IgM<sup>+</sup>/IgD<sup>-</sup>, B220<sup>+</sup>/IgM<sup>+</sup>/IgD<sup>+</sup>, or B220<sup>+</sup>/IgD<sup>+</sup>/CD40<sup>+</sup> cells either tissue (Figure 3-16).

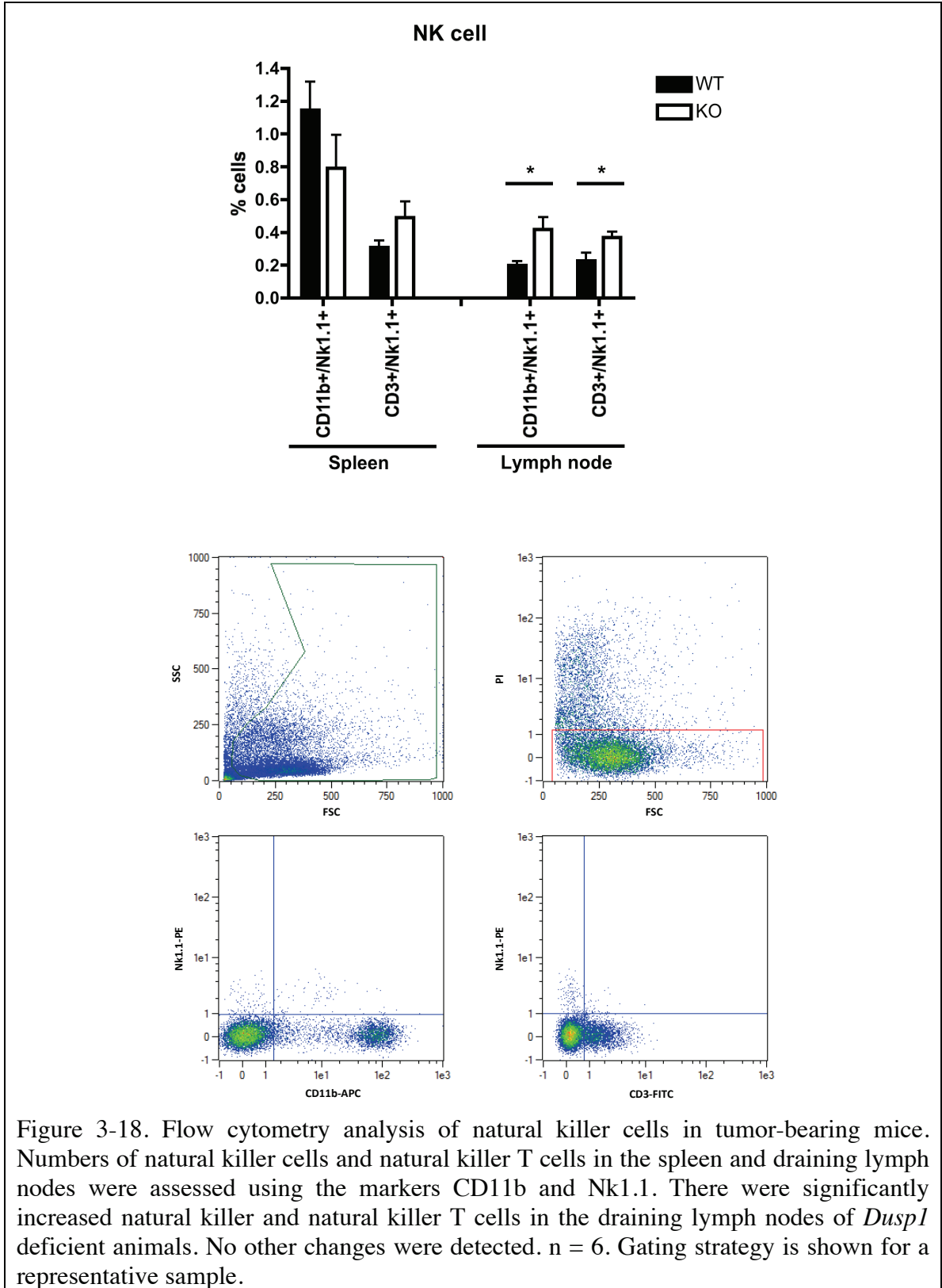




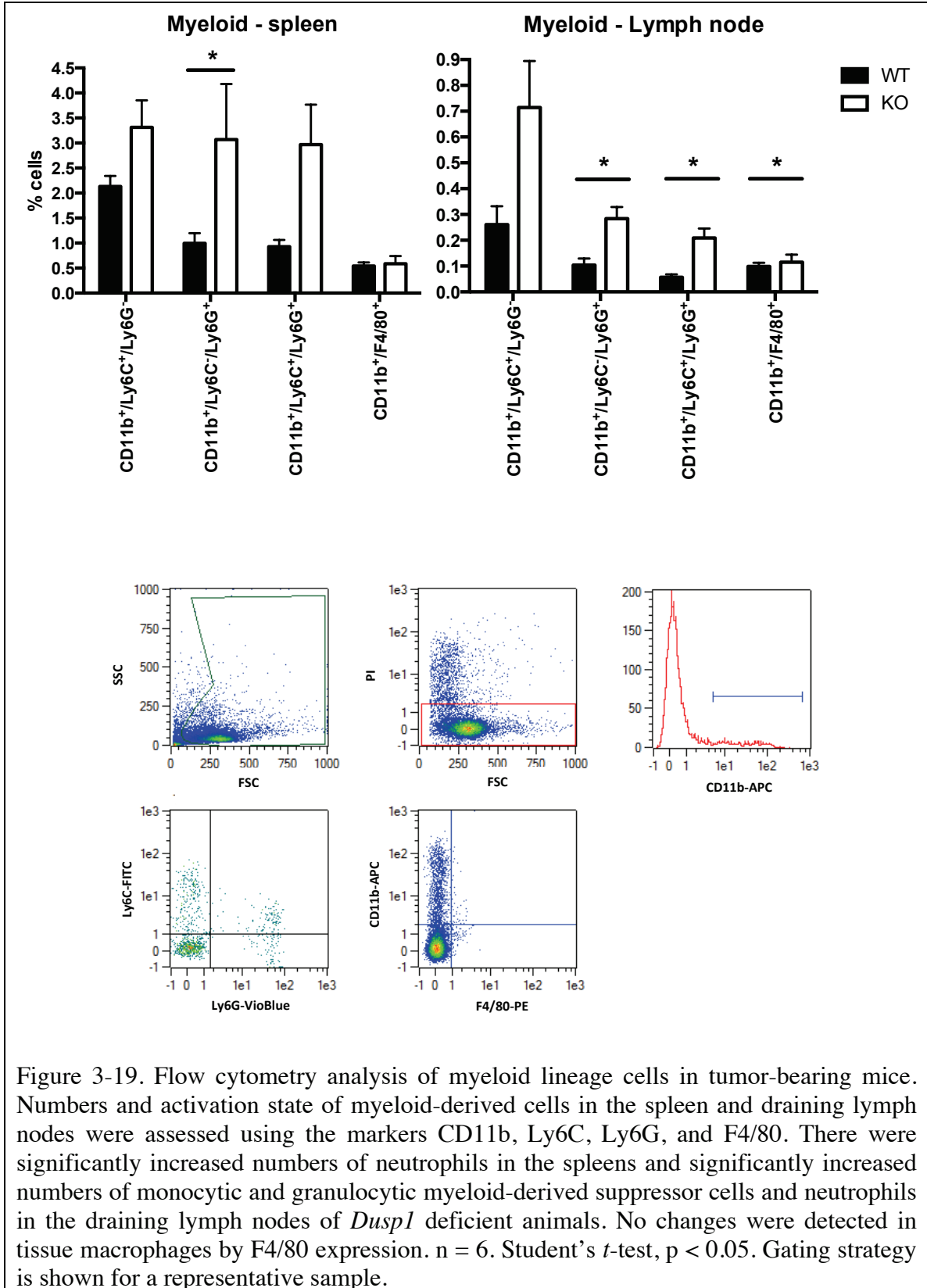


No changes were detected in total levels of dendritic cells, CD11c<sup>+</sup>, or plasmacytoid dendritic cells, CD11c<sup>+</sup>/PDCA-1<sup>+</sup>, in either tissue, but there were significantly decreased levels of activated dendritic cells, CD11c<sup>+</sup>/MHCII<sup>hi</sup> within the spleen of *Dusp1* deficient mice. No changes in activated plasmacytoid dendritic cells were noted in either tissue (Figure 3-17). No changes in natural killer cell populations were detected within the spleen. However, natural killer cells, Cd11b<sup>+</sup>/Nk1.1<sup>+</sup>, and natural killer T cells, CD3<sup>+</sup>/Nk1.1<sup>+</sup>, were significantly elevated in *Dusp1* deficient lymph nodes (Figure 3-18). The most abundant changes were noted in the cells of the myeloid lineage. Cells of interest were defined as monocytic myeloid derived suppressor cells, CD11b<sup>+</sup>/Ly6C<sup>+</sup>/Ly6G<sup>-</sup>, granulocytic myeloid-derived suppressor cells, CD11b<sup>+</sup>/Ly6C<sup>-</sup>/Ly6G<sup>+</sup>, neutrophils, CD11b<sup>+</sup>/Ly6C<sup>+</sup>/Ly6G<sup>+</sup>, or macrophages, CD11b<sup>+</sup>/F4/80<sup>+</sup>. In the spleen, there was a trend toward increased levels of both myeloid derived suppressor cells with significant increase in neutrophils in the *Dusp1* deficient mice. In the lymph node, all populations were elevated in *Dusp1* deficient samples, with the exception of tissue macrophages (Figure 3-19).









***Effects of *Dusp1* deficiency on MAPK activation in oral tumor epithelium.***

To determine how the absence of *Dusp1* affects MAPK activation, esophageal tumor tissue lysates were probed for levels of phosphorylated and total MAPK levels (Figure 3-20). Esophageal tumor tissues were chosen as their larger size enabled a sampling of increased tumor:epithelial ratio, compared to tongue tumors which were unable to be cleanly dissected from surrounding epithelium due to their small size. Western blot analysis revealed no significant changes in MAPK expression or activation in tissues from vehicle-treated mice. However, most striking were elevated levels of total MAPK expression, particularly p38 and ERK1/2, despite equal amounts of protein by bicinchoninic acid quantification and expression of the housekeeper glyceraldehyde 3-phosphate dehydrogenase (GAPDH). Phospho-ERK1/2 MAPK expression was decreased in *Dusp1* deficient tumor tissues compared to wild-type. No significant difference was seen in phospho-p38 MAPK expression between *Dusp1* deficient tumor tissues compared to wild-type; however, densitometry analysis only revealed increases in total MAPK levels (Figure 3-21).

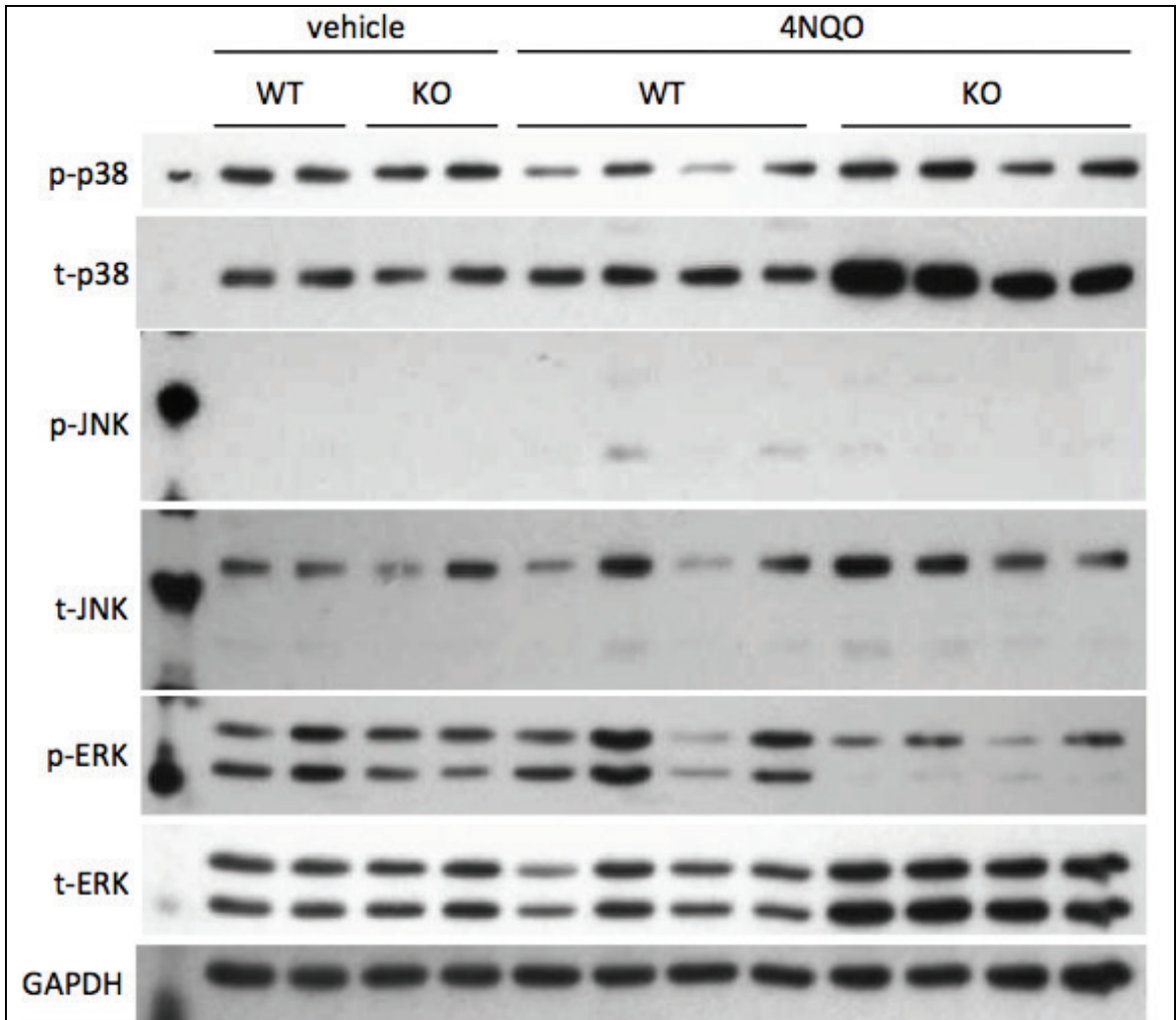
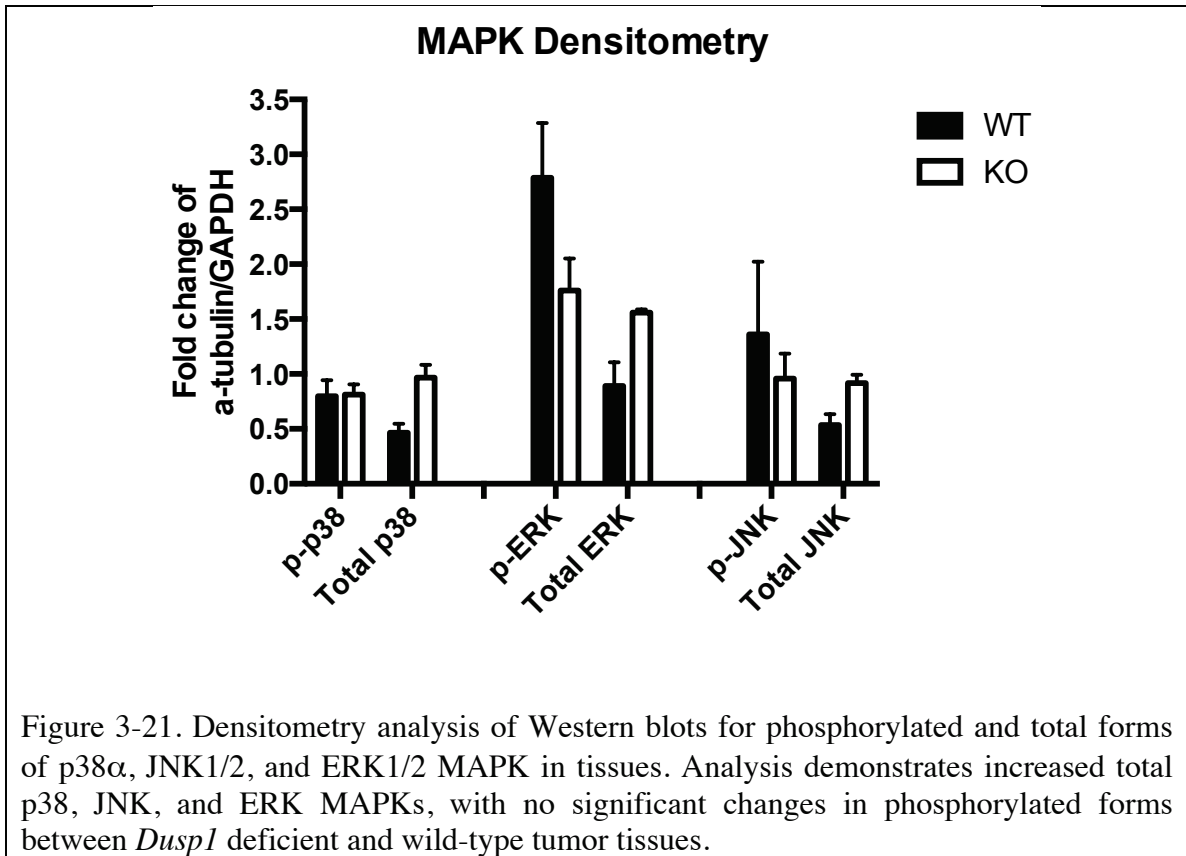


Figure 3-20. MAPK expression and activity in wild-type and *Dusp1* deficient tissues. Western blots for phosphorylated and total forms of p38a, JNK1/2, and ERK1/2 MAPK in tissues show elevations in phospho-p38 in *Dusp1* deficient tumor tissues compared to wild-type. More striking are elevations in total p38, JNK, and ERK MAPKs in *Dusp1* deficient tissue samples compared to wild-type. No significant changes are noted between wild-type and *Dusp1* deficient tumor-free mice.



To address whether alterations in MAPK activation were due to tumor epithelial tissue, immunohistochemistry was performed to assess levels of phosphorylated MAPK expression in tumor epithelium (Figure 3-22). Only the tumor epithelium was assessed in scoring the staining percentage and positivity. No significant differences were detected in levels of phosphorylated JNK or ERK MAPK. Although levels of phospho-p38 MAPK were elevated in tumor tissues compared to vehicle-treated tissues, no differences were detected in wild-type, compared to *Dusp1* deficient mice (Figure 3-23). Immunohistochemistry for the proliferation marker Ki67 also revealed no significant differences in proliferation rates between wild-type and *Dusp1* deficient tumor tissues. Immunohistochemistry for markers of angiogenesis and proliferation, CD31 and TUNEL respectively, were not quantified, as TUNEL expression was extensive throughout tissue

sections due to physiologic epithelium turnover, and minimal CD31 positivity was detected in these tissues. The small size of many of the oral cancer tissues made it difficult obtain multiple serial sections to accurately assess angiogenesis by CD31 expression.

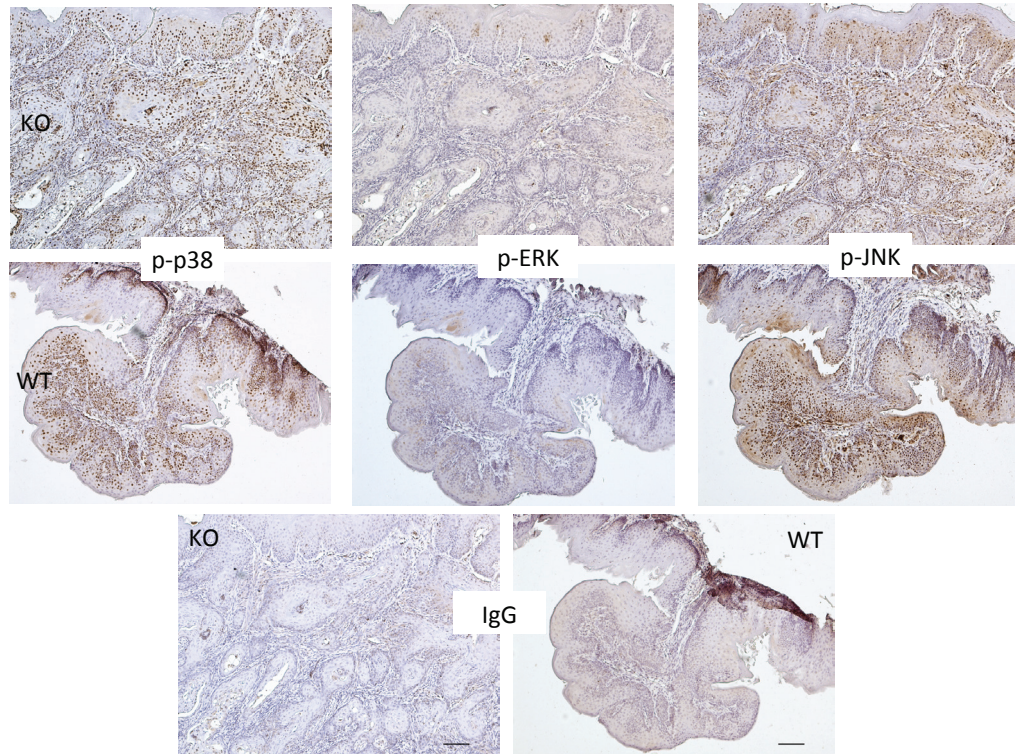


Figure 3-22. Immunohistochemistry of phosphorylated MAPK in oral tumor tissues. Immunohistochemistry was performed to detect phospho-p38, ERK1/2, and JNK1/2 MAPK in oral tumor tissues in wild-type and *Dusp1* deficient animals. Representative staining from serial sections for the three kinases and antibody isotype controls are shown from data in Figure 3-24. The majority of tissues showed phospho-p38 MAPK activation, with little phospho-ERK or phospho-JNK. n = 12 (vehicle), 15 (4NQO).

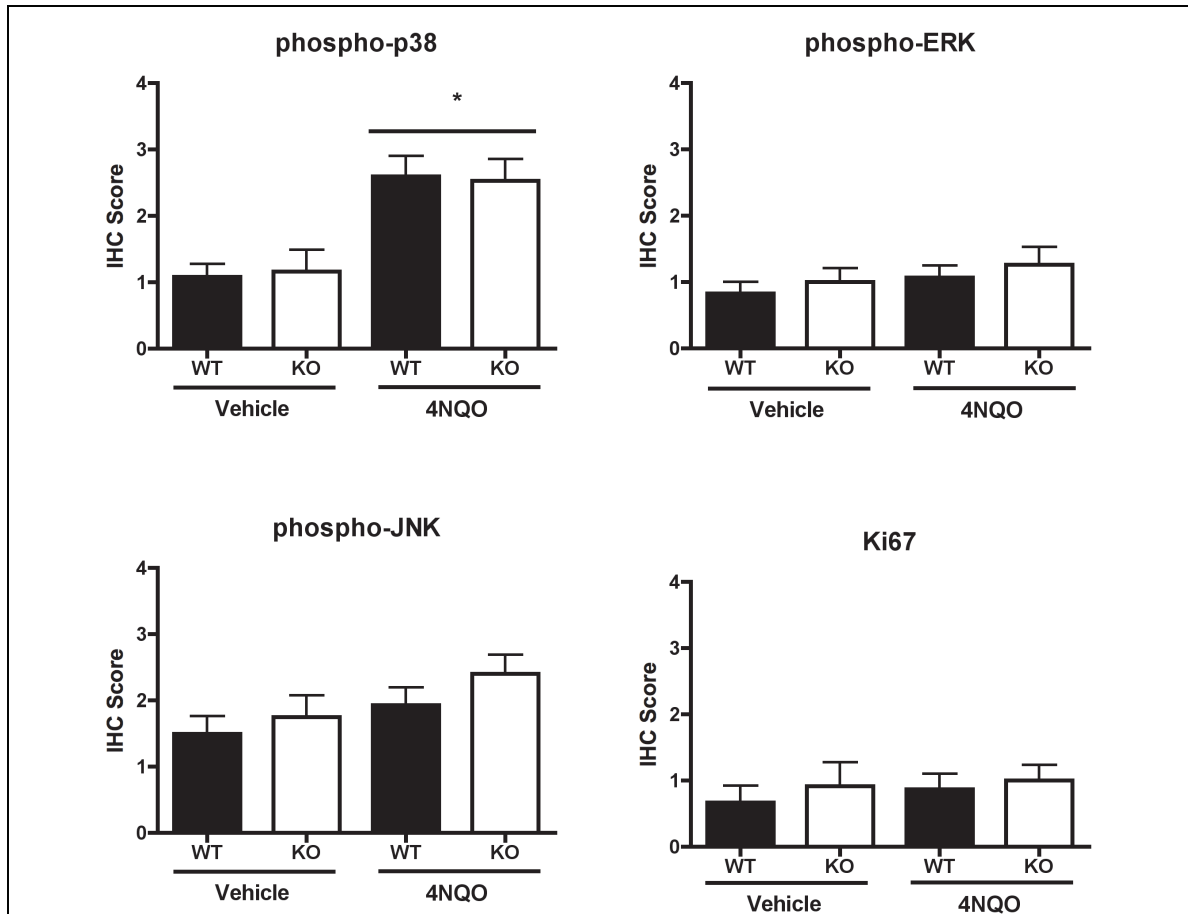


Figure 3-23. Quantification of MAPK and Ki67 immunohistochemistry staining. Immunohistochemistry scores were generated based on assessment of staining intensity and area within the tumor epithelium. Of the three MAPK, p38 was significantly increased in tumor tissues compared to vehicle-treated tissues. However, no differences were detected in MAPK activity between wild-type and *Dusp1* deficient tumor epithelium. In addition, no significant differences in tumor proliferation, as assessed by Ki67 staining were detected. n = 12 (vehicle), 15 (4NQO). Kruskal-Wallis test,  $p = 0.006$ .

### ***Effect of hematopoietic *Dusp1* deficiency in carcinogen-induced oral cancer.***

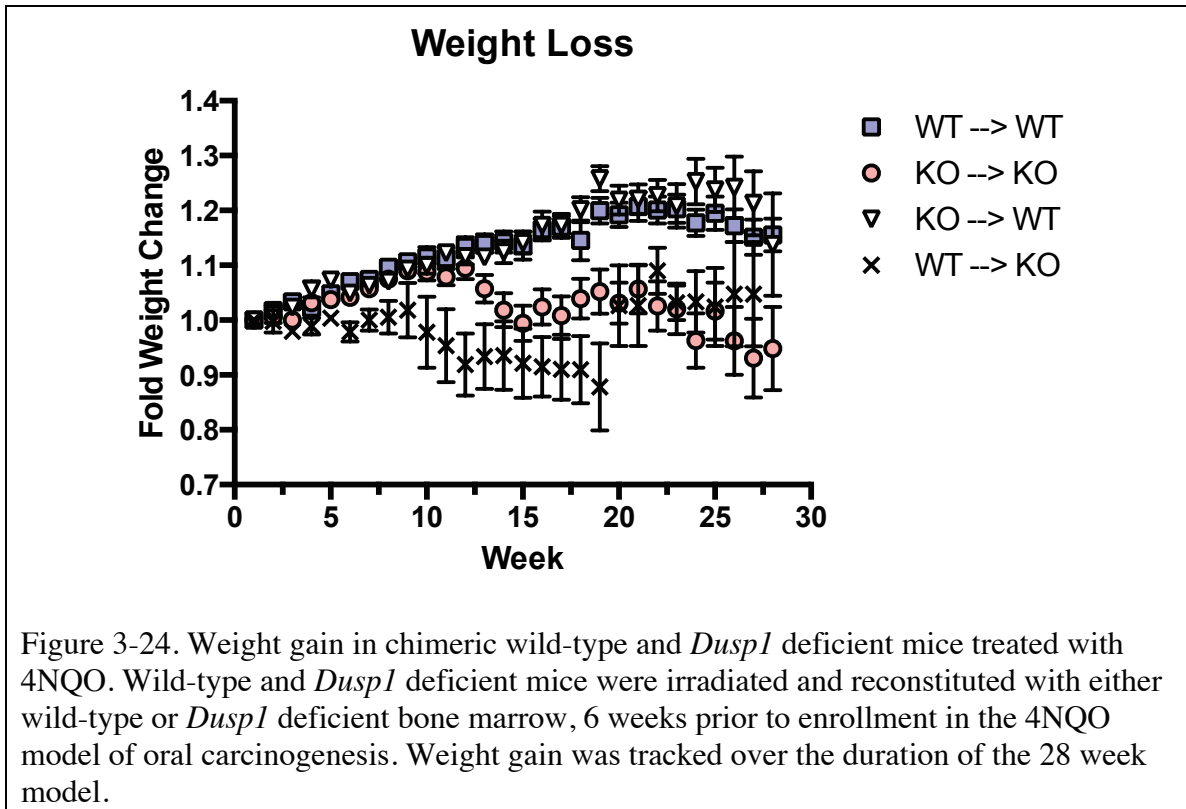
To delineate the contribution of the immunologic constituents versus tumor epithelium to the advanced disease phenotype in *Dusp1* deficient mice, bone marrow chimeras were generated with *Dusp1* deficient and wild-type mice on a C57BL/6 background and wild-type mice bearing the congenic allele CD45.1. Engraftment was assessed by expression of the CD45 alleles on peripheral blood at 6-8 weeks after

transplant. After transplant and engraftment, animals were treated with 4NQO at 50µg/mL for 16 weeks, at a treatment dose and schedule as previously described (337). Earlier treatment of wild-type and *Dusp1* deficient mice on a mixed C57/129 genetic background required a lower dose of 25µg/mL, due to enhanced susceptibility of *Dusp1* deficient mice to the carcinogen and were monitored for an extended period of 32 weeks to achieve sufficient tumor development on wild-type animals.

After backcrossing to a C57BL/6 genetic background, the *Dusp1* deficient mice and chimeras were treated with the originally described 50µg/mL dose and monitored for a total of 28 weeks, rather than 32 weeks. Weight gain was assessed as a surrogate measure of tumor burden (Figure 3-24). Comparison of wild-type and *Dusp1* deficient mice both on a C57BL/6 genetic background demonstrates the same enhanced susceptibility of *Dusp1* deficient animals to 4NQO-induced disease as previously seen on a mixed genetic background. Chimeric wild-type animals reconstituted with *Dusp1* deficient hematopoietic cells had similar changes in weight to wild-type animals. Surprisingly, chimeric *Dusp1* deficient animals reconstituted with wild-type hematopoietic cells were more susceptible to 4NQO-induced weight loss than wild-type animals or wild-type animals with *Dusp1* deficient hematopoietic cells. These chimeric animals appeared to be more sensitive to 4NQO-induced weight loss early in the model, before returning to a similar pattern of weight change to the *Dusp1* deficient animals by week 20. These results suggest *Dusp1* deficiency in the radiation-resistant compartment is responsible for the increased disease burden described in Figure 3-4. At this time, additional analyses of histologic disease and inflammation scores from paraffin-embedded tumor tissues as well as mRNA and protein analyses from snap frozen tissues



remain to be evaluated to assess how hematopoietic *Dusp1* deficiency alters tumor-associated inflammation.



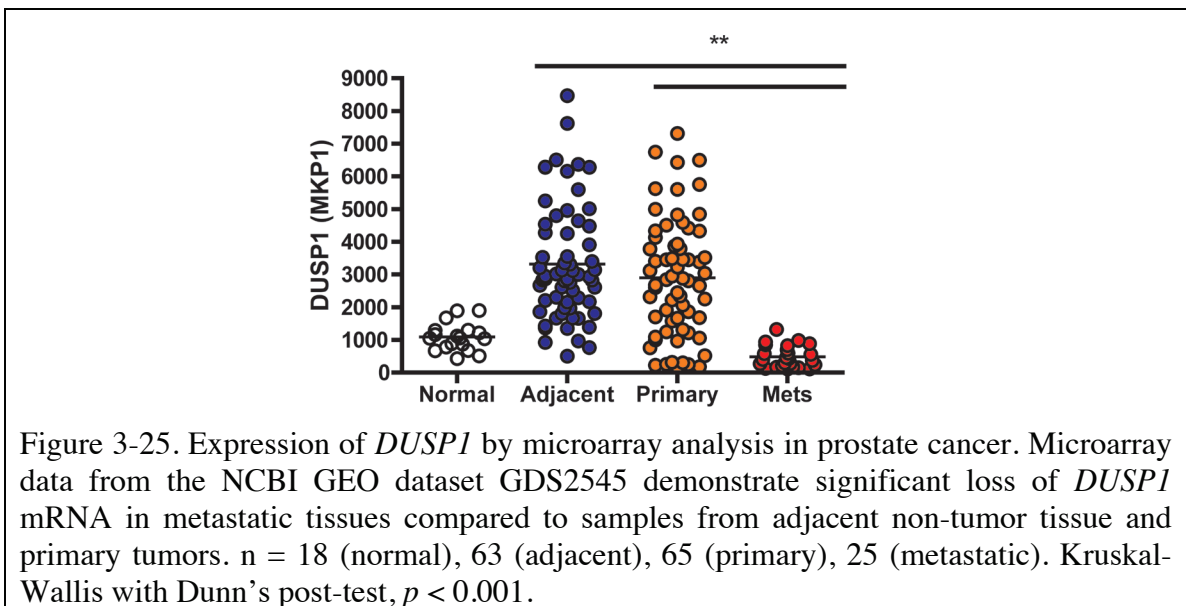
***Dusp1* deficient mice support enhanced syngeneic tumor growth.**

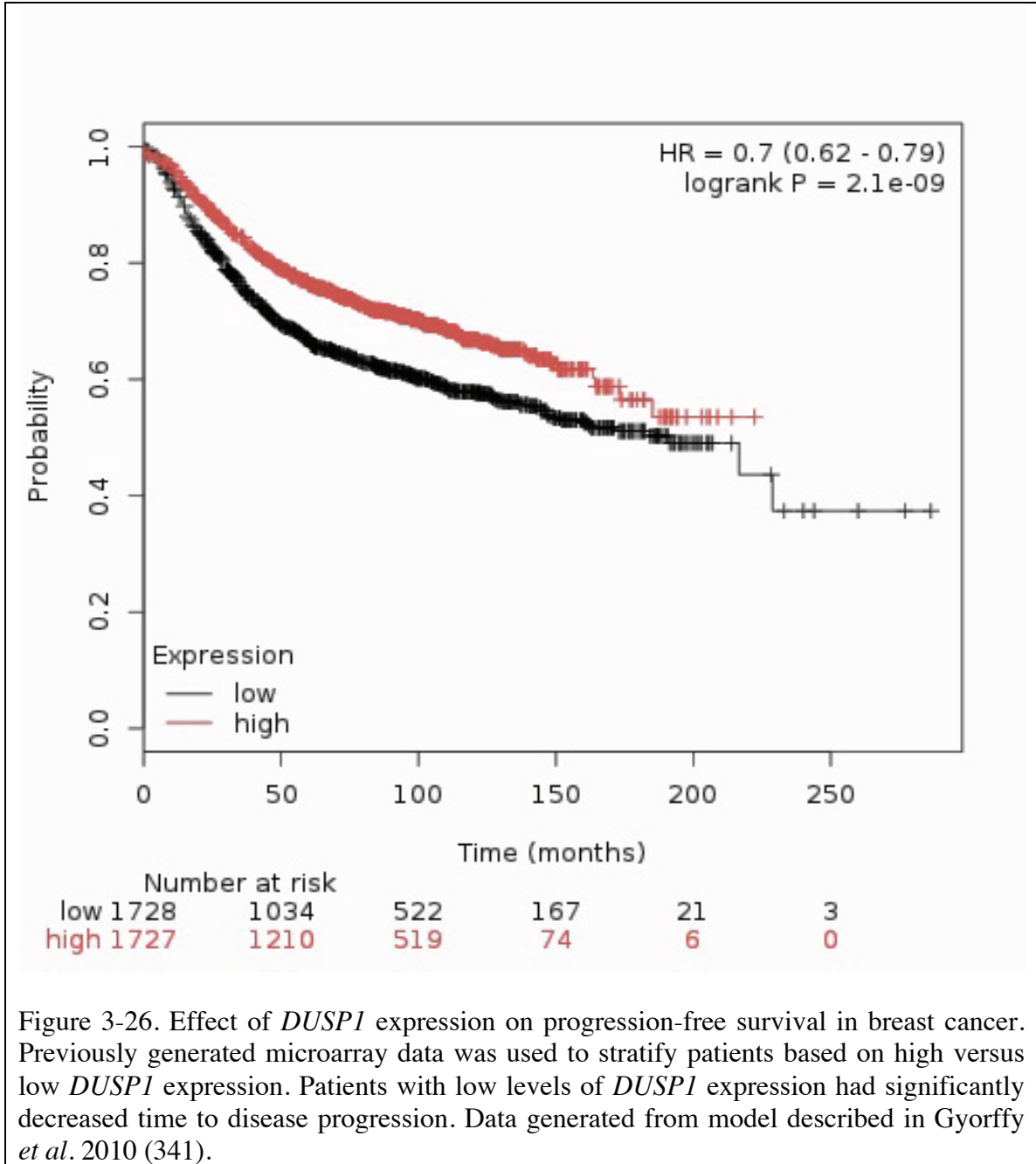
To understand how *Dusp1* expression within only the microenvironment affects tumor progression, wild-type and *Dusp1* deficient mice were injected with syngeneic tumor cells to form subcutaneous allografts. Few murine oral cancer cell lines have been described, with SCCVII being the best characterized. Although SCCVII readily forms tumors in mice (338), the cell line was derived from a mouse on the C3H/HeJ genetic background, which is protected from endotoxin challenge due to a spontaneous *Tlr4* mutation (339). Murine cancer cell lines on a C57BL/6 background are limited to other



tissue origins, including colorectal, breast, and prostate adenocarcinomas, melanoma, lymphoma, and lung carcinomas.

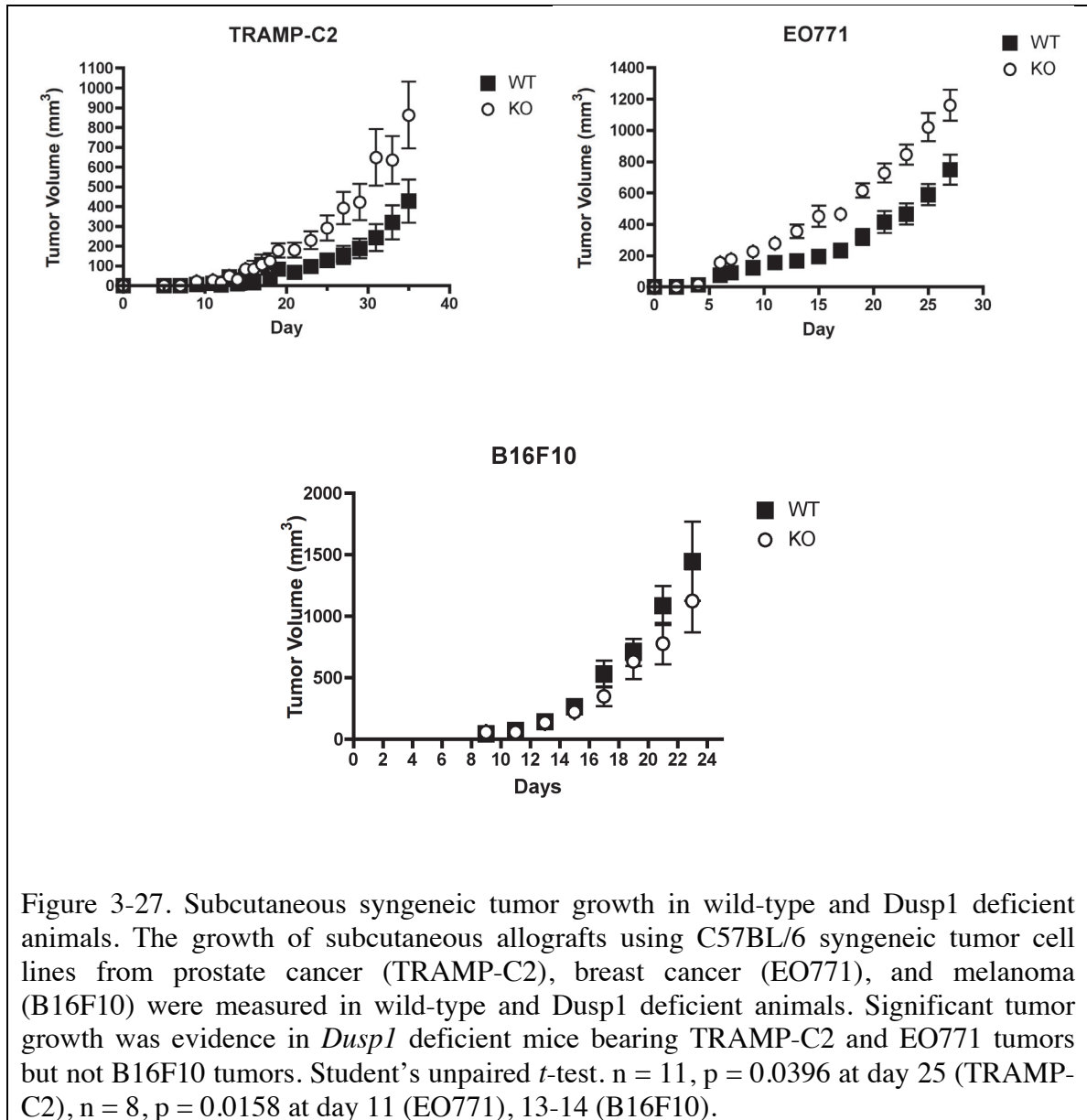
Previous studies have demonstrated *DUSP1* expression is lost in advanced stages of human breast and prostate cancer (174, 176, 340). Furthermore, analysis of *DUSP1* gene expression in publicly available databases has revealed the same trend, with loss of *DUSP1* expression in metastatic lesions compared to adjacent non-tumor tissue and primary prostate cancer tissues (Figure 3-25). In breast cancer, patients stratified as having high *DUSP1* expression compared to those with low *DUSP1* expression have significantly enhanced progression-free survival (Figure 3-26). Based on these data suggesting these malignancies mirror the trend seen in HNSCC, the murine prostate adenocarcinoma cell line TRAMP-C2 and the murine breast adenocarcinoma cell line EO771 were selected for subcutaneous allografts. In contrast, *DUSP1* expression has not been well characterized in melanoma, and no reports have identified a consistent correlation between expression levels and disease stage or survival. In that regard, the murine B16F10 melanoma cell line was used for comparison.





Measurements of allografts were taken with digital calipers every other day after the formation of palpable tumors, usually occurring after ~ 3-5 days for EO771 and B16F10 cell lines and after ~14-16 days for TRAMP-C2 cells. For both EO771 and

TRAMP-C2 cell lines, implanted tumors in *Dusp1* deficient mice were significantly larger than wild-type mice. However, B16F10 allografts grew at the same rate in wild-type and *Dusp1* deficient mice (Figure 3-27). Histological analysis of inflammatory infiltrate was scored as previously described for 4NQO-induced tumors on a 0-4 scale. No differences in distribution of inflammation scores were detected in either EO771 or TRAMP-C2 tumors (Figure 3-28). To determine whether enhanced p38 $\alpha$  MAPK activation was responsible for the increase in tumor growth, the small molecule inhibitor SB203580 was injected intraperitoneally daily following establishment of subcutaneous tumors 7 days after initial tumor cell injection (Figure 3-29). SB203580 did not have an effect on EO771 tumor growth in wild-type mice, and no difference was seen between SB203580 versus vehicle treatment in wild-type mice. However, in *Dusp1* deficient mice, SB203580 injection abrogated the enhanced tumor growth seen in *Dusp1* deficient mice compared to wild-type mice, suggesting enhanced tumor growth in *Dusp1* deficient mice is driven by p38 $\alpha$  MAPK activity within the tumor microenvironment.



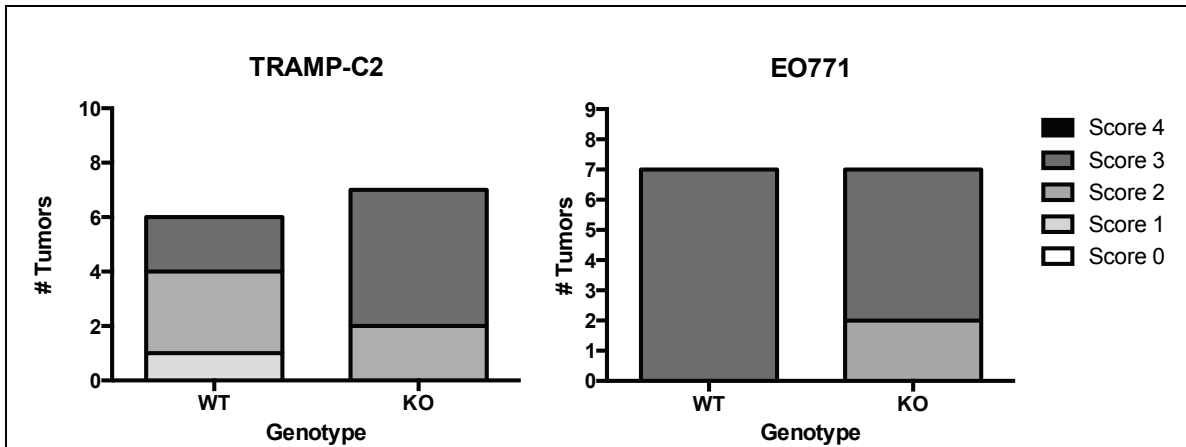


Figure 3-28. Inflammation scores of syngeneic subcutaneous tumors in wild-type and *Dusp1* deficient animals. Histological scores of inflammatory infiltrate within tumors of injected syngeneic TRAMP-C2, EO771, and B16F10 cells were performed on a 0-4 scale, as previously described. n = 6-7, p = 0.6585 (TRAMP-C2), n = 7, p = 0.6747 (EO771). Fisher's exact test.

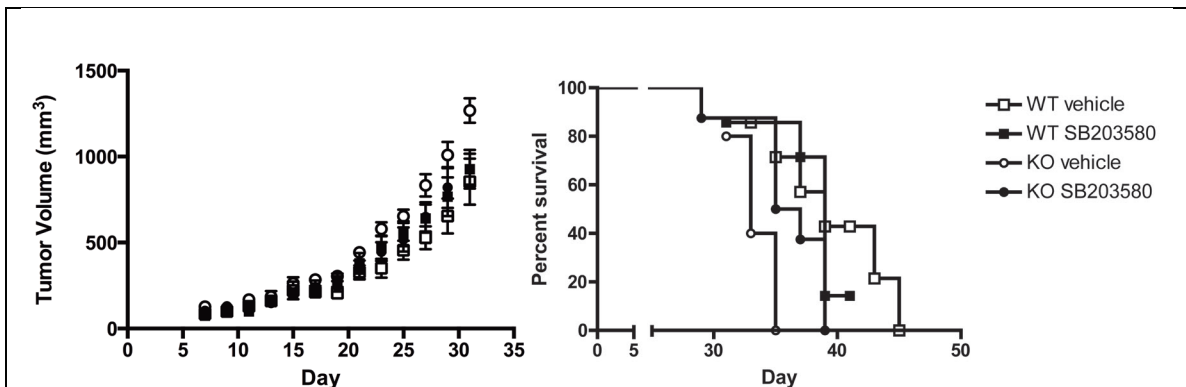


Figure 3-29. Inhibition of p38 $\alpha$  MAPK in wild-type and *Dusp1* deficient mice with subcutaneous syngeneic EO771 tumors. Wild-type and *Dusp1* deficient mice were injected subcutaneously with syngeneic EO771 cells, as previously described. Starting on day 7, mice received daily intraperitoneal injections of SB203580 (5mg/kg) or vehicle control. Rate of tumor growth is increased in *Dusp1* deficient vehicle-treated animals (p < 0.0001) and *Dusp1* deficient SB203580-treated animals (p = 0.0098). *Dusp1* deficient animals had decreased survival compared to wild-type animals (p = 0.0123). Survival was enhanced in *Dusp1* deficient animals treated with SB203580 compared to vehicle treatment group (p = 0.0086). n = 6-8.

### 3.3 Summary & Discussion

Although the mechanisms of pro-tumorigenic inflammation in gastric and colorectal cancer have been well described, only recently has there been an appreciation of the contribution of chronic inflammation to other processes of tumorigenesis. The development of cancer is now better understood as the interplay between genomic alterations, such as those induced by carcinogen exposure, and a supportive tumor microenvironment. To understand how *Dusp1* deficiency alters the development and progression of oral cancer, wild-type and *Dusp1* deficient mice were subjected to a carcinogen-induced oral cancer model, previously optimized to generate heterogeneous oral lesions that evolve into squamous cell carcinomas (337). This carcinogen-induced model of oral cancer has previously been described, in wild-type animals, as generating little inflammation with low levels of COX-2 expression and stromal infiltrate (337, 342). Results from these studies demonstrate the immense alteration of the inflammatory milieu within these tumors that develops in the absence of *Dusp1* negative regulation.

In this model system designed to mirror human disease progression from hyperplasia to dysplasia to *in situ* and invasive squamous cell carcinoma, *Dusp1* deficient mice demonstrated accelerated oral tumorigenesis with associated inflammation and provides the first evidence for a mechanistic link between loss of DUSP1 expression and advanced disease progression in human cancers. Furthermore, this is the first experimental evidence to demonstrate the pro-tumorigenic effect of enhanced inflammatory cytokine expression in oral cancer. The particularly enhanced tumor burden within esophageal tissues (Figure 3-7) suggests the same mechanism lies true for esophageal squamous cell carcinoma. Whether the dramatic increase in esophageal tumor

volume in *Dusp1* deficient animals is due to tissue-specific effects of *Dusp1* regulation or characteristics of the esophageal tissue architecture that might render it more susceptible to rapid tumor proliferation and expansion requires further investigation.

The panel of increased cytokines and chemokines identified by Nanostring analyses suggests a wide-scale activation of immune signaling. Although IL-1 $\beta$  was one of the most highly elevated mRNAs, it is unclear if this cytokine is sufficient to generate the development of the pro-inflammatory microenvironment that promotes tumor progression. The gradual process of tumorigenesis in the 4NQO model makes antibody blockade of IL-1 $\beta$  prohibitively expensive. Repeating the model with *Casp1*<sup>-/-</sup> and *Casp1*<sup>-/-</sup>*Dusp1*<sup>-/-</sup> double knockout animals or *Il1r*<sup>-/-</sup> animals could better address the functional role of elevated IL-1 $\beta$  in oral tumorigenesis and tumor progression.

Although the identification of a precise cytokine driver has not been identified in this model, these studies highlight the potential of targeting an upstream regulator of the pro-tumorigenic inflammatory response rather than single, secreted factors with biologics, which have not yielded significant improvement in clinical trials (343, 344). Pharmaceutical methods of increasing *DUSP1* expression have been described in a number of *in vitro* studies (345-347) and merit further investigation, particularly in cancer models.

The loss of *DUSP1* expression has implications on the biologic activities of many cellular constituents within the tumor, which have yet to be clearly dissected in these experiments. A recent survey of over 400 human HNSCC tissues revealed p38 MAPK activity to be highly elevated in nearly 80% of cases studied by immunohistochemistry, with significant impact on cancer cell growth, lymphangiogenesis, and angiogenesis in

xenograft studies (348). The discrepancy between elevated phosphorylated p38 MAPK in immunoblotting whole tissue lysates versus equal immunohistochemical staining of tumor epithelium suggests a more critical role for Dusp1-mediated p38 regulation in the supporting stromal and immune cells.

Results from the bone marrow chimeric model suggest hematopoietic-derived cells alone cannot recapitulate the enhanced disease progression in the long-term model of carcinogenesis and tumor progression driven by 4NQO exposure. An initial hypothesis for advanced disease progression in *Dusp1* deficient mice centered on inflammatory cells driving an enhanced immune response that promoted tumor growth. Although *Dusp1* hematopoietic deficiency did not recapitulate the original phenotype, the possibility remains increased immune activation with infiltrating leukocytes and cytokine production are still necessary for the enhanced disease production seen in *Dusp1* deficient animals, both with wild-type and *Dusp1* deficient bone marrow. Although the 4NQO model produces heterogeneous tumors of the oral cavity, bearing numerous molecular alterations similar to human HNSCC, the slow, carcinogen-driven disease process encompasses a wide spectrum of tumor biology, including carcinogenesis and neoplastic transformation, immune escape, tumor proliferation, and early local invasion, which makes identification of specific points of regulation difficult. More specific models to address immune escape, e.g. MCA-induced fibrosarcoma, or suppression of anti-tumor responses, e.g. adoptive transfer of pmel-1 T cells against B16 melanoma, could begin to more precisely answer how *Dusp1* deficiency enhances tumor progression through immune modulation.



These initial findings from the chimer and syngeneic subcutaneous tumor models suggest non-hematopoietic, non-epithelial tissues within the tumor microenvironment, including endothelium, lymphatic vessels, and cancer-associated fibroblasts, may also be a driving force. Xenograft studies with a small molecular inhibitor of p38 $\alpha$  MAPK demonstrated a crucial role for p38-mediated regulation of tumor-promoting secreted factors from cancer-associated fibroblasts (349). Inactivation of the RNA decay factor AUF1 increased expression of a panel of cytokines and chemokines, including IL-1 $\beta$ , CXCL1, and GM-CSF, validated in larger datasets of stromal-specific factors present in human breast cancer. In a murine hindlimb ischemia model, *Dusp1* expression in endothelial cells promoted angiogenesis by modulating histone H3 dephosphorylation to induce expression of the proangiogenic chemokine fractalkine (350). As *DUSP1* is ubiquitously expressed, the potential impact it has on tumorigenesis may vary across different cell types.

*DUSP1* is capable of regulating activation of multiple MAPKs, although it has greatest affinity for p38. In HNSCC, p38 $\alpha$  activation fails to inactivate ERK1/2 signaling, as in normal oral keratinocytes, due to a failure to inactivate MEK1/2 (351). The enhanced p38 $\alpha$  and p38 $\delta$  activity promoted tumor cell proliferation and survival, both *in vitro* and *in vivo* (351). In peripheral blood mononuclear cells isolated from 83 HNSCC patients, p38 $\alpha$  MAPK was significantly elevated compared to healthy donors (352). Levels of p38 $\alpha$  were also found to be elevated in sera from HNSCC patients, with significant decreases during and after radiation therapy in the group of responders (70 patients), not seen in the non-responders (11 patients) (353). Based on these previous characterizations of human HNSCC samples and the MAPK activation profile in *Dusp1*

deficient 4NQO-induced tumor tissues, the candidate MAPK target responsible for the enhancement of tumor progression in *Dusp1* deficient animals is p38 $\alpha$ , as suggested by small molecule inhibition of subcutaneous syngeneic tumor cell growth (Figure 3-29).

Already, several orally available p38 MAPK inhibitors are in phase II and III clinical trials for inflammatory conditions with no signs of clinical toxicity (354, 355). A xenograft model of tumor progression using co-injected cancer-associated fibroblasts and preneoplastic cell lines demonstrated oral p38 inhibitor treatment could preferentially target stromal production of pro-inflammatory mediators (349). However, xenograft studies using a systemically administered p38 inhibitor blocked HNSCC tumor cell growth (356), suggesting inhibition of p38 signaling within tumor epithelium may also have beneficial effects.

However, the tumor-promoting effect of *Dusp1* deficiency may be through increased activation of other pathways, such as JNK1/2. Small molecular inhibitors of JNK1/2 were effective at targeting *in vitro* HNSCC cell lines and in xenograft models, reducing tumor proliferation and microvasculature, EGFR expression, and secretion of IL-6, IL-8, and VEGF (357). In rat tongue cancers, resulting from 4NQO treatment, of all the AP-1 family members, JunB and *cfos* mRNA and protein were elevated in cancerous tissue compared to normal control, although only *cfos* was elevated during the dysplastic stage (358). In addition, a targeted qPCR array described in Chapter 4.2 revealed *cfos* to be highly elevated in the *Dusp1* deficient tumor sample, although this result was not selected for further validation.

Histological scores, flow cytometry, immunohistochemistry, and Nanostring analyses describe a highly inflammatory tumor tissue in *Dusp1* deficient mice subjected

to 4NQO. The panel of cytokines and chemokines suggest a mechanism by which recruited myeloid-derived immune cells traffick to the tumor site to promote tumor progression in *Dusp1* deficient animals. Potential cellular mediators include myeloid-derived suppressor cells, tumor-associated macrophages, neutrophils, and other granulocytes. In a murine model of rhabdomyosarcoma, the recruitment of  $Cxcr2^+$  granulocytic myeloid derived suppressor cells ( $CD11b^+/Ly6G^+$ ), via *Cxcl1/2* expression, inhibited anti-PD1 therapy. Tumor regression after anti-PD1 treatment was restored on *Cxcr2* deficient mice or with a CXCR2 neutralizing antibody (359). Genetic deletion of eosinophils in Balb/c mice challenged with 4-nitroquinoline 1-oxide resulted in reduced disease burden (360).

A similar association between increased numbers of myeloid-derived granulocytes and disease progression has been described in HNSCC. A study of HNSCC patients revealed high levels of neutrophilic infiltrate in HNSCC tissue with greater infiltrate correlating to poorer survival in advanced disease (361). Furthermore, HNSCC cell line conditioned medium enhanced neutrophil survival and increased chemotaxis and secretory function (361). A later study of neutrophils isolated from peripheral blood of HNSCC patients identified impairment of HNSCC-conditioned neutrophilic inducible ROS production but not cytokine secretion, with elevated cytokine levels in HNSCC serum compared to controls. Similar to previous studies, these cells had enhanced survival with lower rates of spontaneous apoptosis. Importantly, HNSCC patients had increased numbers of immature PMNs, suggesting a systemic response engaging hematopoietic precursors to traffick to the tumor site (362).

Little changes were detected in members of the adaptive immune response, with low levels of activation markers in T cell subsets, suggesting T cell exhaustion may be occurring, as described in other characterizations of the 4NQO model (342). Slight decreases in expression of dendritic cell activation markers may be signs of impaired recruitment of an anti-tumor immune response. A dendritic cell-based vaccination strategy using 4NQO-treated animals suggests these cells are capable of promoting an immune response to premalignant and HNSCC lesions (363). In previous characterizations of 4NQO-induced lesions on wild-type mice, cervical lymph nodes contained higher levels of immunosuppressive T regulatory cells but also conventional T cells, albeit with decreased proliferative capacity (342). A study of circulating and intratumoral T regulatory cells isolated from HNSCC patients found higher levels of immune checkpoint markers (CTLA-4 and PD-1) in intratumoral cells with corresponding greater immunosuppressive ability (364). The development of such a potent immunosuppressive microenvironment may result, in part, from the enhanced secretion of cytokines within earlier premalignant lesions (365). In a small study of 11 patients and 10 healthy donors, peripheral blood-isolated regulatory T cells from HNSCC patients were significantly elevated with increased TLR expression and enhanced immunosuppressive effect following LPS and Hsp60 stimulation (366). However, no differences in effector T cell proliferative ability were detected. At this time, it is unclear how these immunosuppressive mechanisms develop in HNSCC, but *Dusp1* deficiency does not appear to immediately affect these pathways in the 4NQO model.

Although 4NQO treatment generated lymph node metastases only in *Dusp1* deficient animals, whether loss of DUSP1 protein promotes metastasis is still unclear. A

previous group's modification of the 4NQO delivery model, using a higher dose with prolonged monitoring period, has been used to establish lymph node metastasis with complete penetrance in Balb/c mice (367). This and other more rapid models could be used to address this question, especially if DUSP1 is postulated to be a regulator of the supporting soil for tumor initiation and development.

The subcutaneous allogeneic tumor model was performed to address whether an equivalent tumor burden, with wild-type *Dusp1* expression, would progress more rapidly in a *Dusp1* deficient tumor microenvironment compared to wild-type. A limitation of this model is the tissue-specific effects of the oral cavity, in particular, potential sources of innate immune activation in the microflora. The syngeneic murine oral squamous cell line SCCVII can be used on a C3H/HeJ genetic background to model oral squamous cell carcinoma with local invasion into the local muscle and mandible, and cervical lymph node and pulmonary metastases (368). Unfortunately, the C3H/HeJ genetic background necessary for a syngeneic transplant contains a spontaneous mutation in *Tlr4*, rendering these mice resistant to endotoxin challenge (339).

Due to supporting evidence from human tissue datasets, breast and prostate adenocarcinoma cell lines were selected for allogeneic tumor cell experiments, results of which support the role of *Dusp1* in the microenvironment as a suppressor of tumor growth. This effect was not seen across all tumor cell lines, with no statistical difference in the growth curves of B16F10 allografts. The spontaneous murine B16 melanoma cell line is highly tumorigenic and rapidly growing but has generally been described as poorly immunogenic (369, 370). Furthermore, the characterization of *DUSP1* in human melanoma samples is not consistent, with much smaller sample sizes available in public

databases such as NCBI Gene Expression Omnibus and Oncomine. Thus, in future investigation of *DUSP1* as a target of therapeutic induction, careful consideration of the tumor type and molecular patterns of MAPK and cytokine expression should be made.

## **CHAPTER 4. *Dusp1* regulates inflammatory mediators *ex vivo*.**

### **4.1 Rationale & Hypothesis**

Animal models of tumor progression, both carcinogen-induced and transplanted tumors, suggest *Dusp1* deficiency enhances disease progression and generates a more inflammatory phenotype than in wild-type animals. Although DUSP1 is well described as a negative regulator of the innate immune response to acute endotoxin stimuli in models of sepsis and other bacterial-driven disease processes (143, 144, 150, 153, 334, 371), how it affects tumor-associated inflammation has not been addressed. Within the oral cavity, tissues are constantly exposed to pathogen-associated molecular patterns (PAMPs) through the diverse microbiota (372). Correlations between altered microbiota and cancer development have been made, in patients with periodontitis or poor oral hygiene (373, 374). However, the functional impact of these bacterial triggers and host inflammatory responses on HNSCC carcinogenesis are not well characterized.

In HNSCC, IL-1 $\beta$  has been identified as a potential diagnostic biomarker, through mRNA and protein studies of tumor tissue and patient saliva samples (375, 376). IL-1 $\beta$  was initially discovered as a secreted cytokine from activated monocytes (377) and has been shown to be expressed primarily by innate myeloid cells. A study of cytokine secretion from well-established UMSCC cell lines revealed varying levels of IL-6, VEGF, and IL-8 secretion but no detectable IL-1 $\beta$  (378), suggesting an alternative

cellular source of IL-1 $\beta$  within the microenvironment is driving transcription of these cytokines and growth factors.

Due to the highly elevated levels of IL-1 $\beta$  mRNA and increase in myeloid-lineage cells within *Dusp1* deficient tumor tissues, we hypothesize *Dusp1* negatively regulates expression of IL-1 $\beta$  in macrophages. Of the elevated cytokines and chemokines identified by Nanostring analysis in the 4NQO tumor model, IL-1 $\beta$  had previously been shown to upregulated in human HNSCC. Furthermore, IL-1 $\beta$  signaling has been described as an activator of a number of inflammatory mediators, making it an attractive candidate for validation as a downstream target of *Dusp1* for future therapeutic targeting.

## 4.2 Results

### *Macrophage polarization is not skewed in Dusp1 deficient primary cells.*

Immunohistochemistry previously identified similar numbers of infiltrating F4/80<sup>+</sup> tumor-associated macrophages within 4NQO-induced lesions in wild-type and *Dusp1* deficient mice. However, Nanostring analysis suggested the phenotype of these macrophages might differ between wild-type and *Dusp1* deficient animals, based on expression of macrophage polarization genes, such as *Il12a*, *Arg1*, and *Il4ra*. To determine whether *Dusp1* deficiency generated an intrinsic defect in M1 polarization, primary bone marrow-derived macrophages from wild-type and *Dusp1* deficient mice were treated *ex vivo* to classic M1 (LPS and IFN- $\gamma$ ) or M2 (IL-4) polarizing conditions and assessed for cytokine response.

There have been conflicting reports of whether IL-12 is within a group of cytokines negatively regulated by DUSP1 (142, 379). In this study, *Dusp1* deficient



macrophages express less *Iil2b* mRNA and IL-12p40 protein following stimulation, although the difference was not statistically significant. Levels of *Nos2* mRNA and IL-23 protein were also decreased in *Dusp1* deficient macrophages. However, examination of markers of M2 polarization did not reveal a consistent trend. There were no significant changes in *Iil10* mRNA and no detectable IL-10 protein secreted. There was a trend toward decreased *Arg1* mRNA and no significant difference in IL-1RA expression (Figure 4-1). These data suggest *Dusp1* deficient macrophages may have impaired M1 polarization, but the effect of *Dusp1* deficiency on M2 polarization is still unclear.

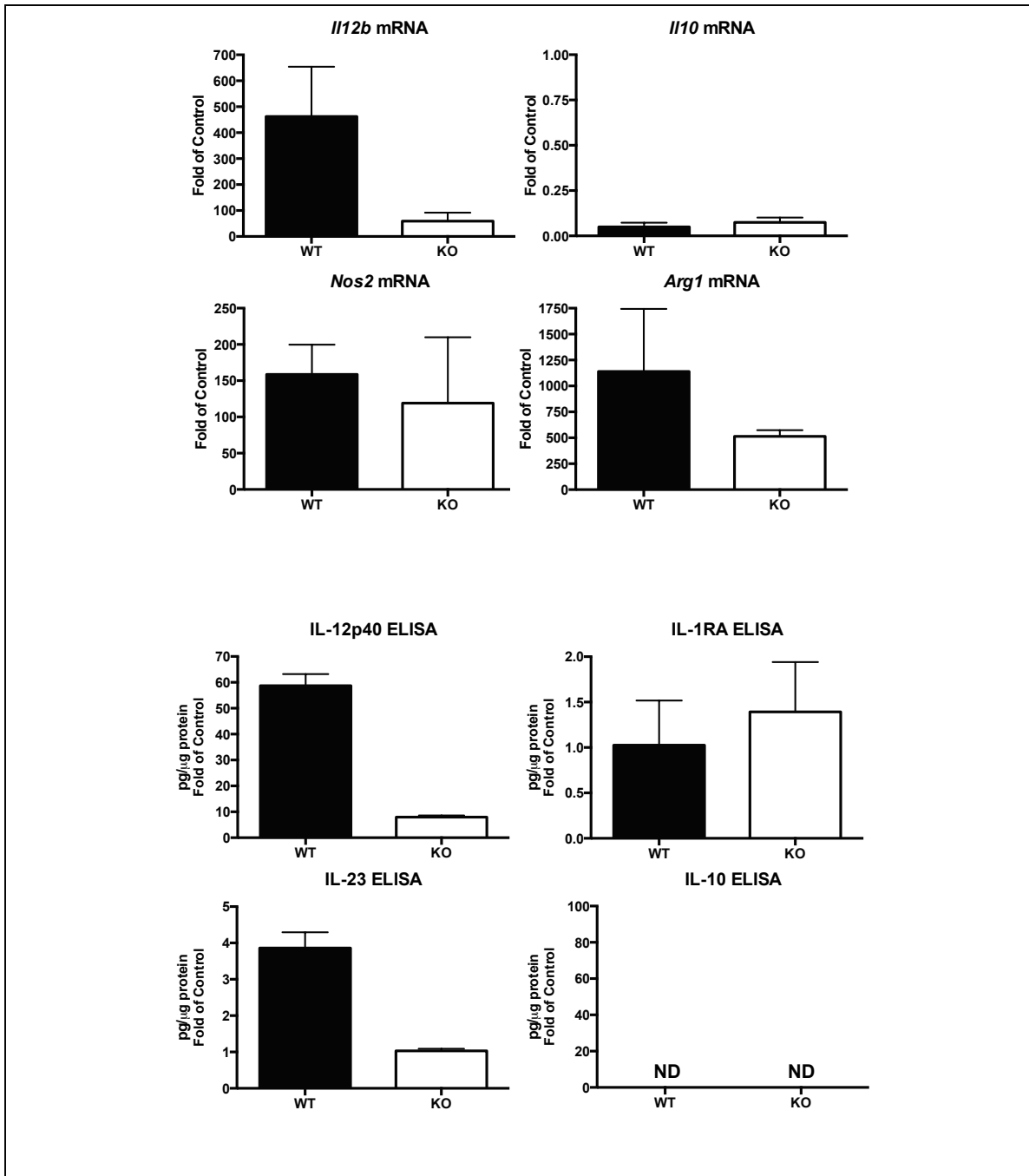


Figure 4-1. Effect of *Dusp1* deficiency on macrophage polarization. Primary bone marrow-derived macrophages from wild-type and *Dusp1* deficient mice were treated with LPS and IFN- $\gamma$  to induce M1 polarization or IL-4 to induce M2 polarization. *Il12b* and *Nos2* gene expression and IL-12p40 and IL-23 cytokine secretion were assessed as measures of M1 polarization. *Il10* and *Arg1* gene expression and IL-1RA and IL-10 cytokine secretion were assessed as measures of M2 polarization. n = 4.

***Dusp1* deficient tumor tissues express significantly higher levels of inflammatory chemokines and cytokines.**

A targeted qPCR array was used to assess a panel of 89 inflammatory cytokines, chemokines, and receptors comparing expression between a pair of wild-type and *Dusp1* deficient tumor tissues matched for sex, tumor grade, and inflammation score. Fifteen targets were expressed greater than 5-fold in the *Dusp1* deficient sample, with the three highest being *Il20*, *Il1b*, and *Cxcl1* (Appendix A). Of these three targets, *Il1b* was validated in a larger panel of 4NQO and vehicle-treated tissue samples with significant increased in *Il1b* in *Dusp1* deficient tumor tissues (Figure 4-2). *Il1b* was also selected for further investigation, due to the supportive evidence that IL-1 $\beta$  is up-regulated in human HNSCC. A similar qPCR array targeted towards members of the MAPK signaling family identified 6 genes up-regulated greater than 5-fold in at the *Dusp1* deficient tumor tissue sample compared to a wild-type match, but validation of the most highly expressed gene, *p16<sup>INK4A</sup>*, in a larger panel of tissue samples was unsuccessful (Appendix B).

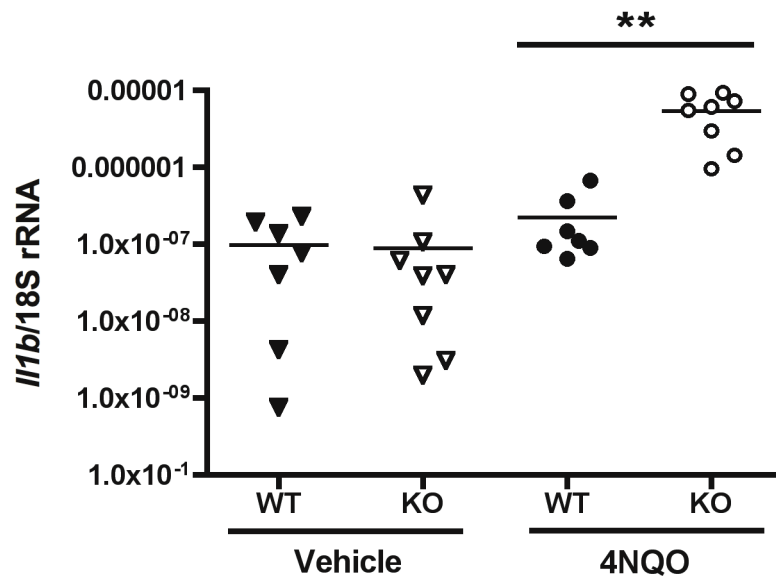
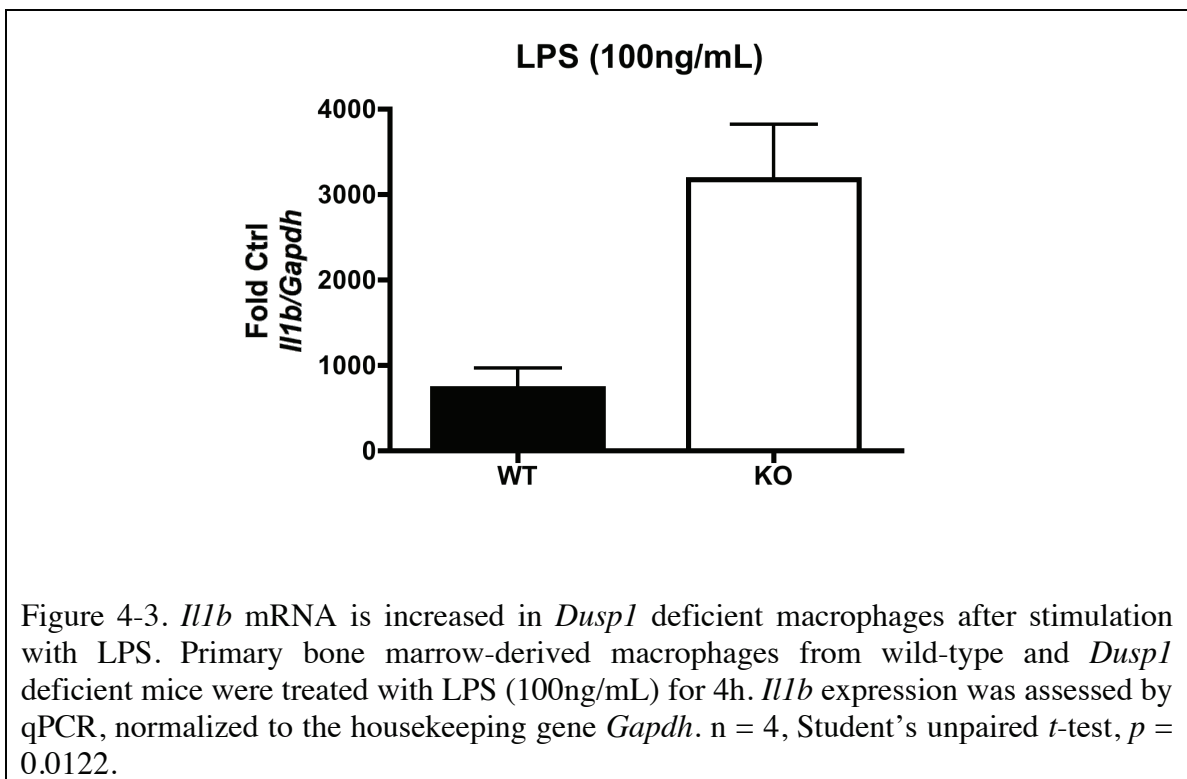


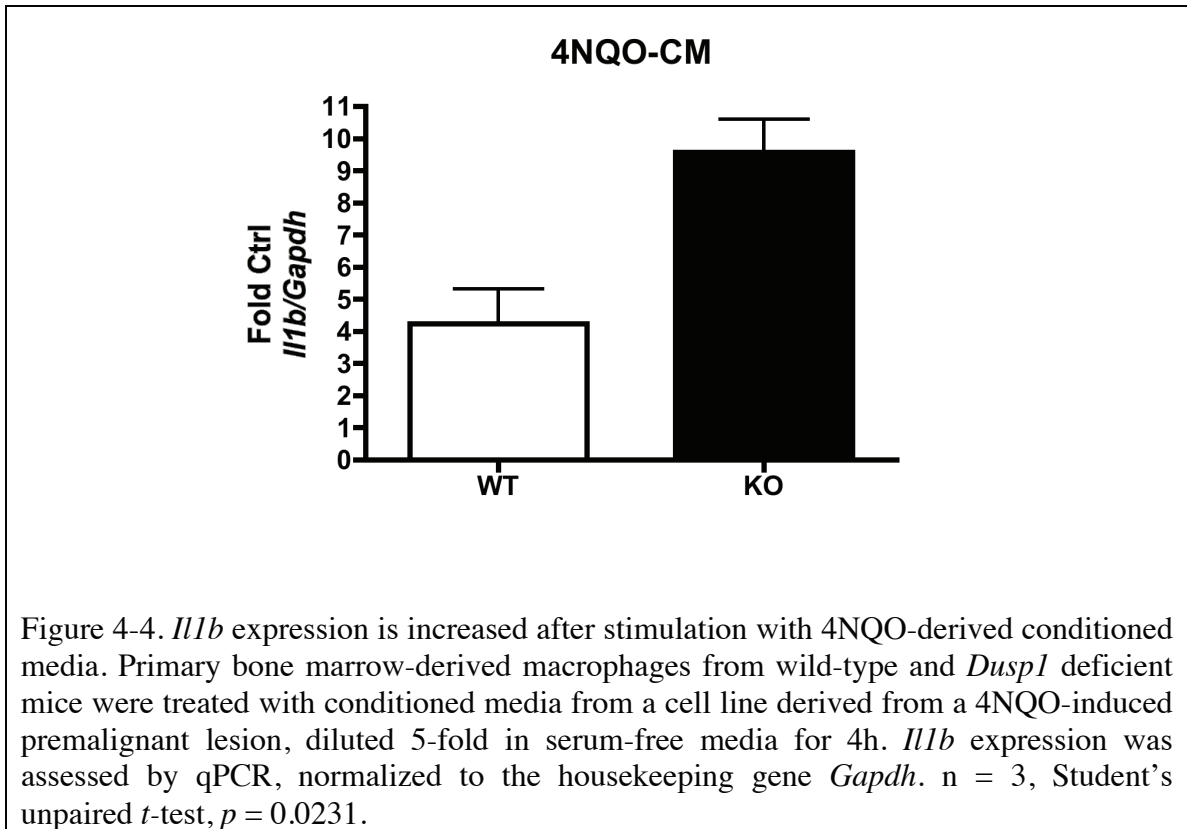
Figure 4-2. Increased *I11b* gene expression in *Dusp1* deficient tumor tissues. Validation of *I11b* as an upregulated gene in *Dusp1* deficient tumor tissues was performed by qPCR in a panel of wild-type and *Dusp1* deficient tumor and control-treated tissues. *I11b* mRNA was significantly increased in *Dusp1* deficient tumor tissues, with no differences between tumor-free animals. n = 7-8, Mann-Whitney test,  $p = 0.0003$ .

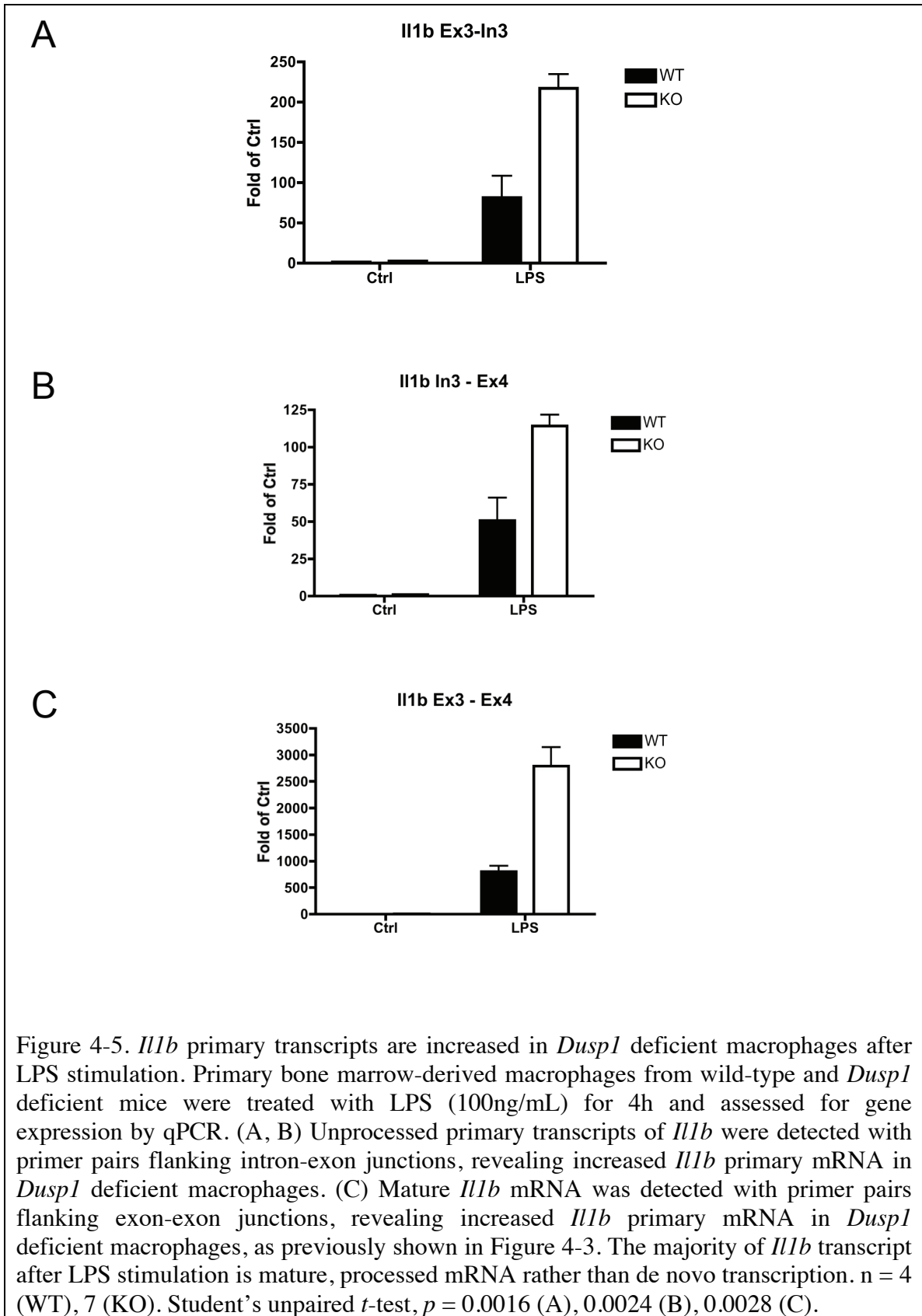
***Dusp1* deficient macrophages express more *I11b* mRNA after stimulation.**

Stimulation of primary bone marrow-derived macrophages with LPS confirmed enhanced expression of *I11b* mRNA in *Dusp1* deficient cells compared to wild-type (Figure 4-3). The same trend was seen when conditioned media from a premalignant cell line obtained from a 4NQO-induced lesion was used as an activation stimulus, although to a much lesser extent than with LPS (Figure 4-4). IL-1 $\beta$  expression is carefully controlled at both the mRNA and protein level. To understand whether the increase in steady-state mRNA was due to increased *de novo* transcription or enhanced mRNA stability, levels of primary mRNA transcripts were quantified by qPCR using primers targeting the exon-intron junction present only in unprocessed mRNA compared to amplicons generated from primers targeting exon-exon junctions of mature, fully

processed mRNA. These data revealed increases in both primary transcripts as well as mature mRNA after LPS stimulation, both with greater levels in *Dusp1* deficient cells (Figure 4-5). However, mature mRNA appeared to constitute the majority of *I11b* mRNA present after LPS stimulation. The expression levels of mature mRNA detected by exon-exon primer pairs were identical to that detected by TaqMan assays using fluorescent probes specific for exon-exon junctions performed in independent experiments (Figure 4-3).

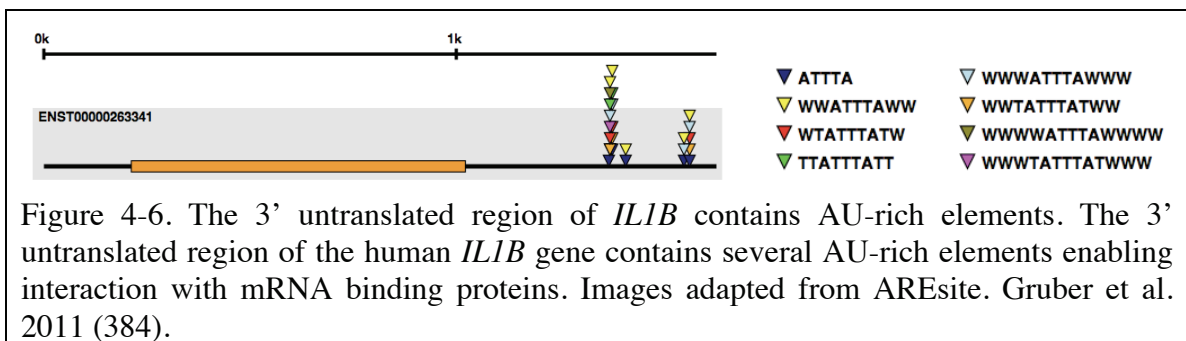




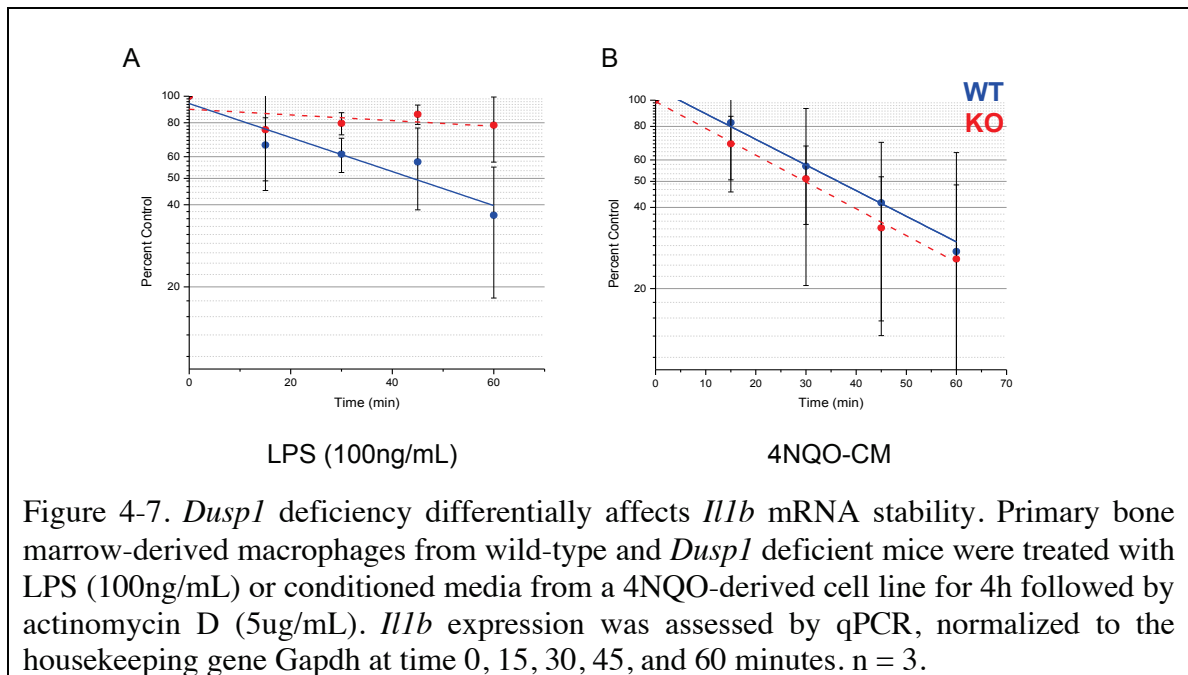


***Il1b mRNA stability is enhanced in Dusp1 deficient macrophages.***

The 3' untranslated region of *Il1b* mRNA, like many other cytokines, contains multiple AU-rich elements capable of interacting with RNA binding proteins, such as AUF1, HuR, and TTP (Figure 4-6) (380). The activity of these RNA binding proteins can be regulated by p38MAPK-mediated phosphorylation downstream of DUSP1, affecting their cellular localization or targeting them for degradation (381-383). To determine whether enhanced *Il1b* expression after stimulation was due to increased mRNA stability following LPS stimulation, primary bone marrow-derived macrophages were treated with actinomycin D to inhibit *de novo* transcription. After actinomycin D treatment, levels of *Il1b* mRNA were quantified to assess rates of mRNA decay. In these experiments, LPS stimulation revealed enhanced *Il1b* stability in *Dusp1* deficient macrophages with a half-life of approximately 45 minutes in wild-type macrophages compared to greater than 60 minutes in *Dusp1* deficient cells (Figure 4-7A). However, treatment with conditioned media from the 4NQO-derived cell line did not reveal significant differences in mRNA half-life, both between 30-35 minutes (Figure 4-7B), possibly due to the low levels of induction as seen in steady-state experiments.



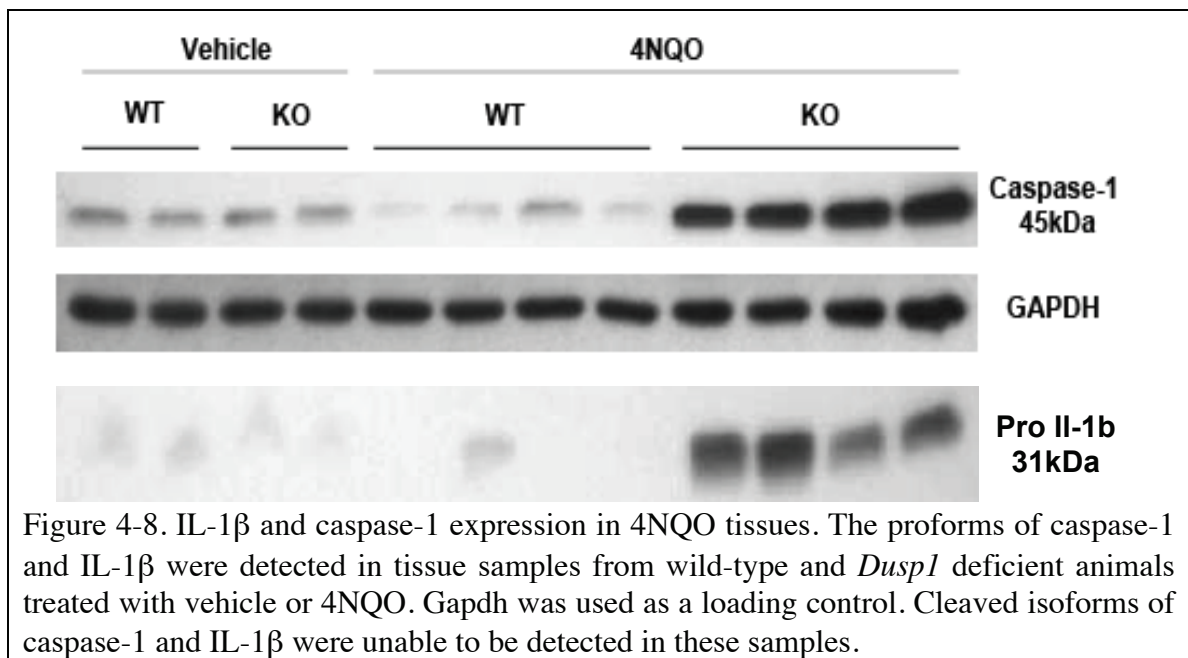




***Dusp1* deficiency does not affect inflammasome activation.**

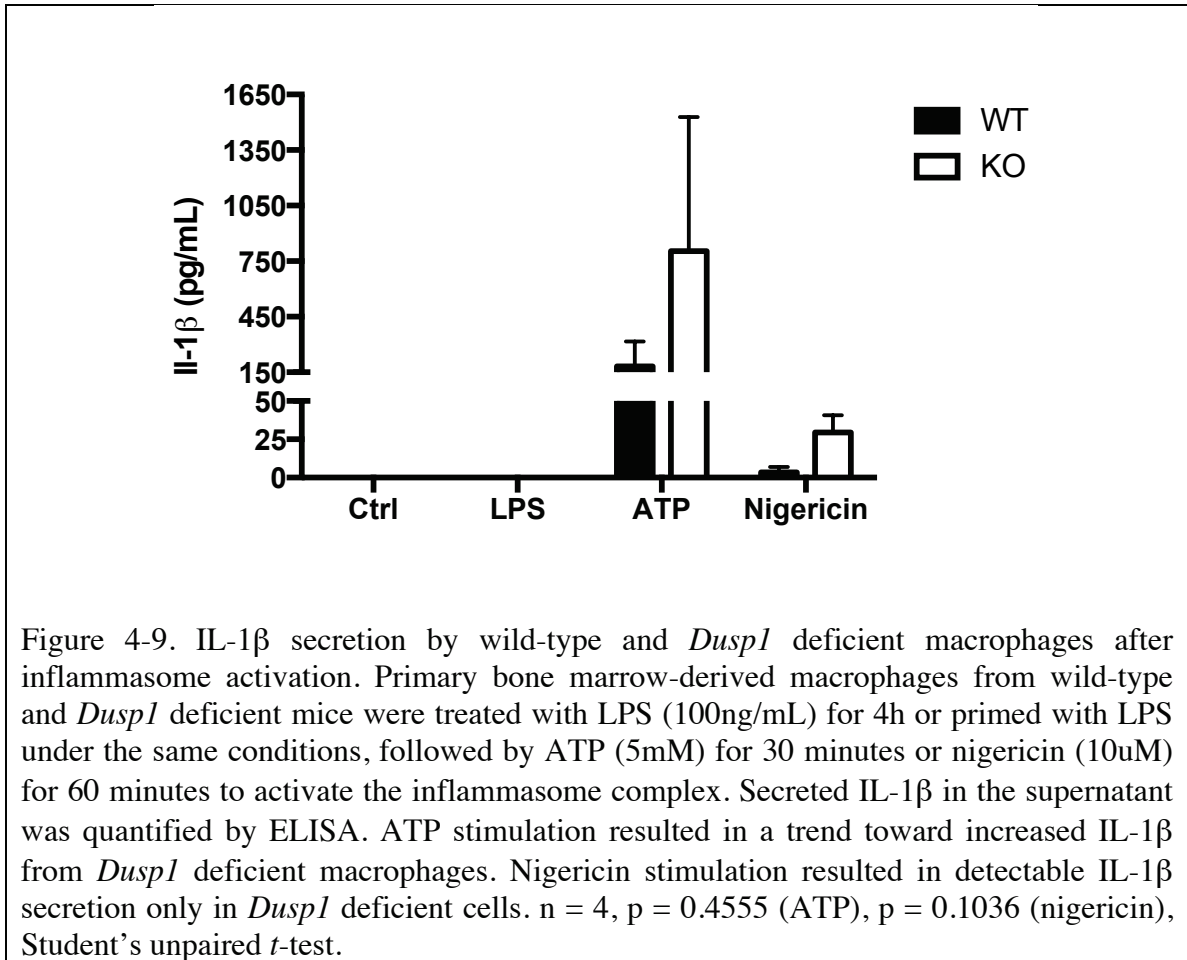
After transcription of *Il1b* mRNA, the message must be translated as a 34kDa protein and then cleaved by the inflammasome protein complex before being secreted in its active 17kDa form. Examination of tumor tissues from the 4NQO model revealed the proform of IL-1 $\beta$  to be elevated only in *Dusp1* deficient tumor samples. Furthermore, these samples contained highly elevated levels of procaspase-1, the enzyme within the inflammasome complex responsible for cleavage and activation of IL-1 $\beta$  (Figure 4-8). These data support increased production of IL-1 $\beta$  within the 4NQO-induced tumor microenvironment, with both elevated transcriptional and translational products. However, the increased levels of procaspase-1 within *Dusp1* deficient tumor tissues

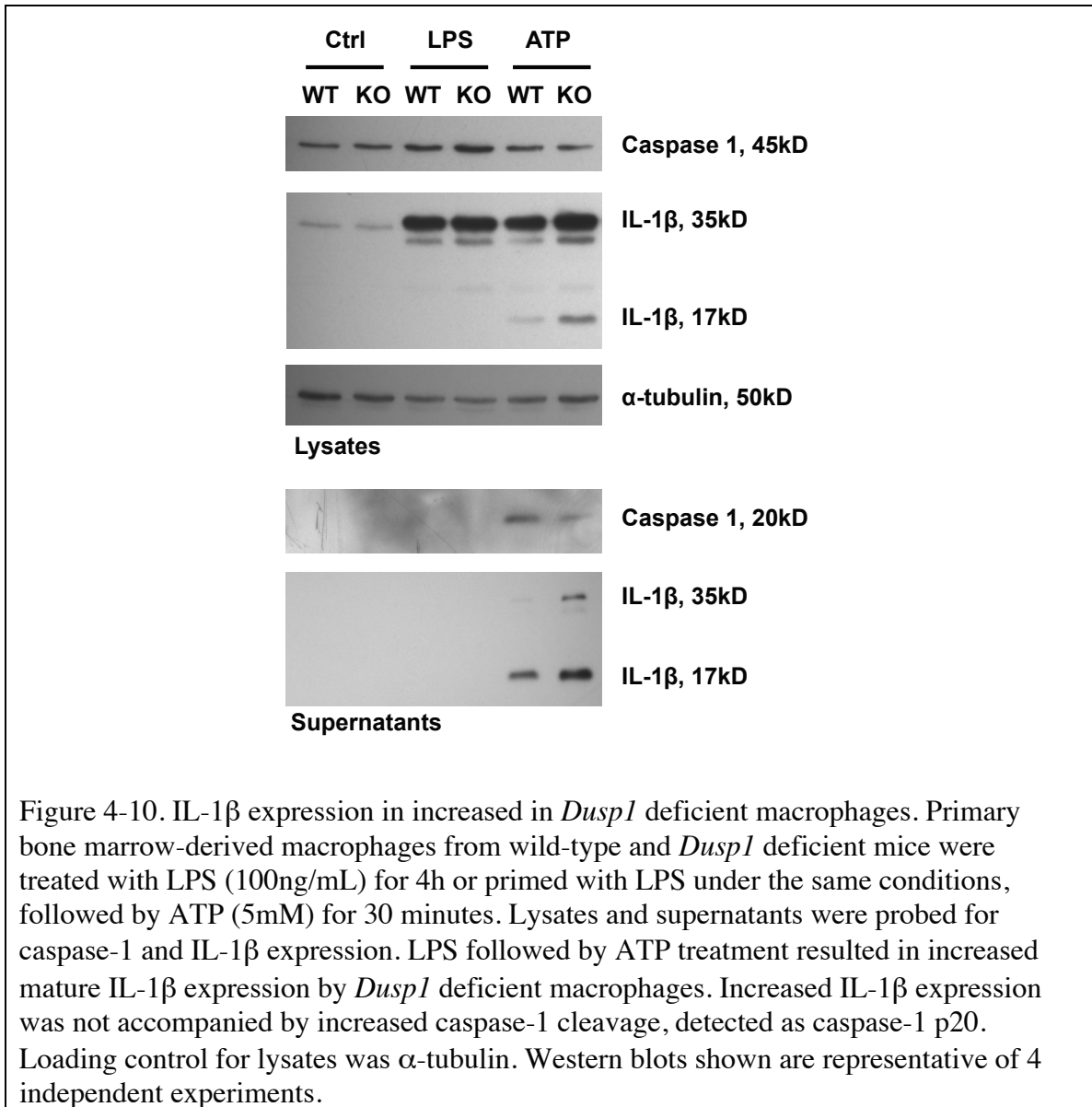
suggested *Dusp1* could potentially modulate an additional point of post-translational regulation by the inflammasome.



To determine whether this was the case, primary bone marrow-derived macrophages from wild-type and *Dusp1* deficient mice were treated with LPS for 4 hours to prime these cells to express *Il1b* mRNA. Following this treatment, cells were stimulated with either adenosine tri-phosphate (ATP) or nigericin to induce formation of the Nlrp3 inflammasome complex necessary to cleave Il1b to its mature, secreted form. Activation of inflammasomes requires this secondary treatment to recruit members of the complex with subsequent cleavage of procaspase-1 into active p10 and p20 subunits. ELISA of supernatants collected revealed enhanced IL-1 $\beta$  secretion by *Dusp1* deficient macrophages after ATP or nigericin treatment, although this was not statistically significant (Figure 4-9). Western blotting showed similar increases of IL-1 $\beta$  protein in lysates as well as supernatants in *Dusp1* deficient samples. However, no changes were

seen in procaspase-1 expression or its cleaved caspase 1 p20 subunit (Figure 4-10), suggesting enhanced IL-1 $\beta$  secretion is due to increased influx of *Il1b* mRNA and its translational product rather than increased inflammasome recruitment or activation.





### 4.3 Summary & Discussion

Immunohistochemistry and flow cytometry analysis did not suggest alterations in macrophage numbers within *Dusp1* deficient tumor tissues. However, the phenotype of infiltrating macrophages was only indirectly assessed by Nanostring analysis. These gene expression results suggest a skewing toward M2 polarization, which would promote tumor progression through immunosuppressive effects on other immune cells and

enhancing angiogenesis (287, 385, 386). Macrophage polarization was assessed *ex vivo* using primary bone marrow-derived macrophages and revealed no intrinsic bias toward M2 polarization but did demonstrate decreased IL-12 expression, which could lead to a less effective anti-tumor immune response. *Dusp1* deficient dendritic cells have been shown to express lower levels of IL-12, rescued by p38 but not JNK inhibition, which impaired effective recruitment of Th1 and Th17 but not Th2 responses (387).

*Dusp1* deficient macrophages have been well characterized as expressing enhanced levels of IL-10 after LPS challenge (143, 144, 151, 371), but this effect was not seen in M2-polarized primary cells. Enhanced IL-10 may promote the development of an immunosuppressive tumor microenvironment (286, 388). It is unclear whether recombinant IL-4 treatment can sufficiently mimic the conditions that promote the development of tumor-associated macrophages. Furthermore, debate continues as to whether M2 polarized macrophages from primary cells can accurately recapitulate these cells or whether tumor-associated macrophages are a truly distinct entity (389).

The inflammatory component of 4NQO-induced tumors in *Dusp1* deficient mice was characterized by qPCR array to identify cytokine mediators for more in-depth validation. Both Nanostring analyses, performed in Chapter 3.2, and targeted qPCR array results, described in Chapter 4.3, found *Il1b* mRNA to be significantly elevated in *Dusp1* deficient tumor tissues. To address the mechanism of IL-1 $\beta$  regulation by *Dusp1*, primary bone marrow-derived macrophages were used for an *ex vivo* culture model, based on these observations. A previous study of 4NQO-induced lesions in Balb/c mice revealed *Il1b* mRNA was elevated in HNSCC lesions but not in epithelial-enriched samples examined by laser-capture microdissection, with prominent CD11b<sup>+</sup> cells in the

underlying stroma (390). Examination of secreted supernatants from HNSCC cell lines compared to supernatants from freshly derived tumors and tumor-draining lymph nodes from HNSCC patients found similar results with elevated levels of IL-1 $\beta$  only in the tumor lysates and lymph nodes but not isolated cell lines (391).

Results from the experiments detailed in this chapter demonstrate multiple points of regulation of IL-1 $\beta$  expression by *Dusp1*, both transcriptionally and post-transcriptionally. Transcriptional regulation of IL-1 $\beta$  has been shown to be mediated by NF- $\kappa$ B and AP-1 (392), both key members of the TLR-MAPK innate immune signaling pathway, suggesting similar mechanisms may be increased in *Dusp1* deficient cells. Identifying the MAPK responsible for increased transcription by inhibitor treatment, followed by chromatin immunoprecipitation of the putative transcription factor and promoter region will more clearly delineate this pathway.

Following stimulation, the majority of *Illb* mRNA was determined to be mature, processed transcript suggesting enhanced mRNA stability as the main mechanism by which IL-1 $\beta$  is rapidly elevated following stimulation. Like other cytokines rapidly induced following TLR4 activation, the 3' UTR of IL-1 $\beta$  contains several ARE sites for interactions with RNA binding proteins to regulate its stability (393). Specifically in HNSCC tissues, the RNA binding protein tristetraprolin down-regulates expression of IL-6, VEGF, and PGE<sub>2</sub> by decreasing mRNA stability, with an inverse correlation between TTP and IL-6 expression, serving as a biomarker for poor prognosis (394). More recently, the tumor-promoting effects of p38 $\alpha$  MAPK activity in senescent and cancer-associated fibroblasts was found to be mediated through post-transcriptional regulation of secretory products known collectively as the senescence-associated secretory phenotype,

which includes IL-1 $\beta$ , by RNA binding protein AUF1 (349). As the ARE sites within IL-1 $\beta$  have been identified to bind to at least three RNA binding proteins (395-399), more thorough ribonucleoprotein immunoprecipitation reactions with 3' UTR mutation screens are needed to dissect the regulatory pathway involved.

Functionally, IL-1 $\beta$  may have several distinct roles within the tumor microenvironment. In Epstein Barr virus-associated nasopharyngeal carcinoma, tumor-derived IL-1 $\beta$  was shown to recruit neutrophils to generate an anti-tumor immune response, associated with increased survival (400). Other knockout studies have also suggested hematopoietic-derived IL-1 $\beta$  may have beneficial anti-tumor effects (325, 401). IL-1 $\beta$  has the potential to induce dendritic cell-mediated activation of adaptive immune cells (401). However, the effects of IL-1 $\beta$  may vary greatly depending upon the cellular constituents of the microenvironment. In a xenograft model, tumor cells engineered to overexpress IL-1 $\beta$  were shown to preferentially induce expansion of a Ly6C<sup>+</sup> MDSC population, particularly immunosuppressive against NK cell function (402). *Il1r* and *Myd88* deficiency protected mice from topical skin carcinogenesis, but orthotopic tumor growth was only inhibited in *Myd88* deficient keratinocytes and not *Il1r* deficient cells (403). Deficiency in IL-1 $\beta$  but not IL-1 $\alpha$  was shown to protect mice from 3-methylcholanthrene-induced fibrosarcoma, an effect reversed with addition of recombinant IL-1RA, an endogenous inhibitor of IL-1 $\beta$  signaling (300). In mouse models of obesity, inflammasome activation in adipose tissue macrophages occurs in response to secreted factors from adipocytes; the increase in circulating IL-1 $\beta$  then promotes the expansion and recruitment of bone marrow-derived myeloid progenitors (404). Data from the *Dusp1* deficient animals challenged with 4NQO, described in chapter 3, suggest

IL-1 $\beta$  may play a similar role in recruiting myeloid lineage immune cells to the tumor microenvironment. Understanding the direct contribution of IL-1 $\beta$  in these models of tumor progression could be better addressed in the future with *Casp1*<sup>-/-</sup> or *Il1b*<sup>-/-</sup> animals.

In addition to tumor-associated macrophages, other cellular sources of IL-1 $\beta$  could further modulate the immune response. Sublethal doses of radiation and chemotherapeutics 5-fluorouracil and cisplatin were shown to increase levels of IL-1 $\beta$  in a panel of HNSCC cell lines (405). Surprisingly, enhanced tumorigenesis in colitis-associated cancer through *Nlr4* inflammasome activation has been attributed to caspase-1 regulation of colonic epithelium (406). However, *Nlrp3* has been shown in the same model of colitis-associated cancer to regulate tumorigenesis through the hematopoietic compartment (325). Whether these complex regulatory pathways impact HNSCC development are exciting avenues for future investigation.



## **CHAPTER 5. Assessment of DUSP1 expression in human HNSCC**

### **5.1 Rationale & Hypothesis**

*DUSP1* gene and protein expression have been shown to be lost in a number of human malignancies, including prostate, breast, and colon, with increasing tumor grade (174, 176, 340). Based on characterization of the knockout animal, *Dusp1* has been shown to be necessary for timely inactivation of immune responses to bacterial challenges, including LPS, peptidoglycan, and other innate immune stimuli (144, 153, 407). The oral microenvironment contains a unique complement of dense bacterial pathogens and constant immune surveillance, with important implications in head and neck cancer (374, 408). Animal studies presented in Chapter 3 suggest *Dusp1* may have a tumor suppressive role in head and neck cancer, due in part to alterations of the immunologic milieu. Thus, we hypothesize expression of DUSP1 is decreased in human HNSCC tissues.

### **5.2 Results**

#### ***Decreased DUSP1 expression in human HNSCC***

Expression of *DUSP1* mRNA and protein levels were examined in tumor tissue from patients diagnosed with HNSCC in comparison to matched adjacent non-tumor tissue. RNA and protein were isolated from snap frozen tissues and assessed by qPCR

and immunoblotting. *DUSP1* mRNA was significantly decreased in ten pairs of HNSCC tissues compared to non-tumor controls (Figure 5-1). Protein levels of DUSP1 were also down-regulated in tumor tissues in 8 of the 11 pairs of tissue samples. Expression of *IL1B* mRNA was also examined to determine if there was a similar inverse relationship as seen in the 4NQO animal model and in *ex vivo* macrophage experiments. A linear regression of *IL1B* and *DUSP1* gene expression from each patient, using fold change of gene expression in the tumor tissue normalized to the adjacent non-tumor tissue sample did not detect an inverse linear relationship between fold change of *DUSP1* versus fold change of *IL1B* for each patient sample pair. However, this method of comparison is not well suited for these data, in which a single patient provides two pairs of (x, y) data. Using an alternative statistical test, an association ( $\beta = 1.34$ ,  $p = 0.011$ ) was detected between *IL1B* and *DUSP1* in this sample set. However, the available sample size limits the interpretation that can be made from this comparison. As expression of IL-1 $\beta$  is regulated at multiple points, both in gene expression and post-translational processing, protein expression of IL-1 $\beta$  by Western blotting was assessed (Figure 5-2). These blots demonstrate increased levels of 35kD proform and cleaved 17kD IL-1 $\beta$  in eight of eleven pairs of these HNSCC tumor tissues, likely a more appropriate measure of IL-1 $\beta$  expression within the tumor microenvironment than mRNA.

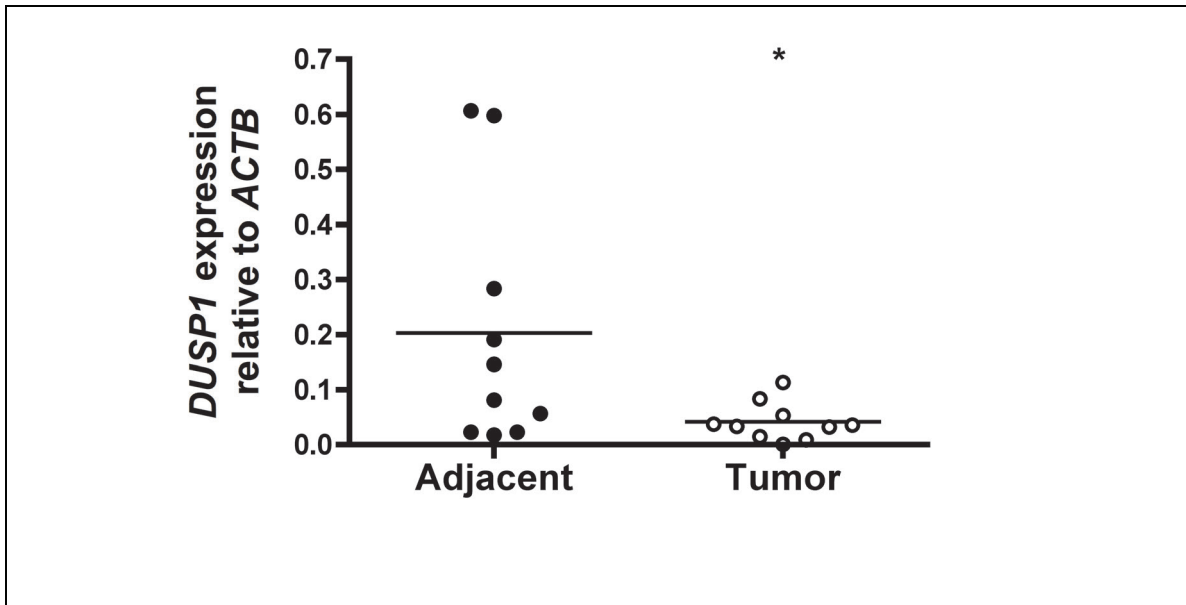


Figure 5-1. *DUSP1* mRNA is decreased in human HNSCC. Tissues from patients diagnosed with HNSCC were assessed for *DUSP1* expression by qPCR. *DUSP1* expression was significantly decreased in tumor tissues compared to matched adjacent non-tumor tissue. n = 10, Student's paired *t*-test,  $p = 0.0378$ .

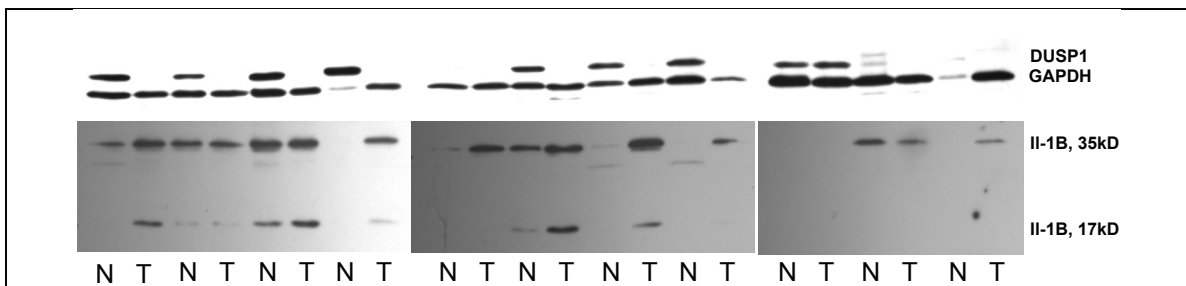
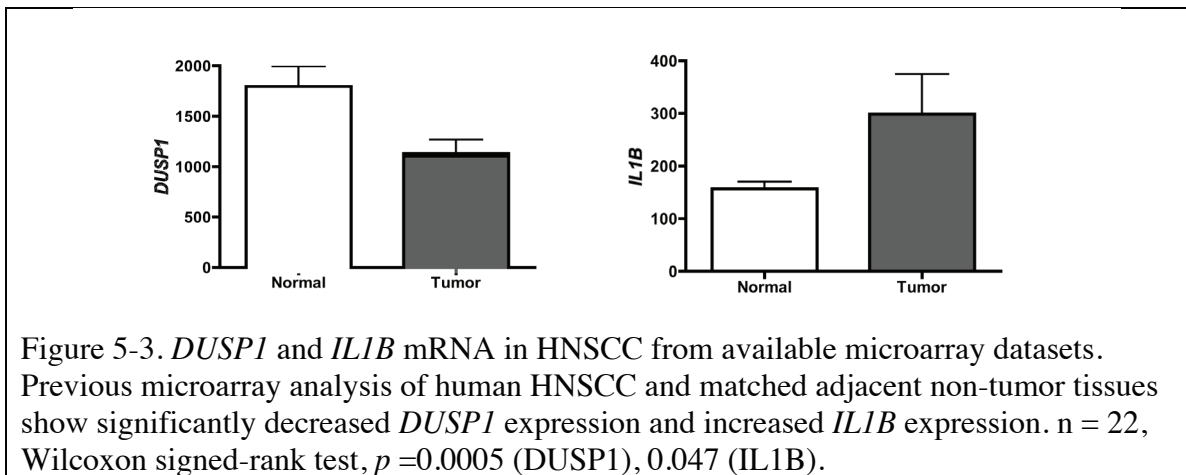


Figure 5-2. *DUSP1* and IL-1 $\beta$  expression in human HNSCC. Tissues from patients diagnosed with HNSCC were assessed for *DUSP1* and IL-1 $\beta$  expression by Western blotting. *DUSP1* expression was decreased in nine of the eleven tumor tissues compared to matched adjacent non-tumor tissue. IL-1 $\beta$  expression was increased eight of the eleven tumor tissues. n = 11.

### *DUSP1* expression in other HNSCC datasets

Previously generated microarray data from a set of 22 patients diagnosed with HNSCC were also examined for *DUSP1* expression. Five of the 22 pairs of patient samples were obtained from a hospital in Shanghai, China, and the remainder during

surgical resection at New York University. Thirteen of the 22 tumors were located within the oral cavity. Three of the tumor samples were located within the oropharynx. Nine patients were diagnosed with stage T<sub>1</sub> or T<sub>2</sub> disease with no nodal involvement, and none of the patients had any distant metastatic disease (409). In this sample set, comparing HNSCC expression with that of non-tumor adjacent tissue revealed significantly decreased *DUSP1* and significantly increased *IL1B* mRNA (Figure 5-3).



### ***Correlation between DUSP1 expression and cytokine levels in HNSCC***

Linear regression analysis of *DUSP1* and *IL1B* mRNA expression from the ten sample sets obtained from the Hollings Cancer Center did not reveal a significant correlation. This analysis was performed using a linear regression of *IL1B* and *DUSP1* gene expression from each patient, comparing fold change of gene expression in the tumor tissue normalized to the adjacent non-tumor tissue sample, for both *DUSP1* and *IL1B* gene levels, which did not detect an inverse linear relationship between fold change of *DUSP1* versus fold change of *IL1B* for each patient sample pair. As previously discussed, this statistical method is not well suited for these data, in which a single patient provides two pairs of (x, y) data. Although an association ( $\beta = 1.34$ , p = 0.011)

was detected between *IL1B* and *DUSP1* using an alternative statistical test, the available sample size limits the interpretation that can be made from this comparison.

### **5.3 Summary & Discussion**

These experiments demonstrated that *DUSP1* gene and protein expression is reduced in human HNSCC compared to adjacent non-tumor tissue, as previously described in other tumor types (88, 174, 182). The interpretation of these results is limited by a disease-free tissue sample to account for potential changes in gene expression due to a tumor field effect. Although adjacent non-tumor tissue samples were used as controls, the field of precancerous epithelium, seen early in the progression of OSCC (410), has likely already begun to accumulate genomic and epigenetic alterations. An alternative option for control tissues from cancer-free patients includes samples from uvulopharyngoplasty for obstructive sleep apnea. These tissues offer similar anatomical location but often are complicated by long-standing inflammation and hypoxia (411). In the available tissue pairs, the difference between HNSCC and adjacent non-tumor tissue was significant, even in a small sample size, suggesting loss of *DUSP1* is a common molecular occurrence. Searches of available genome-wide association studies and copy number variation analyses have not identified sites of mutation or deletion to explain its loss. Recently, an unbiased promoter hypermethylation screen identified *DUSP1* (89), suggesting its down-regulation can be mediated by epigenetic means. The upstream epigenetic modifiers responsible and whether loss of expression can be reversed with pharmaceutical inhibitors, such as azacytidine and decitabine, should be addressed in future studies.

A shortcoming of these studies is the inability to address whether regulation of IL-1 $\beta$  is deregulated by loss of *DUSP1* expression, as seen in murine macrophages *ex vivo*. Correlation analysis suggests a trend toward increasing IL-1 $\beta$  mRNA expression with decreasing *DUSP1* mRNA expression, but analysis of IL-1 $\beta$  gene levels may not be sufficient as its expression is highly regulated post-translationally by inflammasome activation. Furthermore, the small sample size limits the associations that could be drawn to understand whether *DUSP1* and/or IL-1 $\beta$  expression may have prognostic or predictive value in HNSCC. In future studies with a larger sample set, ideally these tissues can be stratified based on tissue site, stage, grade, patient sex, exposure to tobacco, alcohol, and chemotherapeutic and radiotherapeutic treatments. The tissues used for these analyses did not include tumors from the oropharynx, limiting likelihood of HPV-positive status. However, in future studies with larger datasets, stratification of HPV-positive versus negative tissues will be an important distinction, as pathophysiology of these tumors, particularly with respect to immune involvement, differs dramatically. In addition, analysis of tissues from primary tumors versus lymph node or distant metastases might answer whether *DUSP1* expression level is involved in metastatic progression.

Immunohistochemical studies were not performed due to non-specific background staining in testing of several commercially available *DUSP1* antibodies. The consequences of altered subcellular localization must be considered, as *DUSP1* immunohistochemistry has been characterized as cytoplasmic in certain cancers (184) (182). With a more specific antibody for immunohistochemistry, subcellular localization can be assessed as well as identifying which cells within the tumor express *DUSP1* and whether these colocalize with specific cytokines, such as IL-1 $\beta$ . The latter question can

be addressed by laser-capture microdissection of epithelial versus stromal expression within HNSCC tissues, but delineating key immune cell players will require more precise techniques.

Already a recombinant form of IL-1RA, an endogenous antagonist to IL-1R1, approved for use in rheumatoid arthritis, is showing signs of efficacy in clinical trials for smoldering myeloma and numerous murine cancer models (412, 413). A dose-escalation phase I clinical trial of a monoclonal antibody against IL-1 $\alpha$  demonstrated 29% stable disease and 3% partial response in a group of 34 patients with metastatic disease of 18 tumor types. Furthermore, 70% of patients with cancer-associated cachexia demonstrated reduced IL-6 plasma levels with increased lean body mass (414). Before expanding these to other disease models, additional studies must be done to better understand the cellular constituents and downstream mechanisms targeted by these inhibitors.

## **CHAPTER 6. General Discussion & Future Directions**

Although previous reports have identified down-regulation of DUSP1 across a diversity of tumor tissues, this is the first study to demonstrate a tumor suppressive role for this MAPK phosphatase. Results from these *in vivo* and *ex vivo* studies also highlight a potential mechanism for up-regulation of the pro-inflammatory cytokine IL-1 $\beta$  in oral cancer, previously shown to be elevated both as mRNA in salivary exosomes (376) and secreted protein (375). Using a model that closely mimics the genetic heterogeneity of HNSCC following long-term carcinogen exposure, these findings support the role of IL-1 $\beta$  as a potential biomarker for human disease. However, additional work must be done to address the functional impact of IL-1 $\beta$  on tumor progression.

The implications of these findings may extend well beyond HNSCC, as DUSP1 expression has been shown to be dysregulated in a number of other cancers and may even be predictive of response to targeted therapies, such as cetuximab (174, 415). Genomic studies have not identified common mutation or deletions, but a recent DNA methylation screen identified significantly increased promoter hypermethylation in over 80% of oral cancer tissues compared to normal samples (89). Furthermore, aberrant ERK signaling in cancer cells may enhance DUSP1 degradation through the proteasomal pathway (136, 137). The delineation of regulatory mechanisms in different cell types will enhance the understanding of expression changes in pathologic states and enhance development of specific therapeutic agents.



Bone marrow chimeric and subcutaneous syngeneic tumor experiments suggest the loss of *DUSP1* expression in the tumor microenvironment, but not hematopoietic cells, supports tumor progression. Additional studies must be performed to address how *Dusp1* deficiency in non-hematopoietic cells alters tumor-associated inflammation and the specific cell types involved. This finding presents an opportunity to design therapeutics with the benefit of targeting cell types with decreased heterogeneity, compared to tumor cells, with the goal of generating a consistent anti-tumor response. In addition, modulation of an immune regulator, such as DUSP1, has the potential to go beyond simply reducing inflammation and shifts the immune response to reprogram it toward a less immunosuppressive phenotype.

An unanswered question remains the potential inflammatory trigger that initiates the inflammatory response seen in the 4NQO model of oral cancer. Although tumor-associated inflammation is commonly referred to as “sterile inflammation,” possibly driven, in this scenario, by the interleukin-1 response to necrotic tissue, the context of the oral cavity brings up potential involvement of the abundant and diverse microflora. Recent studies of germ-free mice have identified crucial roles of the gut microbiome in shaping immune system development with broad-reaching effects on metabolism, autoimmunity, and cancer. Additional work must be done to address how the complex biodiversity in the oral cavity may interact with the immune cells within the head and neck tumor microenvironment and its effects on tumor growth and progression.

Pharmaceutical intervention to induce *DUSP1* expression, with agents such as rosiglitazone and mapracorat, are currently being explored with promising results, suppressing MMP-2 and CXCR4 expression and xenograft growth in NSCLC cells and

LPS-induced activation in macrophages, respectively (345, 347). Additional agonists of DUSP1 include aurothiomalate and auranofin, which increase *DUSP1* expression and inhibit p38 MAPK phosphorylation, are anti-rheumatic gold compounds (416). Phosphodiesterase 4 (PDE4) inhibitors, recently used to treat chronic obstructive pulmonary disease, plaque psoriasis, and psoriatic arthritis (417-419), inhibit the cyclic AMP (cAMP) degradation pathway regulating the signaling through this second messenger in a number of cell types (420). DUSP1 has been shown to mediate the anti-inflammatory effect of the PDE4 inhibitor rolipram through transcriptional activation by the cAMP-PKA-CREB pathway (421-424). Vitamin D has also been shown to induce DUSP1 expression and inhibit p38 MAPK phosphorylation in macrophages (83), as one of a number of mechanisms for its role as an endogenous anti-inflammatory agent. The use of thiazolidinediones as an anti-diabetic agent was previously shown in a retrospective study to be associated with reduced risk of lung, prostate, and colon cancer (425). Concerns over adverse cardiovascular events associated with rosiglitazone use have dampened enthusiasm over its potential as a chemopreventive agent. However, on November 25, 2013, the Food and Drug Administration released an update removing prescribing restrictions on the drug following evaluation of the Rosiglitazone Evaluated for Cardiovascular Outcomes and Regulation of Glycemia in Diabetes (RECORD) clinical trial when no increase in risk of heart attack or death was found. Within the same family of thiazolidinediones, pioglitazone was recently examined in a Phase IIa clinical trial for prevention of head and neck cancer in patients with oral leukoplakia, with partial or complete responses in 15 out of 21 patients, as reported to [clinicaltrials.gov](http://clinicaltrials.gov)

(NCT00099021). Given these promising early findings, additional investigation as to whether these agents could enhance current therapies is needed.

In summary, these studies demonstrate DUSP1 plays an important role within the tumor microenvironment, regulating key cytokines such as IL-1 $\beta$ . Loss of *DUSP1* expression, as shown here in head and neck cancer, alters the inflammatory milieu of the tissue, with enhanced expression of pro-tumorigenic cytokines that enhance immune cell recruitment and activation while promoting suppression of anti-tumor immunity. In animal tumor models, down regulation of *Dusp1* leads to enhanced disease progression through increased activation of MAPK-driven signaling pathways. Thus, restoring *DUSP1* expression represents a promising target of pharmacological intervention and merits further investigation as a suppressor of tumor-promoting inflammation.

Appendix A. Comparison of inflammatory cytokine, chemokine and receptor expression in wild-type and *Dusp1* deficient tumor tissue by targeted qPCR array.

Gene Symbol	Fold Change (KO/WT)
Abcf1	0.6329
Bcl6	0.6875
Cxcr5	0.3248
C3	0.1073
Casp1	1.4903
Ccl1	2.7989
Ccl11	4.7209
Ccl12	1.7519
Ccl17	0.2741
Ccl19	0.1674
Ccl2	1.9337
Ccl20	10.2795
Ccl22	0.4401
Ccl24	0.4618
Ccl25	3.3507
Ccl3	6.182
Ccl4	2.9434
Ccl5	0.9409
Ccl6	0.1186
Ccl7	4.1278
Ccl8	7.7008
Ccl9	0.3585
Ccr1	1.9907
Ccr2	0.093
Ccr3	0.4918
Ccr4	0.8927
Ccr5	1.7285
Ccr6	0.4775
Ccr7	1.7226
Ccr8	2.1032
Ccr9	0.9698
Crp	0.5606
Cx3cl1	4.0198
Cxcl1	61.9138
Cxcl10	8.8977
Cxcl11	0.2104

Cxcl12	0.0616
Cxcl13	0.2982
Cxcl15	14.1112
Pf4	0.2629
Cxcl5	38.2254
Cxcl9	2.5912
Cxcr3	0.4102
Ccr10	0.595
Ifng	1.6071
Il10	4.7894
Il10ra	0.6025
Il10rb	1.001
Il11	4.4849
Il13	1.0203
Il13ral	3.471
Il15	0.1727
Il16	0.2565
Il17b	3.2297
Il18	0.2697
Il1a	17.6278
Il1b	70.8116
Il1f6	1.0531
Il1f8	0.3074
Il1r1	1.1472
Il1r2	0.1121
Il20	98.0404
Il2rb	1.5139
Il2rg	1.3098
Il3	1.2666
Il4	2.3206
Il5ra	0.4031
Il6ra	0.4937
Il6st	0.2467
Il8rb	10.4981
Itgam	0.5867
Itgb2	0.5232
Lta	1.1531
Ltb	0.65
Mif	1.5026

Scye1	0.3676
Spp1	32.0843
Tgfb1	4.3959
Tnf	11.3496
Tnfrsf1a	1.5127
Tnfrsf1b	1.3287
Cd40lg	31.3148
Tollip	0.7192
Xcr1	5.7944
Gusb	2.2192
Hprt1	1.9778
Hsp90ab1	0.7519
Gapdh	0.172
Actb	1.7619
MGDC	4.4951

Appendix B. Comparison of the expression levels of MAPK signaling pathway members in wild-type and *Dusp1* deficient tumor tissue by targeted qPCR array.

<b>Gene Symbol</b>	<b>Fold Change (KO/WT)</b>
Araf	1.06
Atf2	1.93
Ccna1	0.81
Ccna2	0.01
Ccnb1	4.01
Ccnb2	11.16
Ccnd1	2.47
Ccnd2	1.09
Ccnd3	1.07
Ccne1	3.29
Cdc42	2.91
Cdk2	3.05
Cdk4	1.16
Cdk6	4.7
Cdkn1a	1.07
Cdkn1b	0.88
Cdkn1c	1.49
Cdkn2a	124.88
Cdkn2b	27.25
Cdkn2c	1.17
Cdkn2d	0.63
Chuk	3.7
Col1a1	0.17
Creb1	1.39
Crebbp	0.7
Dlk1	0.81
E2f1	2.56
Egfr	0.62
Egr1	7.55
Elk1	0.74
Ets1	5.48
Ets2	0.44
Fos	102.33
Grb2	1.04
Hras1	1.21
Hspa5	2.12

Hspb1	0.86
Jun	0.56
Kcnn1	0.11
Kras	3.46
Ksr1	0.13
Map2k1	1.47
Mapksp1	2.96
Map2k2	0.56
Map2k3	1.01
Map2k4	1
Map2k5	1.11
Map2k6	0.75
Map2k7	0.42
Map3k1	0.89
Map3k2	1.42
Map3k3	3.01
Map3k4	0.31
Map4k1	0.7
Mapk1	0.88
Mapk10	0.16
Mapk11	2.89
Mapk12	0.15
Mapk13	4.69
Mapk14	0.42
Mapk3	1.06
Mapk6	4.59
Mapk7	2.38
Mapk8	0.81
Mapk8ip1	0.35
Mapk8ip2	0.67
Mapk8ip3	1.93
Mapk9	0.7
Mapkapk2	0.3
Mapkapk5	0.34
Max	0.89
Mef2c	0.03
Mknk1	1.16
Mos	1.2
Myc	2.68

Nfatc4	0.21
Nras	2.7
Pak1	4.26
Rac1	1.81
Raf1	0.87
Rb1	0.58
Sfn	2.57
Smad4	0.94
Trp53	1.32
Gusb	1.93
Hprt1	2.18
Hsp90ab1	1.07
Gapdh	0.14
Actb	1.55

Appendix C. Nanostring gene counts from wild-type and *Dusp1* deficient tumor tissues.

Gene counts are shown for individual tumor tissue lysates, after normalization against positive and negative in-assay controls and housekeeping genes. n = 6.

	a-SMA	Activin AB	Acvr2a	ADAM17	ALK-1
WT	11775.74	13.16	1266.01	2303.91	3407.61
WT	12400.28	13.23	1284.19	2389.29	3476.07
WT	1489.83	5.02	1696.78	2935.46	561.58
WT	12312.11	11.72	1529.42	2195.55	1032.76
WT	6367.13	22.76	1473.21	3544.08	892.31
WT	9517.23	25.36	1483.79	3163.57	900.42
KO	9980.18	12.16	1087.9	3462.71	1265.9
KO	2372.75	14.97	1468	4034.42	794.35
KO	2283.04	11.14	1426.2	3961.06	728.7
KO	2861.85	7.53	1308.97	4579.52	720.41
KO	6599.72	8.93	1275.89	2604.37	804.63
KO	1818.34	21.6	1583.38	4706.96	453.51

	ALK-2 (Acvr 1)	ALK-3 (BMR1A)	ALK-4 (Acvr 1B)	ALK-5 (TGFbR I)	ALK-6 (BMPR1B)
WT	1203.72	6603.78	4139.32	1946.83	644.85
WT	1333.04	6820.87	4136.48	2029.06	706.2
WT	1018.67	6231.58	4353.97	2206.12	343.58
WT	1130.81	6497.11	4368.71	2282.94	751.39
WT	1389.37	6224.6	4418.42	2003.8	476.7
WT	1292.41	6240.68	4883.71	1776.63	537.25
KO	1478.18	6724.21	5472.68	2340.54	357.11
KO	1414.67	6384.71	4170.08	2917.28	188.06
KO	1325.92	6384.49	4227.36	2959.37	172.7
KO	1520.86	7440.42	4582.34	2873.15	136.55
KO	1061.59	5700.84	3225.45	1787.84	335.34
KO	2146.59	11267.68	5760.82	4127.34	80.34

	ALK-7 (Acvr1C)	Alpl	AMH	APRIL	Arg-1
WT	23.69	206.18	7.02	108.79	6703.8
WT	31.55	194.36	5.09	123.13	6988.77
WT	52.24	239.1	5.02	164.76	12976.52
WT	62.88	313.35	9.59	181.19	7331.63

WT	141.33	267.09	7.19	179.66	13404.98
WT	29.98	198.3	6.92	227.12	14945.11
KO	17.69	504.15	4.42	135.99	39627.73
KO	165.61	145.96	14.97	130.05	160061.26
KO	171.59	122.56	11.14	141.51	155674.57
KO	5.65	542.42	5.65	80.99	86303.61
KO	49.61	200.41	7.94	84.33	9542.4
KO	9.5	38.87	6.91	50.1	24022.86

	Arginase	Atf4	Axin2	Bad	Bax
WT	89.49	9329.7	420.25	364.1	1262.5
WT	86.49	9760.67	423.32	401.95	1297.42
WT	25.12	10790.5	301.38	459.11	1477.78
WT	38.37	7856.01	510.52	363.44	1170.25
WT	22.76	10674.16	352.13	420.4	1143.83
WT	42.66	9732.83	408.13	447.33	1127.54
KO	160.31	13104.58	375.9	509.68	1451.64
KO	236.71	12309.09	245.13	589.44	1963.88
KO	240.67	12043.62	222.84	563.8	1896.4
KO	367.27	12590.61	344.66	543.36	1777
KO	33.73	11155.62	278.79	373.04	1116.16
KO	126.12	16403.09	188.31	597.76	2265.8

	Bcl2	Bcl2l1	Bcl2l11	Bcl6	Bglap
WT	310.58	1706.44	485.17	914.19	6679.24
WT	345.98	1722.77	528.13	936.18	6835.11
WT	115.53	1423.53	318.46	798.66	20252.9
WT	262.19	1164.92	447.64	840.92	12957.99
WT	222.78	1349.84	421.6	1002.5	11506.58
WT	249.03	1254.36	469.23	832.4	9053.76
KO	192.37	1795.48	724.16	1072.42	1460.49
KO	109.47	2055.57	747.57	906.62	1217.25
KO	93.59	2089.17	726.47	915.89	1246.81
KO	113	1618.79	761.84	741.12	459.55
KO	70.44	907.81	299.63	872.09	1088.38
KO	155.49	1161.84	694.51	1102.24	251.37

	Bmp-1	Bmp2	Bmp4	BMPR-II	C-fos
WT	1547.64	450.96	1898.58	2263.55	1444.11

WT	1502.97	487.42	1953.76	2269.21	1507.04
WT	816.75	744.41	888.07	2799.84	958.4
WT	962.42	820.67	1606.16	2940.54	1289.62
WT	1052.8	589.28	958.18	2617.04	1913.97
WT	1215.16	645.63	1423.84	2712.79	1165.59
KO	1822.02	674.41	1223.89	2672.22	3153.15
KO	2170.65	1007.67	712.01	3360.77	10835.48
KO	2071.34	947.09	677.45	3295.87	10536.08
KO	2058.57	730.76	1280.72	2608.53	2936.24
KO	714.34	369.08	1018.93	2352.36	1433.64
KO	5028.3	1921.14	1224.9	3905.33	15322.45

	C1qa	C1qb	C3ar1	C5ar1	Calcr
WT	1712.58	3354.09	547.46	374.63	37.73
WT	1821.48	3395.68	590.2	365.31	38.67
WT	1819.35	3333.29	494.27	339.56	31.14
WT	2550.46	4242.95	940.04	331.46	28.78
WT	1948.71	3287.77	1203.72	406.03	41.92
WT	2526.02	4613.93	1035.31	440.41	24.21
KO	3147.62	5973.51	1169.72	705.37	16.58
KO	4553.69	9327.25	1756.17	1274.32	8.42
KO	4507.03	9220.18	1644.59	1331.49	17.83
KO	3254.54	5420.46	2217.72	921.93	11.3
KO	1494.16	3338.55	540.72	303.59	26.79
KO	2101.68	4063.41	1591.16	446.6	10.37

	CCL2	CCR5	Cd 44	Cd 47	Cd 9
WT	504.47	106.16	11211.61	3898.05	13505.87
WT	525.07	135.34	11338.94	4029.63	14243.13
WT	445.04	115.53	11416.37	5073.27	20856.67
WT	540.36	185.45	10892.47	4500.87	13942.79
WT	1366.61	209.6	15350.1	4525.02	15465.08
WT	840.47	228.28	14834.43	4949.42	14910.52
KO	794.92	256.5	24304.22	5984.57	22548.55
KO	2137.91	377.06	39415.11	8776.17	50118.67
KO	2152.68	384.41	38495.24	8796.78	49367.81
KO	1214.8	509.46	32803.39	8977.29	39992.38
KO	655.8	157.75	10609.95	3605.44	11283.61
KO	3063.11	332.57	50665.68	9912.34	56344.44



	CD105	CD109	CD11b	CD16	CD163
WT	1759.08	2347.78	423.76	219.34	959.82
WT	1926.29	2419.82	443.67	241.17	979.93
WT	697.2	3527.18	546.51	341.57	882.05
WT	1316.26	3418.02	653.34	274.98	1108.43
WT	1234.86	2327.19	450.35	202.42	945.01
WT	1378.87	2361.15	737.86	319.35	1265.89
KO	1670.55	2546.18	740.75	479.83	1678.29
KO	1156.43	3188.61	1442.74	1424.02	4221.54
KO	1080.79	3221.21	1520.91	1352.66	4169.42
KO	1244.94	2830.77	833.41	838.12	1554.76
KO	1149.89	1676.72	536.75	302.6	540.72
KO	801.63	8969.92	404.27	374.03	375.76

	CD32	CD40lg	CD46	CD55	CD56
WT	1473.06	13.16	26.32	3350.59	1350.24
WT	1490.76	21.37	18.32	3506.6	1374.76
WT	1403.44	9.04	12.06	2343.75	931.27
WT	1303.47	29.84	22.38	3080.16	1235.26
WT	1353.43	34.73	28.75	2421.81	983.34
WT	1596.77	29.98	18.45	2588.27	990.35
KO	3138.78	38.7	23.22	2640.15	885.58
KO	6517.57	27.13	12.16	2264.21	786.86
KO	6138.25	23.4	20.06	2184.99	699.73
KO	4228.26	32.02	14.13	1438.93	431.3
KO	1097.31	26.79	21.83	2690.68	882.01
KO	2521.49	16.41	20.73	567.53	1844.26

	Col10a1	Colla1	CD86	Cdh1	CEBPb
WT	4.39	4788.56	296.54	9626.24	8791.89
WT	6.11	4880.33	306.29	9845.13	9098.22
WT	4.02	3398.59	240.1	10433.86	11097.91
WT	4.26	4995.4	436.98	8474.17	8942.06
WT	11.98	4413.63	554.55	11681.45	12782.17
WT	13.83	7221.8	526.88	12096.28	10289.68
KO	12.16	9460.55	671.09	15243.9	11820.99
KO	11.23	12267.93	265.72	20376.06	11453.93
KO	21.17	11987.91	269.64	20265.46	11015.19
KO	19.78	9013.07	652.6	15222.68	10204.33
KO	6.94	4705.72	326.41	8153.41	9482.88

KO	244.46	4910.82	310.98	14060.41	6772.35
----	--------	---------	--------	----------	---------

	Chordin	Col10a1	Colla1	CollA2	Col2a1
WT	163.19	4.39	4788.56	3107.56	11.41
WT	180.11	6.11	4880.33	3231.85	14.25
WT	112.52	4.02	3398.59	1482.8	14.06
WT	187.58	4.26	4995.4	3731.36	20.25
WT	135.34	11.98	4413.63	3260.22	25.15
WT	177.55	13.83	7221.8	4853.73	16.14
KO	127.14	12.16	9460.55	5199.6	13.27
KO	78.59	11.23	12267.93	3752.8	25.26
KO	60.17	21.17	11987.91	3613.42	31.2
KO	65.92	19.78	9013.07	5009.88	25.43
KO	99.21	6.94	4705.72	1886.06	10.91
KO	50.97	244.46	4910.82	2074.03	38.01

	Cpt1a	Crim1	CSF1	CSF2	CSF3
WT	3472.54	1612.56	1067.73	21.93	35.97
WT	3613.44	1801.12	1120.36	36.63	46.81
WT	4810.06	1114.11	894.1	14.06	8.04
WT	3208.06	1711.67	1187.3	27.71	24.51
WT	3630.32	1206.11	1269.59	22.76	69.47
WT	3637.42	1324.69	1207.09	25.36	13.83
KO	4412.42	1556.67	1055.84	16.58	202.32
KO	3428.13	1882.48	880.42	55.2	152.51
KO	3387.23	1908.66	817.84	46.8	134.82
KO	3594.49	1573.59	823.05	61.21	259.91
KO	3341.53	1323.52	929.64	12.9	7.94
KO	4144.61	2888.62	848.27	55.28	119.21

	Ctla4	Ctnnb1	Ctsk	CXCL1	CXCL10
WT	129.85	20536.04	464.99	100.02	42.11
WT	121.09	20424.95	436.54	98.71	42.74
WT	97.45	22674.01	259.19	48.22	53.24
WT	228.08	23931.46	699.16	106.58	121.5
WT	231.16	24639.68	492.27	332.97	415.61
WT	244.42	25083.76	707.88	103.76	198.3
KO	464.35	26059.9	824.77	1174.14	456.61
KO	178.7	32609.37	1959.2	1250.93	246.07

KO	193.87	32197.66	1808.38	1128.71	233.99
KO	836.24	27795.4	747.71	1544.4	457.67
KO	81.36	19792.21	353.2	78.38	101.2
KO	199.54	38908.22	344.66	2392.78	374.03

	CXCL11	CXCL13	CXCL2	CXCL9	CXCR5
WT	23.69	202.67	48.25	41.24	35.97
WT	31.55	202.5	49.86	42.74	58
WT	47.22	589.7	11.05	120.55	49.23
WT	105.51	344.25	35.17	160.94	96.99
WT	79.05	1245.64	38.33	168.88	80.25
WT	117.6	1065.28	62.26	387.38	99.15
KO	26.53	547.27	906.59	347.16	35.38
KO	31.81	2408.3	1215.38	364.89	27.13
KO	25.63	2313.12	1270.21	324.24	33.43
KO	48.03	433.18	2536.96	1107.45	30.13
KO	31.75	104.17	11.91	128.98	15.87
KO	32.83	31.1	610.72	377.49	26.78

	Decorin	Dermatopontin	Dkk1	DMP-1	Dspg
WT	66434.41	25010.51	15.79	9.65	8.77
WT	67027.26	25073.28	13.23	20.35	3.05
WT	75432	20581.41	8.04	10.05	11.05
WT	97661.33	25296.75	30.91	19.18	24.51
WT	57691.02	26109.3	20.36	10.78	20.36
WT	77477.54	26981.44	21.91	12.68	17.29
KO	67276.37	26277.71	14.37	14.37	12.16
KO	49692.03	9735.19	8.42	25.26	11.23
KO	49153.88	9468.65	10.03	20.06	10.03
KO	30450.07	11938.01	11.3	26.37	11.3
KO	48463.07	19216.76	7.94	5.95	16.87
KO	7776.11	7115.29	11.23	13.82	9.5

	Erbin	Ets1	Eif4a2	Elastase	Emr1
WT	7349.53	1823.13	32873.28	10.53	294.79
WT	7390.72	1888.64	33172.23	9.16	317.49
WT	7451.18	1031.73	30200.53	12.06	654
WT	7525.61	1393	30605.49	12.79	597.91
WT	7033.07	1569.03	28751.49	15.57	601.26

WT	6968.16	1468.8	30991.24	12.68	718.26
KO	7233.89	1817.59	30459.05	15.48	372.58
KO	8424.38	1714.07	20233.85	14.97	813.06
KO	8280.89	1608.94	20080.5	15.6	821.18
KO	7404.64	1756.28	32189.4	5.65	483.1
KO	4855.53	1248.11	31393.3	11.91	383.96
KO	9261.02	1652.49	33940.38	11.23	301.47

	EOMES	Erbin	Ets1	Factor B	Fgf2
WT	10.53	7349.53	1823.13	214.95	1156.34
WT	17.3	7390.72	1888.64	178.08	1098.99
WT	5.02	7451.18	1031.73	294.35	585.69
WT	21.32	7525.61	1393	401.81	1165.98
WT	15.57	7033.07	1569.03	328.18	722.23
WT	25.36	6968.16	1468.8	457.7	780.52
KO	5.53	7233.89	1817.59	637.93	657.83
KO	22.46	8424.38	1714.07	946.85	277.88
KO	31.2	8280.89	1608.94	937.06	287.47
KO	13.18	7404.64	1756.28	657.31	152.56
KO	9.92	4855.53	1248.11	529.8	640.92
KO	32.83	9261.02	1652.49	343.8	101.07

	Fgf23	Fgf4	Fgf8	Fizz1	FKBP51
WT	8.77	14.91	5.26	16235.29	1137.92
WT	8.14	18.32	8.14	16512.34	1097.97
WT	17.08	28.13	13.06	40055.73	655
WT	38.37	30.91	6.39	33439.46	690.64
WT	63.48	39.53	11.98	27507.05	839.61
WT	38.05	39.2	5.76	34869.62	667.53
KO	49.75	15.48	7.74	15194.15	1911.57
KO	34.62	14.97	7.49	33161.39	1698.16
KO	55.71	18.94	8.91	32078.44	1598.91
KO	68.74	15.07	6.59	12470.07	606.46
KO	16.87	24.8	4.96	23334.15	459.36
KO	21.6	18.14	12.09	2810.01	324.8

	FLT3L	Follistatin	Foxo1	FoxP3	Fstl3
WT	372.87	599.23	1208.98	34.22	67.56
WT	387.7	579.01	1231.28	31.55	89.55

WT	211.97	503.31	1023.7	28.13	36.17
WT	339.99	522.24	1470.8	103.38	93.79
WT	396.45	352.13	1143.83	140.13	85.04
WT	317.05	499.21	1062.98	136.04	83.01
KO	302.93	1060.26	1166.4	107.24	89.55
KO	244.2	1091.88	1409.05	31.81	130.05
KO	226.19	1021.74	1372.72	26.74	123.68
KO	285.34	1488.84	747.71	122.42	77.22
KO	218.27	376.02	749.07	31.75	40.68
KO	416.36	8448.17	1151.47	31.1	158.94

	Fstl4	Furin (PACE)	G6pd2	Gata3	GDF1
WT	16.67	4412.17	3260.22	135.11	52.64
WT	29.51	4404.11	3490.31	129.23	68.18
WT	15.07	5261.13	3367.45	95.44	31.14
WT	40.5	4466.77	3253.89	266.45	77.8
WT	17.97	5180.18	3833.93	173.67	68.27
WT	34.59	5080.85	3300.77	279	48.42
KO	22.11	8414.66	3599.81	174.68	32.06
KO	17.78	12194.01	4503.17	105.73	16.84
KO	18.94	12311.03	4518.17	114.76	18.94
KO	12.24	10256.12	3330.81	184.57	22.6
KO	7.94	4822.79	2152.94	94.25	40.68
KO	22.46	16334.85	2179.42	143.39	11.23

	GDF15 (MIC-1)	GDF2 (BMP9)	GDF3 (Vgr-2)	GDNFR alpha-2	GDNFR alpha-3
WT	5.26	8.77	14.04	366.73	28.95
WT	8.14	6.11	11.19	391.77	39.69
WT	11.05	13.06	12.06	278.28	16.07
WT	19.18	22.38	29.84	395.41	49.03
WT	34.73	19.16	13.18	346.14	37.13
WT	23.06	21.91	29.98	386.22	35.74
KO	13.27	11.06	44.22	392.49	38.7
KO	14.97	9.36	14.97	422.9	16.84
KO	17.83	17.83	20.06	441.23	12.26
KO	21.66	10.36	20.72	358.79	11.3
KO	8.93	13.89	28.77	403.8	31.75
KO	14.68	11.23	30.23	214.23	10.37

	GFR alpha-1	Gfra4	Gli1	GP49A	Gprasp1
WT	215.83	286.89	251.8	541.32	529.92
WT	253.38	296.12	276.78	623.78	533.21
WT	240.1	181.83	57.26	203.94	371.71
WT	222.75	311.21	142.82	341.06	525.44
WT	198.82	194.03	82.64	519.81	516.22
WT	168.32	250.18	129.13	515.35	500.36
KO	123.83	208.96	105.03	1902.72	286.35
KO	69.24	151.57	50.52	3142.77	174.03
KO	62.4	141.51	55.71	3132.08	192.76
KO	52.74	154.44	57.44	5239.65	144.08
KO	92.27	90.28	64.49	375.03	312.52
KO	63.06	67.38	59.6	1760.47	187.45

	Gprasp2	Gr1	Gremlin	GusB	GzmB
WT	131.6	6.14	660.64	626.43	10.53
WT	117.02	10.18	668.55	641.08	13.23
WT	67.31	3.01	44.2	619.84	22.1
WT	229.15	12.79	474.28	614.97	33.04
WT	156.9	11.98	457.53	606.05	22.76
WT	157.95	25.36	600.66	722.87	38.05
KO	50.86	17.69	1656.18	986.19	33.17
KO	29	56.14	1370.69	1136.79	101.05
KO	28.97	49.03	1422.86	1184.42	90.25
KO	36.73	34.84	1699.78	946.41	117.71
KO	24.8	7.94	147.83	667.71	16.87
KO	21.6	18.14	501.88	1208.49	87.25

	HAVCR2	Hk2	Hmgb1	Hmox1	Ibsp
WT	149.15	7147.74	5464.99	3448.85	6.14
WT	161.8	7405.98	5522.43	3514.74	6.11
WT	83.38	6423.46	6713.8	3909.93	15.07
WT	101.25	6575.98	6591.97	3053.52	11.72
WT	152.11	8646.41	5792.22	3734.52	3.59
WT	142.96	6512.76	5622.72	2597.5	8.07
KO	280.82	8892.27	5513.59	5964.67	3.32
KO	185.25	8276.55	6671.01	6017.01	18.71

KO	162.68	7965.57	6554.96	5825.15	11.14
KO	334.31	5998.67	6074	5559.83	10.36
KO	82.35	8668.33	5609.56	3558.81	9.92
KO	225.46	4083.28	8817.88	2154.37	19.87

	IFNG	Ift122	Ift139	Ift140	Ift172
WT	19.3	634.32	455.34	735.22	858.92
WT	17.3	674.66	447.74	742.84	845.61
WT	15.07	516.37	355.63	575.64	730.35
WT	27.71	609.64	448.7	685.31	882.48
WT	29.94	528.2	424	842	887.52
WT	21.91	510.74	455.4	902.72	760.92
KO	15.48	636.82	382.53	719.74	623.55
KO	29	682.07	510.85	918.78	705.46
KO	13.37	667.42	547.08	929.26	601.68
KO	11.3	550.9	513.23	765.61	387.98
KO	22.82	437.53	311.53	502.02	626.04
KO	12.09	1047.81	1015.85	1267.23	743.75

	Ift88	Igsf1	Ihh	IL-10	IL-12a
WT	259.69	24.57	9.65	14.91	566.77
WT	252.36	23.4	19.33	12.21	565.78
WT	223.02	15.07	8.04	5.02	713.27
WT	249.4	25.58	10.66	13.86	563.81
WT	289.85	37.13	13.18	26.35	455.14
WT	257.1	20.75	12.68	13.83	348.18
KO	243.23	24.32	6.63	15.48	241.02
KO	331.21	19.65	10.29	21.52	58.01
KO	373.26	13.37	10.03	24.51	42.34
KO	247.67	14.13	10.36	24.48	78.16
KO	162.71	19.84	8.93	18.85	421.66
KO	574.44	9.5	19.87	19	33.69

	IL-13	IL-15	IL-15Ra	IL-17a	IL-1B
WT	7.9	241.27	269.35	16.67	304.44
WT	12.21	257.45	317.49	10.18	290.01
WT	13.06	321.47	184.85	15.07	42.19
WT	25.58	379.42	301.62	44.76	88.46
WT	14.37	376.09	337.76	34.73	332.97

WT	33.43	522.27	325.12	57.65	244.42
KO	12.16	319.52	430.08	27.64	2276.41
KO	24.33	222.68	226.42	25.26	4731.46
KO	18.94	197.22	203.9	33.43	4423.46
KO	31.08	271.21	351.26	48.97	8111.86
KO	13.89	456.38	191.48	19.84	71.43
KO	29.37	125.25	248.78	27.64	3077.79

	IL-2	IL-21r	IL-2RB	IL-2Rg	IL-4
WT	7.02	102.65	493.07	206.18	14.91
WT	5.09	78.35	493.53	237.1	5.09
WT	8.04	56.26	178.82	148.68	16.07
WT	23.45	156.67	442.31	211.03	21.32
WT	14.37	179.66	582.1	261.1	29.94
WT	23.06	234.04	575.3	270.93	27.67
KO	13.27	175.79	799.34	407.96	17.69
KO	4.68	107.6	272.27	234.84	110.4
KO	12.26	124.79	283.01	280.78	147.08
KO	7.53	328.66	882.38	440.72	80.05
KO	9.92	64.49	210.33	213.31	8.93
KO	4.32	182.27	241.87	245.33	106.25

	IL-4Ra	IL-6	IL-7	IL-7Ra	IL18r1
WT	1589.75	38.6	129.85	573.78	634.32
WT	1594.55	32.56	132.29	594.27	658.38
WT	1135.21	15.07	124.57	317.46	271.24
WT	944.3	31.97	150.28	516.91	429.52
WT	1922.36	45.51	136.54	837.21	469.51
WT	1965.7	35.74	168.32	866.98	534.95
KO	6754.06	116.09	171.37	1408.52	604.76
KO	15117.84	227.36	205.84	459.39	469.68
KO	14708.84	230.64	215.04	452.37	473.54
KO	10327.69	199.64	239.19	1182.78	637.54
KO	1830.5	17.86	149.81	421.66	274.82
KO	11254.72	205.59	107.98	440.55	376.63

	IL1RL1	IL2ra	IL9R	iNOS	Irf-5
WT	200.91	62.29	18.42	45.62	784.35
WT	206.57	52.91	16.28	51.9	800.84



WT	236.08	93.43	17.08	44.2	1287.91
WT	325.07	165.2	38.37	66.08	1406.86
WT	318.6	141.33	37.13	65.88	1237.25
WT	436.95	197.15	26.52	59.95	1407.7
KO	453.29	179.11	18.8	63.02	1089.01
KO	758.79	105.73	15.91	87.95	1351.98
KO	698.62	114.76	14.48	76.88	1322.58
KO	655.43	277.8	14.13	59.33	1482.25
KO	193.47	75.4	8.93	53.58	802.64
KO	152.9	112.3	12.09	63.92	1058.18

	Lag3	Ldha	Lef1	Lefty	Lilrb4
WT	82.47	56098.39	114.93	441.31	327.25
WT	82.42	56527.83	117.02	460.97	320.54
WT	81.37	65711.42	27.12	308.41	155.71
WT	124.7	52390.43	36.24	442.31	187.58
WT	147.32	69859.95	46.71	255.12	194.03
WT	134.89	56214.51	47.27	403.52	219.05
KO	142.62	72462.7	54.17	613.6	728.59
KO	158.12	92997.47	43.97	541.73	1445.54
KO	154.88	91134.4	37.88	463.52	1368.26
KO	305.11	63465.35	105.47	549.01	1505.79
KO	67.47	70321.91	56.55	275.81	228.19
KO	243.6	84590.51	47.51	900.1	777.44

	LRRC32	MCP-1	Amhr2	Mmp1	MMP2
WT	898.4	75.45	1559.92	5.26	3649.76
WT	907.69	86.49	1607.78	7.12	3851.56
WT	233.07	102.47	1530.02	14.06	3437.77
WT	478.54	296.29	1236.33	12.79	4824.87
WT	444.36	366.51	1337.86	7.19	3379.99
WT	519.96	220.2	1207.09	13.83	4751.12
KO	835.83	143.73	1279.17	7.74	5301.31
KO	569.8	597.86	796.22	10.29	3776.19
KO	583.85	533.71	750.99	10.03	3583.34
KO	521.71	155.38	667.67	16.01	2862.79
KO	383.96	87.31	1655.88	7.94	2793.87
KO	456.96	209.04	752.39	16.41	1146.29

	MMP9	Msx1	Msx2	MMP14	MMP16
WT	172.84	60.54	64.92	1708.19	71.94
WT	181.13	76.32	61.06	1613.89	73.27
WT	245.12	34.16	47.22	1320.06	53.24
WT	193.98	60.75	69.28	1873.68	95.92
WT	247.93	64.68	49.11	2115.19	55.1
WT	216.75	65.72	42.66	2185.91	71.48
KO	1049.21	61.91	100.61	2723.07	46.43
KO	1126.49	63.62	83.27	4303.88	36.49
KO	1181.07	34.54	65.74	4162.73	39
KO	2314.71	48.97	108.3	4210.37	19.78
KO	60.52	38.69	52.58	1176.68	60.52
KO	12239.48	112.3	266.06	6945.12	21.6

	Nanog	ND4	Nfatc1	Nfkb	NGF
WT	12.28	2772.41	705.39	2198.63	64.92
WT	10.18	2733.23	738.77	2349.6	71.23
WT	21.1	2584.86	500.29	2282.47	72.33
WT	29.84	2851.01	613.9	2208.34	81
WT	37.13	3177.58	613.24	3100.92	92.23
WT	38.05	2858.05	545.32	2644.76	86.47
KO	11.06	2836.95	538.42	4059.73	106.14
KO	15.91	2635.66	445.36	5718.55	214.26
KO	16.71	2405.6	425.63	5583.36	168.25
KO	10.36	3291.26	448.25	4574.81	151.61
KO	11.91	3911.02	497.06	2141.04	97.23
KO	15.55	2899.85	407.72	5806.6	72.56

	Nicalin	Noggin	Nox1	Oaz1	Ocstamp
WT	1521.32	318.48	59.66	20699.23	21.93
WT	1440.9	329.7	56.98	20273.33	19.33
WT	1797.24	262.2	32.15	25134.29	18.08
WT	1531.55	394.35	67.15	20482.53	19.18
WT	1825.34	267.09	41.92	20897.98	22.76
WT	1642.89	145.27	44.96	19305.4	20.75
KO	1585.42	234.39	40.91	20030.01	19.9
KO	2042.47	117.89	52.4	21721.49	55.2
KO	2056.85	112.54	40.11	20831.48	42.34
KO	1443.64	115.83	30.13	22769.51	27.31
KO	1376.1	340.3	22.82	21762.6	30.76

KO	1939.28	296.29	19	26923.57	46.65
----	---------	--------	----	----------	-------

	Pcx	Pdcd1	PDGFA	Pdlim7	Pfkl
WT	1108.09	78.96	1868.75	12937.35	3024.21
WT	1136.64	67.16	1931.38	13029.15	3208.44
WT	2005.2	33.15	1287.91	11025.57	4440.37
WT	2612.27	99.12	1611.49	12334.5	4143.83
WT	1939.12	130.55	1426.5	11130.5	5715.56
WT	1706.3	176.39	1472.26	10747.38	4006.35
KO	1247.11	385.85	1520.19	10987.37	5939.24
KO	2622.56	112.28	1928.32	8305.55	11006.7
KO	2514.8	119.22	1928.72	8378.95	10774.52
KO	873.9	384.22	1782.65	7723.87	5629.52
KO	1793.79	54.57	1128.06	13943.54	2891.1
KO	609.86	61.33	3615.09	9393.19	11751.42

	PGAM1	Pgd	PGE2	Pilrb1	Plasmin
WT	3025.09	6594.13	936.13	63.17	28.95
WT	2983.56	6657.04	999.27	63.09	26.46
WT	3839.61	6177.34	964.42	55.25	14.06
WT	3690.86	5509.12	1081.79	75.67	116.17
WT	5662.86	6625.84	1036.04	105.4	15.57
WT	4827.21	6100.02	1039.92	127.97	17.29
KO	6761.8	6921	1197.36	91.76	21.01
KO	9174.75	8307.42	1276.19	84.21	23.39
KO	9242.47	7854.15	1260.18	83.57	17.83
KO	8034.64	6219.97	1010.45	108.3	16.95
KO	2970.47	4384.27	1208.43	50.6	13.89
KO	10763.21	4754.47	1094.46	58.74	11.23

	POSTN	Pou5f1	PPARG	Ppargc1a	Prdm1
WT	7610.1	4.39	308.83	930.86	1229.16
WT	7680.73	7.12	302.22	932.11	1275.03
WT	3219.77	6.03	183.84	632.9	3584.44
WT	8961.24	14.92	295.23	830.26	2244.57
WT	5194.55	20.36	361.71	656.36	3285.37
WT	7742.91	20.75	216.75	589.13	2707.02
KO	7176.4	12.16	152.57	864.57	2326.17
KO	9714.6	11.23	499.62	574.47	2921.96

KO	9327.15	8.91	454.6	592.77	2774.41
KO	4733.02	8.48	65.92	227.89	3090.68
KO	2307.72	6.94	155.77	1312.6	1566.59
KO	4148.93	6.91	52.69	121.8	2600.96

	Prf1	Ptch1	Ptgs2	Pth1r	Pthlh
WT	44.74	378.14	994.91	216.7	363.22
WT	49.86	402.96	989.09	212.68	360.22
WT	12.06	192.88	267.23	171.79	140.65
WT	35.17	278.17	376.23	330.4	214.23
WT	50.3	258.71	445.56	362.91	118.58
WT	56.49	270.93	624.87	264.02	446.17
KO	23.22	235.49	3923.75	213.38	1760.1
KO	28.07	175.9	4411.48	272.27	5590.36
KO	28.97	198.33	4434.6	269.64	5512.05
KO	33.9	213.77	5877.19	124.31	2865.61
KO	20.83	141.88	203.39	232.16	90.28
KO	19.87	226.32	8461.99	77.74	5651.98

	PTPRC	RGM-A	RGM-B	RGM-C	Rorc
WT	1354.62	1128.27	4772.76	6072.99	1337.95
WT	1355.42	1196.68	4601.52	6284.6	1364.58
WT	841.86	767.52	4069.67	4287.67	2123.74
WT	1243.79	1018.9	5389.75	3634.38	1566.73
WT	1509.14	1020.47	3995.62	3235.07	1469.61
WT	1684.39	951.15	4009.8	3298.46	1242.83
KO	1473.75	933.12	3379.79	3567.74	1202.88
KO	1241.58	878.55	2409.24	1279.94	1048.84
KO	1189.99	824.52	2347.66	1257.96	1062.97
KO	2681.04	644.13	1834.44	1487.9	717.58
KO	849.27	805.62	3305.81	9342.98	1960.47
KO	1012.4	1916.82	3149.49	843.95	539.02

	Runx2	SCF	SDF-1	Serpib9	Shh
WT	216.7	2075.8	1771.36	321.11	64.92
WT	216.75	2031.1	1943.59	366.33	49.86
WT	112.52	1425.54	1736.97	166.76	6.03
WT	102.32	2206.2	2596.29	308.02	14.92
WT	178.46	1182.16	1752.28	253.92	5.99

WT	189.08	1570.26	2129.42	314.74	16.14
KO	298.51	1741.31	3003.89	228.86	3.32
KO	310.63	2058.38	1880.61	208.64	10.29
KO	301.95	1958.8	1851.84	231.76	2.23
KO	351.26	1167.72	1433.28	261.79	2.83
KO	80.36	1430.67	2812.72	155.77	2.98
KO	638.36	2226.07	513.97	348.98	6.05

	Slc2a1	Slc2a4	Smad3	SOCS1	SOST
WT	2145.11	5058.78	4678.01	193.89	7.02
WT	2212.23	5110.31	4899.67	163.83	4.07
WT	3740.16	3894.87	4719.65	237.09	11.05
WT	1977.06	5627.42	4630.9	276.04	19.18
WT	3781.23	4460.34	4310.63	323.39	13.18
WT	3140.51	3947.55	3553.25	359.71	12.68
KO	9818.76	3681.62	3125.51	718.63	1.11
KO	26045.95	2644.08	1991.95	606.29	29.94
KO	25275	2688.62	1924.26	518.11	28.97
KO	17462.06	960.54	2048.21	646.01	1.88
KO	3281.01	7544.23	3975.51	241.09	2.98
KO	27263.05	1069.41	2555.18	1445.17	6.91

	Sox9	Sp7	Sparc	Sphk1	SPON-1
WT	205.3	7.02	1319.53	479.91	615.9
WT	198.43	13.23	1331	515.92	625.81
WT	146.67	9.04	805.7	125.58	67.31
WT	224.88	18.12	999.72	160.94	321.87
WT	155.7	15.57	919.86	149.72	155.7
WT	259.4	14.99	1065.28	200.61	249.03
KO	329.47	12.16	1208.41	417.91	517.42
KO	1055.39	20.58	1075.03	430.39	804.64
KO	1044.03	22.28	1007.26	426.75	729.82
KO	523.59	20.72	872.02	412.47	602.69
KO	199.42	9.92	1066.55	178.59	121.04
KO	2585.42	28.51	862.09	398.22	133.89

	Spp1	Sprouty2	Sprouty4	Stat1	Stk36
WT	200.91	951.04	516.76	1331.81	40.36
WT	220.82	965.69	466.05	1363.56	39.69

WT	118.54	725.33	168.77	1809.3	19.09
WT	72.47	755.65	280.31	2491.84	25.58
WT	389.26	968.96	287.45	2304.43	31.14
WT	118.75	642.17	230.58	1876.93	27.67
KO	552.8	621.34	379.22	2184.65	23.22
KO	2186.56	875.75	208.64	2184.69	29.94
KO	2130.39	854.61	249.59	2211.73	37.88
KO	2250.68	524.53	180.81	2448.44	20.72
KO	93.26	610.17	192.48	1407.85	11.91
KO	3178.86	1433.08	182.27	2515.45	41.46

	Tbx21	Tceb1	Tcf7	Tdgl1 (Cripto)	TFAM
WT	9.65	3018.07	261.45	10.53	1519.56
WT	14.25	3150.44	263.55	10.18	1497.88
WT	12.06	4039.53	112.52	14.06	1670.66
WT	35.17	3351.94	219.55	18.12	1621.08
WT	22.76	3366.82	212	35.93	1545.07
WT	26.52	3230.44	277.85	25.36	1506.85
KO	17.69	3768.96	379.22	12.16	1688.24
KO	16.84	4554.63	422.9	25.26	1969.49
KO	18.94	4683.07	408.92	21.17	1937.63
KO	15.07	4862.03	408.7	16.01	1844.8
KO	6.94	3765.17	212.32	9.92	1880.11
KO	15.55	4861.58	494.11	13.82	2550.86

	TGF-B1	TGF-beta 2	TGF-b 3	TGFb R II	TGFBRIII
WT	1374.8	353.57	1455.52	3700.65	3624.32
WT	1397.14	374.47	1466.34	3753.87	3740.64
WT	1107.08	215.99	1014.65	2870.17	2023.28
WT	1268.3	289.9	1257.64	3808.1	3557.64
WT	1451.65	222.78	1031.24	3637.5	2267.3
WT	1525.29	231.73	1148.29	3856.47	2471.83
KO	2715.33	390.27	1276.96	4290.8	2234.4
KO	4829.7	443.49	874.81	5343.36	1375.37
KO	4644.08	411.15	909.2	5408.43	1401.69
KO	3245.12	353.14	1018.93	4556.92	666.73
KO	926.66	236.13	1522.94	2929.79	1421.74
KO	6773.22	2646.75	1123.83	4268.14	523.48

	TNF	Tnfrsf11a	Tnfrsf11b	TNFRSF4	Tnfsf11
WT	24.57	200.03	43.87	71.07	15.79
WT	22.39	203.52	53.93	63.09	24.42
WT	35.16	132.61	39.18	36.17	28.13
WT	60.75	292.03	74.61	74.61	30.91
WT	101.81	233.56	63.48	85.04	33.54
WT	102.61	254.79	101.46	66.87	33.43
KO	96.19	195.69	116.09	80.71	54.17
KO	87.01	181.51	126.31	93.56	75.79
KO	92.48	187.19	99.17	67.97	74.65
KO	150.67	183.63	160.09	153.5	50.85
KO	29.76	126	58.54	29.76	14.88
KO	209.91	142.53	85.52	115.75	20.73

	Tnfsf13b	Tubb4a	VEGF	VHL	Wnt5a
WT	204.42	189.51	4428.84	395.68	2276.71
WT	209.62	194.36	4524.18	397.88	2254.97
WT	86.4	79.36	2129.77	342.57	1554.13
WT	192.91	139.62	2533.41	670.39	1926.97
WT	177.26	94.62	2584.7	904.29	1816.96
WT	193.69	86.47	2079.84	968.44	2097.13
KO	290.77	70.76	4689.92	687.68	1772.26
KO	223.61	26.2	8483.32	281.62	1964.81
KO	198.33	30.08	8409.03	330.92	1930.95
KO	290.05	24.48	5273.55	558.43	2692.34
KO	115.09	49.61	3283.98	305.58	1316.57
KO	112.3	10.37	11494	641.82	4409.81

	Wnt7a	Yml
WT	23.69	122.83
WT	17.3	102.78
WT	12.06	95.44
WT	25.58	92.72
WT	22.76	59.89
WT	21.91	92.23
KO	23.22	1054.73
KO	17.78	54121.28
KO	15.6	53186.25

KO	22.6	1001.03
KO	12.9	46.63
KO	20.73	887.14



## List of References

1. Parkin DM, Ferlay J, Curado MP, Bray F, Edwards B, Shin HR, et al. Fifty years of cancer incidence: CI5 I-IX. *Int J Cancer*. 2010;127:2918-27.
2. Jemal A, Bray F, Center MM, Ferlay J, Ward E, Forman D. Global cancer statistics. *CA Cancer J Clin*. 2011;61:69-90.
3. American Cancer Society. *Cancer facts & figures*. Atlanta, GA: The Society; 2014. p. v.
4. National Cancer Institute. *Surveillance epidemiology and end results*. Available online: <http://seer.cancer.gov/statfacts/html/oralcav.html/>; National Cancer Institute; 2014.
5. Sturgis EM, Cinciripini PM. Trends in head and neck cancer incidence in relation to smoking prevalence: an emerging epidemic of human papillomavirus-associated cancers? *Cancer*. 2007;110:1429-35.
6. Schlecht NF, Franco EL, Pintos J, Kowalski LP. Effect of smoking cessation and tobacco type on the risk of cancers of the upper aero-digestive tract in Brazil. *Epidemiology*. 1999;10:412-8.
7. Marur S, D'Souza G, Westra WH, Forastiere AA. HPV-associated head and neck cancer: a virus-related cancer epidemic. *Lancet Oncol*. 2010;11:781-9.
8. D'Souza G, Kreimer AR, Viscidi R, Pawlita M, Fakhry C, Koch WM, et al. Case-control study of human papillomavirus and oropharyngeal cancer. *N Engl J Med*. 2007;356:1944-56.
9. de Villiers EM, Fauquet C, Broker TR, Bernard HU, zur Hausen H. Classification of papillomaviruses. *Virology*. 2004;324:17-27.
10. Gillison ML, D'Souza G, Westra W, Sugar E, Xiao W, Begum S, et al. Distinct risk factor profiles for human papillomavirus type 16-positive and human papillomavirus type 16-negative head and neck cancers. *J Natl Cancer Inst*. 2008;100:407-20.
11. Ragin CC, Taioli E. Survival of squamous cell carcinoma of the head and neck in relation to human papillomavirus infection: review and meta-analysis. *Int J Cancer*. 2007;121:1813-20.
12. Scheffner M, Werness BA, Huibregtse JM, Levine AJ, Howley PM. The E6 oncoprotein encoded by human papillomavirus types 16 and 18 promotes the degradation of p53. *Cell*. 1990;63:1129-36.

13. Dyson N, Howley PM, Munger K, Harlow E. The human papilloma virus-16 E7 oncoprotein is able to bind to the retinoblastoma gene product. *Science*. 1989;243:934-7.
14. Kuo KT, Hsiao CH, Lin CH, Kuo LT, Huang SH, Lin MC. The biomarkers of human papillomavirus infection in tonsillar squamous cell carcinoma-molecular basis and predicting favorable outcome. *Mod Pathol*. 2008;21:376-86.
15. Harris SL, Thorne LB, Seaman WT, Hayes DN, Couch ME, Kimple RJ. Association of p16(INK4a) overexpression with improved outcomes in young patients with squamous cell cancers of the oral tongue. *Head Neck*. 2011;33:1622-7.
16. Ragin CC, Taioli E, Weissfeld JL, White JS, Rossie KM, Modugno F, et al. 11q13 amplification status and human papillomavirus in relation to p16 expression defines two distinct etiologies of head and neck tumours. *Br J Cancer*. 2006;95:1432-8.
17. Bolt J, Vo QN, Kim WJ, McWhorter AJ, Thomson J, Hagenssee ME, et al. The ATM/p53 pathway is commonly targeted for inactivation in squamous cell carcinoma of the head and neck (SCCHN) by multiple molecular mechanisms. *Oral Oncol*. 2005;41:1013-20.
18. Rothenberg SM, Ellisen LW. The molecular pathogenesis of head and neck squamous cell carcinoma. *J Clin Invest*. 2012;122:1951-7.
19. Poeta ML, Manola J, Goldwasser MA, Forastiere A, Benoit N, Califano JA, et al. TP53 mutations and survival in squamous-cell carcinoma of the head and neck. *N Engl J Med*. 2007;357:2552-61.
20. Agrawal N, Frederick MJ, Pickering CR, Bettegowda C, Chang K, Li RJ, et al. Exome sequencing of head and neck squamous cell carcinoma reveals inactivating mutations in NOTCH1. *Science*. 2011;333:1154-7.
21. Stransky N, Egloff AM, Tward AD, Kostic AD, Cibulskis K, Sivachenko A, et al. The mutational landscape of head and neck squamous cell carcinoma. *Science*. 2011;333:1157-60.
22. Molinolo AA, Amornphimoltham P, Squarize CH, Castilho RM, Patel V, Gutkind JS. Dysregulated molecular networks in head and neck carcinogenesis. *Oral Oncol*. 2009;45:324-34.
23. Ozanne B, Richards CS, Hendler F, Burns D, Gusterson B. Over-expression of the EGF receptor is a hallmark of squamous cell carcinomas. *J Pathol*. 1986;149:9-14.
24. Wheeler S, Siwak DR, Chai R, LaValle C, Seethala RR, Wang L, et al. Tumor epidermal growth factor receptor and EGFR PY1068 are independent prognostic indicators for head and neck squamous cell carcinoma. *Clin Cancer Res*. 2012;18:2278-89.

25. Takes RP, Baatenburg de Jong RJ, Schuurin E, Litvinov SV, Hermans J, Van Krieken JH. Differences in expression of oncogenes and tumor suppressor genes in different sites of head and neck squamous cell. *Anticancer Res.* 1998;18:4793-800.
26. Bonner JA, Harari PM, Giralt J, Azarnia N, Shin DM, Cohen RB, et al. Radiotherapy plus cetuximab for squamous-cell carcinoma of the head and neck. *N Engl J Med.* 2006;354:567-78.
27. Vermorken JB, Mesia R, Rivera F, Remenar E, Kawecki A, Rottey S, et al. Platinum-based chemotherapy plus cetuximab in head and neck cancer. *N Engl J Med.* 2008;359:1116-27.
28. Sok JC, Coppelli FM, Thomas SM, Lango MN, Xi S, Hunt JL, et al. Mutant epidermal growth factor receptor (EGFRvIII) contributes to head and neck cancer growth and resistance to EGFR targeting. *Clin Cancer Res.* 2006;12:5064-73.
29. Sharafinski ME, Ferris RL, Ferrone S, Grandis JR. Epidermal growth factor receptor targeted therapy of squamous cell carcinoma of the head and neck. *Head Neck.* 2010;32:1412-21.
30. Scott AM, Lee FT, Tebbutt N, Herbertson R, Gill SS, Liu Z, et al. A phase I clinical trial with monoclonal antibody ch806 targeting transitional state and mutant epidermal growth factor receptors. *Proc Natl Acad Sci U S A.* 2007;104:4071-6.
31. Sampson JH, Heimberger AB, Archer GE, Aldape KD, Friedman AH, Friedman HS, et al. Immunologic escape after prolonged progression-free survival with epidermal growth factor receptor variant III peptide vaccination in patients with newly diagnosed glioblastoma. *J Clin Oncol.* 2010;28:4722-9.
32. Yu CL, Meyer DJ, Campbell GS, Larner AC, Carter-Su C, Schwartz J, et al. Enhanced DNA-binding activity of a Stat3-related protein in cells transformed by the Src oncoprotein. *Science.* 1995;269:81-3.
33. Sriuranpong V, Park JI, Amornphimoltham P, Patel V, Nelkin BD, Gutkind JS. Epidermal growth factor receptor-independent constitutive activation of STAT3 in head and neck squamous cell carcinoma is mediated by the autocrine/paracrine stimulation of the interleukin 6/gp130 cytokine system. *Cancer Res.* 2003;63:2948-56.
34. Grandis JR, Drenning SD, Zeng Q, Watkins SC, Melhem MF, Endo S, et al. Constitutive activation of Stat3 signaling abrogates apoptosis in squamous cell carcinogenesis in vivo. *Proc Natl Acad Sci U S A.* 2000;97:4227-32.
35. Nagpal JK, Mishra R, Das BR. Activation of Stat-3 as one of the early events in tobacco chewing-mediated oral carcinogenesis. *Cancer.* 2002;94:2393-400.
36. Koppikar P, Lui VW, Man D, Xi S, Chai RL, Nelson E, et al. Constitutive activation of signal transducer and activator of transcription 5 contributes to tumor

growth, epithelial-mesenchymal transition, and resistance to epidermal growth factor receptor targeting. *Clin Cancer Res.* 2008;14:7682-90.

37. Xi S, Zhang Q, Gooding WE, Smithgall TE, Grandis JR. Constitutive activation of Stat5b contributes to carcinogenesis in vivo. *Cancer Res.* 2003;63:6763-71.
38. Leeman-Neill RJ, Seethala RR, Singh S, Freilino ML, Bednash JS, Thomas SM, et al. Inhibition of EGFR-STAT3 signaling with erlotinib prevents carcinogenesis in a mouse model of oral squamous cell carcinoma. *Cancer Prev Res (Phila Pa).* 2010.
39. Sharafinski ME, Ferris RL, Ferrone S, Grandis JR. Epidermal growth factor receptor targeted therapy of squamous cell carcinoma of the head and neck. *Head Neck.* 2010.
40. Sen M, Thomas SM, Kim S, Yeh JI, Ferris RL, Johnson JT, et al. First-in-Human Trial of a STAT3 Decoy Oligonucleotide in Head and Neck Tumors: Implications for Cancer Therapy. *Cancer discovery.* 2012;2:694-705.
41. Garzon R, Marcucci G, Croce CM. Targeting microRNAs in cancer: rationale, strategies and challenges. *Nat Rev Drug Discov.* 2010;9:775-89.
42. Johnson SM, Grosshans H, Shingara J, Byrom M, Jarvis R, Cheng A, et al. RAS is regulated by the let-7 microRNA family. *Cell.* 2005;120:635-47.
43. Scott GK, Goga A, Bhaumik D, Berger CE, Sullivan CS, Benz CC. Coordinate suppression of ERBB2 and ERBB3 by enforced expression of micro-RNA miR-125a or miR-125b. *J Biol Chem.* 2007;282:1479-86.
44. Park SM, Gaur AB, Lengyel E, Peter ME. The miR-200 family determines the epithelial phenotype of cancer cells by targeting the E-cadherin repressors ZEB1 and ZEB2. *Genes Dev.* 2008;22:894-907.
45. Park NJ, Zhou H, Elashoff D, Henson BS, Kastratovic DA, Abemayor E, et al. Salivary microRNA: discovery, characterization, and clinical utility for oral cancer detection. *Clin Cancer Res.* 2009;15:5473-7.
46. Childs G, Fazzari M, Kung G, Kawachi N, Brandwein-Gensler M, McLemore M, et al. Low-level expression of microRNAs let-7d and miR-205 are prognostic markers of head and neck squamous cell carcinoma. *Am J Pathol.* 2009;174:736-45.
47. Wong TS, Liu XB, Chung-Wai Ho A, Po-Wing Yuen A, Wai-Man Ng R, Ignace Wei W. Identification of pyruvate kinase type M2 as potential oncoprotein in squamous cell carcinoma of tongue through microRNA profiling. *Int J Cancer.* 2008;123:251-7.
48. Ivanovska I, Ball AS, Diaz RL, Magnus JF, Kibukawa M, Schelter JM, et al. MicroRNAs in the miR-106b family regulate p21/CDKN1A and promote cell cycle progression. *Mol Cell Biol.* 2008;28:2167-74.

49. Qu C, Liang Z, Huang J, Zhao R, Su C, Wang S, et al. MiR-205 determines the radioresistance of human nasopharyngeal carcinoma by directly targeting PTEN. *Cell Cycle*. 2012;11:785-96.
50. Babu JM, Prathibha R, Jijith VS, Hariharan R, Pillai MR. A miR-centric view of head and neck cancers. *Biochim Biophys Acta*. 2011;1816:67-72.
51. Raman M, Chen W, Cobb MH. Differential regulation and properties of MAPKs. *Oncogene*. 2007;26:3100-12.
52. Widmann C, Gibson S, Jarpe MB, Johnson GL. Mitogen-activated protein kinase: conservation of a three-kinase module from yeast to human. *Physiol Rev*. 1999;79:143-80.
53. Wada T, Penninger JM. Mitogen-activated protein kinases in apoptosis regulation. *Oncogene*. 2004;23:2838-49.
54. Turjanski AG, Vaque JP, Gutkind JS. MAP kinases and the control of nuclear events. *Oncogene*. 2007;26:3240-53.
55. Kyriakis JM, Avruch J. Mammalian MAPK signal transduction pathways activated by stress and inflammation: a 10-year update. *Physiol Rev*. 2012;92:689-737.
56. Rincon M, Davis RJ. Regulation of the immune response by stress-activated protein kinases. *Immunol Rev*. 2009;228:212-24.
57. Dhillon AS, Hagan S, Rath O, Kolch W. MAP kinase signalling pathways in cancer. *Oncogene*. 2007;26:3279-90.
58. Lawrence MC, Jivan A, Shao C, Duan L, Goad D, Zaganjor E, et al. The roles of MAPKs in disease. *Cell Res*. 2008;18:436-42.
59. Marshall CJ. MAP kinase kinase kinase, MAP kinase kinase and MAP kinase. *Curr Opin Genet Dev*. 1994;4:82-9.
60. Cobb MH. MAP kinase pathways. *Prog Biophys Mol Biol*. 1999;71:479-500.
61. Coulombe P, Meloche S. Atypical mitogen-activated protein kinases: structure, regulation and functions. *Biochim Biophys Acta*. 2007;1773:1376-87.
62. Marshall CJ. Specificity of receptor tyrosine kinase signaling: transient versus sustained extracellular signal-regulated kinase activation. *Cell*. 1995;80:179-85.
63. Keyse SM. Protein phosphatases and the regulation of mitogen-activated protein kinase signalling. *Curr Opin Cell Biol*. 2000;12:186-92.
64. Dickinson RJ, Keyse SM. Diverse physiological functions for dual-specificity MAP kinase phosphatases. *J Cell Sci*. 2006;119:4607-15.

65. Owens DM, Keyse SM. Differential regulation of MAP kinase signalling by dual-specificity protein phosphatases. *Oncogene*. 2007;26:3203-13.
66. Slack DN, Seternes OM, Gabrielsen M, Keyse SM. Distinct binding determinants for ERK2/p38alpha and JNK map kinases mediate catalytic activation and substrate selectivity of map kinase phosphatase-1. *J Biol Chem*. 2001;276:16491-500.
67. Nichols A, Camps M, Gillieron C, Chabert C, Brunet A, Wilsbacher J, et al. Substrate recognition domains within extracellular signal-regulated kinase mediate binding and catalytic activation of mitogen-activated protein kinase phosphatase-3. *J Biol Chem*. 2000;275:24613-21.
68. Farooq A, Zhou MM. Structure and regulation of MAPK phosphatases. *Cell Signal*. 2004;16:769-79.
69. Alonso A, Sasin J, Bottini N, Friedberg I, Friedberg I, Osterman A, et al. Protein tyrosine phosphatases in the human genome. *Cell*. 2004;117:699-711.
70. Boutros T, Chevet E, Metrakos P. Mitogen-activated protein (MAP) kinase/MAP kinase phosphatase regulation: roles in cell growth, death, and cancer. *Pharmacol Rev*. 2008;60:261-310.
71. Theodosiou A, Ashworth A. MAP kinase phosphatases. *Genome Biol*. 2002;3:REVIEWS3009.
72. Camps M, Nichols A, Arkinstall S. Dual specificity phosphatases: a gene family for control of MAP kinase function. *FASEB J*. 2000;14:6-16.
73. Raingeaud J, Gupta S, Rogers JS, Dickens M, Han J, Ulevitch RJ, et al. Pro-inflammatory cytokines and environmental stress cause p38 mitogen-activated protein kinase activation by dual phosphorylation on tyrosine and threonine. *J Biol Chem*. 1995;270:7420-6.
74. Stewart AE, Dowd S, Keyse SM, McDonald NQ. Crystal structure of the MAPK phosphatase Pyst1 catalytic domain and implications for regulated activation. *Nat Struct Biol*. 1999;6:174-81.
75. Zhou B, Zhang ZY. Mechanism of mitogen-activated protein kinase phosphatase-3 activation by ERK2. *J Biol Chem*. 1999;274:35526-34.
76. Chen P, Hutter D, Yang X, Gorospe M, Davis RJ, Liu Y. Discordance between the binding affinity of mitogen-activated protein kinase subfamily members for MAP kinase phosphatase-2 and their ability to activate the phosphatase catalytically. *J Biol Chem*. 2001;276:29440-9.
77. Zhang Q, Muller M, Chen CH, Zeng L, Farooq A, Zhou MM. New insights into the catalytic activation of the MAPK phosphatase PAC-1 induced by its substrate MAPK ERK2 binding. *J Mol Biol*. 2005;354:777-88.

78. Lau LF, Nathans D. Identification of a set of genes expressed during the G0/G1 transition of cultured mouse cells. *EMBO J.* 1985;4:3145-51.
79. Kwak SP, Hakes DJ, Martell KJ, Dixon JE. Isolation and characterization of a human dual specificity protein-tyrosine phosphatase gene. *J Biol Chem.* 1994;269:3596-604.
80. Caunt CJ, Keyse SM. Dual-specificity MAP kinase phosphatases (MKPs): shaping the outcome of MAP kinase signalling. *FEBS J.* 2013;280:489-504.
81. Boutros T, Chevet E, Metrakos P. Mitogen-activated protein (MAP) kinase/MAP kinase phosphatase regulation: roles in cell growth, death, and cancer. *Pharmacol Rev.* 2008;60:261-310.
82. Shipp LE, Lee JV, Yu CY, Pufall M, Zhang P, Scott DK, et al. Transcriptional regulation of human dual specificity protein phosphatase 1 (DUSP1) gene by glucocorticoids. *PLoS ONE.* 2010;5:e13754.
83. Zhang Y, Leung DY, Richers BN, Liu Y, Remigio LK, Riches DW, et al. Vitamin D inhibits monocyte/macrophage proinflammatory cytokine production by targeting MAPK phosphatase-1. *J Immunol.* 2012;188:2127-35.
84. Wang Z, Cao N, Nantajit D, Fan M, Liu Y, Li JJ. Mitogen-activated protein kinase phosphatase-1 represses c-Jun NH2-terminal kinase-mediated apoptosis via NF-kappaB regulation. *J Biol Chem.* 2008;283:21011-23.
85. Noguchi T, Metz R, Chen L, Mattei MG, Carrasco D, Bravo R. Structure, mapping, and expression of erp, a growth factor-inducible gene encoding a nontransmembrane protein tyrosine phosphatase, and effect of ERP on cell growth. *Mol Cell Biol.* 1993;13:5195-205.
86. Sommer A, Burkhardt H, Keyse SM, Luscher B. Synergistic activation of the mkp-1 gene by protein kinase A signaling and USF, but not c-Myc. *FEBS Lett.* 2000;474:146-50.
87. Li J, Gorospe M, Hutter D, Barnes J, Keyse SM, Liu Y. Transcriptional induction of MKP-1 in response to stress is associated with histone H3 phosphorylation-acetylation. *Mol Cell Biol.* 2001;21:8213-24.
88. Rauhala HE, Porkka KP, Tolonen TT, Martikainen PM, Tammela TL, Visakorpi T. Dual-specificity phosphatase 1 and serum/glucocorticoid-regulated kinase are downregulated in prostate cancer. *International journal of cancer Journal international du cancer.* 2005;117:738-45.
89. Khor GH, Froemming GR, Zain RB, Abraham MT, Omar E, Tan SK, et al. DNA methylation profiling revealed promoter hypermethylation-induced silencing of p16, DDAH2 and DUSP1 in primary oral squamous cell carcinoma. *International journal of medical sciences.* 2013;10:1727-39.



90. Bokemeyer D, Sorokin A, Yan M, Ahn NG, Templeton DJ, Dunn MJ. Induction of mitogen-activated protein kinase phosphatase 1 by the stress-activated protein kinase signaling pathway but not by extracellular signal-regulated kinase in fibroblasts. *J Biol Chem.* 1996;271:639-42.
91. Wu W, Chaudhuri S, Brickley DR, Pang D, Karrison T, Conzen SD. Microarray analysis reveals glucocorticoid-regulated survival genes that are associated with inhibition of apoptosis in breast epithelial cells. *Cancer Res.* 2004;64:1757-64.
92. Wu W, Pew T, Zou M, Pang D, Conzen SD. Glucocorticoid receptor-induced MAPK phosphatase-1 (MPK-1) expression inhibits paclitaxel-associated MAPK activation and contributes to breast cancer cell survival. *J Biol Chem.* 2005;280:4117-24.
93. Schliess F, Kurz AK, Haussinger D. Glucagon-induced expression of the MAP kinase phosphatase MKP-1 in rat hepatocytes. *Gastroenterology.* 2000;118:929-36.
94. Lornejad-Schafer MR, Schafer C, Graf D, Haussinger D, Schliess F. Osmotic regulation of insulin-induced mitogen-activated protein kinase phosphatase (MKP-1) expression in H4IIE rat hepatoma cells. *Biochem J.* 2003;371:609-19.
95. Furst R, Brueckl C, Kuebler WM, Zahler S, Krotz F, Grolach A, et al. Atrial natriuretic peptide induces mitogen-activated protein kinase phosphatase-1 in human endothelial cells via Rac1 and NAD(P)H oxidase/Nox2-activation. *Circ Res.* 2005;96:43-53.
96. Keyse SM, Emslie EA. Oxidative stress and heat shock induce a human gene encoding a protein-tyrosine phosphatase. *Nature.* 1992;359:644-7.
97. Wong HR, Dunsmore KE, Page K, Shanley TP. Heat shock-mediated regulation of MKP-1. *Am J Physiol Cell Physiol.* 2005;289:C1152-8.
98. Schliess F, Heinrich S, Haussinger D. Hyperosmotic induction of the mitogen-activated protein kinase phosphatase MKP-1 in H4IIE rat hepatoma cells. *Arch Biochem Biophys.* 1998;351:35-40.
99. Seta KA, Kim R, Kim HW, Millhorn DE, Beitner-Johnson D. Hypoxia-induced regulation of MAPK phosphatase-1 as identified by subtractive suppression hybridization and cDNA microarray analysis. *J Biol Chem.* 2001;276:44405-12.
100. Bernaudin M, Tang Y, Reilly M, Petit E, Sharp FR. Brain genomic response following hypoxia and re-oxygenation in the neonatal rat. Identification of genes that might contribute to hypoxia-induced ischemic tolerance. *J Biol Chem.* 2002;277:39728-38.
101. Liu C, Shi Y, Han Z, Pan Y, Liu N, Han S, et al. Suppression of the dual-specificity phosphatase MKP-1 enhances HIF-1 trans-activation and increases expression of EPO. *Biochem Biophys Res Commun.* 2003;312:780-6.



102. Takano S, Fukuyama H, Fukumoto M, Hirashimizu K, Higuchi T, Takenawa J, et al. Induction of CL100 protein tyrosine phosphatase following transient forebrain ischemia in the rat brain. *J Cereb Blood Flow Metab.* 1995;15:33-41.
103. Wiessner C, Neumann-Haefelin T, Vogel P, Back T, Hossmann KA. Transient forebrain ischemia induces an immediate-early gene encoding the mitogen-activated protein kinase phosphatase 3CH134 in the adult rat brain. *Neuroscience.* 1995;64:959-66.
104. Franklin CC, Srikanth S, Kraft AS. Conditional expression of mitogen-activated protein kinase phosphatase-1, MKP-1, is cytoprotective against UV-induced apoptosis. *Proc Natl Acad Sci U S A.* 1998;95:3014-9.
105. Staples CJ, Owens DM, Maier JV, Cato AC, Keyse SM. Cross-talk between the p38alpha and JNK MAPK pathways mediated by MAP kinase phosphatase-1 determines cellular sensitivity to UV radiation. *J Biol Chem.* 2010;285:25928-40.
106. Kasid U, Wang FH, Whiteside TL. Ionizing radiation and TNF-alpha stimulate gene expression of a Thr/Tyr-protein phosphatase HVH1 and inhibitory factor IkappaB alpha in human squamous carcinoma cells. *Mol Cell Biochem.* 1997;173:193-7.
107. Zhu QY, Liu Q, Chen JX, Lan K, Ge BX. MicroRNA-101 targets MAPK phosphatase-1 to regulate the activation of MAPKs in macrophages. *J Immunol.* 2010;185:7435-42.
108. Kuwano Y, Kim HH, Abdelmohsen K, Pullmann R, Jr., Martindale JL, Yang X, et al. MKP-1 mRNA stabilization and translational control by RNA-binding proteins HuR and NF90. *Mol Cell Biol.* 2008;28:4562-75.
109. Kim HS, Ullevig SL, Zamora D, Lee CF, Asmis R. Redox regulation of MAPK phosphatase 1 controls monocyte migration and macrophage recruitment. *Proc Natl Acad Sci U S A.* 2012;109:E2803-12.
110. Takehara N, Kawabe J, Aizawa Y, Hasebe N, Kikuchi K. High glucose attenuates insulin-induced mitogen-activated protein kinase phosphatase-1 (MKP-1) expression in vascular smooth muscle cells. *Biochim Biophys Acta.* 2000;1497:244-52.
111. Lornejad-Schafer M, Schafer C, Richter L, Grune T, Haussinger D, Schliess F. Osmotic regulation of MG-132-induced MAP-kinase phosphatase MKP-1 expression in H4IIE rat hepatoma cells. *Cell Physiol Biochem.* 2005;16:193-206.
112. Wu JJ, Bennett AM. Essential role for mitogen-activated protein (MAP) kinase phosphatase-1 in stress-responsive MAP kinase and cell survival signaling. *J Biol Chem.* 2005;280:16461-6.
113. Mishra OP, Delivoria-Papadopoulos M. Effect of hypoxia on the expression and activity of mitogen-activated protein (MAP) kinase-phosphatase-1 (MKP-1) and MKP-3 in neuronal nuclei of newborn piglets: the role of nitric oxide. *Neuroscience.* 2004;129:665-73.

114. Liu C, Shi Y, Du Y, Ning X, Liu N, Huang D, et al. Dual-specificity phosphatase DUSP1 protects overactivation of hypoxia-inducible factor 1 through inactivating ERK MAPK. *Exp Cell Res.* 2005;309:410-8.
115. Liu CJ, Shi YQ, Du YL, Pan YL, Liang J, Han S, et al. [Inhibition of the in vitro interaction between hypoxia inducible factor 1alpha and p300 by mitogen-activated protein kinase phosphatase 1]. *Zhonghua Yi Xue Za Zhi.* 2005;85:2344-8.
116. Metzler B, Hu Y, Sturm G, Wick G, Xu Q. Induction of mitogen-activated protein kinase phosphatase-1 by arachidonic acid in vascular smooth muscle cells. *J Biol Chem.* 1998;273:33320-6.
117. Charles CH, Ablner AS, Lau LF. cDNA sequence of a growth factor-inducible immediate early gene and characterization of its encoded protein. *Oncogene.* 1992;7:187-90.
118. Yaglom J, O'Callaghan-Sunol C, Gabai V, Sherman MY. Inactivation of dual-specificity phosphatases is involved in the regulation of extracellular signal-regulated kinases by heat shock and hsp72. *Mol Cell Biol.* 2003;23:3813-24.
119. Wang Z, Xu J, Zhou JY, Liu Y, Wu GS. Mitogen-activated protein kinase phosphatase-1 is required for cisplatin resistance. *Cancer Res.* 2006;66:8870-7.
120. Wu JJ, Zhang L, Bennett AM. The noncatalytic amino terminus of mitogen-activated protein kinase phosphatase 1 directs nuclear targeting and serum response element transcriptional regulation. *Mol Cell Biol.* 2005;25:4792-803.
121. Rauch J, Volinsky N, Romano D, Kolch W. The secret life of kinases: functions beyond catalysis. *Cell Commun Signal.* 2011;9:23.
122. Rodriguez J, Crespo P. Working without kinase activity: phosphotransfer-independent functions of extracellular signal-regulated kinases. *Sci Signal.* 2011;4:re3.
123. Keyse SM. Dual-specificity MAP kinase phosphatases (MKPs) and cancer. *Cancer Metastasis Rev.* 2008;27:253-61.
124. Rosini P, De Chiara G, Bonini P, Lucibello M, Marcocci ME, Garaci E, et al. Nerve growth factor-dependent survival of CESS B cell line is mediated by increased expression and decreased degradation of MAPK phosphatase 1. *J Biol Chem.* 2004;279:14016-23.
125. Hutter D, Chen P, Li J, Barnes J, Liu Y. The carboxyl-terminal domains of MKP-1 and MKP-2 have inhibitory effects on their phosphatase activity. *Mol Cell Biochem.* 2002;233:107-17.
126. Franklin CC, Kraft AS. Conditional expression of the mitogen-activated protein kinase (MAPK) phosphatase MKP-1 preferentially inhibits p38 MAPK and stress-activated protein kinase in U937 cells. *J Biol Chem.* 1997;272:16917-23.

127. Sarkozi R, Miller B, Pollack V, Feifel E, Mayer G, Sorokin A, et al. ERK1/2-driven and MKP-mediated inhibition of EGF-induced ERK5 signaling in human proximal tubular cells. *J Cell Physiol*. 2007;211:88-100.
128. Venema RC, Venema VJ, Eaton DC, Marrero MB. Angiotensin II-induced tyrosine phosphorylation of signal transducers and activators of transcription 1 is regulated by Janus-activated kinase 2 and Fyn kinases and mitogen-activated protein kinase phosphatase 1. *J Biol Chem*. 1998;273:30795-800.
129. Kinney CM, Chandrasekharan UM, Yang L, Shen J, Kinter M, McDermott MS, et al. Histone H3 as a novel substrate for MAP kinase phosphatase-1. *Am J Physiol Cell Physiol*. 2009;296:C242-9.
130. Robinson FL, Whitehurst AW, Raman M, Cobb MH. Identification of novel point mutations in ERK2 that selectively disrupt binding to MEK1. *J Biol Chem*. 2002;277:14844-52.
131. Amit I, Citri A, Shay T, Lu Y, Katz M, Zhang F, et al. A module of negative feedback regulators defines growth factor signaling. *Nat Genet*. 2007;39:503-12.
132. Nunes-Xavier CE, Tarrega C, Cejudo-Marin R, Frijhoff J, Sandin A, Ostman A, et al. Differential up-regulation of MAP kinase phosphatases MKP3/DUSP6 and DUSP5 by Ets2 and c-Jun converge in the control of the growth arrest versus proliferation response of MCF-7 breast cancer cells to phorbol ester. *J Biol Chem*. 2010;285:26417-30.
133. Avraham R, Yarden Y. Feedback regulation of EGFR signalling: decision making by early and delayed loops. *Nat Rev Mol Cell Biol*. 2011;12:104-17.
134. Cagnol S, Rivard N. Oncogenic KRAS and BRAF activation of the MEK/ERK signaling pathway promotes expression of dual-specificity phosphatase 4 (DUSP4/MKP2) resulting in nuclear ERK1/2 inhibition. *Oncogene*. 2013;32:564-76.
135. Brondello JM, Pouyssegur J, McKenzie FR. Reduced MAP kinase phosphatase-1 degradation after p42/p44MAPK-dependent phosphorylation. *Science*. 1999;286:2514-7.
136. Lin YW, Chuang SM, Yang JL. ERK1/2 achieves sustained activation by stimulating MAPK phosphatase-1 degradation via the ubiquitin-proteasome pathway. *J Biol Chem*. 2003;278:21534-41.
137. Lin YW, Yang JL. Cooperation of ERK and SCF<sup>Skp2</sup> for MKP-1 destruction provides a positive feedback regulation of proliferating signaling. *J Biol Chem*. 2006;281:915-26.
138. Cao W, Bao C, Padalko E, Lowenstein CJ. Acetylation of mitogen-activated protein kinase phosphatase-1 inhibits Toll-like receptor signaling. *J Exp Med*. 2008;205:1491-503.

139. Jeffrey KL, Camps M, Rommel C, Mackay CR. Targeting dual-specificity phosphatases: manipulating MAP kinase signalling and immune responses. *Nat Rev Drug Discov.* 2007;6:391-403.
140. Dorfman K, Carrasco D, Gruda M, Ryan C, Lira SA, Bravo R. Disruption of the *erp/mkp-1* gene does not affect mouse development: normal MAP kinase activity in ERP/MKP-1-deficient fibroblasts. *Oncogene.* 1996;13:925-31.
141. Salojin KV, Owusu IB, Millerchip KA, Potter M, Platt KA, Oravec T. Essential role of MAPK phosphatase-1 in the negative control of innate immune responses. *J Immunol.* 2006;176:1899-907.
142. Hammer M, Mages J, Dietrich H, Servatius A, Howells N, Cato AC, et al. Dual specificity phosphatase 1 (DUSP1) regulates a subset of LPS-induced genes and protects mice from lethal endotoxin shock. *J Exp Med.* 2006;203:15-20.
143. Zhao Q, Wang X, Nelin LD, Yao Y, Matta R, Manson ME, et al. MAP kinase phosphatase 1 controls innate immune responses and suppresses endotoxic shock. *J Exp Med.* 2006;203:131-40.
144. Chi H, Barry SP, Roth RJ, Wu JJ, Jones EA, Bennett AM, et al. Dynamic regulation of pro- and anti-inflammatory cytokines by MAPK phosphatase 1 (MKP-1) in innate immune responses. *Proc Natl Acad Sci U S A.* 2006;103:2274-9.
145. Korhonen R, Turpeinen T, Taimi V, Nieminen R, Goulas A, Moilanen E. Attenuation of the acute inflammatory response by dual specificity phosphatase 1 by inhibition of p38 MAP kinase. *Mol Immunol.* 2011;48:2059-68.
146. Huang G, Wang Y, Shi LZ, Kanneganti TD, Chi H. Signaling by the phosphatase MKP-1 in dendritic cells imprints distinct effector and regulatory T cell fates. *Immunity.* 2011;35:45-58.
147. Zhang Y, Reynolds JM, Chang SH, Martin-Orozco N, Chung Y, Nurieva RI, et al. MKP-1 is necessary for T cell activation and function. *J Biol Chem.* 2009;284:30815-24.
148. Turpeinen T, Nieminen R, Taimi V, Heittola T, Sareila O, Clark AR, et al. Dual specificity phosphatase 1 regulates human inducible nitric oxide synthase expression by p38 MAP kinase. *Mediators Inflamm.* 2011;2011:127587.
149. Wang X, Zhao Q, Matta R, Meng X, Liu X, Liu CG, et al. Inducible nitric-oxide synthase expression is regulated by mitogen-activated protein kinase phosphatase-1. *J Biol Chem.* 2009;284:27123-34.
150. Sartori R, Li F, Kirkwood KL. MAP kinase phosphatase-1 protects against inflammatory bone loss. *J Dent Res.* 2009;88:1125-30.

151. Yu H, Li Q, Herbert B, Zinna R, Martin K, Junior CR, et al. Anti-inflammatory effect of MAPK phosphatase-1 local gene transfer in inflammatory bone loss. *Gene Ther.* 2010.
152. Vattakuzhi Y, Abraham SM, Freidin A, Clark AR, Horwood NJ. Dual-specificity phosphatase 1-null mice exhibit spontaneous osteolytic disease and enhanced inflammatory osteolysis in experimental arthritis. *Arthritis Rheum.* 2012;64:2201-10.
153. Frazier WJ, Wang X, Wancket LM, Li XA, Meng X, Nelin LD, et al. Increased inflammation, impaired bacterial clearance, and metabolic disruption after gram-negative sepsis in Mkp-1-deficient mice. *J Immunol.* 2009;183:7411-9.
154. Hammer M, Echtenachter B, Weighardt H, Jozefowski K, Rose-John S, Mannel DN, et al. Increased inflammation and lethality of Dusp1<sup>-/-</sup> mice in polymicrobial peritonitis models. *Immunology.* 2010;131:395-404.
155. Rodriguez N, Dietrich H, Mossbrugger I, Weintz G, Scheller J, Hammer M, et al. Increased inflammation and impaired resistance to *Chlamydomydia pneumoniae* infection in Dusp1<sup>-/-</sup> mice: critical role of IL-6. *J Leukoc Biol.* 2010;88:579-87.
156. Wang X, Meng X, Kuhlman JR, Nelin LD, Nicol KK, English BK, et al. Knockout of Mkp-1 enhances the host inflammatory responses to gram-positive bacteria. *J Immunol.* 2007;178:5312-20.
157. Wu JJ, Roth RJ, Anderson EJ, Hong EG, Lee MK, Choi CS, et al. Mice lacking MAP kinase phosphatase-1 have enhanced MAP kinase activity and resistance to diet-induced obesity. *Cell Metab.* 2006;4:61-73.
158. Han MS, Jung DY, Morel C, Lakhani SA, Kim JK, Flavell RA, et al. JNK expression by macrophages promotes obesity-induced insulin resistance and inflammation. *Science.* 2013;339:218-22.
159. Bueno OF, De Windt LJ, Lim HW, Tymitz KM, Witt SA, Kimball TR, et al. The dual-specificity phosphatase MKP-1 limits the cardiac hypertrophic response in vitro and in vivo. *Circ Res.* 2001;88:88-96.
160. Dean JL, Sully G, Clark AR, Saklatvala J. The involvement of AU-rich element-binding proteins in p38 mitogen-activated protein kinase pathway-mediated mRNA stabilisation. *Cell Signal.* 2004;16:1113-21.
161. Rousseau S, Morrice N, Peggie M, Campbell DG, Gaestel M, Cohen P. Inhibition of SAPK2a/p38 prevents hnRNP A0 phosphorylation by MAPKAP-K2 and its interaction with cytokine mRNAs. *EMBO J.* 2002;21:6505-14.
162. Bollig F, Winzen R, Gaestel M, Kostka S, Resch K, Holtmann H. Affinity purification of ARE-binding proteins identifies polyA-binding protein 1 as a potential substrate in MK2-induced mRNA stabilization. *Biochem Biophys Res Commun.* 2003;301:665-70.

163. Lin NY, Lin CT, Chang CJ. Modulation of immediate early gene expression by tristetraprolin in the differentiation of 3T3-L1 cells. *Biochem Biophys Res Commun.* 2008;365:69-74.
164. Claffey KP, Shih SC, Mullen A, Dziennis S, Cusick JL, Abrams KR, et al. Identification of a human VPF/VEGF 3' untranslated region mediating hypoxia-induced mRNA stability. *Mol Biol Cell.* 1998;9:469-81.
165. Akool el S, Kleinert H, Hamada FM, Abdelwahab MH, Forstermann U, Pfeilschifter J, et al. Nitric oxide increases the decay of matrix metalloproteinase 9 mRNA by inhibiting the expression of mRNA-stabilizing factor HuR. *Mol Cell Biol.* 2003;23:4901-16.
166. Huwiler A, Akool el S, Aschrafi A, Hamada FM, Pfeilschifter J, Eberhardt W. ATP potentiates interleukin-1 beta-induced MMP-9 expression in mesangial cells via recruitment of the ELAV protein HuR. *J Biol Chem.* 2003;278:51758-69.
167. Li Q, Valerio MS, Kirkwood KL. MAPK usage in periodontal disease progression. *Journal of signal transduction.* 2012;2012:308943.
168. Bhattacharyya S, Brown DE, Brewer JA, Vogt SK, Muglia LJ. Macrophage glucocorticoid receptors regulate Toll-like receptor 4-mediated inflammatory responses by selective inhibition of p38 MAP kinase. *Blood.* 2007;109:4313-9.
169. Perdiguero E, Sousa-Victor P, Ruiz-Bonilla V, Jardí M, Caelles C, Serrano AL, et al. p38/MKP-1-regulated AKT coordinates macrophage transitions and resolution of inflammation during tissue repair. *J Cell Biol.* 2011;195:307-22.
170. Tchen CR, Martins JR, Paktiawal N, Perelli R, Saklatvala J, Clark AR. Glucocorticoid regulation of mouse and human dual specificity phosphatase 1 (DUSP1) genes: unusual cis-acting elements and unexpected evolutionary divergence. *J Biol Chem.* 2010;285:2642-52.
171. Abraham SM, Lawrence T, Kleiman A, Warden P, Medghalchi M, Tuckermann J, et al. Antiinflammatory effects of dexamethasone are partly dependent on induction of dual specificity phosphatase 1. *J Exp Med.* 2006;203:1883-9.
172. Jin Y, Hu D, Peterson EL, Eng C, Levin AM, Wells K, et al. Dual-specificity phosphatase 1 as a pharmacogenetic modifier of inhaled steroid response among asthmatic patients. *J Allergy Clin Immunol.* 2010;126:618-25 e1-2.
173. Wang X, Nelin LD, Kuhlman JR, Meng X, Welty SE, Liu Y. The role of MAP kinase phosphatase-1 in the protective mechanism of dexamethasone against endotoxemia. *Life Sci.* 2008;83:671-80.
174. Loda M, Capodici P, Mishra R, Yao H, Corless C, Grigioni W, et al. Expression of mitogen-activated protein kinase phosphatase-1 in the early phases of human epithelial carcinogenesis. *Am J Pathol.* 1996;149:1553-64.



175. Manzano RG, Montuenga LM, Dayton M, Dent P, Kinoshita I, Vicent S, et al. CL100 expression is down-regulated in advanced epithelial ovarian cancer and its re-expression decreases its malignant potential. *Oncogene*. 2002;21:4435-47.
176. Magi-Galluzzi C, Mishra R, Fiorentino M, Montironi R, Yao H, Capodieci P, et al. Mitogen-activated protein kinase phosphatase 1 is overexpressed in prostate cancers and is inversely related to apoptosis. *Lab Invest*. 1997;76:37-51.
177. Rauhala HE, Porkka KP, Tolonen TT, Martikainen PM, Tammela TL, Visakorpi T. Dual-specificity phosphatase 1 and serum/glucocorticoid-regulated kinase are downregulated in prostate cancer. *Int J Cancer*. 2005;117:738-45.
178. Shimada K, Nakamura M, Ishida E, Higuchi T, Tanaka M, Ota I, et al. c-Jun NH2 terminal kinase activation and decreased expression of mitogen-activated protein kinase phosphatase-1 play important roles in invasion and angiogenesis of urothelial carcinomas. *Am J Pathol*. 2007;171:1003-12.
179. Liu YX, Wang J, Guo J, Wu J, Lieberman HB, Yin Y. DUSP1 is controlled by p53 during the cellular response to oxidative stress. *Mol Cancer Res*. 2008;6:624-33.
180. Fuchs SY, Adler V, Buschmann T, Yin Z, Wu X, Jones SN, et al. JNK targets p53 ubiquitination and degradation in nonstressed cells. *Genes Dev*. 1998;12:2658-63.
181. Bang YJ, Kwon JH, Kang SH, Kim JW, Yang YC. Increased MAPK activity and MKP-1 overexpression in human gastric adenocarcinoma. *Biochem Biophys Res Commun*. 1998;250:43-7.
182. Denkert C, Schmitt WD, Berger S, Reles A, Pest S, Siegert A, et al. Expression of mitogen-activated protein kinase phosphatase-1 (MKP-1) in primary human ovarian carcinoma. *Int J Cancer*. 2002;102:507-13.
183. Tsujita E, Taketomi A, Gion T, Kuroda Y, Endo K, Watanabe A, et al. Suppressed MKP-1 is an independent predictor of outcome in patients with hepatocellular carcinoma. *Oncology*. 2005;69:342-7.
184. Vicent S, Garayoa M, Lopez-Picazo JM, Lozano MD, Toledo G, Thunnissen FB, et al. Mitogen-activated protein kinase phosphatase-1 is overexpressed in non-small cell lung cancer and is an independent predictor of outcome in patients. *Clin Cancer Res*. 2004;10:3639-49.
185. Sanchez-Perez I, Martinez-Gomariz M, Williams D, Keyse SM, Perona R. CL100/MKP-1 modulates JNK activation and apoptosis in response to cisplatin. *Oncogene*. 2000;19:5142-52.
186. Small GW, Shi YY, Higgins LS, Orlowski RZ. Mitogen-activated protein kinase phosphatase-1 is a mediator of breast cancer chemoresistance. *Cancer Res*. 2007;67:4459-66.

187. Wang J, Zhou JY, Wu GS. ERK-dependent MKP-1-mediated cisplatin resistance in human ovarian cancer cells. *Cancer Res.* 2007;67:11933-41.
188. Brondello JM, Brunet A, Pouyssegur J, McKenzie FR. The dual specificity mitogen-activated protein kinase phosphatase-1 and -2 are induced by the p42/p44MAPK cascade. *J Biol Chem.* 1997;272:1368-76.
189. Cook SJ, Beltman J, Cadwallader KA, McMahon M, McCormick F. Regulation of mitogen-activated protein kinase phosphatase-1 expression by extracellular signal-related kinase-dependent and Ca<sup>2+</sup>-dependent signal pathways in Rat-1 cells. *J Biol Chem.* 1997;272:13309-19.
190. Jeanneteau F, Deinhardt K, Miyoshi G, Bennett AM, Chao MV. The MAP kinase phosphatase MKP-1 regulates BDNF-induced axon branching. *Nat Neurosci.* 2010;13:1373-9.
191. Xu Q, Konta T, Nakayama K, Furuu A, Moreno-Manzano V, Lucio-Cazana J, et al. Cellular defense against H<sub>2</sub>O<sub>2</sub>-induced apoptosis via MAP kinase-MKP-1 pathway. *Free Radic Biol Med.* 2004;36:985-93.
192. Melhem A, Yamada SD, Fleming GF, Delgado B, Brickley DR, Wu W, et al. Administration of glucocorticoids to ovarian cancer patients is associated with expression of the anti-apoptotic genes SGK1 and MKP1/DUSP1 in ovarian tissues. *Clin Cancer Res.* 2009;15:3196-204.
193. Pascoe JM, Roberts JJ. Interactions between mammalian cell DNA and inorganic platinum compounds. I. DNA interstrand cross-linking and cytotoxic properties of platinum(II) compounds. *Biochem Pharmacol.* 1974;23:1359-65.
194. Pascoe JM, Roberts JJ. Interactions between mammalian cell DNA and inorganic platinum compounds. II. Interstrand cross-linking of isolated and cellular DNA by platinum(IV) compounds. *Biochem Pharmacol.* 1974;23:1345-57.
195. Jordan MA, Wilson L. Microtubules as a target for anticancer drugs. *Nat Rev Cancer.* 2004;4:253-65.
196. Song JJ, Lee YJ. Differential cleavage of Mst1 by caspase-7/-3 is responsible for TRAIL-induced activation of the MAPK superfamily. *Cell Signal.* 2008;20:892-906.
197. Lamkanfi M, Festjens N, Declercq W, Vanden Berghe T, Vandenabeele P. Caspases in cell survival, proliferation and differentiation. *Cell Death Differ.* 2007;14:44-55.
198. Yoshida M, Horinouchi S. Trichostatin and leptomycin. Inhibition of histone deacetylation and signal-dependent nuclear export. *Ann N Y Acad Sci.* 1999;886:23-36.
199. Bentzen SM. Preventing or reducing late side effects of radiation therapy: radiobiology meets molecular pathology. *Nat Rev Cancer.* 2006;6:702-13.



200. Nyati MK, Feng FY, Maheshwari D, Varambally S, Zielske SP, Ahsan A, et al. Ataxia telangiectasia mutated down-regulates phospho-extracellular signal-regulated kinase 1/2 via activation of MKP-1 in response to radiation. *Cancer Res.* 2006;66:11554-9.
201. Hamdi M, Kool J, Cornelissen-Steijger P, Carlotti F, Popeijus HE, van der Burgt C, et al. DNA damage in transcribed genes induces apoptosis via the JNK pathway and the JNK-phosphatase MKP-1. *Oncogene.* 2005;24:7135-44.
202. Li M, Zhou JY, Ge Y, Matherly LH, Wu GS. The phosphatase MKP1 is a transcriptional target of p53 involved in cell cycle regulation. *J Biol Chem.* 2003;278:41059-68.
203. Brondello JM, McKenzie FR, Sun H, Tonks NK, Pouyssegur J. Constitutive MAP kinase phosphatase (MKP-1) expression blocks G1 specific gene transcription and S-phase entry in fibroblasts. *Oncogene.* 1995;10:1895-904.
204. Verde P, Casalino L, Talotta F, Yaniv M, Weitzman JB. Deciphering AP-1 function in tumorigenesis: fra-ternizing on target promoters. *Cell Cycle.* 2007;6:2633-9.
205. Liao Q, Guo J, Kleeff J, Zimmermann A, Buchler MW, Korc M, et al. Down-regulation of the dual-specificity phosphatase MKP-1 suppresses tumorigenicity of pancreatic cancer cells. *Gastroenterology.* 2003;124:1830-45.
206. Wellbrock C, Karasarides M, Marais R. The RAF proteins take centre stage. *Nat Rev Mol Cell Biol.* 2004;5:875-85.
207. Kinney CM, Chandrasekharan UM, Mavrakis L, DiCorleto PE. VEGF and thrombin induce MKP-1 through distinct signaling pathways: role for MKP-1 in endothelial cell migration. *Am J Physiol Cell Physiol.* 2008;294:C241-50.
208. Rousseau S, Dolado I, Beardmore V, Shpiro N, Marquez R, Nebreda AR, et al. CXCL12 and C5a trigger cell migration via a PAK1/2-p38alpha MAPK-MAPKAP-K2-HSP27 pathway. *Cell Signal.* 2006;18:1897-905.
209. Cuenda A, Rousseau S. p38 MAP-kinases pathway regulation, function and role in human diseases. *Biochim Biophys Acta.* 2007;1773:1358-75.
210. Iyer NG, Ozdag H, Caldas C. p300/CBP and cancer. *Oncogene.* 2004;23:4225-31.
211. Schwartsburd PM. Chronic inflammation as inductor of pro-cancer microenvironment: pathogenesis of dysregulated feedback control. *Cancer Metastasis Rev.* 2003;22:95-102.
212. O'Byrne KJ, Dalglish AG. Chronic immune activation and inflammation as the cause of malignancy. *Br J Cancer.* 2001;85:473-83.

213. Kuper H, Adami HO, Trichopoulos D. Infections as a major preventable cause of human cancer. *J Intern Med.* 2000;248:171-83.
214. Ardies CM. Inflammation as cause for scar cancers of the lung. *Integr Cancer Ther.* 2003;2:238-46.
215. Itzkowitz SH, Yio X. Inflammation and cancer IV. Colorectal cancer in inflammatory bowel disease: the role of inflammation. *Am J Physiol Gastrointest Liver Physiol.* 2004;287:G7-17.
216. Ben-Baruch A. Inflammation-associated immune suppression in cancer: the roles played by cytokines, chemokines and additional mediators. *Semin Cancer Biol.* 2006;16:38-52.
217. Ridnour LA, Cheng RY, Switzer CH, Heinecke JL, Ambs S, Glynn S, et al. Molecular pathways: toll-like receptors in the tumor microenvironment--poor prognosis or new therapeutic opportunity. *Clin Cancer Res.* 2013;19:1340-6.
218. Akira S, Takeda K. Toll-like receptor signalling. *Nat Rev Immunol.* 2004;4:499-511.
219. Karin M, Lawrence T, Nizet V. Innate immunity gone awry: linking microbial infections to chronic inflammation and cancer. *Cell.* 2006;124:823-35.
220. Belmont L, Rabbe N, Antoine M, Cathelin D, Guignabert C, Kurie J, et al. Expression of TLR9 in tumor-infiltrating mononuclear cells enhances angiogenesis and is associated with a worse survival in lung cancer. *Int J Cancer.* 2014;134:765-77.
221. Mao L, Hong WK, Papadimitrakopoulou VA. Focus on head and neck cancer. *Cancer Cell.* 2004;5:311-6.
222. Szczepanski MJ, Czystowska M, Szajnik M, Harasymczuk M, Boyiadzis M, Kruk-Zagajewska A, et al. Triggering of Toll-like receptor 4 expressed on human head and neck squamous cell carcinoma promotes tumor development and protects the tumor from immune attack. *Cancer Res.* 2009;69:3105-13.
223. Ren G, Hu J, Wang R, Han W, Zhao M, Zhou G, et al. Rapamycin inhibits Toll-like receptor 4-induced pro-oncogenic function in head and neck squamous cell carcinoma. *Oncol Rep.* 2014;31:2804-10.
224. Erridge C. Endogenous ligands of TLR2 and TLR4: agonists or assistants? *J Leukoc Biol.* 2010;87:989-99.
225. Karin M. Nuclear factor-kappaB in cancer development and progression. *Nature.* 2006;441:431-6.
226. Brown M, Cohen J, Arun P, Chen Z, Van Waes C. NF-kappaB in carcinoma therapy and prevention. *Expert Opin Ther Targets.* 2008;12:1109-22.

227. Greten FR, Eckmann L, Greten TF, Park JM, Li ZW, Egan LJ, et al. IKKbeta links inflammation and tumorigenesis in a mouse model of colitis-associated cancer. *Cell*. 2004;118:285-96.
228. Pikarsky E, Porat RM, Stein I, Abramovitch R, Amit S, Kasem S, et al. NF-kappaB functions as a tumour promoter in inflammation-associated cancer. *Nature*. 2004;431:461-6.
229. Ki SH, Choi MJ, Lee CH, Kim SG. Galpha12 specifically regulates COX-2 induction by sphingosine 1-phosphate. Role for JNK-dependent ubiquitination and degradation of IkappaBalpha. *J Biol Chem*. 2007;282:1938-47.
230. Lee TL, Yeh J, Friedman J, Yan B, Yang X, Yeh NT, et al. A signal network involving coactivated NF-kappaB and STAT3 and altered p53 modulates BAX/BCL-XL expression and promotes cell survival of head and neck squamous cell carcinomas. *Int J Cancer*. 2008;122:1987-98.
231. Allen C, Duffy S, Teknos T, Islam M, Chen Z, Albert PS, et al. Nuclear factor-kappaB-related serum factors as longitudinal biomarkers of response and survival in advanced oropharyngeal carcinoma. *Clin Cancer Res*. 2007;13:3182-90.
232. Van Waes C, Yu M, Nottingham L, Karin M. Inhibitor-kappaB kinase in tumor promotion and suppression during progression of squamous cell carcinoma. *Clin Cancer Res*. 2007;13:4956-9.
233. Camacho M, Leon X, Fernandez-Figueras MT, Quer M, Vila L. Prostaglandin E(2) pathway in head and neck squamous cell carcinoma. *Head Neck*. 2008;30:1175-81.
234. Lin DT, Subbaramaiah K, Shah JP, Dannenberg AJ, Boyle JO. Cyclooxygenase-2: a novel molecular target for the prevention and treatment of head and neck cancer. *Head Neck*. 2002;24:792-9.
235. Kwak YE, Jeon NK, Kim J, Lee EJ. The cyclooxygenase-2 selective inhibitor celecoxib suppresses proliferation and invasiveness in the human oral squamous carcinoma. *Ann N Y Acad Sci*. 2007;1095:99-112.
236. Papadimitrakopoulou VA, William WN, Jr., Dannenberg AJ, Lippman SM, Lee JJ, Ondrey FG, et al. Pilot randomized phase II study of celecoxib in oral premalignant lesions. *Clin Cancer Res*. 2008;14:2095-101.
237. Mulshine JL, Atkinson JC, Greer RO, Papadimitrakopoulou VA, Van Waes C, Rudy S, et al. Randomized, double-blind, placebo-controlled phase IIb trial of the cyclooxygenase inhibitor ketorolac as an oral rinse in oropharyngeal leukoplakia. *Clin Cancer Res*. 2004;10:1565-73.
238. Lathers DM, Clark JI, Achille NJ, Young MR. Phase 1B study to improve immune responses in head and neck cancer patients using escalating doses of 25-hydroxyvitamin D3. *Cancer Immunol Immunother*. 2004;53:422-30.

239. Park CC, Bissell MJ, Barcellos-Hoff MH. The influence of the microenvironment on the malignant phenotype. *Mol Med Today*. 2000;6:324-9.
240. Jakobisiak M, Lasek W, Golab J. Natural mechanisms protecting against cancer. *Immunol Lett*. 2003;90:103-22.
241. Brigati C, Noonan DM, Albin A, Benelli R. Tumors and inflammatory infiltrates: friends or foes? *Clin Exp Metastasis*. 2002;19:247-58.
242. Maleki S, Schlecht NF, Keller C, Diaz J, Moss J, Prystowsky MB, et al. Lymphocytic host response to oral squamous cell carcinoma: an adaptive T-cell response at the tumor interface. *Head and neck pathology*. 2011;5:117-22.
243. Tourkova IL, Shurin GV, Chatta GS, Perez L, Finke J, Whiteside TL, et al. Restoration by IL-15 of MHC class I antigen-processing machinery in human dendritic cells inhibited by tumor-derived gangliosides. *J Immunol*. 2005;175:3045-52.
244. Bergmann C, Strauss L, Wieckowski E, Czystowska M, Albers A, Wang Y, et al. Tumor-derived microvesicles in sera of patients with head and neck cancer and their role in tumor progression. *Head Neck*. 2009;31:371-80.
245. Katou F, Ohtani H, Watanabe Y, Nakayama T, Yoshie O, Hashimoto K. Differing phenotypes between intraepithelial and stromal lymphocytes in early-stage tongue cancer. *Cancer Res*. 2007;67:11195-201.
246. Strome SE, Dong H, Tamura H, Voss SG, Flies DB, Tamada K, et al. B7-H1 blockade augments adoptive T-cell immunotherapy for squamous cell carcinoma. *Cancer Res*. 2003;63:6501-5.
247. Green VL, Michno A, Stafford ND, Greenman J. Increased prevalence of tumour infiltrating immune cells in oropharyngeal tumours in comparison to other subsites: relationship to peripheral immunity. *Cancer Immunol Immunother*. 2013.
248. Hawiger D, Inaba K, Dorsett Y, Guo M, Mahnke K, Rivera M, et al. Dendritic cells induce peripheral T cell unresponsiveness under steady state conditions in vivo. *J Exp Med*. 2001;194:769-79.
249. Jonuleit H, Schmitt E, Schuler G, Knop J, Enk AH. Induction of interleukin 10-producing, nonproliferating CD4(+) T cells with regulatory properties by repetitive stimulation with allogeneic immature human dendritic cells. *J Exp Med*. 2000;192:1213-22.
250. Bingle L, Brown NJ, Lewis CE. The role of tumour-associated macrophages in tumour progression: implications for new anticancer therapies. *J Pathol*. 2002;196:254-65.

251. Di Carlo E, Forni G, Lollini P, Colombo MP, Modesti A, Musiani P. The intriguing role of polymorphonuclear neutrophils in antitumor reactions. *Blood*. 2001;97:339-45.
252. Pollard JW. Tumour-educated macrophages promote tumour progression and metastasis. *Nat Rev Cancer*. 2004;4:71-8.
253. Mantovani A, Sozzani S, Locati M, Allavena P, Sica A. Macrophage polarization: tumor-associated macrophages as a paradigm for polarized M2 mononuclear phagocytes. *Trends Immunol*. 2002;23:549-55.
254. Crowther M, Brown NJ, Bishop ET, Lewis CE. Microenvironmental influence on macrophage regulation of angiogenesis in wounds and malignant tumors. *J Leukoc Biol*. 2001;70:478-90.
255. Mills CD, Kincaid K, Alt JM, Heilman MJ, Hill AM. M-1/M-2 macrophages and the Th1/Th2 paradigm. *J Immunol*. 2000;164:6166-73.
256. Li C, Shintani S, Terakado N, Nakashiro K, Hamakawa H. Infiltration of tumor-associated macrophages in human oral squamous cell carcinoma. *Oncol Rep*. 2002;9:1219-23.
257. Marcus B, Arenberg D, Lee J, Kleer C, Chepeha DB, Schmalbach CE, et al. Prognostic factors in oral cavity and oropharyngeal squamous cell carcinoma. *Cancer*. 2004;101:2779-87.
258. Liu SY, Chang LC, Pan LF, Hung YJ, Lee CH, Shieh YS. Clinicopathologic significance of tumor cell-lined vessel and microenvironment in oral squamous cell carcinoma. *Oral Oncol*. 2008;44:277-85.
259. Mantovani A, Ming WJ, Balotta C, Abdeljalil B, Bottazzi B. Origin and regulation of tumor-associated macrophages: the role of tumor-derived chemotactic factor. *Biochim Biophys Acta*. 1986;865:59-67.
260. Sallusto F, Mackay CR, Lanzavecchia A. The role of chemokine receptors in primary, effector, and memory immune responses. *Annu Rev Immunol*. 2000;18:593-620.
261. Kim CH, Broxmeyer HE. Chemokines: signal lamps for trafficking of T and B cells for development and effector function. *J Leukoc Biol*. 1999;65:6-15.
262. Albert S, Riveiro ME, Halimi C, Hourseau M, Couvelard A, Serova M, et al. Focus on the role of the CXCL12/CXCR4 chemokine axis in head and neck squamous cell carcinoma. *Head Neck*. 2013.
263. Barreda DR, Hanington PC, Belosevic M. Regulation of myeloid development and function by colony stimulating factors. *Dev Comp Immunol*. 2004;28:509-54.

264. Lin EY, Nguyen AV, Russell RG, Pollard JW. Colony-stimulating factor 1 promotes progression of mammary tumors to malignancy. *J Exp Med*. 2001;193:727-40.
265. Lin EY, Gouon-Evans V, Nguyen AV, Pollard JW. The macrophage growth factor CSF-1 in mammary gland development and tumor progression. *J Mammary Gland Biol Neoplasia*. 2002;7:147-62.
266. Liss C, Fekete MJ, Hasina R, Lam CD, Lingen MW. Paracrine angiogenic loop between head-and-neck squamous-cell carcinomas and macrophages. *Int J Cancer*. 2001;93:781-5.
267. Liss C, Fekete MJ, Hasina R, Lingen MW. Retinoic acid modulates the ability of macrophages to participate in the induction of the angiogenic phenotype in head and neck squamous cell carcinoma. *Int J Cancer*. 2002;100:283-9.
268. Li AG, Lu SL, Zhang MX, Deng C, Wang XJ. Smad3 knockout mice exhibit a resistance to skin chemical carcinogenesis. *Cancer Res*. 2004;64:7836-45.
269. Almofti A, Uchida D, Begum NM, Tomizuka Y, Iga H, Yoshida H, et al. The clinicopathological significance of the expression of CXCR4 protein in oral squamous cell carcinoma. *Int J Oncol*. 2004;25:65-71.
270. Katayama A, Ogino T, Bandoh N, Nonaka S, Harabuchi Y. Expression of CXCR4 and its down-regulation by IFN-gamma in head and neck squamous cell carcinoma. *Clin Cancer Res*. 2005;11:2937-46.
271. Uchida D, Onoue T, Tomizuka Y, Begum NM, Miwa Y, Yoshida H, et al. Involvement of an autocrine stromal cell derived factor-1/CXCR4 system on the distant metastasis of human oral squamous cell carcinoma. *Mol Cancer Res*. 2007;5:685-94.
272. Ishikawa T, Nakashiro K, Hara S, Klosek SK, Li C, Shintani S, et al. CXCR4 expression is associated with lymph-node metastasis of oral squamous cell carcinoma. *Int J Oncol*. 2006;28:61-6.
273. Yoon Y, Liang Z, Zhang X, Choe M, Zhu A, Cho HT, et al. CXC chemokine receptor-4 antagonist blocks both growth of primary tumor and metastasis of head and neck cancer in xenograft mouse models. *Cancer Res*. 2007;67:7518-24.
274. Biswas SK, Mantovani A. Macrophage plasticity and interaction with lymphocyte subsets: cancer as a paradigm. *Nat Immunol*. 2010;11:889-96.
275. Sica A, Schioppa T, Mantovani A, Allavena P. Tumour-associated macrophages are a distinct M2 polarised population promoting tumour progression: potential targets of anti-cancer therapy. *Eur J Cancer*. 2006;42:717-27.
276. Allavena P, Sica A, Garlanda C, Mantovani A. The Yin-Yang of tumor-associated macrophages in neoplastic progression and immune surveillance. *Immunol Rev*. 2008;222:155-61.

277. Condeelis J, Pollard JW. Macrophages: obligate partners for tumor cell migration, invasion, and metastasis. *Cell*. 2006;124:263-6.
278. Yang L, Huang J, Ren X, Gorska AE, Chytil A, Aakre M, et al. Abrogation of TGF beta signaling in mammary carcinomas recruits Gr-1+CD11b+ myeloid cells that promote metastasis. *Cancer Cell*. 2008;13:23-35.
279. Mantovani A, Schioppa T, Porta C, Allavena P, Sica A. Role of tumor-associated macrophages in tumor progression and invasion. *Cancer Metastasis Rev*. 2006;25:315-22.
280. Murdoch C, Muthana M, Coffelt SB, Lewis CE. The role of myeloid cells in the promotion of tumour angiogenesis. *Nat Rev Cancer*. 2008;8:618-31.
281. Shime H, Yabu M, Akazawa T, Kodama K, Matsumoto M, Seya T, et al. Tumor-secreted lactic acid promotes IL-23/IL-17 proinflammatory pathway. *J Immunol*. 2008;180:7175-83.
282. Sica A, Bronte V. Altered macrophage differentiation and immune dysfunction in tumor development. *J Clin Invest*. 2007;117:1155-66.
283. Huang B, Pan PY, Li Q, Sato AI, Levy DE, Bromberg J, et al. Gr-1+CD115+ immature myeloid suppressor cells mediate the development of tumor-induced T regulatory cells and T-cell anergy in tumor-bearing host. *Cancer Res*. 2006;66:1123-31.
284. Nagaraj S, Gabilovich DI. Tumor escape mechanism governed by myeloid-derived suppressor cells. *Cancer Res*. 2008;68:2561-3.
285. Sinha P, Clements VK, Bunt SK, Albelda SM, Ostrand-Rosenberg S. Cross-talk between myeloid-derived suppressor cells and macrophages subverts tumor immunity toward a type 2 response. *J Immunol*. 2007;179:977-83.
286. Elgert KD, Alleva DG, Mullins DW. Tumor-induced immune dysfunction: the macrophage connection. *J Leukoc Biol*. 1998;64:275-90.
287. Sica A, Sacconi A, Mantovani A. Tumor-associated macrophages: a molecular perspective. *Int Immunopharmacol*. 2002;2:1045-54.
288. Malmberg KJ. Effective immunotherapy against cancer: a question of overcoming immune suppression and immune escape? *Cancer Immunol Immunother*. 2004;53:879-92.
289. Van Waes C. Nuclear factor-kappaB in development, prevention, and therapy of cancer. *Clin Cancer Res*. 2007;13:1076-82.
290. Sawanobori Y, Ueha S, Kurachi M, Shimaoka T, Talmadge JE, Abe J, et al. Chemokine-mediated rapid turnover of myeloid-derived suppressor cells in tumor-bearing mice. *Blood*. 2008;111:5457-66.



291. Mantovani A, Allavena P, Sica A, Balkwill F. Cancer-related inflammation. *Nature*. 2008;454:436-44.
292. Pries R, Nitsch S, Wollenberg B. Role of cytokines in head and neck squamous cell carcinoma. *Expert Rev Anticancer Ther*. 2006;6:1195-203.
293. Lee TL, Yeh J, Van Waes C, Chen Z. Epigenetic modification of SOCS-1 differentially regulates STAT3 activation in response to interleukin-6 receptor and epidermal growth factor receptor signaling through JAK and/or MEK in head and neck squamous cell carcinomas. *Mol Cancer Ther*. 2006;5:8-19.
294. Duffy SA, Taylor JM, Terrell JE, Islam M, Li Y, Fowler KE, et al. Interleukin-6 predicts recurrence and survival among head and neck cancer patients. *Cancer*. 2008;113:750-7.
295. Kanazawa T, Nishino H, Hasegawa M, Ohta Y, Iino Y, Ichimura K, et al. Interleukin-6 directly influences proliferation and invasion potential of head and neck cancer cells. *Eur Arch Otorhinolaryngol*. 2007;264:815-21.
296. Chen CJ, Kono H, Golenbock D, Reed G, Akira S, Rock KL. Identification of a key pathway required for the sterile inflammatory response triggered by dying cells. *Nat Med*. 2007;13:851-6.
297. Marhaba R, Nazarenko I, Knofler D, Reich E, Voronov E, Vitacolonna M, et al. Opposing effects of fibrosarcoma cell-derived IL-1 alpha and IL-1 beta on immune response induction. *Int J Cancer*. 2008;123:134-45.
298. Elkabets M, Krelin Y, Dotan S, Cerwenka A, Porgador A, Lichtenstein RG, et al. Host-derived interleukin-1alpha is important in determining the immunogenicity of 3-methylcholantrene tumor cells. *J Immunol*. 2009;182:4874-81.
299. Voronov E, Shouval DS, Krelin Y, Cagnano E, Benharroch D, Iwakura Y, et al. IL-1 is required for tumor invasiveness and angiogenesis. *Proc Natl Acad Sci U S A*. 2003;100:2645-50.
300. Krelin Y, Voronov E, Dotan S, Elkabets M, Reich E, Fogel M, et al. Interleukin-1beta-driven inflammation promotes the development and invasiveness of chemical carcinogen-induced tumors. *Cancer Res*. 2007;67:1062-71.
301. Zhu P, Baek SH, Bourk EM, Ohgi KA, Garcia-Bassets I, Sanjo H, et al. Macrophage/cancer cell interactions mediate hormone resistance by a nuclear receptor derepression pathway. *Cell*. 2006;124:615-29.
302. El-Omar EM, Carrington M, Chow WH, McColl KE, Bream JH, Young HA, et al. Interleukin-1 polymorphisms associated with increased risk of gastric cancer. *Nature*. 2000;404:398-402.



303. Tu S, Bhagat G, Cui G, Takaishi S, Kurt-Jones EA, Rickman B, et al. Overexpression of interleukin-1beta induces gastric inflammation and cancer and mobilizes myeloid-derived suppressor cells in mice. *Cancer Cell*. 2008;14:408-19.
304. Giavazzi R, Garofalo A, Bani MR, Abbate M, Ghezzi P, Boraschi D, et al. Interleukin 1-induced augmentation of experimental metastases from a human melanoma in nude mice. *Cancer Res*. 1990;50:4771-5.
305. Luo JL, Tan W, Ricono JM, Korchynskiy O, Zhang M, Gonias SL, et al. Nuclear cytokine-activated IKKalpha controls prostate cancer metastasis by repressing Maspin. *Nature*. 2007;446:690-4.
306. Mukhopadhyay P, Ali MA, Nandi A, Carreon P, Choy H, Saha D. The cyclin-dependent kinase 2 inhibitor down-regulates interleukin-1beta-mediated induction of cyclooxygenase-2 expression in human lung carcinoma cells. *Cancer Res*. 2006;66:1758-66.
307. Teruel A, Romero M, Cacalano NA, Head C, Jewett A. Potential contribution of naive immune effectors to oral tumor resistance: role in synergistic induction of VEGF, IL-6, and IL-8 secretion. *Cancer Immunol Immunother*. 2008;57:359-66.
308. St John MA, Dohadwala M, Luo J, Wang G, Lee G, Shih H, et al. Proinflammatory mediators upregulate snail in head and neck squamous cell carcinoma. *Clin Cancer Res*. 2009;15:6018-27.
309. Lyons JG, Patel V, Roue NC, Fok SY, Soon LL, Halliday GM, et al. Snail up-regulates proinflammatory mediators and inhibits differentiation in oral keratinocytes. *Cancer Res*. 2008;68:4525-30.
310. Chen Z, Malhotra PS, Thomas GR, Ondrey FG, Duffey DC, Smith CW, et al. Expression of proinflammatory and proangiogenic cytokines in patients with head and neck cancer. *Clin Cancer Res*. 1999;5:1369-79.
311. Asirvatham AJ, Magner WJ, Tomasi TB. miRNA regulation of cytokine genes. *Cytokine*. 2009;45:58-69.
312. Ting JP, Lovering RC, Alnemri ES, Bertin J, Boss JM, Davis BK, et al. The NLR gene family: a standard nomenclature. *Immunity*. 2008;28:285-7.
313. Davis BK, Wen H, Ting JP. The inflammasome NLRs in immunity, inflammation, and associated diseases. *Annu Rev Immunol*. 2011;29:707-35.
314. Ting JP, Willingham SB, Bergstralh DT. NLRs at the intersection of cell death and immunity. *Nat Rev Immunol*. 2008;8:372-9.
315. Rathinam VA, Jiang Z, Waggoner SN, Sharma S, Cole LE, Waggoner L, et al. The AIM2 inflammasome is essential for host defense against cytosolic bacteria and DNA viruses. *Nat Immunol*. 2010;11:395-402.

316. Poeck H, Bscheider M, Gross O, Finger K, Roth S, Rebsamen M, et al. Recognition of RNA virus by RIG-I results in activation of CARD9 and inflammasome signaling for interleukin 1 beta production. *Nat Immunol.* 2010;11:63-9.
317. Mariathasan S, Weiss DS, Newton K, McBride J, O'Rourke K, Roose-Girma M, et al. Cryopyrin activates the inflammasome in response to toxins and ATP. *Nature.* 2006;440:228-32.
318. Dostert C, Petrilli V, Van Bruggen R, Steele C, Mossman BT, Tschopp J. Innate immune activation through Nalp3 inflammasome sensing of asbestos and silica. *Science.* 2008;320:674-7.
319. Chen GY, Liu M, Wang F, Bertin J, Nunez G. A functional role for Nlrp6 in intestinal inflammation and tumorigenesis. *J Immunol.* 2011;186:7187-94.
320. Elinav E, Strowig T, Kau AL, Henao-Mejia J, Thaiss CA, Booth CJ, et al. NLRP6 inflammasome regulates colonic microbial ecology and risk for colitis. *Cell.* 2011;145:745-57.
321. Normand S, Delanoye-Crespin A, Bressenot A, Huot L, Grandjean T, Peyrin-Biroulet L, et al. Nod-like receptor pyrin domain-containing protein 6 (NLRP6) controls epithelial self-renewal and colorectal carcinogenesis upon injury. *Proc Natl Acad Sci U S A.* 2011;108:9601-6.
322. Zaki MH, Vogel P, Body-Malapel M, Lamkanfi M, Kanneganti TD. IL-18 production downstream of the Nlrp3 inflammasome confers protection against colorectal tumor formation. *J Immunol.* 2010;185:4912-20.
323. Siegmund B, Lehr HA, Fantuzzi G, Dinarello CA. IL-1 beta -converting enzyme (caspase-1) in intestinal inflammation. *Proc Natl Acad Sci U S A.* 2001;98:13249-54.
324. Bauer C, Duewell P, Mayer C, Lehr HA, Fitzgerald KA, Dauer M, et al. Colitis induced in mice with dextran sulfate sodium (DSS) is mediated by the NLRP3 inflammasome. *Gut.* 2010;59:1192-9.
325. Allen IC, TeKippe EM, Woodford RM, Uronis JM, Holl EK, Rogers AB, et al. The NLRP3 inflammasome functions as a negative regulator of tumorigenesis during colitis-associated cancer. *J Exp Med.* 2010;207:1045-56.
326. Dupaul-Chicoine J, Yeretssian G, Doiron K, Bergstrom KS, McIntire CR, LeBlanc PM, et al. Control of intestinal homeostasis, colitis, and colitis-associated colorectal cancer by the inflammatory caspases. *Immunity.* 2010;32:367-78.
327. Zaki MH, Vogel P, Malireddi RK, Body-Malapel M, Anand PK, Bertin J, et al. The NOD-like receptor NLRP12 attenuates colon inflammation and tumorigenesis. *Cancer Cell.* 2011;20:649-60.

328. Zaki MH, Boyd KL, Vogel P, Kastan MB, Lamkanfi M, Kanneganti TD. The NLRP3 inflammasome protects against loss of epithelial integrity and mortality during experimental colitis. *Immunity*. 2010;32:379-91.
329. Staley EM, Tanner SM, Daft JG, Stanus AL, Martin SM, Lorenz RG. Maintenance of host leukocytes in peripheral immune compartments following lethal irradiation and bone marrow reconstitution: implications for graft versus host disease. *Transpl Immunol*. 2013;28:112-9.
330. Wu S, Rhee KJ, Albesiano E, Rabizadeh S, Wu X, Yen HR, et al. A human colonic commensal promotes colon tumorigenesis via activation of T helper type 17 T cell responses. *Nat Med*. 2009;15:1016-22.
331. Detre S, Saclani Jotti G, Dowsett M. A "quickscore" method for immunohistochemical semiquantitation: validation for oestrogen receptor in breast carcinomas. *J Clin Pathol*. 1995;48:876-8.
332. Wilson ME, Hamilton RG. Immunoglobulin G subclass response of localized juvenile periodontitis patients to *Actinobacillus actinomycetemcomitans* Y4 lipopolysaccharide. *Infect Immun*. 1992;60:1806-12.
333. Tang XH, Knudsen B, Bemis D, Tickoo S, Gudas LJ. Oral cavity and esophageal carcinogenesis modeled in carcinogen-treated mice. *Clinical cancer research : an official journal of the American Association for Cancer Research*. 2004;10:301-13.
334. McAbee J, Li Q, Yu H, Kirkwood KL. Sexual Dimorphism in Periapical Inflammation and Bone Loss from Mitogen-activated Protein Kinase Phosphatase-1 Deficient Mice. *J Endod*. 2012;38:1097-100.
335. Roth RJ, Le AM, Zhang L, Kahn M, Samuel VT, Shulman GI, et al. MAPK phosphatase-1 facilitates the loss of oxidative myofibers associated with obesity in mice. *The Journal of clinical investigation*. 2009;119:3817-29.
336. Wu JJ, Roth RJ, Anderson EJ, Hong EG, Lee MK, Choi CS, et al. Mice lacking MAP kinase phosphatase-1 have enhanced MAP kinase activity and resistance to diet-induced obesity. *Cell Metab*. 2006;4:61-73.
337. Czerninski R, Amornphimoltham P, Patel V, Molinolo AA, Gutkind JS. Targeting mammalian target of rapamycin by rapamycin prevents tumor progression in an oral-specific chemical carcinogenesis model. *Cancer Prev Res (Phila Pa)*. 2009;2:27-36.
338. Nomura T, Shibahara T, Katakura A, Matsubara S, Takano N. Establishment of a murine model of bone invasion by oral squamous cell carcinoma. *Oral Oncol*. 2007;43:257-62.
339. Poltorak A, He X, Smirnova I, Liu MY, Van Huffel C, Du X, et al. Defective LPS signaling in C3H/HeJ and C57BL/10ScCr mice: mutations in Tlr4 gene. *Science*. 1998;282:2085-8.

340. Hou MF, Chang CW, Chen FM, Wang SN, Yang SF, Chen PH, et al. Decreased Total MKP-1 Protein Levels Predict Poor Prognosis in Breast Cancer. *World J Surg.* 2012.
341. Gyorffy B, Lanczky A, Eklund AC, Denkert C, Budczies J, Li Q, et al. An online survival analysis tool to rapidly assess the effect of 22,277 genes on breast cancer prognosis using microarray data of 1,809 patients. *Breast Cancer Res Treat.* 2010;123:725-31.
342. De Costa AM, Schuyler CA, Walker DD, Young MR. Characterization of the evolution of immune phenotype during the development and progression of squamous cell carcinoma of the head and neck. *Cancer immunology, immunotherapy : CII.* 2011.
343. Bayliss TJ, Smith JT, Schuster M, Dragnev KH, Rigas JR. A humanized anti-IL-6 antibody (ALD518) in non-small cell lung cancer. *Expert Opin Biol Ther.* 2011;11:1663-8.
344. Voorhees PM, Manges RF, Sonneveld P, Jagannath S, Somlo G, Krishnan A, et al. A phase 2 multicentre study of siltuximab, an anti-interleukin-6 monoclonal antibody, in patients with relapsed or refractory multiple myeloma. *Br J Haematol.* 2013;161:357-66.
345. Tai CJ, Wu AT, Chiou JF, Jan HJ, Wei HJ, Hsu CH, et al. The investigation of mitogen-activated protein kinase phosphatase-1 as a potential pharmacological target in non-small cell lung carcinomas, assisted by non-invasive molecular imaging. *BMC Cancer.* 2010;10:95.
346. Jan HJ, Lee CC, Lin YM, Lai JH, Wei HW, Lee HM. Rosiglitazone reduces cell invasiveness by inducing MKP-1 in human U87MG glioma cells. *Cancer Lett.* 2009;277:141-8.
347. Vollmer TR, Stockhausen A, Zhang JZ. Anti-inflammatory effects of mapracorat, a novel selective glucocorticoid receptor agonist, is partially mediated by MAP kinase phosphatase-1 (MKP-1). *J Biol Chem.* 2012.
348. Leelahavanichkul K, Amornphimoltham P, Molinolo AA, Basile JR, Koontongkaew S, Gutkind JS. A role for p38 MAPK in head and neck cancer cell growth and tumor-induced angiogenesis and lymphangiogenesis. *Mol Oncol.* 2014;8:105-18.
349. Alspach E, Flanagan KC, Luo X, Ruhland MK, Huang H, Pazolli E, et al. p38MAPK Plays a Crucial Role in Stromal-Mediated Tumorigenesis. *Cancer discovery.* 2014.
350. Boerckel JD, Chandrasekharan UM, Waitkus MS, Tillmaand EG, Bartlett R, Dicorleto PE. Mitogen-Activated Protein Kinase Phosphatase-1 Promotes Neovascularization and Angiogenic Gene Expression. *Arterioscler Thromb Vasc Biol.* 2014.

351. Junttila MR, Ala-Aho R, Jokilehto T, Peltonen J, Kallajoki M, Grenman R, et al. p38alpha and p38delta mitogen-activated protein kinase isoforms regulate invasion and growth of head and neck squamous carcinoma cells. *Oncogene*. 2007;26:5267-79.
352. Gill K, Kumar R, Mohanti BK, Dey S. Assessment of p38alpha in peripheral blood mononuclear cells (PBMC): a potential blood protein marker of head and neck squamous cell carcinoma. *Clin Transl Oncol*. 2013.
353. Gill K, Mohanti BK, Ashraf MS, Singh AK, Dey S. Quantification of p38alphaMAP kinase: A prognostic marker in HNSCC with respect to radiation therapy. *Clinica chimica acta; international journal of clinical chemistry*. 2011.
354. Cohen P. Protein kinases--the major drug targets of the twenty-first century? *Nat Rev Drug Discov*. 2002;1:309-15.
355. Saklatvala J. The p38 MAP kinase pathway as a therapeutic target in inflammatory disease. *Curr Opin Pharmacol*. 2004;4:372-7.
356. Leelahavanichkul K, Amornphimoltham P, Molinolo AA, Basile JR, Koontongkaew S, Gutkind JS. A role for p38 MAPK in head and neck cancer cell growth and tumor-induced angiogenesis and lymphangiogenesis. *Mol Oncol*. 2013.
357. Gross ND, Boyle JO, Du B, Kekatpure VD, Lantowski A, Thaler HT, et al. Inhibition of Jun NH2-terminal kinases suppresses the growth of experimental head and neck squamous cell carcinoma. *Clinical cancer research : an official journal of the American Association for Cancer Research*. 2007;13:5910-7.
358. Ohyama M, Hirayama Y, Tanuma J, Hirano M, Semba I, Shisa H, et al. Expressions of junB and c-fos are enhanced in 4-nitroquinoline 1-oxide-induced rat tongue cancers. *Pathol Int*. 2004;54:35-40.
359. Highfill SL, Cui Y, Giles AJ, Smith JP, Zhang H, Morse E, et al. Disruption of CXCR2-Mediated MDSC Tumor Trafficking Enhances Anti-PD1 Efficacy. *Science translational medicine*. 2014;6:237ra67.
360. da Silva JM, Queiroz-Junior CM, Batista AC, Rachid MA, Teixeira MM, da Silva TA. Eosinophil depletion protects mice from tongue squamous cell carcinoma induced by 4-nitroquinoline-1-oxide. *Histol Histopathol*. 2013.
361. Trellakis S, Bruderek K, Dumitru CA, Gholaman H, Gu X, Bankfalvi A, et al. Polymorphonuclear granulocytes in human head and neck cancer: Enhanced inflammatory activity, modulation by cancer cells and expansion in advanced disease. *International journal of cancer Journal international du cancer*. 2010.
362. Trellakis S, Farjah H, Bruderek K, Dumitru CA, Hoffmann TK, Lang S, et al. Peripheral blood neutrophil granulocytes from patients with head and neck squamous cell carcinoma functionally differ from their counterparts in healthy donors. *Int J Immunopathol Pharmacol*. 2011;24:683-93.

363. De Costa AM, Justis DN, Schuyler CA, Young MR. Administration of a vaccine composed of dendritic cells pulsed with premalignant oral lesion lysate to mice bearing carcinogen-induced premalignant oral lesions stimulates a protective immune response. *Int Immunopharmacol*. 2012;13:322-30.
364. Jie HB, Gildener-Leapman N, Li J, Srivastava RM, Gibson SP, Whiteside TL, et al. Intratumoral regulatory T cells upregulate immunosuppressive molecules in head and neck cancer patients. *Br J Cancer*. 2013.
365. Johnson SD, De Costa AM, Young MR. Effect of the premalignant and tumor microenvironment on immune cell cytokine production in head and neck cancer. *Cancers*. 2014;6:756-70.
366. Wild CA, Brandau S, Lindemann M, Lotfi R, Hoffmann TK, Lang S, et al. Toll-like Receptors in Regulatory T Cells of Patients With Head and Neck Cancer. *Arch Otolaryngol Head Neck Surg*. 2010;136:1253-9.
367. Li J, Liang F, Yu D, Qing H, Yang Y. Development of a 4-nitroquinoline-1-oxide model of lymph node metastasis in oral squamous cell carcinoma. *Oral Oncol*. 2012.
368. O'Malley BW, Jr., Cope KA, Johnson CS, Schwartz MR. A new immunocompetent murine model for oral cancer. *Arch Otolaryngol Head Neck Surg*. 1997;123:20-4.
369. Bystryjn JC. Release of tumor-associated antigens by murine melanoma cells. *J Immunol*. 1976;116:1302-5.
370. Leveson SH, Howell JH, Paolini NS, Tan MH, Holyoke ED, Goldrosen MH. Correlations between the leukocyte adherence inhibition microassay and in vivo tests of transplantation resistance. *Cancer Res*. 1979;39:582-6.
371. Salojin KV, Owusu IB, Millerchip KA, Potter M, Platt KA, Oravec T. Essential role of MAPK phosphatase-1 in the negative control of innate immune responses. *J Immunol*. 2006;176:1899-907.
372. Ahn J, Chen CY, Hayes RB. Oral microbiome and oral and gastrointestinal cancer risk. *Cancer Causes Control*. 2012;23:399-404.
373. Meyer MS, Joshipura K, Giovannucci E, Michaud DS. A review of the relationship between tooth loss, periodontal disease, and cancer. *Cancer Causes Control*. 2008;19:895-907.
374. Meurman JH. Oral microbiota and cancer. *Journal of oral microbiology*. 2010;2.
375. Arellano-Garcia ME, Hu S, Wang J, Henson B, Zhou H, Chia D, et al. Multiplexed immunobead-based assay for detection of oral cancer protein biomarkers in saliva. *Oral Dis*. 2008;14:705-12.

376. Li Y, St John MA, Zhou X, Kim Y, Sinha U, Jordan RC, et al. Salivary transcriptome diagnostics for oral cancer detection. *Clinical cancer research : an official journal of the American Association for Cancer Research*. 2004;10:8442-50.
377. Auron PE, Webb AC, Rosenwasser LJ, Mucci SF, Rich A, Wolff SM, et al. Nucleotide sequence of human monocyte interleukin 1 precursor cDNA. *Proc Natl Acad Sci U S A*. 1984;81:7907-11.
378. Chen Z, Malhotra PS, Thomas GR, Ondrey FG, Duffey DC, Smith CW, et al. Expression of proinflammatory and proangiogenic cytokines in patients with head and neck cancer. *Clinical cancer research : an official journal of the American Association for Cancer Research*. 1999;5:1369-79.
379. Korhonen R, Huotari N, Hommo T, Leppanen T, Moilanen E. The expression of interleukin-12 is increased by MAP kinase phosphatase-1 through a mechanism related to interferon regulatory factor 1. *Mol Immunol*. 2012;51:219-26.
380. Gruber AR, Fallmann J, Kratochvill F, Kovarik P, Hofacker IL. AREsite: a database for the comprehensive investigation of AU-rich elements. *Nucleic Acids Res*. 2011;39:D66-9.
381. Yu H, Sun Y, Haycraft C, Palanisamy V, Kirkwood KL. MKP-1 regulates cytokine mRNA stability through selectively modulation subcellular translocation of AUF1. *Cytokine*. 2011.
382. Huotari N, Hommo T, Taimi V, Nieminen R, Moilanen E, Korhonen R. Regulation of tristetraprolin expression by mitogen-activated protein kinase phosphatase-1. *APMIS*. 2012.
383. Sun L, Stoecklin G, Van Way S, Hinkovska-Galcheva V, Guo RF, Anderson P, et al. Tristetraprolin (TTP)-14-3-3 complex formation protects TTP from dephosphorylation by protein phosphatase 2a and stabilizes tumor necrosis factor-alpha mRNA. *The Journal of biological chemistry*. 2007;282:3766-77.
384. Gruber AR, Fallmann J, Kratochvill F, Kovarik P, Hofacker IL. AREsite: a database for the comprehensive investigation of AU-rich elements. *Nucleic Acids Res*. 2011;39:D66-9.
385. Biswas SK, Sica A, Lewis CE. Plasticity of macrophage function during tumor progression: regulation by distinct molecular mechanisms. *J Immunol*. 2008;180:2011-7.
386. Qualls JE, Murray PJ. Tumor macrophages protective and pathogenic roles in cancer development. *Curr Top Dev Biol*. 2011;94:309-28.
387. Huang G, Wang Y, Shi LZ, Kanneganti TD, Chi H. Signaling by the Phosphatase MKP-1 in Dendritic Cells Imprints Distinct Effector and Regulatory T Cell Fates. *Immunity*. 2011.



388. Biswas SK, Gangi L, Paul S, Schioppa T, Saccani A, Sironi M, et al. A distinct and unique transcriptional program expressed by tumor-associated macrophages (defective NF-kappaB and enhanced IRF-3/STAT1 activation). *Blood*. 2006;107:2112-22.
389. Franklin RA, Liao W, Sarkar A, Kim MV, Bivona MR, Liu K, et al. The cellular and molecular origin of tumor-associated macrophages. *Science*. 2014;344:921-5.
390. Gannot G, Buchner A, Keisari Y. Interaction between the immune system and tongue squamous cell carcinoma induced by 4-nitroquinoline N-oxide in mice. *Oral Oncol*. 2004;40:287-97.
391. Kesselring R, Thiel A, Pries R, Trenkle T, Wollenberg B. Human Th17 cells can be induced through head and neck cancer and have a functional impact on HNSCC development. *Br J Cancer*. 2010.
392. Perez RL, Ritzenthaler JD, Roman J. Transcriptional regulation of the interleukin-1beta promoter via fibrinogen engagement of the CD18 integrin receptor. *Am J Respir Cell Mol Biol*. 1999;20:1059-66.
393. Rattenbacher B, Bohjanen PR. Evaluating posttranscriptional regulation of cytokine genes. *Methods Mol Biol*. 2012;820:71-89.
394. Van Tubergen E, Vander Broek R, Lee J, Wolf G, Carey T, Bradford C, et al. Tristetraprolin regulates interleukin-6, which is correlated with tumor progression in patients with head and neck squamous cell carcinoma. *Cancer*. 2011.
395. Bros M, Wiechmann N, Besche V, Art J, Pautz A, Grabbe S, et al. The RNA binding protein tristetraprolin influences the activation state of murine dendritic cells. *Mol Immunol*. 2010;47:1161-70.
396. Chen YL, Huang YL, Lin NY, Chen HC, Chiu WC, Chang CJ. Differential regulation of ARE-mediated TNFalpha and IL-1beta mRNA stability by lipopolysaccharide in RAW264.7 cells. *Biochem Biophys Res Commun*. 2006;346:160-8.
397. Lu JY, Sadri N, Schneider RJ. Endotoxic shock in AUF1 knockout mice mediated by failure to degrade proinflammatory cytokine mRNAs. *Genes Dev*. 2006;20:3174-84.
398. Lopez de Silanes I, Zhan M, Lal A, Yang X, Gorospe M. Identification of a target RNA motif for RNA-binding protein HuR. *Proc Natl Acad Sci U S A*. 2004;101:2987-92.
399. Sirenko O, Bocker U, Morris JS, Haskill JS, Watson JM. IL-1 beta transcript stability in monocytes is linked to cytoskeletal reorganization and the availability of mRNA degradation factors. *Immunol Cell Biol*. 2002;80:328-39.



400. Chen LC, Wang LJ, Tsang NM, Ojcius DM, Chen CC, Ouyang CN, et al. Tumour inflammasome-derived IL-1beta recruits neutrophils and improves local recurrence-free survival in EBV-induced nasopharyngeal carcinoma. *EMBO Mol Med.* 2012;4:1276-93.
401. Ghiringhelli F, Apetoh L, Tesniere A, Aymeric L, Ma Y, Ortiz C, et al. Activation of the NLRP3 inflammasome in dendritic cells induces IL-1beta-dependent adaptive immunity against tumors. *Nat Med.* 2009;15:1170-8.
402. Elkabets M, Ribeiro VS, Dinarello CA, Ostrand-Rosenberg S, Di Santo JP, Apte RN, et al. IL-1beta regulates a novel myeloid-derived suppressor cell subset that impairs NK cell development and function. *Eur J Immunol.* 2010;40:3347-57.
403. Cataisson C, Salcedo R, Hakim S, Moffitt BA, Wright L, Yi M, et al. IL-1R-MyD88 signaling in keratinocyte transformation and carcinogenesis. *J Exp Med.* 2012;209:1689-702.
404. Nagareddy PR, Kraakman M, Masters SL, Stirzaker RA, Gorman DJ, Grant RW, et al. Adipose tissue macrophages promote myelopoiesis and monocytosis in obesity. *Cell Metab.* 2014;19:821-35.
405. Reers S, Pfannerstill AC, Rades D, Maushagen R, Andratschke M, Pries R, et al. Cytokine changes in response to radio-/chemotherapeutic treatment in head and neck cancer. *Anticancer Res.* 2013;33:2481-9.
406. Hu B, Elinav E, Huber S, Booth CJ, Strowig T, Jin C, et al. Inflammation-induced tumorigenesis in the colon is regulated by caspase-1 and NLRC4. *Proc Natl Acad Sci U S A.* 2010.
407. Li L, Chen SF, Liu Y. MAP kinase phosphatase-1, a critical negative regulator of the innate immune response. *Int J Clin Exp Med.* 2009;2:48-67.
408. Hooper SJ, Wilson MJ, Crean SJ. Exploring the link between microorganisms and oral cancer: a systematic review of the literature. *Head Neck.* 2009;31:1228-39.
409. Kuriakose MA, Chen WT, He ZM, Sikora AG, Zhang P, Zhang ZY, et al. Selection and validation of differentially expressed genes in head and neck cancer. *Cell Mol Life Sci.* 2004;61:1372-83.
410. Argiris A, Karamouzis MV, Raben D, Ferris RL. Head and neck cancer. *Lancet.* 2008;371:1695-709.
411. Leinum CJ, Dopp JM, Morgan BJ. Sleep-disordered breathing and obesity: pathophysiology, complications, and treatment. *Nutr Clin Pract.* 2009;24:675-87.
412. Lust JA, Lacy MQ, Zeldenrust SR, Dispenzieri A, Gertz MA, Witzig TE, et al. Induction of a chronic disease state in patients with smoldering or indolent multiple myeloma by targeting interleukin 1{beta}-induced interleukin 6 production and the myeloma proliferative component. *Mayo Clin Proc.* 2009;84:114-22.

413. Zitvogel L, Kepp O, Galluzzi L, Kroemer G. Inflammasomes in carcinogenesis and anticancer immune responses. *Nat Immunol.* 2012;13:343-51.
414. Hong DS, Hui D, Bruera E, Janku F, Naing A, Falchook GS, et al. MABp1, a first-in-class true human antibody targeting interleukin-1alpha in refractory cancers: an open-label, phase 1 dose-escalation and expansion study. *Lancet Oncol.* 2014;15:656-66.
415. Montagut C, Iglesias M, Arumi M, Bellosillo B, Gallen M, Martinez-Fernandez A, et al. Mitogen-activated protein kinase phosphatase-1 (MKP-1) impairs the response to anti-epidermal growth factor receptor (EGFR) antibody cetuximab in metastatic colorectal cancer patients. *Br J Cancer.* 2010;102:1137-44.
416. Nieminen R, Korhonen R, Moilanen T, Clark AR, Moilanen E. Aurothiomalate inhibits cyclooxygenase 2, matrix metalloproteinase 3, and interleukin-6 expression in chondrocytes by increasing MAPK phosphatase 1 expression and decreasing p38 phosphorylation: MAPK phosphatase 1 as a novel target for antirheumatic drugs. *Arthritis Rheum.* 2010;62:1650-9.
417. Rabe KF. Update on roflumilast, a phosphodiesterase 4 inhibitor for the treatment of chronic obstructive pulmonary disease. *Br J Pharmacol.* 2011;163:53-67.
418. Papp K, Cather JC, Rosoph L, Sofen H, Langley RG, Matheson RT, et al. Efficacy of apremilast in the treatment of moderate to severe psoriasis: a randomised controlled trial. *Lancet.* 2012;380:738-46.
419. Schett G, Wollenhaupt J, Papp K, Joos R, Rodrigues JF, Vessey AR, et al. Oral apremilast in the treatment of active psoriatic arthritis: results of a multicenter, randomized, double-blind, placebo-controlled study. *Arthritis Rheum.* 2012;64:3156-67.
420. Houslay MD. Underpinning compartmentalised cAMP signalling through targeted cAMP breakdown. *Trends Biochem Sci.* 2010;35:91-100.
421. Brion L, Maloberti PM, Gomez NV, Poderoso C, Gorostizaga AB, Mori Sequeiros Garcia MM, et al. MAPK phosphatase-1 (MKP-1) expression is up-regulated by hCG/cAMP and modulates steroidogenesis in MA-10 Leydig cells. *Endocrinology.* 2011;152:2665-77.
422. Lee J, Komatsu K, Lee BC, Lim JH, Jono H, Xu H, et al. Phosphodiesterase 4B mediates extracellular signal-regulated kinase-dependent up-regulation of mucin MUC5AC protein by *Streptococcus pneumoniae* by inhibiting cAMP-protein kinase A-dependent MKP-1 phosphatase pathway. *J Biol Chem.* 2012;287:22799-811.
423. Zhang J, Wang Q, Zhu N, Yu M, Shen B, Xiang J, et al. Cyclic AMP inhibits JNK activation by CREB-mediated induction of c-FLIP(L) and MKP-1, thereby antagonizing UV-induced apoptosis. *Cell Death Differ.* 2008;15:1654-62.
424. Korhonen R, Hommo T, Keranen T, Laavola M, Hamalainen M, Vuolteenaho K, et al. Attenuation of TNF production and experimentally induced inflammation by PDE4

inhibitor rolipram is mediated by MAPK phosphatase-1. *Br J Pharmacol.* 2013;169:1525-36.

425. Govindarajan R, Ratnasinghe L, Simmons DL, Siegel ER, Midathada MV, Kim L, et al. Thiazolidinediones and the risk of lung, prostate, and colon cancer in patients with diabetes. *J Clin Oncol.* 2007;25:1476-81.

## **Biography**

Xiaoyi Tina Zhang was born in Xi'An in the People's Republic of China. At the age of four, she moved to the United States with her parents, Yunke Zhang and Yumei Yang. She attended the South Carolina Governor's School of Science and Mathematics in Hartsville, South Carolina. During her undergraduate work at the University of South Carolina Honors College in Columbia, SC, Tina maintained a 4.0 GPA and received awards for leadership, community service, and promoting diversity in the student campus. She graduated *summa cum laude* with honors from the Honors College in May 2008. She matriculated into the Medical University of South Carolina's Medical Scientist Training Program in Charleston, SC, in the summer of 2008. She is married to Joseph Cheng, M.D. Ph.D., and they have a son Elliott.